Stony Brook University

Exploring Protein-Protein and Protein-Ligand Interactions in the Bacterial Fatty Acid Biosynthesis Pathway

A Dissertation Presented

by

Janine Borgaro

to

The Graduate School

in Partial Fulfillment of the

Requirements

for the Degree of

Doctor of Philsophy

in

Chemistry

Stony Brook University

August 2011

Stony Brook University

The Graduate School

Janine Borgaro

We, the dissertation committee for the above candidate for the

Doctor of Philosophy degree, hereby recommend

acceptance of this dissertation.

Peter J. Tonge, Ph. D., Advisor
Department of Chemistry, Stony Brook University

Isaac Carrico, Ph. D., Chair
Department of Chemistry, Stony Brook University

Carlos Simmerling, Ph. D., Third Member
Department of Chemistry, Stony Brook University

John Shanklin, Ph. D., Outside Member
Department of Biology, Brookhaven National Lab

This dissertation is accepted by the Graduate School

Lawrence Martin
Dean of the Graduate School

Abstract of the Dissertation

Exploring Protein-Protein and Protein-Ligand Interactions in the Bacterial Fatty Acid Biosynthesis Pathway

by

Janine Borgaro

Doctor of Philosophy

In

Chemistry

Stony Brook University

2011

The bacterial fatty acid biosynthesis (FASII) pathway is a promising target for antibacterial drug discovery and current research is focused on elucidating the substrate specificity of the β-ketoacyl-ACP synthase (KAS) enzymes in this pathway, identify the interactions between the components of the FASII pathway and discovering the

unknown dehydratase, and studying the interaction of current enzyme inhibitors with FASII components in whole cells.

Substrates are shuttled between the FASII enzymes by acyl carrier protein, a phosphopantetheinylated protein with a MW of 13 kDa in *Mycobacterium tuberculosis* and 7 kDa in *Escherichia coli*. While the KAS enzyme(s) involved in fatty acid elongation (KASI and KASII) utilize ACP-based substrates, the priming KAS enzyme (KASIII) is initially acylated by an acyl-CoA substrate. In order to compare and contrast the specificity of KASI/II and KASIII for the substrate carrier, we have synthesized substrates based on phosphopantetheine, CoA, ACP and ACP peptide mimics, and explored their interactions with the KASI enzyme from *M. tuberculosis* (KasA) as well as with the KASI and KASII enzymes from *E. coli* (ecFabB and ecFabF). Highlights of this work include the observation that a 14 residue malonyl-phosphopantetheine peptide can replace malonyl-ACP as the acceptor substrate in the ecFabF reaction. In addition, it was observed that the KASI enzymes ecFabB and KasA have an absolute requirement for an ACP substrate as the donor substrate, and that, provided this requirement was met, variation in the acceptor carrier had only had a small effect on k_{cat}/K_m. For the KASI enzymes it is proposed that the binding of ACP results in a conformational change toward a more accessible open form, thus facilitating the binding of the second substrate.

Studies involving the components of the FASII system also involve the utilization of techniques to identify protein-protein interactions. Several data in the literature suggest the existence of protein–protein interactions within the FASII pathway. Efforts we employed toward characterizing this noncovalent complex include the development of a

photoprobe by attaching a benzophenone group to the prosthetic PPant arm of AcpM (B4M-AcpM), the development of a bioorthogonal ω-azido fatty acid probe to determine fatty acylated proteins in the cell and lastly, the incorporation of fluorescent tags into InhA in order to quantitate an interaction to KasA. Preliminary results indicated a covalent interaction between B4M-AcpM and proteins in *M. smegmatis* cell lysate. However, future optimizations of this method along with the incorporation of ω-azido fatty acids into cells and the appropriate position to insert fluorescent probes into InhA are required to definitely identify physiologically relevant protein-protein interactions.

In separate studies a novel drug-target identification method has been developed that relies on the incorporation of short-lived isotopes such as carbon-11 into the drug of interest. Radiolabeling is accomplished without altering the structure of the drug and size exclusion chromatography (SEC) is used to fractionate proteins following exposure to the radiotracer. Proof of concept experiments have so demonstrated interactions between the FabI enoyl-ACP reductase and the front-line tuberculosis drug ^{11}C-isoniazid as well as with a carbon-11 labeled alkyl diaryl ether FabI inhibitor.

Table of Contents

List of Figures……xiii

List of Schemes……..…xvi

List of Tables xvii

List of Equations xviii

List of Abbreviations..... xix

Acknowledgements..... xxiv

Chapter I. *Mycobacterium Tuberculosis* and Anti-Bacterial Drug Discovery

The History of Tuberculosis…….....1

TB Regimen History……..2

Maturation of Drug Resistance…….....6

Cell Wall Biosynthesis……..9

Enzymes and function in FASII Pathway…….....13

Inhibitors of Bacterial Fatty Acid Biosynthesis…….....15

Isoniazid……..16

Triclosan…….....18

KAS inhibitors……...21

Summary…….....23

References……..…24

Chapter II. Substrate Specificity between *β*-ketoacyl ACP Synthases

Introduction…….....38

β-ketoacyl ACP synthase…….38

Catalytic Mechanism of KAS…….....40

KAS Essentiality…….....42

Acyl Carrier Protein……...43

Minimal Peptide Carrier Potein (PCP) or ACP fragment required for recognition……..46

Substrate Specificity of KAS……47

Materials and Methods…….....49

Materials……...49

KasA and C171Q KasA Expression and Purification…….....49

ecFabB, ecFabF and PantK Expression and Purification……50

KasA R214G and ecFabF R206G Mutagenesis……50

Holo-ACP Synthase Expression and Purification…….....51

ecACP Expression and Purification……...51

ecACP and AcpM Substrate Synthesis…….....52

Peptide Synthesis and Purification…….....53

Peptide Substrate Synthesis……...54

Panthetheine **(1)**……...54

Phosphopantetheine **(2)**……...55

Malonylthiophenol **(3)**……..56

Malonyl Phosphopantetheine **(4)**…….....56

KAS Enzyme Assays……...57

Direct Binding Fluorescence Titrations……..59

Results……..61

*Kinetic Characterization of KAS Enzymes with ACP and CoA Substrates……*61

ecFabF Activity with CoA……62

ecFabB Activity with CoA……67

KasA Activity with CoA……73

Direct Binding Experiment……..78

KAS Discrimination of ACP vs. CoA……82

Kinetic Characterization of KAS Enzymes with Malonyl-phosphopantetheine…….....84

Kinetic Characterization of KAS Enzymes with Short Peptide Mimics of ACP……86

ecFabF Activity with Peptide Mimics……..90

ecFabB Activity with Peptide Mimics……..94

KasA Activity with Peptide Mimics……..98

Discussion……102

Summary……,……...111

References…….....113

Chapter III. The Use of Short Lived Isotopes for Exploring Drug Binding Partners in *Mycobacterium Tuberculosis*

Introduction……...124

Challenges of Identifying Protein Targets……....124

Rifampicin……...125

Enoyl-ACP reductase Structure activity relationship and target validation.....125

Reactive Species of INH…….....127

Mechanism of Action of INH……128

Current Methods to study Drug binding partners……130

Proteomic and Genomic Approaches……130

Affinity Chromatography using Small Molecules……....131

Drug Affinity Response Target Stability (DARTS)……...132

Positron Emission Tomography and Radiochemistry……132

Incorporation of Short Lived Radio-isotopes……135

Materials and Methods

Expression and Purification of InhA……137

The synthesis of ^{11}C-rifampicin, ^{11}C-INH and ^{11}C-PT70……..137

Identification of Protein Targets using ^{11}C-rifampicin……...139

Conditions for INH-NAD Adduct Formation……....139

InhA Inactivation……..139

^{11}C-INH Binds to InhA……140

Identification of Cellular Protein Targets Using ^{11}C-INH……141

Results

Expression and Purification of InhA, AcpM and KasA……..142

^{11}C-rifampicin Binds to High Molecular Weight Proteins……..142

^{11}C-PT70 binds to InhA……143

Proof of INH-NAD Adduct Formation……..145

InhA Inactivation Conditions……146

^{11}C-INH Binds to and Inhibits InhA……..149

^{11}C- INH Binding in a Complex Mixture……152

Discussion……155

Summary……...162

References…….....161

Chapter IV. Studying Protein-Protein Interactions in the FASII Pathway

Introduction*…….*.....170

Protein-Protein Interactions……170

Evidence of a Fatty Acid Biosynthesis Pathway Complex……170

General Protein-Protein Identification Methods……..171

Yeast or Bacterial Hybrid (Y2H, B2H)……..172

Phage Display…….....172

Protein Affinity Chromatography..……...173

Crosslinkers……..173

Chemical Crosslinkers ……174

Photo Crosslinkers…….....175

Bio-orthognal Probes…….....175

Fluorescence……..…….....176

Elucidating a FASII Complex.……..…….177

Materials and Methods

Chemical Synthesis of ω-Azido-fatty Acids ……..…….....179

ω-Hydroxy-dodecanoic Acid Methyl Ester ***(2)***…….....180

ω-Mesyl-dodecanoic Acid Methyl Ester ***(3)***……..……..180

ω-Azido-dodecanoic Acid Methyl Ester ***(4)***……...……..181

ω-Azido-dodecanoic Acid ***(5)***…….....181

Benzophenone-4-maleimide Coenzyme A (B4M-CoA) Synthesis……181

Expression and Purification of AcpM……..……..182

Expression and Purification of KasA ……..…….....183

Expression and Purification of InhA ……183

Expression and Purification of S200C and S73C InhA……184

B4M-AcpM Synthesis……..184

M. Smegmatis Growth……184

Identiyfing Protein-Protein Interactions with B4M-AcpM……184

Metabolic Labeling with ω-azido-hexadecanoic Acid……...186

Reaction of Azide Labeled Cells with a Biotin Alkyne or Alkyne-FLAG Tag……186

Western Blotting……..…….....186

Fluorescently Labeling InhA…….……..187

Direct Binding Fluorescence Titrations…….....188

Results

Expression and Purification of InhA (wild type, S200C, S73C), AcpM and KasA……...……...190

Identifying Protein Interactions with B4M-AcpM…….....…….....190

Incorporation of ω-Azido-fatty Acids…..……..……...193

InhA-KasA Fluorescence…….....194

Discussion……...198

Summary……..201

References…….....203

Bibliography……211

List of Figures

Figure 1.1: Frontline Drugs Used for Tuberculosis Treatment……..3

Figure 1.2: Second Line (A) and Third Line (B) TB Drugs…….....8

Figure 1.3: Mycobacterial Cell Wall…….....10

Figure 1.4: MTb Fatty Acid Biosynthesis FASII Cycle…….....11

Figure 1.5: Structure of ACP…….....12

Figure 1.6: Structure of *Mycobacterium* β-ketoacyl-ACP synthase KasA (KASI)……...14

Figure 1.7: Structure of INH-NAD^+ Adduct Bound to InhA……..…….....17

Figure 1.8: Inhibitors of FabI…….....18

Figure 1.9*:* Structure of Triclosan and PT70 Bound to InhA…….20

Figure 1.10: KAS Inhibitors.……...21

Figure 2.1*:* Structure of KasA……..…….39

Figure 2.2: Ping-Pong Catalytic Mechanism for KasA……..41

Figure 2.3: Structure of ACP with Stearic Acid Bound…..…….45

Figure 2.4: Coupled Assay for KAS Activity……..……....59

Figure 2.5: Synthesis of ACP Substrates……....61

Figure 2.6: Kinetic Analysis of ecFabF for Malonyl-CoA…….....63

Figure 2.7: Kinetic Analysis of ecFabF for Lauroyl-CoA..……..64

Figure 2.8: Kinetic Analysis of ecFabF for Malonyl-ecACP…..……65

Figure 2.9: Kinetic Analysis of ecFabB for Lauroyl-ecACP……..68

Figure 2.10: Kinetic Analysis of ecFabB for Malonyl-ecACP……69

Figure 2.11: Kinetic Analysis of ecFabB for Malonyl-CoA……..……....70

Figure 2.12: Kinetic Analysis of ecFabB for Lauroyl-CoA……..……..71

Figure 2.13: Kinetic Analysis of KasA for Malonyl-AcpM……..……74

Figure 2.14: Kinetic Analysis of KasA for Malonyl-CoA…….....75

Figure 2.15: Interaction Between KasA and Palmitoyl-CoA……..…....76

Figure 2.16: Interaction Between apo-KasA and Palmitoyl-CoA……..……..79

Figure 2.17: Interaction Between acyl-KasA and Palmitoyl-CoA……..…....80

Figure 2.18: Interaction of C171Q KasA with Palmitoyl-CoA……..…....81

Figure 2.19: Kinetic Analysis of R206G ecFabF for Malonyl-CoA……...83

Figure 2.20: Kinetic Analysis of R214G KasA for Malonyl-CoA……...84

Figure 2.21: Kinetic Analysis of ecFabF for MalPPant…….....86

Figure 2.22: Phosphopantethenylation Reaction Catalyzed by AcpS……...88

Figure 2.23: CD Spectra of MalPPant-14mer……..……..89

Figure 2.24: CD Spectra of MalPPant-16mer……..……..89

Figure 2.25: Kinetic Analysis of ecFabF for MalPPant-8mer……...91

Figure 2.26: Kinetic Analysis of ecFabF for MalPPant-14mer……..……..92

Figure 2.27: Kinetic Analysis of ecFabF for MalPPant-16mer…….....93

Figure 2.28: Kinetic Analysis of ecFabB for MalPPant-8mer…….....95

Figure 2.29: Kinetic Analysis of ecFabB for MalPPant-14mer……....96

Figure 2.30: Kinetic Analysis of ecFabB for MalPPant-16mer……....97

Figure 2.31: Kinetic analysis of KasA for MalPPant-8mer……..... 99

Figure 2.32: Kinetic Analysis of KasA for MalPPant-14mer…….. 100

Figure 2.33: Kinetic Analysis of KasA for MalPPant-16mer…….. 101

Figure 2.34: Synthesized AcpM Peptide Mimic…….....103

Figure 2.35: Structure of ecFabH-CoA complex superimposed with …….....105

Figure 2.36: Proposed binding interactions between ACP and ecFabB, ecFabF and KasA ……..107

Figure 3.1: InhA Inhibitors……..127

Figure 3.2: INH Oxidation Products..…….....128

Figure 3.3: Scheme for the Formation of the INH-NAD Adduct…..……..130

Figure 3.4: Radioactive Decay by Positron Emission..……..134

Figure 3.5: ^{11}C-rifampicin Binding to *M. smegmatis* Protein Lysate..……...143

Figure 3.6: HPLC Based SEC of ^{11}C-PT70 Incubated with InhA……144

Figure 3.7: UV Analysis of INH-NAD Adduct Formation……..146

Figure 3.8: Remaining InhA Activity……147

Figure 3.9: Remaining InhA Activity……148

Figure 3.10: HPLC Based SEC of ^{11}C-INH Incubated with InhA…..……...150

Figure 3.11: NADH Oxidation……152

Figure 3.12: HPLC Based SEC of ^{11}C-INH Incubated with *E. coli* overexpressing InhA……..……154

Figure 4.1: Structure of Alexa Fluor 350……188

Figure 4.2: Structure of Bimane Fluorophore……..188

Figure 4.3: Reaction with Purified MabA, KasA and InhA and B4M-AcpM..……....192

Figure 4.4: Reaction *with M. smegmatis* Cell Lysate and B4M-AcpM…….....193

Figure 4.5: Reaction of ω-Azido-hexadecanoic Acid with Protein Lysate…....194

Figure 4.6: Structure of InhA Tetramer…..……....196

Figure 4.7: Structure of InhA Tetramer…….....197

List of Schemes

Scheme 2.1 Synthesis of Malonylphosphopantetheine…….....83

Scheme 3.1: Radiosynthesis of ^{11}C-RIF…….....138

Scheme 3.2: Radiosynthesis of ^{11}C-INH……138

Scheme 3.3: Radiosynthesis of ^{11}C-PT70……138

Scheme 4.1: Synthesis of ω-Azido-hexadecanoic Acid..……...179

Scheme 4.2: Synthesis of B4M-CoA……...182

Scheme 4.3: Benzophenone Photochemistry……...185

List of Tables

Table 1.1: Drug Regimen for Culture Positive Pulmonary Tuberculosis……...5

Table 2.1: Mutagenesis Primers for ecFabF & KasA…….....50

Table 2.2: Kinetic Parameters for ecFabF…….....66

Table 2.3: Kinetic Parameters for ecFabB…….....72

Table 2.4: Kinetic Parameters for KasA…….....77

Table 2.5: Interaction of KasA and C171Q KasA with Palmitoyl-CoA…… 81

Table 2.6: Sequence Homology of α-helix 2 Between ACPs……...87

Table 3.1: Short Lived Radioactive Isotopes and Their Half Lives……...135

List of Equations

Equation 1: $v = V_{max} [S] / (K_m + [S])$

Equation 2: $k_{cat} = V_{max} / [E]$

Equation 3: $v = V_{max}*[S] / (K_m + [S] + [S]^2 / K_d)$

Equation 4: [Bound] = (Capacity * [Free]) / (K_d + [Free])

Equation 5: $A_x/\in$ * MW of protein/mg protein/mL = molesof dye/moles of protein

List of Abbreviations

8PP	5-octyl-2-phenoxyphenol
Å	Angstom
AaCl	Acetyl chloride
ACP	Acyl carrier protein
AcpM	Acyl carrier protein from *M. Tuberculosis*
AcpS	*holo*-ACP synthase
AD	Activating domain
B2H	Bacterial two hybrid
B4M	*Benzophenone-4-maleimide*
B. mallei	*Burkholderia Mallei*
B. subtilis	*Bacillus subtilis*
BD	Binding domain
^{11}C-INH	Carbon-11 labeled isoniazid
^{11}C-RIF	Carbon-11 labeled rifampicin
^{11}C-PT70	Carbon-11 labeled PT70
CAP	Catabolite activating protein
CD	Circular dichroism
CDC	Center for disease control
CESTET	Conditional expression and specialized transduction essentiality test
CoA	Coenzyme A
CurF	ACP-specific decarboxylase

Da	Dalton
DD-CoA	Dodecenoyl-CoA
DMF	Dimethylformaide
DNA	Deoxyribonucleic acid
DOTS	directly observed therapy short course
DTNB	5,5'-Dithio-bis(2-nitrobenzoic acid)
DTT	Dithiothreitol
E. coli	*Escherichia coli*
ecACP	Acyl carrier protein from *Escherichia coli*
ecFabB	β-Ketoacyl synthases I from *Escherichia coli*
ecFabF	β-Ketoacyl synthases II from *Escherichia coli*
ecFabH	β-Ketoacyl synthases III from *Escherichia coli*
ecFabI	Enoyl-ACP reductase from *Escherichia coli*
EDTA	
ELISA	Enzyme-linked immunosorban assays
EMB	Ethambutol
ESI-MS	Electrospray ionization mass spectrometry
ER	Enoyl redutase
EtoAc	Ethyl acetate
F. tularensis	*Francisella tularensis*
FabA	β-Hydroxyacyl-ACP dehydrases
FabD	malonyl-CoA:ACP transacylase
FabG	β-Ketoacyl-ACP reductase

FabH	β-Ketoacyl synthases III
FabI	Enoyl-ACP reductase
FabZ	β-Hydroxyacyl-ACP dehydrases
FAS-I	Eukaryotic fatty acid biosynthesis
FAS-II	Bacterial fatty acid biosynthesis
Fmoc	9-fluornylmethoxycarbonyl
FPLC	Fast protein liquid chromatography
HPLC	High performance liquid chromatography
HRP	Horseradish peroxidase
INH	Isoniazid
INH-NAD^+	Isonazid Nicotinamide adenine dinucleotide adduct
InhA	Enoyl-ACP reductase from *Mycobacterium tuberculosis*
IPTG	Isopropyl-1-thio-β-D-galactopyranoside
IUATLD	International Union Against Tuberculosis and Lung Disease
KASI	β-Ketoacyl synthases I
KASII	β-Ketoacyl synthases II
KasB	β-Ketoacyl synthases II from *Mycobacterium tuberculosis*
KatG	Mycobacterial catalase-peroxidase
kD	Kila-dalton

LB	Luria Broth
LC-MS	Liquid chromatography mass spectrometry
M. tuberculosis	*Mycobacterium tuberculosis*
MALDI-TOF	Matrix-assisted laser desorption ionization-time of fly
MalPPant-8mer	8 residue malonyl-phosphopantetheine
MalPPant-14mer	14 residue malonyl-phosphopantetheine
MalPPant-16mer	16 residue malonyl-phosphopantetheine
MDR-TB	Multi-drug resistanttuberculosis
MeOH	Methanol
MES	4-morpholineethanesulfonic acid monohydrate
MIC	Minimal inhibitory concentration
MsCl	Mesyl chloride
MTB	*Mycobacterium tuberculosis*
NAD+	Nicotinamide adenine dinucleotide, oxidized form
NADH	Nicotinamide adenine dinucleotide, reduced form
NADPH	Nicotinamide adenine dinucleotide phosphate, reduced form
NaOH	Sodium chloride
NMR	Nuclear magnetic resonance
NYC	New York city
O.D. 600	Optical density at 600 nm
PAL-PEG	5-(4’-Fmocaminomethyl-3’, 5-dimethoxyphenol) valeric acid

PantK	Pantothenate kinase
PDIM	phthiocerol dimycocerosate
PET	Positron emission tomography
PPant	Phophopantetheine
PT70	2-(o-tolyloxy)-5-hexylphenol
PZA	Pyrazinamide
RIF	Rifampicin
RNA	Ribonucleic acid
S. aurues	*Staphylococcus aureus*
S. pneumoniae	*Streptococcus pneumoniae*
SAR	Structure activity relationship
SDS-PAGE	sodium dodecyl sulfate-polyacrylamide gel electrophoresis
SEC	Size exclusion chromatography
TB	Tuberculosis
TCEP	Tris(2-carboxyethyl)phosphine
TEA	Triethylamine
TFA	Trifluoroacetic acid
THF	Tertahydrofuran
TLM	Thiolactomycin
UV	Ultra Violet
WHO	World Health Organization
Y2H	Yeast two hybrid

Acknowledgement

I would like to start by thanking my advisor Prof. Peter J. Tonge, whose guidance and support has been an invaluable asset to my scientific career. His mentorship was vital in training me to be a creative and independent thinker and his passion and work ethic towards science is definitely something to be admired.

I would also like to thank Prof. Issac Carrico and Prof. Carlos Simmerling for serving as my dissertation committee and for their helpful suggestions in guiding my research over the years. For Dr. John Shanklin, whose interest and vast knowledge in acyl carrier proteins make him an ideal candidate to serve as the outside member on my committee and I appreciate him taking the time to do so.

I would also like to thank all the friends I've made at Stony Brook University who have made the PhD. experience an extraordinary one. More specifically, I would like to say thanks to all my friends in the 5^{th}, 6^{th} and 7^{th} floor labs, especially the Tonge and Goroff groups. True friends are hard to come by and I will cherish our friendship throughout my life.

Lastly, I would like to thank my family and loved ones, especially my father who has been a role model of strength and preservation throughout my whole life. I truly appreciate all your encouragement towards my education over the years.

Mycobacterium Tuberculosis and Anti-Bacterial Drug Discovery

The History of Tuberculosis

Mycobacterium tuberculosis (MTb), the causative agent of tuberculosis (TB), remains a serious global health concern with an estimated death toll of 2-3 million people annually (*1, 2*). The world health organization (WHO) estimates an annual occurrence of 8 million new cases a year, of which 95% are in developing countries. The effect of the pandemic is mostly noticed in areas such as sub-Saharan Africa where nearly 70% of the population is infected due to low incomes and poor health care. Other groups of people such as those who are in close contact with TB infected patients and people who abuse injectable drugs, are also at higher risk of exposure to infection (*3*). TB poses a deadly co-infection in HIV/AIDS patients, especially in sub-Saharan Africa. One-third of patients co-infected with TB will die, making it the primary cause of death (*4*).

MTb, a gram positive bacillus, has existed in the human population since ancient times. Analysis of the remains of Egyptian mummies from 2400 BCE, indicate characteristic signs of TB (*5*). In the late seventeenth century, written observations of consistent and distinctive changes in the lungs of patients with TB (also known as consumption patients) emerged, indicating an understanding of the anatomy and pathology of the disease. Two centuries later new advances were made by a French military doctor, Jean-Antoine Villemin who confirmed that consumption could be passed from humans to livestock and from livestock to rabbits. This ground-breaking evidence led him to postulate that the disease was likely caused by an explicit microorganism but the causative agent remained elusive and skeptics prevailed. Shortly after in 1882, Dr.

Robert Koch was able to visualize MTb using a staining technique. What delighted the world was not so much the scientific brilliance of Koch's findings, but the accompanying belief that now the battle against humanity's most feared enemy could really begin.

TB Regimen History

The survival of TB is dependent on its ability to persist in human macrophages through complex host pathogen interactions, making the treatment of TB challenging and extensive (*6*). The basic regimen recommended for treating adults with TB is comprised of the four frontline drugs, isoniazid (INH), rifampicin (RIF), pyrizinamide (PZA) and ethambutol (EMB) (**Figure 1.1**). Depending on the circumstances, children may not receive EMB in the initial phase of a 6-month regimen, but the regimens are otherwise identical. Each has an initial phase of 2 months, followed by a choice of several options for the continuation phase of either 4 or 7 months ((*7*), **Table 1.1)**

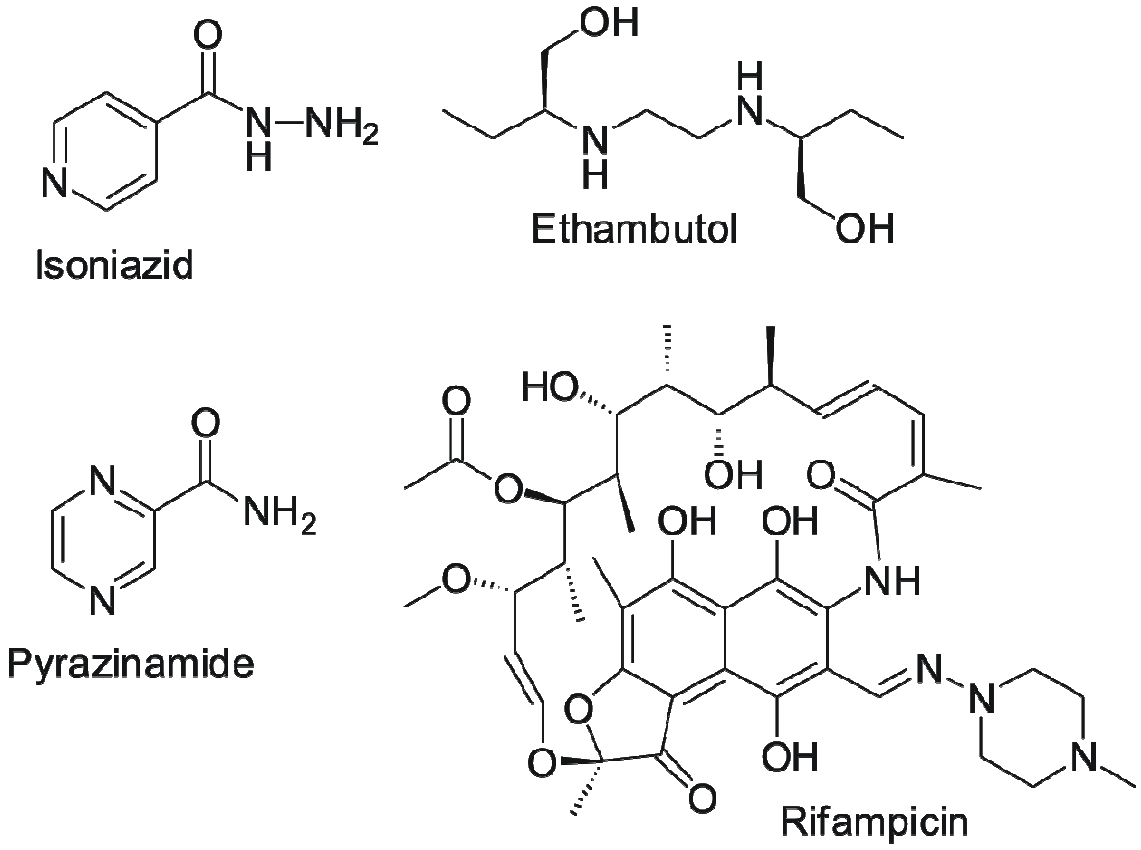

Figure 1.1: Frontline Drugs Used for Tuberculosis Treatment.

For many years, sulfonamides and penicillins have been used in the treatment against infectious diseases. However, these chemotherapeutics showed no efficacy against MTb. The first success was achieved in 1943 when streptomycin efficiently inhibited MTb in animals with moderately low toxicity. Even though streptomycin inhibits protein synthesis, an important factor in TB virulence, it is no longer broadly used due to its toxic effects and required administration by injection (*8*). The following years afforded a number of anti-TB drugs. The timing was vital because resistant mutants started emerging as a result of streptomycin monotherapy which jeopardized the achievement

gained by antibiotic therapy. However, it was quickly discovered that TB resistant mutants could be treated with a combination of two or three drugs.

In 1952 isoniazid was introduced for treatment against TB and is still today one of the most effective front line drugs (*9*). It exhibits its antibacterial activity against the fatty acid biosynthesis pathway (FASII), by primarily inhibiting the enoyl-acyl carrier protein reductase, InhA (*10*).

Pyrazinamide was subsequently introduced in 1954. In highly acidic conditions, pyrazinamidase transforms pyrazinamide to its active form, pyrazinoic acid (*11*). Fatty acid biosynthesis was originally proposed as the target for pyrazinoic acid although this has recently been disproven (*12, 13*). It was also suggested that the influx of pyrazinoic acid disrupts the membrane potential and impedes energy production, necessary for MTb survival (*14*). However, an exact molecular mechanism for the drug's efficacy has remained elusive.

Ethambutol was discovered in 1962 and acts by inhibiting arabinosyl transferase, one enzyme responsible for the synthesis of arabinogalactan. Since arabinogalactan is a key component of the cell wall biosynthesis, inhibition leads to improper formation and thus permeability of the cell wall (*15*). The discovery of rifampicin followed a year later in 1963. Rifampicin, binds to and inhibits the transcriptional factor RNA polymerase β-subunit *rpoB (16).* However, new additions to the frontline drug regimen ceased after the addition of rifampicin, stressing the importance for innovative chemotherapeutics.

Table 1.1: Drug Regimen for Culture Positive Pulmonary Tuberculosis (*17*)

Initial Phase			Continuation Phase			
Regimen	**Drugs**	**Interval and Doses**	**Regimen**	**Drugs**	**Interval and Doses**	**Range of Total Doses (Minimal duration)**
1	INH RIF PZA EMB	Seven d/wk for 56 doses (8 wk) or 5 d/wk for 40 doses (8 wk)‡	1a 1b 1c*	INH/RIF INH/RIF INH/RPT	Seven d/wk for 126 doses (18 wk) or 5 d/wk for 90 doses (18 wk) ‡ Twice weekly for 36 doses (18 wk) Once weekly for 18 doses (18 wk)	182-130 (26 wk)
2	INH RIF PZA EMB	Seven d/wk for 14 doses (2 wk), then twice weekly for 12 doses (6 wk) or 5 d/wk for 10 doses (2 wk)‡, then twice weekly for 12 doses (6 wk)	2a 2b*	INH/RIF INH/RPT	Twice weekly for 36 doses (18 wk) Once weekly for 18 doses (18 wk)	92-76 (26 wk) 74-58 (26 wk)
3	INH RIF PZA EMB	Three times weekly for 24 doses (8 wk)	3a	INH/RIF	Three times weekly for 54 doses (18 wk)	78 (26 wk)
4	INH RIF EMB	Seven d/wk for 56 doses (8 wk) or Five d/wk for 40 doses (8 wk)‡	4a 4b	INH/RIF INH/RIF	Seven d/wk for 217 doses (31 wk) or 5 d/wk for 155 doses (31 wk)‡ Twice weekly for 62 doses	273-195 (39 wk) 118-102 (39 wk)

‡ - Five day a week administration is always given by DOTS

□ - Options 1c and 2b should be used in only HIV negative patients

Although the drugs described above made important advances in the treatment for TB, they are far from optimal therapeutic agents. The recorded side effects associated with these drugs are extremely painful and even fatal. For instance, administration of ethambutol causes optic neuritis and peripheral neuropathy leading to irreversible blindness and nerve damage (*18*). All frontline drugs have been associated with drug induced liver failure. Rifampicin is nearly ineffective in co-infected HIV/AIDS patients due to an interference with anti-retroviral drugs. (*19*). Patient compliance is further

hindered by additional side effects such as, weakness, fever, headache, fatigue, vomiting, weight loss and rash, fueling the emergence of drug resistant strains (*20*).

Maturation of Drug Resistance

A contributing factor to the reappearance of TB is the emergence of multi-drug resistance. The initial exposure of bacilli to an anti-TB drug causes the prevalent bacilli to die, leaving the few drug resistant mutants to multiply at will (*21, 22*). The simultaneous presence of additional effective drugs will prevent the growth of mutant bacilli, emphasizing the importance for physicians to strictly adhere to the recommended four drug regimen of isoniazid, rifampin, pyrazinamide, and ethambutol or streptomycin. Moreover, resistance to anti-TB drugs can occur when these drugs are misused or mismanaged.

A major factor in drug resistance results from patient non-compliance to the full course of treatment due to the harsh side effects. Other contributing factors include, health-care providers prescribing the wrong treatment, dose, or length of time for the regimen, the supply of drugs is not available or the drugs are of poor quality (*23*).

The importance of adhering to the four drug therapy was emphasized when a sudden occurrence of multi-drug resistant TB (MDR-TB) cases surfaced in NYC in the 1990s (*24, 25*). MDR-TB is defined as TB resistant to at least rifampicin and INH and primarily results from multiple mutations in individual drug target genes (*26, 27*). In 2008, the WHO recorded 440,000 new MDR-TB cases, making up 10% of all new cases in Eastern Europe, the region impacted most by the disease. In addition to the number of new cases, the increase in cost for curing MDR-TB is also overwhelming,

since it costs as much as 1400 times that of regular treatment. This new scare initiated TB control programs resulting in a successful decrease in the number of TB cases by 59% and MDR-TB cases by 91% (*25*), indicating that suitable TB control programs can lessen the degree of MDR-TB emergence.

In 2005, three main players involved in TB control programs; the United States Centers for Disease Control and Prevention (CDC), WHO and 14 supranational TB reference laboratories (SRLs), investigated the degree of second line drug resistance in MDR-TB patients. A year later, the results afforded the first definition of extensively drug resistant tuberculosis (XDR-TB). XDR-TB is defined as TB that is resistant to any fluoroquinolone, and at least one of three injectable second-line drugs (capreomycin, kanamycin, and amikacin), in addition to isoniazid and rifampin. This makes XDR-TB treatment tremendously complicated and poses an imminent threat to both developed and undeveloped countries.

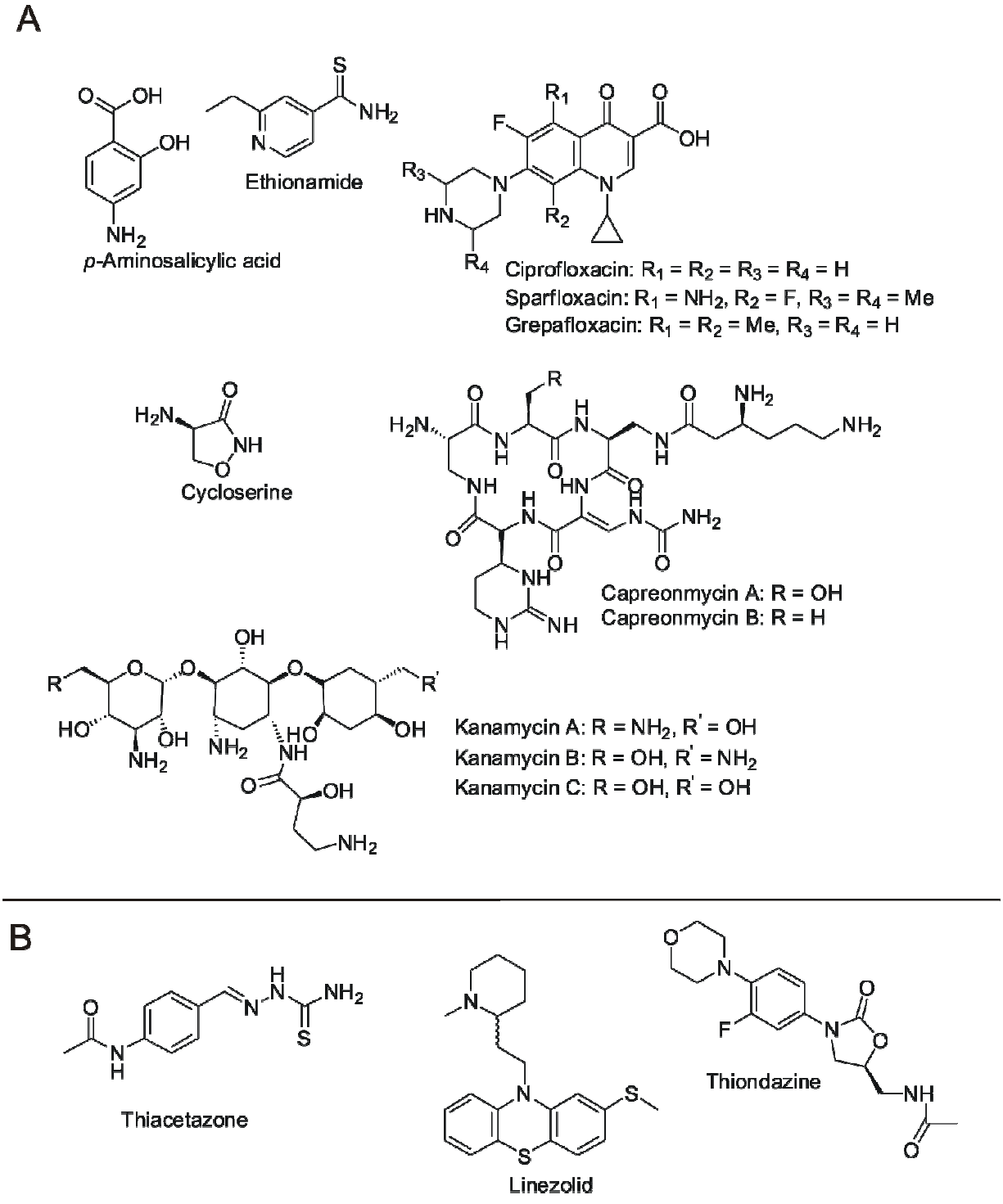

Figure 1.2: Second Line (A) and Third Line (B) TB Drugs.

Figure 1.2 shows one example from each of the six classes of second line drugs along with examples of third line drugs. These drugs are considered third line and are not found on the WHO list of drugs because they are either not very effective or their efficacy has not yet been proven.

The WHO and of the International Union Against Tuberculosis and Lung Disease (IUATLD) compiled a series of recommendations and procedures for the effective treatment of TB. A specialized committee was responsible for creating the document from the WHO, while the IUATLD document is a refinement of IUATLD practice from the field. The recommended treatments and guidelines are built around on a program called DOTS or directly observed therapy short course, employed to ensure the patients were continuing their treatment regimen with regular and appropriate dosing (*25, 28*). Reports from the WHO indicate 84% of patients treated under the guidelines of DOTS are successfully treated. Although improvements have been made towards the global treatment of TB, new cases occur daily. In addition, as long as the treatment of TB consists of a long, complex, decade old drug regimen, drug resistance will continue to flourish. Thus, new novel chemotherapeutics, working through new biological mechanisms of action are of dire need.

Cell Wall Biosynthesis

Cell wall biosynthesis has been established as an effective drug target in a range of bacterial infections (*29*). In mycobacteria, mycolic acids serve as one of the major components that comprise the cell wall (**Figure 1.3**). Mycolic acids are very long chain fatty acids that provide protection for the mycobacteria, thus aiding to its virulence (*30,*

31). The enzymes involved in the biosynthesis of the cell wall have been the subject of intense research for many years (*32*) because they offer attractive and selective targets for the development of novel chemotherapeutics (*32, 33*)

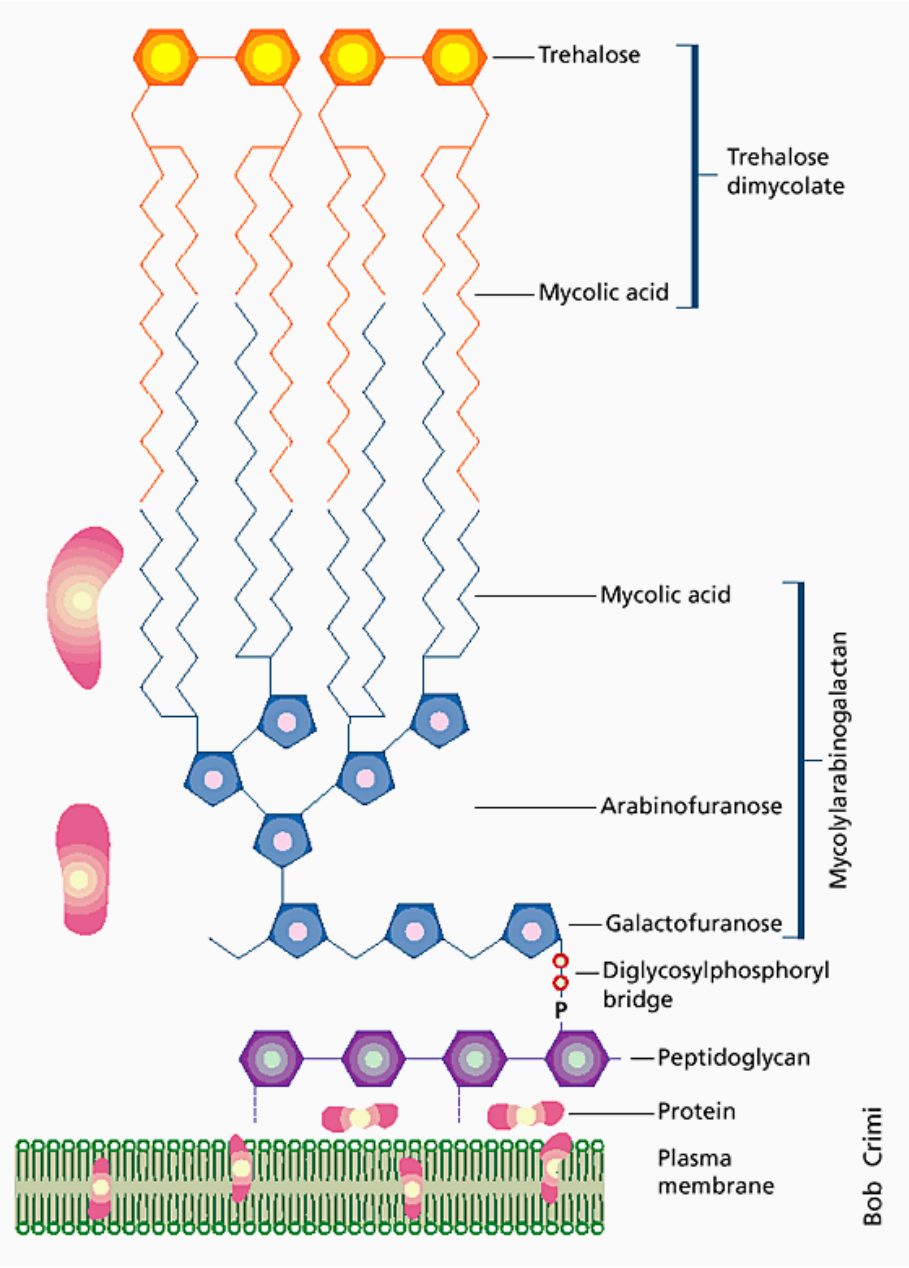

Figure 1.3: Mycobacterial Cell Wall.

Unlike other bacteria, mycobacteria require two distinct fatty acid synthase pathways (FAS) (*34*); the FASI pathway, which is typically found in yeast and mammals and the FASII pathway which is found in bacteria and plants. The synthesis of shorter fatty acids (C_{14}-C_{16}) is performed by the FASI pathway, where all of the catalytic steps are contained on a single multi-functional polypeptide (*35*). These short fatty acids are then elongated by the FASII pathway which is made up of a discrete collection of enzymes **(Figure 1.4)** and is responsible for synthesizing long chain fatty acids that serve as precursors for mycolic acids (C_{50+}) (*36, 37*). In both FASI and FASII, an acyl carrier protein (ACP) is responsible for shuttling the growing fatty acid which is attached via a thioester linkage to a conserved serine found in ACP recognition α-helix 2 (**Figure 1.5**) (*38*). It has been shown that isoniazid, one of the most effective front line drugs for TB inhibits the synthesis of mycolic acids by inhibiting the enoyl-ACP reductase (InhA) (*39-42*) and possibly one of the β-ketoacyl-acyl carrier protein synthase (KAS) enzymes (*43*).

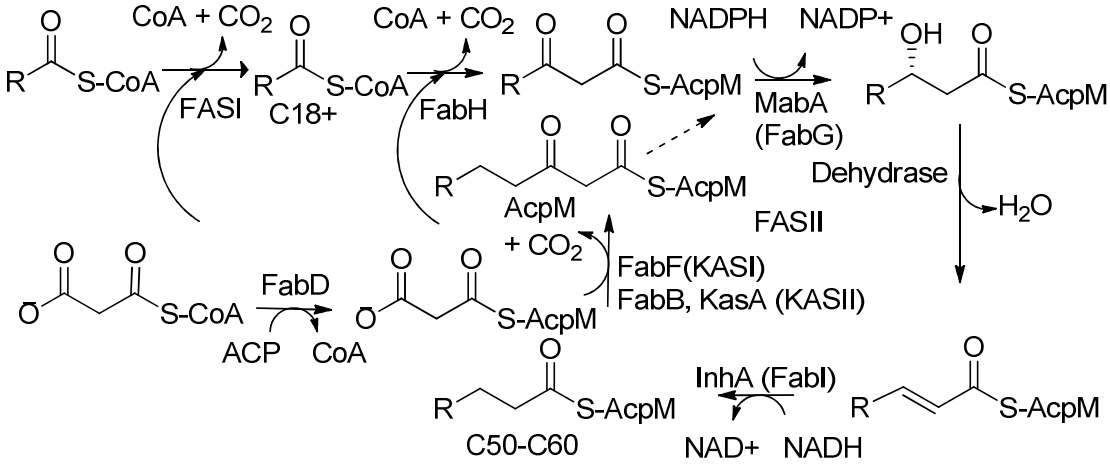

Figure 1.4: MTb Fatty Acid Biosynthesis FASII Cycle.

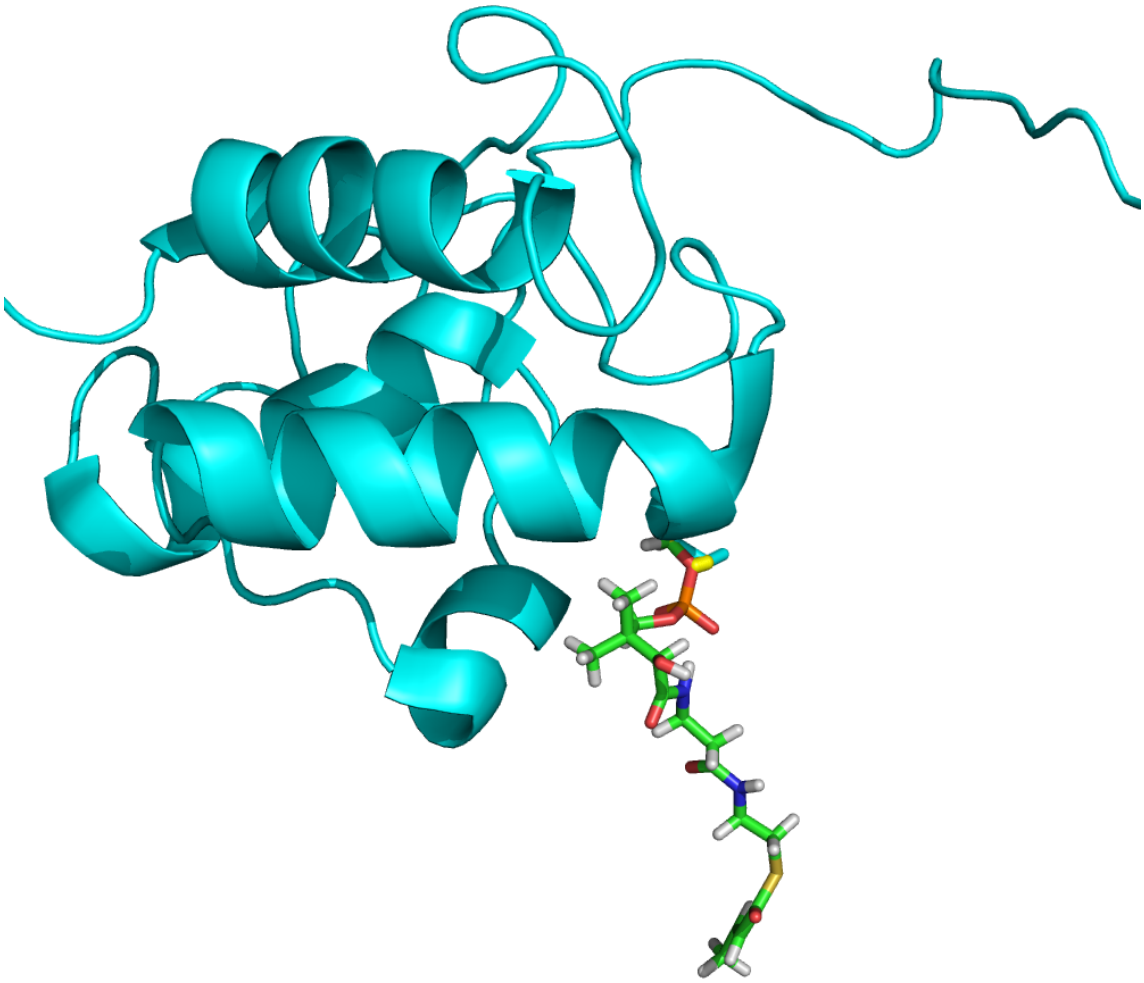

Figure 1.5: Structure of ACP. Alignment of the mycobacterial acyl carrier protein (AcpM) and the acyl carrier protein of *E. coli* (ecAcpM) showing the phosphopantetheine group attached to Serine 41 through a phosphodiester linkage and thioester linkage to the growing fatty acyl chain. This figure was made using PyMOL, AcpM (1klp.pdb); ecAcp.

Enzymes and function in FASII Pathway

Fatty acid biosynthesis plays an essential function in the metabolism of living systems. A considerable degree of research has been performed in biochemically characterizing all the enzymes involved in the fatty acid biosynthetic pathway in *Escherichia coli (44)*. This system serves as a model for understanding FASII systems in other bacteria.

The first enzyme of fatty acid biosynthesis is acetyl-CoA carboxylase, a heterotetrameric enzyme encoded by four genes, accA, accB, accC and accD. The product of the reaction, malonyl-CoA, is then used to produce malonyl-ACP via a transthioesterification reaction catalyzed by the malonyl-CoA:ACP transacylase (FabD) (*45*). The first step in the elongation cycle involves a condensation reaction between the C_{18}-CoA product of the FASI pathway with malonyl-ACP to yield a β-ketoacyl-ACP, catalyzed by the β-ketoacyl synthase, FabH (KASIII) (*46*). The β-ketoacyl-ACP is subsequently reduced to β-hydroxylacyl-ACP catalyzed by the β-ketoacyl dehydrogenase, MabA (FabG in *E. coli*) (*47, 48*). The next step involves a dehydration catalyzed by an unknown dehydrase in MTb and either FabA or FabZ in *E. coli* to yield an enoyl-ACP (*49, 50*). This product is then reduced by the enoyl-ACP reductase, InhA (FabI in *E. coli*) (*10, 51*). A repetitive series of elongation utilizes the same enzymes except that the condensation reaction is catalyzed by ACP-specific KasA (KASI) or KasB (KASII), which are homologues of the FabB (KASI) and FabF (KASII) synthases found in *E. coli (52, 53)*. KasA, KasB and FabH all catalyze a Claisen condensation between malonyl-ACP and acyl-CoA or acyl-ACP. Although there is a high degree of conservation between the β-ketoacyl synthases resulting in analogous three

dimensional structures, they differ in their active site triad which is Cys-His-Asn in FabH and Cys-His-His in KasA/KasB (FabB/FabF) (**Figure 1.6**) (*54*).

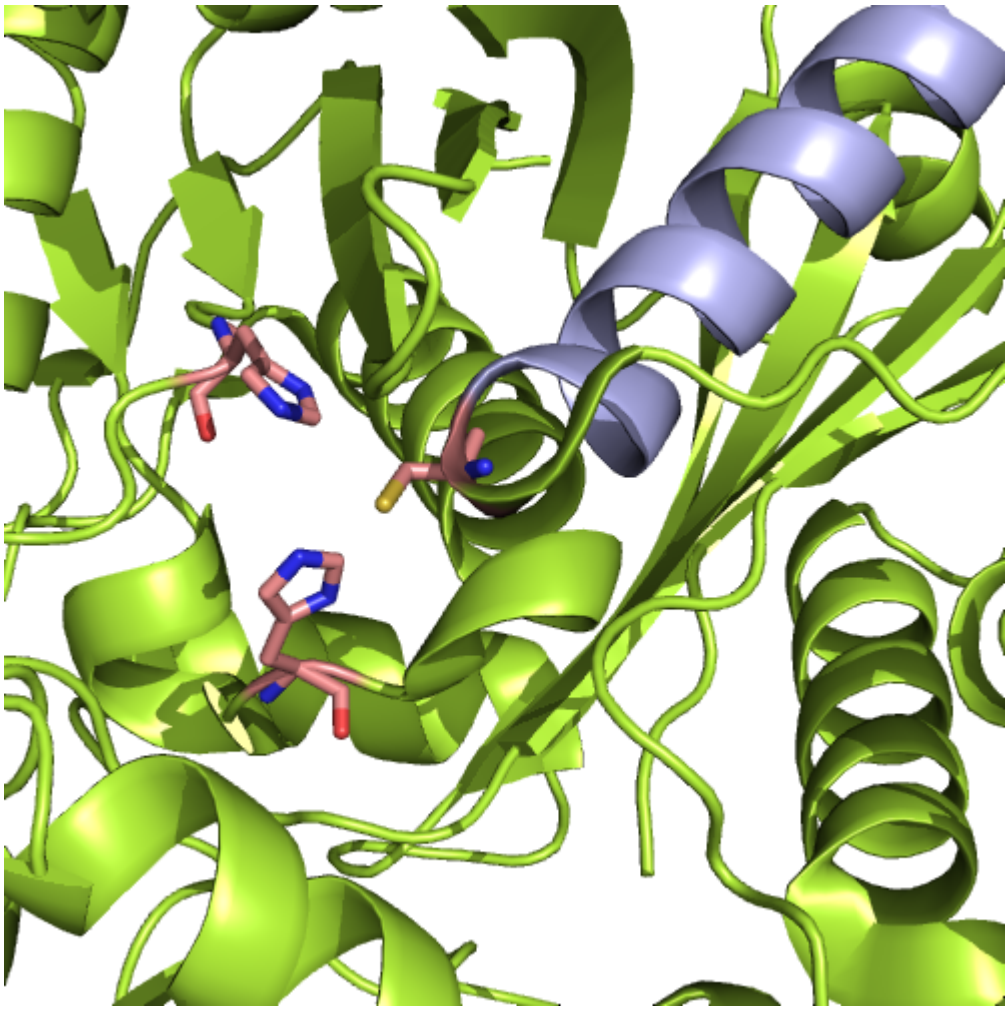

Figure 1.6: Structure of *Mycobacterium* β-ketoacyl-ACP Synthase KasA (KASI).

The Cys-His-His catalytic triad is shown in pink and the helix responsible for the oxyanion hole in shown in lilac. This figure was made using PyMOL, KasA (2WGE.pdb).

FASII has been long recognized as a target for antimicrobial development. The enzymes of this pathway have been well characterized and exhibit a high degree of conservation throughout a variety of bacteria. This coupled with the absence of FASII in mammals make this pathway an attractive drug target. The essentiality of most of the enzymes in the FASII pathway has been confirmed by experiments such as knockdowns, knockouts or through inhibition studies. For instance, Bergler *et al* sought out to determine the essentiality of *E. coli* FabI (ecFabI) by developing an ecFabI mutant strain which caused temperature sensitive growth. Upon growing the strain at non permissive temperatures, lethal effects on lipid biosynthesis were seen, confirming the essentiality of ecFabI (*55*). In addition, numerous inhibitors that are developed to specifically target the enoyl reductase have exhibited promising efficacy (*56*). Lai and Cronan developed an *E. coli* FabH (ecFabH) deletion mutant strain which failed to grow in the absence of supplemental exogenous fatty acids, demonstrating ecFabH essentiality (*57*). However, FabH has yet to be proven essential in MTb (*58*). Bactericidal effects were exhibited through conditional depletion experiments along with KasA specific inhibitors, emphasizing the essentiality of KasA (*59*). MabA and the dehydratase have also shown to be essential for growth (*60, 61*).

Inhibitors of Bacterial Fatty Acid Biosynthesis

To date, FAS inhibition studies have mainly been focused on the ketoacyl synthase (KAS, (*62*)) and the more extensively studied enoyl-ACP reductase (ER, (*63*)).

Isoniazid

Isoniazid has been the leading front line anti-TB drug since 1952 which exhibits excellent bactericidal activity against MTb with an MIC value of 0.02 μg/mL. Thorough research involving crystal structures and genetic knockouts reveal InhA as one of the key cellular targets for INH (*39, 41, 64*). However, due to complexity of the mode of action, other cellular targets such as KasA and a handful of pyridine nucleotide-dependent dehydrogenase/reductases have also been implicated (*43, 65*). INH is a prodrug and must be activated by a catalase-peroxidase enzyme, KatG, which couples the isonicotinic radical with NADH resulting in the formation of the INH-NAD^+ adduct (**Figure 1.8A**, (*10*)) which is responsible for the inhibition of InhA. The mechanism of INH-NAD^+ inhibition classifies the adduct as a slow tight binding inhibitor (K_i = 0.7 nM) where the initial enzyme-inhibitor complex EI is formed rapidly and then slowly converts into a final inhibited complex EI*. Through molecular dynamic simulations and x-ray crystallography, Tonge *et al* demonstrated that the slow step involves a conformational change in InhA resulting in the ordering of the substrate binding loop (**Figure 1.7**, (*56*)). Since most INH resistance is linked to mutations in KatG, inhibitors that do not require activation present a attractive solution to treat INH-resistant TB (*66*).

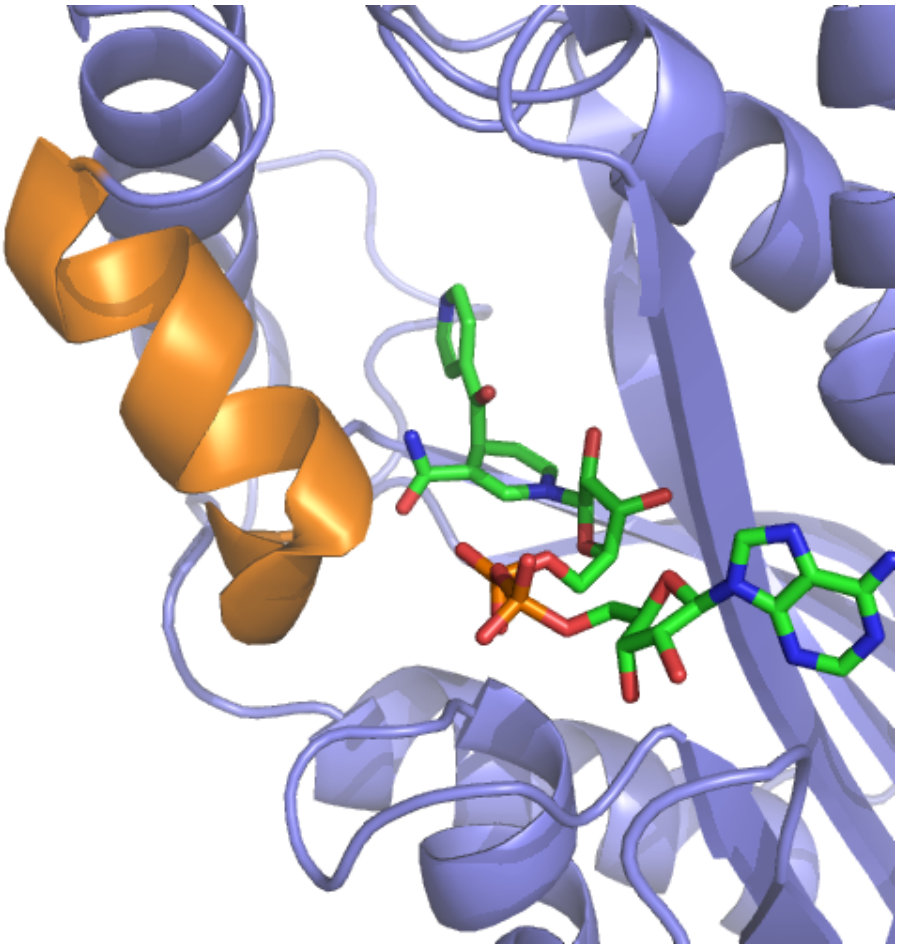

Figure 1.7: Structure of INH-NAD+ Bound to InhA. The ordered substrate binding loop is colored in orange (*42*). This figure was made using PyMOL, InhA (1ZID.pdb).

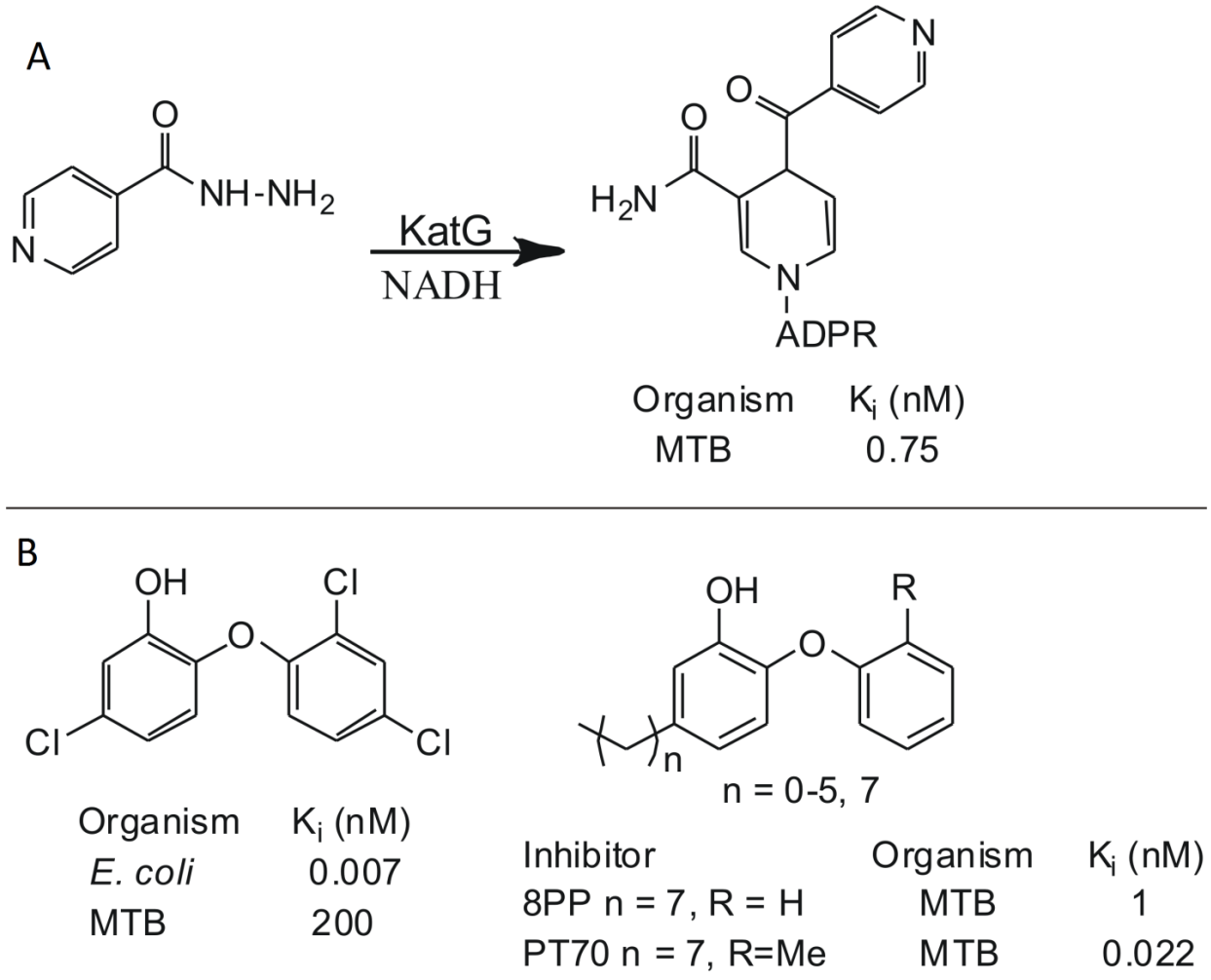

Figure 1.8: Inhibitors of FabI. A) Isoniazid activation by KatG B) Triclosan and structures of the alkyl diaryl ether inhibitors of FabI (*56*).

Triclosan

Triclosan, a broad spectrum antibiotic can be found in a variety of consumer products. Initially, it was considered and administered as a non specific biocide. More recently, the mechanism of action was discovered and it was shown to potently inhibit ER in many bacteria (*67-69*). These include *E. coli*, *Staphylococcus aureus (S. aureus)*

and *Plasmodium falciparum (P. falciparum) (70, 71)*. Structure activity relationship studies were performed in an effort to improve binding affinity and antibacterial efficiency involving the synthesis of a series of analogues with the triclosan pharmacaphore (*56, 72, 73*).

Surprisingly, triclosan is a picomolar inhibitor of ecFabI (K_i = 7 pM) but only weakly inhibits InhA (K_i = 0.2 µM) and exhibits modest bactericidal activity against MTb with an MIC value of 12.5 µg/mL (*74*). Upon evaluation of the crystal structure with triclosan bound to InhA, a hydrophobic binding pocket was discovered (**Figure 1.9A**), resulting in the synthesis of diaryl ether analogues designed to occupy the space left unoccupied by triclosan (**Figure 1.8B**) (*56*). This series of diaryl ethers were shown to inhibit InhA with nM efficacy and exhibit antibacterial activity against both sensitive and INH-resistant strains of MTb (MIC of 1-2 µg/mL) along with *S. aureus* and *Francisella tularensis (F. tularensis)* (*56, 70, 75*).

It should also be noted that the substrate binding loop is disordered in the crystal structure of triclosan bound to InhA and slow onset kinetics are not observed (**Figure 1.9B**). Conversely, slow onset kinetics are observed in the inhibition of InhA by one of the most effective diaryl ether analogues, PT70 (K_i^* = 22 pM) where the substrate binding loop of InhA is ordered as seen in the case of the INH-NAD^+ adduct bound to InhA (**Figure 1.9D**). Taken together, these data suggest the ordering of the substrate binding loop is associated with slow onset enzyme inhibition. PT70 also exhibits efficacy towards MTb with an MIC of 3 µg/mL.

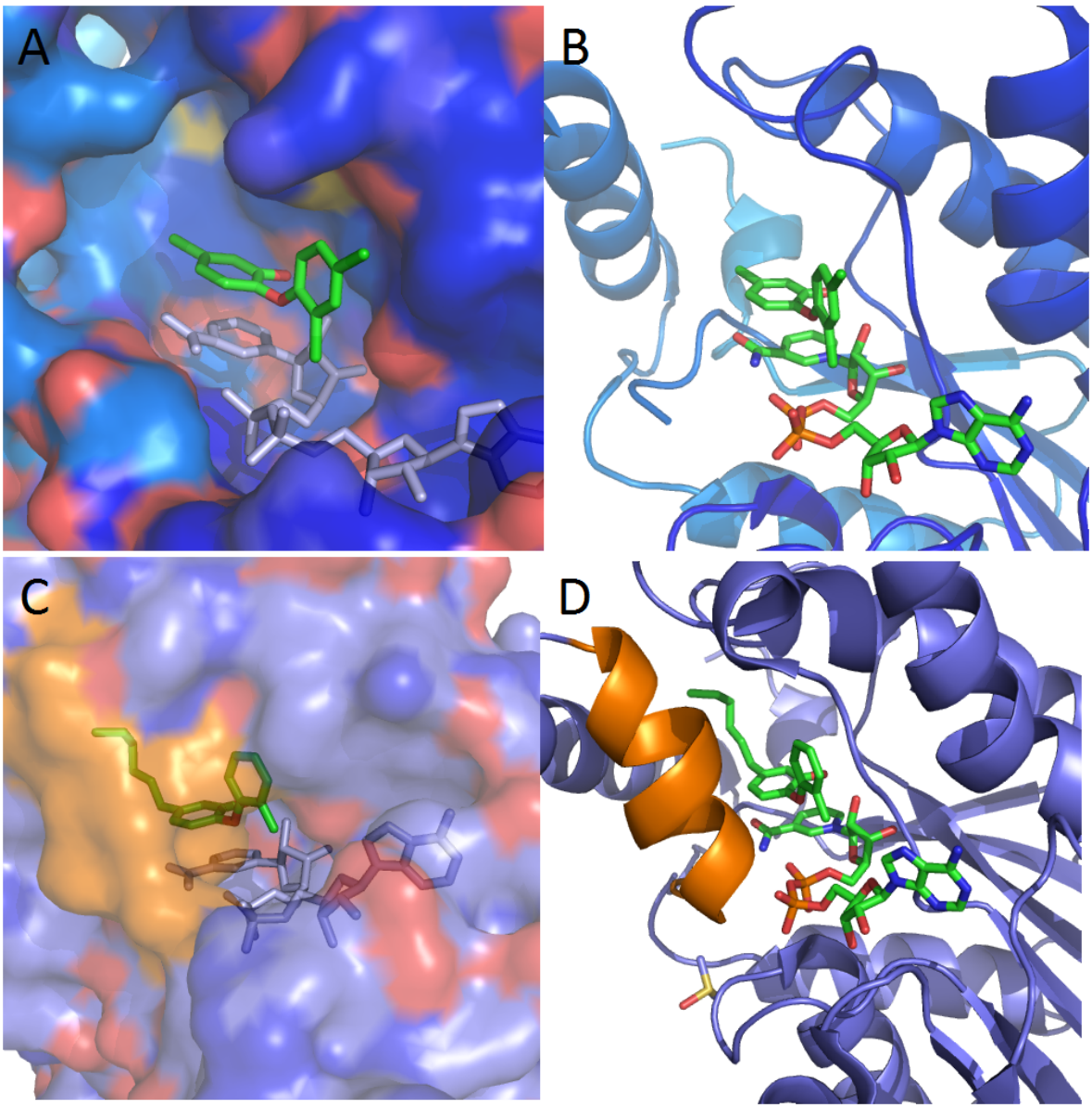

Figure 1.9: Structure of Triclosan and PT70 Bound to InhA. A, B) Triclosan and NAD^+ bound to InhA C, D) PT70 and NAD^+ bound to InhA . The dark blue color in the surface figures represents the electropositive portions, red- electronegative and light blue-neutral. This figure was made using PyMOL, Triclosan-InhA (2B35.pdb); PT70-InhA (2X22.pdb).

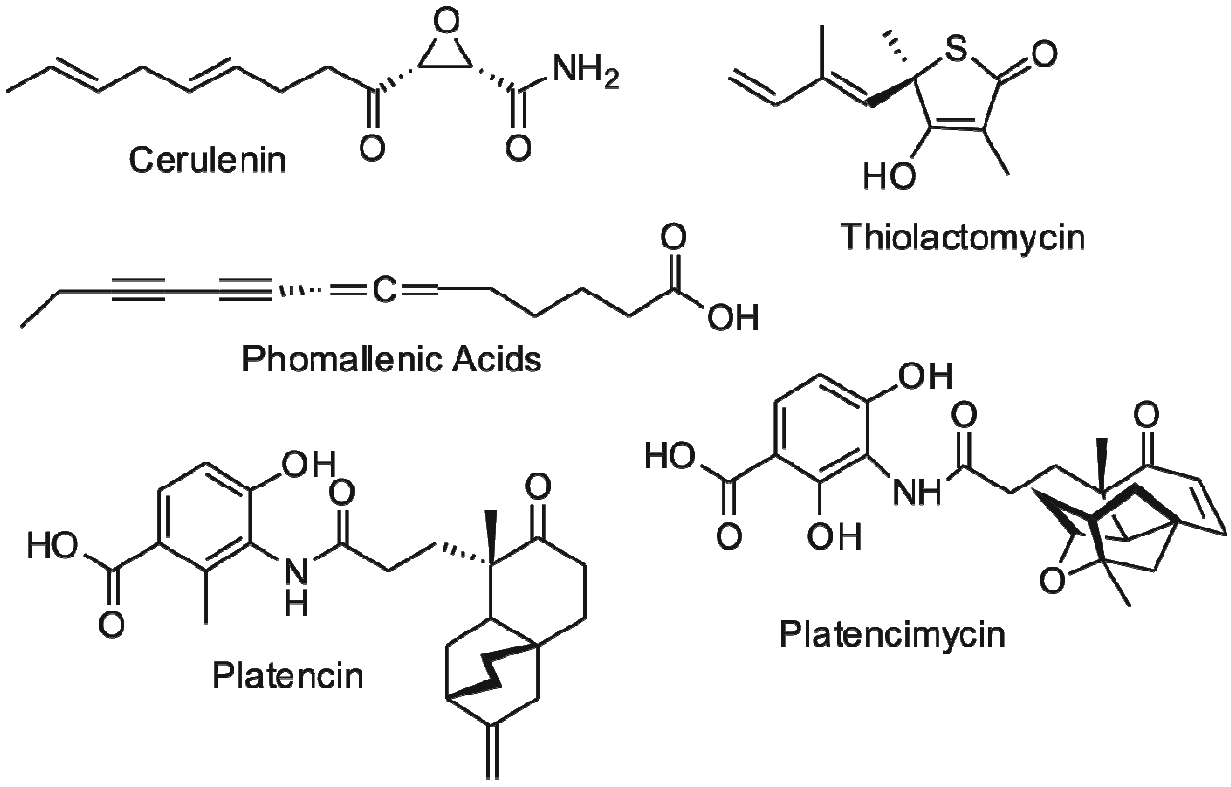

Figure 1.10: KAS Inhibitors.

KAS inhibitors

The currently established ketoacyl synthase inhibitors present a promising lead for the development of novel chemotherapeutics. Cerulenin, an antibacterial discovered in 1960, was originally shown to have antifungal activity. Studies of its mode of action have revealed irreversible inhibition with the active site cysteine in KAS enzymes and exhibited activity against both sensitive and INH-resistant strains of MTb with an MIC value of 2.5 μg/mL (*76, 77*). Unfortunately, the instability of the antibiotic along with its cross reactivity with the mammalian FASI pathway prevent its use in therapy as an

antimicrobial agent (*78*). Thiolactomycin (TLM) was discovered in 1982 and was quickly categorized as a non toxic antibacterial agent owing to its target specificity. TLM is a slow onset tight binding inhibitor of ecFabB and KasA (KASI) and a rapid reversible inhibitor of ecFabF, exhibiting activity against MTb with an MIC value of 12.4 µg/mL (*79*). It has the potential to serve as an antibacterial lead and therefore considerable chemical modifications have been made (*34, 80-87*). Phomallenic acids, platencin and platencimycin were more recently discovered by employing a new spin on whole-cell assays with high-throughput antisense technology. These inhibitors showed target selectivity for ecFabF and ecFabH in both biochemical and whole-cell assays and exhibited antibacterial activity against methicillin-resistant *S. aureus*, *Bacillus subtilis*, and *Haemophilus influenza* with MIC values ranging from 4-16 µg/mL. The antibiotics mentioned above along with other ecFabH and ecFabF/B inhibitors (*88-92*) offer immense opportunities towards the advancement of new antibiotics with novel modes of action.

Summary

TB is serious global health treat affecting 3 million people annually. The current drug regimen is long and has serious side effects leading to patient non compliance to the full course of the treatment. This coupled with drug regimen misuse or mismanagement has led to the emergence of drug resistance. Together, these problems emphasize the need for new novel chemotherapeutics.

The bacterial fatty acid biosynthesis (FASII) pathway is a promising target for antibacterial drug discovery and the current research is focused on elucidating the substrate specificity of the β-ketoacyl-ACP synthase (KAS) enzymes in this pathway, studying the interaction of current enzyme inhibitors with FASII components in whole cells and characterizing the binding interactions between the components of the FASII system. Identifying and characterizing protein-protein and protein-ligand interactions is an important step toward the development of new drugs. Experiments and results to this end are described in the following chapters.

References

1. Snider, D. E., Jr., and La Montagne, J. R. (1994) The neglected global tuberculosis problem: a report of the 1992 World Congress on Tuberculosis, *J Infect Dis 169*, 1189-1196.
2. Dye, C., Scheele, S., Dolin, P., Pathania, V., and Raviglione, M. C. (1999) Consensus statement. Global burden of tuberculosis: estimated incidence, prevalence, and mortality by country. WHO Global Surveillance and Monitoring Project, *JAMA 282*, 677-686.
3. Raviglione, M. C., Snider, D. E., Jr., and Kochi, A. (1995) Global epidemiology of tuberculosis. Morbidity and mortality of a worldwide epidemic, *JAMA 273*, 220-226.
4. Antonucci, G., Girardi, E., Raviglione, M. C., and Ippolito, G. (1995) Risk factors for tuberculosis in HIV-infected persons. A prospective cohort study. The Gruppo Italiano di Studio Tubercolosi e AIDS (GISTA), *JAMA 274*, 143-148.
5. Zink, A. R., Sola, C., Reischl, U., Grabner, W., Rastogi, N., Wolf, H., and Nerlich, A. G. (2003) Characterization of Mycobacterium tuberculosis complex DNAs from Egyptian mummies by spoligotyping, *J Clin Microbiol 41*, 359-367.
6. Schnappinger, D., Schoolnik, G. K., and Ehrt, S. (2006) Expression profiling of host pathogen interactions: how Mycobacterium tuberculosis and the macrophage adapt to one another, *Microbes Infect 8*, 1132-1140.
7. (2000) Diagnostic Standards and Classification of Tuberculosis in Adults and Children. This official statement of the American Thoracic Society and the Centers for Disease Control and Prevention was adopted by the ATS Board of

Directors, July 1999. This statement was endorsed by the Council of the Infectious Disease Society of America, September 1999, *Am J Respir Crit Care Med 161*, 1376-1395.

8. Sacchettini, J. C., Rubin, E. J., and Freundlich, J. S. (2008) Drugs versus bugs: in pursuit of the persistent predator Mycobacterium tuberculosis, *Nat Rev Microbiol 6*, 41-52.

9. Middlebrook, G. (1952) Sterilization of tubercle bacilli by isonicotinic acid hydrazide and the incidence of variants resistant to the drug in vitro, *Am Rev Tuberc 65*, 765-767.

10. Rawat, R., Whitty, A., and Tonge, P. J. (2003) The isoniazid-NAD adduct is a slow, tight-binding inhibitor of InhA, the Mycobacterium tuberculosis enoyl reductase: adduct affinity and drug resistance, *Proc Natl Acad Sci U S A 100*, 13881-13886.

11. Zhang, Y., and Mitchison, D. (2003) The curious characteristics of pyrazinamide: a review, *Int J Tuberc Lung Dis 7*, 6-21.

12. Zimhony, O., Cox, J. S., Welch, J. T., Vilcheze, C., and Jacobs, W. R., Jr. (2000) Pyrazinamide inhibits the eukaryotic-like fatty acid synthetase I (FASI) of Mycobacterium tuberculosis, *Nat Med 6*, 1043-1047.

13. Boshoff, H. I., Mizrahi, V., and Barry, C. E., 3rd. (2002) Effects of pyrazinamide on fatty acid synthesis by whole mycobacterial cells and purified fatty acid synthase I, *J Bacteriol 184*, 2167-2172.

14. Zhang, Y., Wade, M. M., Scorpio, A., Zhang, H., and Sun, Z. (2003) Mode of action of pyrazinamide: disruption of Mycobacterium tuberculosis membrane

transport and energetics by pyrazinoic acid, *J Antimicrob Chemother 52*, 790-795.

15. Takayama, K., and Kilburn, J. O. (1989) Inhibition of synthesis of arabinogalactan by ethambutol in Mycobacterium smegmatis, *Antimicrob Agents Chemother 33*, 1493-1499.
16. Yarbrough, L. R., Wu, F. Y., and Wu, C. W. (1976) Molecular mechanism of the rifampicin -RNA polymerase interaction, *Biochemistry 15*, 2669-2676.
17. CDC. (2003) Treatment of Tuberculosis, *MMWR 52(RR11)*, 1-77.
18. Lim, S. A. (2006) Ethambutol-associated optic neuropathy, *Ann Acad Med Singapore 35*, 274-278.
19. Lopez-Cortes, L. F., Ruiz-Valderas, R., Viciana, P., Alarcon-Gonzalez, A., Gomez-Mateos, J., Leon-Jimenez, E., Sarasanacenta, M., Lopez-Pua, Y., and Pachon, J. (2002) Pharmacokinetic interactions between efavirenz and rifampicin in HIV-infected patients with tuberculosis, *Clin Pharmacokinet 41*, 681-690.
20. Addington, W. W. (1979) The side effects and interactions of antituberculosis drugs, *Chest 76*, 782-784.
21. Gustafson, J. E., Candelaria, P. V., Fisher, S. A., Goodridge, J. P., Lichocik, T. M., McWilliams, T. M., Price, C. T., O'Brien, F. G., and Grubb, W. B. (1999) Growth in the presence of salicylate increases fluoroquinolone resistance in Staphylococcus aureus, *Antimicrob Agents Chemother 43*, 990-992.
22. Lemaitre, N., Sougakoff, W., Truffot-Pernot, C., and Jarlier, V. (1999) Characterization of new mutations in pyrazinamide-resistant strains of Mycobacterium tuberculosis and identification of conserved regions important for

the catalytic activity of the pyrazinamidase PncA, *Antimicrob Agents Chemother 43*, 1761-1763.

23. Addington, W. W. (1979) Patient compliance: the most serious remaining problem in the control of tuberculosis in the United States, *Chest 76*, 741-743.

24. Frieden, T. R., Sterling, T., Pablos-Mendez, A., Kilburn, J. O., Cauthen, G. M., and Dooley, S. W. (1993) The emergence of drug-resistant tuberculosis in New York City, *N Engl J Med 328*, 521-526.

25. Hayward, A. C., and Coker, R. J. (2000) Could a tuberculosis epidemic occur in London as it did in New York?, *Emerg Infect Dis 6*, 12-16.

26. Kwon, H. H., Tomioka, H., and Saito, H. (1995) Distribution and characterization of beta-lactamases of mycobacteria and related organisms, *Tuber Lung Dis 76*, 141-148.

27. Liu, J., Takiff, H. E., and Nikaido, H. (1996) Active efflux of fluoroquinolones in Mycobacterium smegmatis mediated by LfrA, a multidrug efflux pump, *J Bacteriol 178*, 3791-3795.

28. Cox, H. S., Morrow, M., and Deutschmann, P. W. (2008) Long term efficacy of DOTS regimens for tuberculosis: systematic review, *BMJ 336*, 484-487.

29. Heath, R. J., and Rock, C. O. (2004) Fatty acid biosynthesis as a target for novel antibacterials, *Curr Opin Investig Drugs 5*, 146-153.

30. Liu, J., Shworak, N. W., Fritze, L. M., Edelberg, J. M., and Rosenberg, R. D. (1996) Purification of heparan sulfate D-glucosaminyl 3-O-sulfotransferase, *J Biol Chem 271*, 27072-27082.

31. Barry, C. E., 3rd, Lee, R. E., Mdluli, K., Sampson, A. E., Schroeder, B. G., Slayden, R. A., and Yuan, Y. (1998) Mycolic acids: structure, biosynthesis and physiological functions, *Prog Lipid Res 37*, 143-179.

32. Smith, I. (2003) Mycobacterium tuberculosis pathogenesis and molecular determinants of virulence, *Clin Microbiol Rev 16*, 463-496.

33. Brennan, P. J., and Nikaido, H. (1995) The envelope of mycobacteria, *Annu Rev Biochem 64*, 29-63.

34. Kremer, L., Douglas, J. D., Baulard, A. R., Morehouse, C., Guy, M. R., Alland, D., Dover, L. G., Lakey, J. H., Jacobs, W. R., Jr., Brennan, P. J., Minnikin, D. E., and Besra, G. S. (2000) Thiolactomycin and related analogues as novel anti-mycobacterial agents targeting KasA and KasB condensing enzymes in Mycobacterium tuberculosis, *J Biol Chem 275*, 16857-16864.

35. Smith, S., Witkowski, A., and Joshi, A. K. (2003) Structural and functional organization of the animal fatty acid synthase, *Prog Lipid Res 42*, 289-317.

36. Kremer, L., Dover, L. G., Carrere, S., Nampoothiri, K. M., Lesjean, S., Brown, A. K., Brennan, P. J., Minnikin, D. E., Locht, C., and Besra, G. S. (2002) Mycolic acid biosynthesis and enzymic characterization of the beta-ketoacyl-ACP synthase A-condensing enzyme from Mycobacterium tuberculosis, *Biochem J 364*, 423-430.

37. Lu, Y. J., Zhang, Y. M., and Rock, C. O. (2004) Product diversity and regulation of type II fatty acid synthases, *Biochem Cell Biol 82*, 145-155.

38. Campbell, J. W., and Cronan, J. E., Jr. (2001) Bacterial fatty acid biosynthesis: targets for antibacterial drug discovery, *Annu Rev Microbiol 55*, 305-332.

39. Banerjee, A., Dubnau, E., Quemard, A., Balasubramanian, V., Um, K. S., Wilson, T., Collins, D., de Lisle, G., and Jacobs, W. R., Jr. (1994) inhA, a gene encoding a target for isoniazid and ethionamide in Mycobacterium tuberculosis, *Science 263*, 227-230.

40. Dessen, A., Quemard, A., Blanchard, J. S., Jacobs, W. R., Jr., and Sacchettini, J. C. (1995) Crystal structure and function of the isoniazid target of Mycobacterium tuberculosis, *Science 267*, 1638-1641.

41. Quemard, A., Sacchettini, J. C., Dessen, A., Vilcheze, C., Bittman, R., Jacobs, W. R., Jr., and Blanchard, J. S. (1995) Enzymatic characterization of the target for isoniazid in Mycobacterium tuberculosis, *Biochemistry 34*, 8235-8241.

42. Rozwarski, D. A., Grant, G. A., Barton, D. H., Jacobs, W. R., Jr., and Sacchettini, J. C. (1998) Modification of the NADH of the isoniazid target (InhA) from Mycobacterium tuberculosis, *Science 279*, 98-102.

43. Mdluli, K., Slayden, R. A., Zhu, Y., Ramaswamy, S., Pan, X., Mead, D., Crane, D. D., Musser, J. M., and Barry, C. E., 3rd. (1998) Inhibition of a Mycobacterium tuberculosis beta-ketoacyl ACP synthase by isoniazid, *Science 280*, 1607-1610.

44. Magnuson, K., Jackowski, S., Rock, C. O., and Cronan, J. E., Jr. (1993) Regulation of fatty acid biosynthesis in Escherichia coli, *Microbiol Rev 57*, 522-542.

45. Marrakchi, H., Zhang, Y. M., and Rock, C. O. (2002) Mechanistic diversity and regulation of Type II fatty acid synthesis, *Biochem Soc Trans 30*, 1050-1055.

46. White, S. W., Zheng, J., Zhang, Y. M., and Rock. (2005) The structural biology of type II fatty acid biosynthesis, *Annu Rev Biochem 74*, 791-831.

47. Price, A. C., Zhang, Y. M., Rock, C. O., and White, S. W. (2001) Structure of beta-ketoacyl-[acyl carrier protein] reductase from Escherichia coli: negative cooperativity and its structural basis, *Biochemistry 40*, 12772-12781.

48. Silva, R. G., de Carvalho, L. P., Blanchard, J. S., Santos, D. S., and Basso, L. A. (2006) Mycobacterium tuberculosis beta-ketoacyl-acyl carrier protein (ACP) reductase: kinetic and chemical mechanisms, *Biochemistry 45*, 13064-13073.

49. Kimber, M. S., Martin, F., Lu, Y., Houston, S., Vedadi, M., Dharamsi, A., Fiebig, K. M., Schmid, M., and Rock, C. O. (2004) The structure of (3R)-hydroxyacyl-acyl carrier protein dehydratase (FabZ) from Pseudomonas aeruginosa, *J Biol Chem 279*, 52593-52602.

50. Leesong, M., Henderson, B. S., Gillig, J. R., Schwab, J. M., and Smith, J. L. (1996) Structure of a dehydratase-isomerase from the bacterial pathway for biosynthesis of unsaturated fatty acids: two catalytic activities in one active site, *Structure 4*, 253-264.

51. Roujeinikova, A., Sedelnikova, S., de Boer, G. J., Stuitje, A. R., Slabas, A. R., Rafferty, J. B., and Rice, D. W. (1999) Inhibitor binding studies on enoyl reductase reveal conformational changes related to substrate recognition, *J Biol Chem 274*, 30811-30817.

52. Edwards, P., Nelsen, J. S., Metz, J. G., and Dehesh, K. (1997) Cloning of the fabF gene in an expression vector and in vitro characterization of recombinant fabF and fabB encoded enzymes from Escherichia coli, *FEBS Lett 402*, 62-66.

53. Schaeffer, M. L., Agnihotri, G., Volker, C., Kallender, H., Brennan, P. J., and Lonsdale, J. T. (2001) Purification and biochemical characterization of the

Mycobacterium tuberculosis beta-ketoacyl-acyl carrier protein synthases KasA and KasB, *J Biol Chem 276*, 47029-47037.

54. Olsen, J. G., Kadziola, A., von Wettstein-Knowles, P., Siggaard-Andersen, M., and Larsen, S. (2001) Structures of beta-ketoacyl-acyl carrier protein synthase I complexed with fatty acids elucidate its catalytic machinery, *Structure 9*, 233-243.

55. Bergler, H., Fuchsbichler, S., Hogenauer, G., and Turnowsky, F. (1996) The enoyl-[acyl-carrier-protein] reductase (FabI) of Escherichia coli, which catalyzes a key regulatory step in fatty acid biosynthesis, accepts NADH and NADPH as cofactors and is inhibited by palmitoyl-CoA, *Eur J Biochem 242*, 689-694.

56. Sullivan, T. J., Truglio, J. J., Boyne, M. E., Novichenok, P., Zhang, X., Stratton, C. F., Li, H. J., Kaur, T., Amin, A., Johnson, F., Slayden, R. A., Kisker, C., and Tonge, P. J. (2006) High affinity InhA inhibitors with activity against drug-resistant strains of Mycobacterium tuberculosis, *ACS Chem Biol 1*, 43-53.

57. Lai, C. Y., and Cronan, J. E. (2003) Beta-ketoacyl-acyl carrier protein synthase III (FabH) is essential for bacterial fatty acid synthesis, *J Biol Chem 278*, 51494-51503.

58. Sassetti, C. M., and Rubin, E. J. (2003) Genetic requirements for mycobacterial survival during infection, *Proc Natl Acad Sci U S A 100*, 12989-12994.

59. Bhatt, A., Kremer, L., Dai, A. Z., Sacchettini, J. C., and Jacobs, W. R., Jr. (2005) Conditional depletion of KasA, a key enzyme of mycolic acid biosynthesis, leads to mycobacterial cell lysis, *J Bacteriol 187*, 7596-7606.

60. Parish, T., Roberts, G., Laval, F., Schaeffer, M., Daffe, M., and Duncan, K. (2007) Functional complementation of the essential gene fabG1 of

Mycobacterium tuberculosis by Mycobacterium smegmatis fabG but not Escherichia coli fabG, *J Bacteriol 189*, 3721-3728.

61. Silva, R. G., Rosado, L. A., Santos, D. S., and Basso, L. A. (2008) Mycobacterium tuberculosis beta-ketoacyl-ACP reductase: alpha-secondary kinetic isotope effects and kinetic and equilibrium mechanisms of substrate binding, *Arch Biochem Biophys 471*, 1-10.
62. Khandekar, S. S., Daines, R. A., and Lonsdale, J. T. (2003) Bacterial beta-ketoacyl-acyl carrier protein synthases as targets for antibacterial agents, *Curr Protein Pept Sci 4*, 21-29.
63. Zhang, Y. M., White, S. W., and Rock, C. O. (2006) Inhibiting bacterial fatty acid synthesis, *J Biol Chem 281*, 17541-17544.
64. Baldock, C., Rafferty, J. B., Sedelnikova, S. E., Baker, P. J., Stuitje, A. R., Slabas, A. R., Hawkes, T. R., and Rice, D. W. (1996) A mechanism of drug action revealed by structural studies of enoyl reductase, *Science 274*, 2107-2110.
65. Argyrou, A., Jin, L., Siconilfi-Baez, L., Angeletti, R. H., and Blanchard, J. S. (2006) Proteome-wide profiling of isoniazid targets in Mycobacterium tuberculosis, *Biochemistry 45*, 13947-13953.
66. Ramaswamy, S. V., Reich, R., Dou, S. J., Jasperse, L., Pan, X., Wanger, A., Quitugua, T., and Graviss, E. A. (2003) Single nucleotide polymorphisms in genes associated with isoniazid resistance in Mycobacterium tuberculosis, *Antimicrob Agents Chemother 47*, 1241-1250.

67. McMurry, L. M., Oethinger, M., and Levy, S. B. (1998) Triclosan targets lipid synthesis, *Nature 394*, 531-532.

68. Heath, R. J., and Rock, C. O. (1996) Inhibition of beta-ketoacyl-acyl carrier protein synthase III (FabH) by acyl-acyl carrier protein in Escherichia coli, *J Biol Chem 271*, 10996-11000.

69. Levy, C. W., Roujeinikova, A., Sedelnikova, S., Baker, P. J., Stuitje, A. R., Slabas, A. R., Rice, D. W., and Rafferty, J. B. (1999) Molecular basis of triclosan activity, *Nature 398*, 383-384.

70. Xu, H., Sullivan, T. J., Sekiguchi, J., Kirikae, T., Ojima, I., Stratton, C. F., Mao, W., Rock, F. L., Alley, M. R., Johnson, F., Walker, S. G., and Tonge, P. J. (2008) Mechanism and inhibition of saFabI, the enoyl reductase from Staphylococcus aureus, *Biochemistry 47*, 4228-4236.

71. Chhibber, M., Kumar, G., Parasuraman, P., Ramya, T. N., Surolia, N., and Surolia, A. (2006) Novel diphenyl ethers: design, docking studies, synthesis and inhibition of enoyl ACP reductase of Plasmodium falciparum and Escherichia coli, *Bioorg Med Chem 14*, 8086-8098.

72. Freundlich, J. S., Yu, M., Lucumi, E., Kuo, M., Tsai, H. C., Valderramos, J. C., Karagyozov, L., Jacobs, W. R., Jr., Schiehser, G. A., Fidock, D. A., Jacobus, D. P., and Sacchettini, J. C. (2006) Synthesis and biological activity of diaryl ether inhibitors of malarial enoyl acyl carrier protein reductase. Part 2: 2'-substituted triclosan derivatives, *Bioorg Med Chem Lett 16*, 2163-2169.

73. Perozzo, R., Kuo, M., Sidhu, A. S., Valiyaveettil, J. T., Bittman, R., Jacobs, W. R., Jr., Fidock, D. A., and Sacchettini, J. C. (2002) Structural elucidation of the

specificity of the antibacterial agent triclosan for malarial enoyl acyl carrier protein reductase, *J Biol Chem 277*, 13106-13114.

74. Parikh, S. L., Xiao, G., and Tonge, P. J. (2000) Inhibition of InhA, the enoyl reductase from Mycobacterium tuberculosis, by triclosan and isoniazid, *Biochemistry 39*, 7645-7650.

75. Lu, H., England, K., am Ende, C., Truglio, J. J., Luckner, S., Reddy, B. G., Marlenee, N. L., Knudson, S. E., Knudson, D. L., Bowen, R. A., Kisker, C., Slayden, R. A., and Tonge, P. J. (2009) Slow-onset inhibition of the FabI enoyl reductase from francisella tularensis: residence time and in vivo activity, *ACS Chem Biol 4*, 221-231.

76. Price, A. C., Choi, K. H., Heath, R. J., Li, Z., White, S. W., and Rock, C. O. (2001) Inhibition of beta-ketoacyl-acyl carrier protein synthases by thiolactomycin and cerulenin. Structure and mechanism, *J Biol Chem 276*, 6551-6559.

77. Rastogi, N., Goh, K. S., Horgen, L., and Barrow, W. W. (1998) Synergistic activities of antituberculous drugs with cerulenin and trans-cinnamic acid against Mycobacterium tuberculosis, *FEMS Immunol Med Microbiol 21*, 149-157.

78. Omura, S. (1981) Cerulenin, *Methods Enzymol 72*, 520-532.

79. Machutta, C. A., Bommineni, G. R., Luckner, S. R., Kapilashrami, K., Ruzsicska, B., Simmerling, C., Kisker, C., and Tonge, P. J. (2010) Slow onset inhibition of bacterial beta-ketoacyl-acyl carrier protein synthases by thiolactomycin, *J Biol Chem 285*, 6161-6169.

80. Douglas, J. D., Senior, S. J., Morehouse, C., Phetsukiri, B., Campbell, I. B., Besra, G. S., and Minnikin, D. E. (2002) Analogues of thiolactomycin: potential drugs with enhanced anti-mycobacterial activity, *Microbiology 148*, 3101-3109.

81. He, X., Reeve, A. M., Desai, U. R., Kellogg, G. E., and Reynolds, K. A. (2004) 1,2-dithiole-3-ones as potent inhibitors of the bacterial 3-ketoacyl acyl carrier protein synthase III (FabH), *Antimicrob Agents Chemother 48*, 3093-3102.

82. Jones, S. M., Urch, J. E., Brun, R., Harwood, J. L., Berry, C., and Gilbert, I. H. (2004) Analogues of thiolactomycin as potential anti-malarial and anti-trypanosomal agents, *Bioorg Med Chem 12*, 683-692.

83. Kamal, A., Shaik, A. A., Sinha, R., Yadav, J. S., and Arora, S. K. (2005) Antitubercular agents. Part 2: new thiolactomycin analogues active against Mycobacterium tuberculosis, *Bioorg Med Chem Lett 15*, 1927-1929.

84. McFadden, J. M., Medghalchi, S. M., Thupari, J. N., Pinn, M. L., Vadlamudi, A., Miller, K. I., Kuhajda, F. P., and Townsend, C. A. (2005) Application of a flexible synthesis of (5R)-thiolactomycin to develop new inhibitors of type I fatty acid synthase, *J Med Chem 48*, 946-961.

85. Sakya, S. M., Suarez-Contreras, M., Dirlam, J. P., O'Connell, T. N., Hayashi, S. F., Santoro, S. L., Kamicker, B. J., George, D. M., and Ziegler, C. B. (2001) Synthesis and structure-activity relationships of thiotetronic acid analogues of thiolactomycin, *Bioorg Med Chem Lett 11*, 2751-2754.

86. Senior, S. J., Illarionov, P. A., Gurcha, S. S., Campbell, I. B., Schaeffer, M. L., Minnikin, D. E., and Besra, G. S. (2004) Acetylene-based analogues of

thiolactomycin, active against Mycobacterium tuberculosis mtFabH fatty acid condensing enzyme, *Bioorg Med Chem Lett 14*, 373-376.

87. Senior, S. J., Illarionov, P. A., Gurcha, S. S., Campbell, I. B., Schaeffer, M. L., Minnikin, D. E., and Besra, G. S. (2003) Biphenyl-based analogues of thiolactomycin, active against Mycobacterium tuberculosis mtFabH fatty acid condensing enzyme, *Bioorg Med Chem Lett 13*, 3685-3688.

88. Daines, R. A., Pendrak, I., Sham, K., Van Aller, G. S., Konstantinidis, A. K., Lonsdale, J. T., Janson, C. A., Qiu, X., Brandt, M., Khandekar, S. S., Silverman, C., and Head, M. S. (2003) First X-ray cocrystal structure of a bacterial FabH condensing enzyme and a small molecule inhibitor achieved using rational design and homology modeling, *J Med Chem 46*, 5-8.

89. Herath, K. B., Jayasuriya, H., Guan, Z., Schulman, M., Ruby, C., Sharma, N., MacNaul, K., Menke, J. G., Kodali, S., Galgoci, A., Wang, J., and Singh, S. B. (2005) Anthrabenzoxocinones from Streptomyces sp. as liver X receptor ligands and antibacterial agents, *J Nat Prod 68*, 1437-1440.

90. Khandekar, S. S., Gentry, D. R., Van Aller, G. S., Warren, P., Xiang, H., Silverman, C., Doyle, M. L., Chambers, P. A., Konstantinidis, A. K., Brandt, M., Daines, R. A., and Lonsdale, J. T. (2001) Identification, substrate specificity, and inhibition of the Streptococcus pneumoniae beta-ketoacyl-acyl carrier protein synthase III (FabH), *J Biol Chem 276*, 30024-30030.

91. Kodali, S., Galgoci, A., Young, K., Painter, R., Silver, L. L., Herath, K. B., Singh, S. B., Cully, D., Barrett, J. F., Schmatz, D., and Wang, J. (2005) Determination of

selectivity and efficacy of fatty acid synthesis inhibitors, *J Biol Chem 280*, 1669-1677.

92. Young, K., Jayasuriya, H., Ondeyka, J. G., Herath, K., Zhang, C., Kodali, S., Galgoci, A., Painter, R., Brown-Driver, V., Yamamoto, R., Silver, L. L., Zheng, Y., Ventura, J. I., Sigmund, J., Ha, S., Basilio, A., Vicente, F., Tormo, J. R., Pelaez, F., Youngman, P., Cully, D., Barrett, J. F., Schmatz, D., Singh, S. B., and Wang, J. (2006) Discovery of FabH/FabF inhibitors from natural products, *Antimicrob Agents Chemother 50*, 519-526.

Chapter II: Substrate Specificity Between *β*-ketoacyl ACP Synthases

β-ketoacyl ACP Synthase

The formation of a carbon–carbon bond is a crucial step in the biosynthesis of fatty acids, steroids and polyketides. A class of enzymes known as condensing enzymes which belong to the thiolase superfamily are responsible for the formation of a carbon–carbon bond via a Claisen condensation reaction (*1, 2*). Although the enzymes of the thiolase superfamily lack sequence homology, they share a similar three dimensional fold known as the thiolase fold, which was first discovered in *Saccharomyces cerevisiae (3, 4).* Crystal structures of condensing enzymes from *E. coli* and MTb have recently been determined (*5-8*). They indicate a clear structural relationship which encompasses a similar dimeric structure and active site architecture. The active site is buried and only accessible through a hydrophilic tunnel that accommodates the 4′-phosphopantetheine (PPant) prosthetic group of ACP (*6, 7*)). Each monomer has two halves, the N-terminal and the C-terminal half, each having the same βαβαβαββ topology. **Figure 2.1** shows KasA (MTb KASI) emphasizing the conserved catalytic triad Cys-His-His, the conserved catalytic Nα3 helix and the conserved substrate binding loops at Cβ4-Cβ5 and Cβ3-Cα3 (*1*).

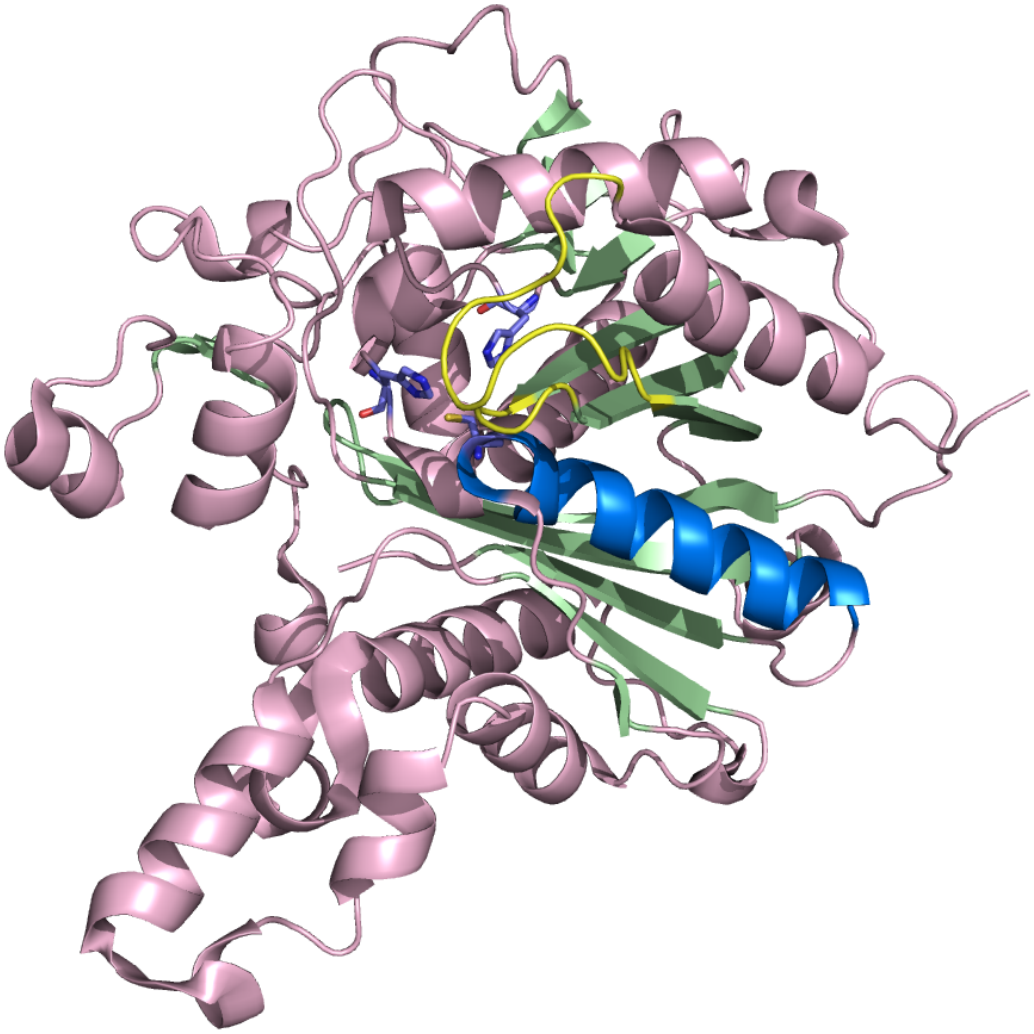

Figure 2.1*:* Structure of KasA. Apo-KasA showing the conserved βαβαβαββ topology with the β-sheets colored in green and helices in pink. Catalytic triad and catalytic helix Nα3 are colored in blue with the conserved thiolase superfamily substrate binding loops in yellow. This figure was made using PyMOL, 2WGD.pdb

The enzymes of the thiolase superfamily can be partitioned into the following categories; the ketoacyl synthases (KAS), the polyketide synthases, and the biosynthetic and degradative thiolases (*1*). The KAS enzyme subgroup is responsible for the synthesis of fatty acids and is the main topic of our drug discovery project in this chapter. Two of these synthases are elongation condensing enzymes (KASI and KASII) which rely on ACP for efficient catalysis. The third class, KASIII, functions as the initiation condensing enzyme which catalyses the first step in the pathway and thus directly regulates the rate of fatty acid synthesis (*9-12*). Unlike KASI and KASII enzymes which utilize an acyl-ACP, KASIII uses acyl-CoA as a donor (*9, 10, 13, 14*) . Although the β-ketoacyl synthases have similar three dimensional structures due to their high degree of conservation, the residues that comprise their active site triad are different. This is where KASIII is further distinguished by a His-Asn-Cys (*2*) catalytic triad as opposed to the His-His-Cys triad in KASI and KASII (*15*).

Catalytic Mechanism of KAS

The KAS enzymes perform a condensation reaction between an acyl primer and malonyl-ACP, yielding a β-ketoacyl-ACP that is lengthened by two carbon units. This reaction occurs via a two step ping-pong mechanism which starts with an acyl group transferred to an active site cysteine via a carrier molecule. After dissociation of the carrier molecule, malonyl-ACP reacts with the acylated enzyme followed by product release **(Figure 2.2).**

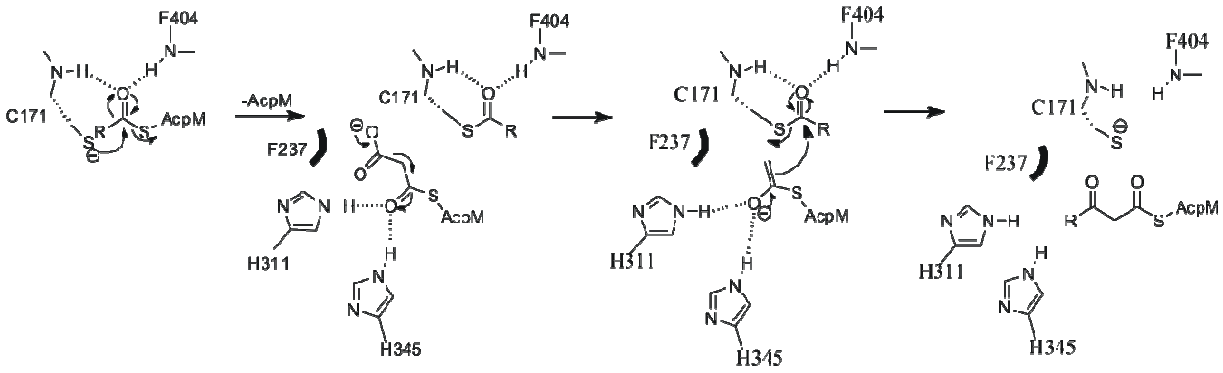

Figure 2.2: Ping-Pong Catalytic Mechanism for KasA.

In the first step, Cys 171 acts as nucleophile and attacks the carbonyl carbon of acyl-AcpM yielding the acyl enzyme intermediate. This is followed by the decarboxylation of malonyl-AcpM and subsequent condensation with the acyl group, which is promoted by two conserved histidines (H311, H345). The conserved phenylalanine (F237) shown is proposed to destabilize the malonate anion, and thus encourage decarboxylation.

An α-helix dipole aids in the initial acylation step that attaches the acyl primer to the active site cysteine (*16, 17*). The high reactivity of this cysteine is a result of its location at the N terminus of helix Nα3 (*18-20*). The electrostatics of this helix decreases the pKa of the cysteine sulfur, thus increasing its nucleophilicity. The decarboylation of malonyl-ACP is stabilized by the formation of two adjacent hydrogen bonds to the thioester carbonyl of the approaching malonyl-ACP. The hydrogen bond donors are two histidines in KASI/KASII and a histidine and an asparagine in KASII (*5, 6*). The subsequent nucleophilic attack of the acyl-enzyme thioester and carbon-carbon bond formation is facilitated through the stabilization of the negative charge in the tetrahedral

intermediate by an oxyanion hole formed by the backbone amides of C171 and F404 (C163 and F392 in *E. coli* FabB/FabF).

KAS Essentiality

The initiation and elongation steps for the fatty acid biosynthesis pathway have been extensively studied. The KAS enzymes involved in these steps have proved essential in both pathogenic and non pathogenic bacteria. The KASI and KASII enzymes in (MTb) carry the designation KasA and KasB, where the corresponding enzymes in *E. coli* are known as FabB (ecFabB) and FabF (ecFabF) (*21, 22*).

ecFabB serves two roles, one in the synthesis of saturated fatty acid biosynthesis and secondly, is required for a critical step in the elongation of unsaturated fatty acids. The essentiality of ecFabB was demonstrated through a knockout experiment in addition to the development of ecFabB null mutants which were only able to grow when supplemented with exogenous unsaturated fatty acids (*23-25*). ecFabF knockouts result in an *E. coli* mutant strain that is incapable of synthesizing C18:1, resulting in the inability to thermally regulate the fatty acid composition (*25, 26*).

KasA essentiality was established by a conditional depletion experiment where the absence of the enzyme proved bactericidal (*27*). In this study, a new method was developed by Jacobs *et al.*, CESTET or Conditional Expression and Specialized Transduction Essentiality Test, to verify the importance of KasA (*27*). CESTET utilizes conditional gene expression (where expression is dependent on an external stimulus) with specialized transduction (transfer of a specific segment of DNA). This technique successfully produced conditional null *kasA* mutants by utilizing an acetamidase

promoter to express KasA during transductant generating experiments, where the depletion of KasA was proven to be bactericidal. A variety of KAS inhibitors have been developed, with the most promising lead compound TLM exhibiting antibacterial activity against MTb with an MIC value of 12.4 µg/mL, (*28-30*) further confirming its essentiality thus making it an attractive and selective target for the development of new novel chemotherapeutics.

Acyl Carrier Protein (ACP)

ACPs are highly conserved, small acidic proteins that are involved in many biosynthetic pathways, including, fatty acid synthesis (FAS), lipopolysaccharide synthesis and polyketide synthesis (*31-35*). In these pathways, ACP acts as a shuttle that immobilizes fatty acid intermediates for efficient entrance into active sites.

Most bacteria and plants possess both FASI and FASII systems. In FASI, ACP is part of a single multidomain protein, as opposed to FASII, where ACP is a discrete protein. ACP is responsible for shuttling the growing fatty acid chain between a collection of enzymes during fatty acid elongation and modification. The functional form of ACP contains a PPant arm that carries the growing fatty acid chain via a thioester linkage. This post translational modification is carried out by the holo-ACP synthase, AcpS, which covalently attaches a PPant moiety of CoA to the hydroxyl oxygen of a highly conserved serine on ACP via a phosphodiester bond (*36, 37*).

Crystal structures have been solved of many FASII ACPs in all three biological relevant forms, apo-, holo, and acyl (*38-47*). Most ACPs not only share high sequence homology, but also structural similarities comprising a group of four α-helices with the

PPant chain attached to the N-terminus of α-helix 2. ACP flexibility in solution enables it to either tuck the growing fatty acyl chain into its hydrophobic core or deliver it to enzymes for further modification. More specifically, recent studies discovered that ACP binds the fatty acid in the middle of the characteristic helices **(Figure 2.3)** (*44, 45, 48, 49*). These investigations also revealed a conformational change or remodeling of the binding pocket in order to accommodate a variety of fatty acyl intermediates.

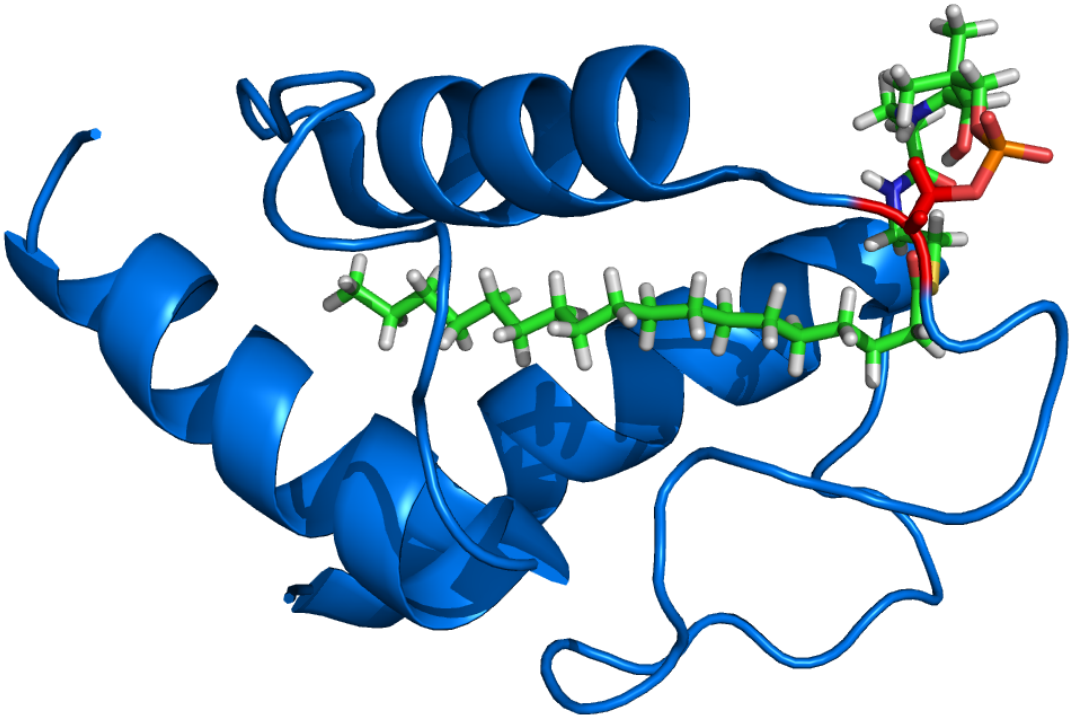

Figure 2.3: **Structure of ACP with Stearic Acid Bound.** ACP showing the position of a stearic fatty acyl chain which is bound in the middle of the helices. The cognate serine is colored in red, and attached to the PPant chain through a thioester linkage. This figure was made using PyMOL, 2FVA.pdb

In general, ACP dependent enzymes interact with the conserved α-helix 2, which has been denoted the recognition helix. Through mutagenesis and NMR experiments,

Rock *et al* demonstrated that conserved acidic residues of α-helix 2 (E41, E48) and basic residues (R129, R172) on the surface of the β-ketoacyl-ACP reductase (FabG) were important for binding and recognition (*50*). In addition, computational docking studies were performed which implicated a basic patch close to the active site of ecFabH as the binding site for α-helix 2. These studies were supported by kinetic analysis, direct binding experiments and mutagenesis where mutations of either basic residues of ecFabH or acidic residues in α-helix 2 resulted in decreased affinity for the binding partner (*51*). The clarification of these enzyme-substrate interactions is a vital step towards the development of new antimicrobial drugs.

Minimal Peptide Carrier Protein (PCP) or ACP Fragment Required for Recognition

More recently, Walsh and coworkers sought out to determine the shortest peptide carrier protein tag that could serve as a surrogate substrate for both AcpS and the *Bacillus subtilis* phosphopantethenyl transferase, Sfp. Through a phage display peptide library, a twelve residue fragment (GDSLDMLEWSLM) was discovered that was efficiently accepted as a substrate for post translational modification. The conserved serine the PPant chain attaches to is underlined and the residues colored in red were identified through NMR as key residues specifically interacting with AcpS. This led to the design of an eight residue fragment containing 5 of the 6 key residues resulting in a minimal fragment capable of efficient post translational phosphopantetheinylation (*52-54*).

Substrate Specificity of KAS

While the KAS enzyme(s) involved in fatty acid elongation (KASI and KASII) utilize ACP-based substrates, the priming KAS enzyme (KASIII) is initially acylated by an acyl-CoA substrate. In order to compare and contrast the specificity of KASI/II and KASIII for the substrate carrier, we have synthesized substrates based on phosphopantetheine, CoA, ACP and ACP peptide mimics, and explored their interactions with the KASI enzyme from *M. tuberculosis* (KasA) as well as with the KASI and KASII enzymes from *E. coli* (ecFabB and ecFabF). Elucidating the substrate-KAS recognition will provide insight towards the development of novel chemotherapeutics for this essential class of enzymes.

Since Walsh and coworkers determined that an eight residue fragment of ACP would suffice for recognition and subsequent post translational modification by AcpS (*54*), we in turn determined the minimal post translationally modified fragment of AcpM that is required for recognition and catalysis by the KAS enzymes. Our peptide sequence design included the important residues from ecACP that are involved in AcpS recognition (discovered by Walsh (*53*)) along with residues from α-helix 2 of AcpM.

Detailed kinetic data of ecFabF with malonylPPant-14mer revealed a 50 fold increase in k_{cat}/K_m relative to CoA and was shown to efficiently replace the activity of *E. coli* ACP (ecACP) as the acceptor substrate. In contrast to ecFabF, it was observed that the KASI enzymes ecFabB and KasA have an absolute requirement for an ACP substrate as the donor substrate, and given this requirement was met, show little variation in k_{cat}/K_m values for the acceptor substrate. For the KASI enzymes it is proposed that the binding of ACP results in a conformational change toward a more

accessible open form, thus facilitating the binding of the second substrate. In addition, palmitoyl-CoA exhibited substrate inhibition for KasA when malonyl-AcpM is the acceptor and through direct binding experiments was shown to bind to apo-KasA, acyl-KasA and the C171Q acyl mimic of KasA with similar affinity.

Materials and Methods

Materials: CoA substrates were purchased from Sigma. All solvents used were either A.C.S. or HPLC grade and all reagents were commercially available unless otherwise noted.

KasA and C171Q KasA Expression and Purification

N-terminally His-tagged KasA proteins were purified from *Mycobacterium smegmatis* strain mc^2155 essentially as described (*24*). pFPCA1 vectors containing the coding regions for these proteins were transformed into *M. smegmatis* competent cells by electroporation and plated on 7H10 solid media containing 30 µg/ml kanamycin, 200 µg/mL ampicillin and 15 µg/mL cyclohexamide. Colonies from these plates were then cultivated in 1 L of 7H9 liquid media supplemented with glycerol, and grown at 37℃ to an optical density (OD_{600}) of 0.6-0.8, after which protein expression was induced with 0.2% acetamide. After incubating overnight at 25℃, cells were harvested by centrifugation, resuspended in 40 mL of 20 mM Tris-HCl, 500 mM NaCl, 5 mM imidizole buffer, pH 7.9 (buffer A) and sonicated for 6 min using 30-s pulses at 4℃. Cellular debris was removed by centrifugation at 33,000 rpm for 1 hr at 4℃ and the supernatant was loaded onto a 8 mL nickel affinity column (8 x 1 cm). The column was washed with 50 mL of buffer A, 50 mL of 20 mM Tris-HCl, 500 mM NaCl and 60 mM imidizole buffer, pH 7.9 (buffer b) and eluted using a linear gradient of imidizole from 100-800 mM imidizole in buffer A. The fractions containing KasA were subsequently loaded onto a G-25 size exclusion chromatography column preequilibrated in 50 mM sodium phosphate

buffer, pH 8.5, 0.3 M NaCl. KasA was eluted in the same buffer and analyzed by SDS-PAGE. The protein was stored at -20 ℃ or -80 ℃ with 50% glycerol (*55*).

ecFabB, ecFabF and PantK Expression and Purification

The KAS enzymes and pantothenate kinase (PantK) were expressed as N-terminally hexahistidine tagged constructs in *E. coli* BL21(DE3)-pLysS cells and purified using standard nickel affinity chromatography as described previously (*16, 37, 56*).

KasA R214G and ecFabF R206G Mutagenesis

The KasA and ecFabF arginine to glycine mutant constructs were prepared using the Quikchange mutagenesis kit and the forward and reverse primers shown in **Tables 2.1**. These mutant proteins were expressed and purified as described for the wild-type enzymes.

Table 2.1: Mutagenesis Primers for ecFabF & KasA

Mutant	Sequence
R214G	Fwrd-5′-GCGTTCTCCATGATGGGCGCCATGTCGACCCGC-3′
	Rvrs-5′-GCGGGTCGACATGGCGCCCATCATGGAGAACGC-3′
R206G	Fwrd-5′-GGTTTTGGCGCGGCAGGCGCATTATCTACCCGC-3′
	Rvrs-5′-GCGGGTAGATAATGCGCCTGCCGCGCCAAAACC-3′

Holo-ACP Synthase Expression and Purification

AcpS was cloned expressed and purified as described previously (*37, 57*). Briefly, transformants containing pET-AcpS were selected on solid LB-ampicillin (200 µg/mL) media and individual colonies were grown to an OD_{600} 0.8-1.0 on a 1L scale in YT media (1 L H_2O, 16 g Tryptone, 10 g Yeast, 5 g (85 mM) NaCl, 2.4 g (20 mM) sodium phosphate). Cells were induced with 0.1 mM isopropyl-β- dithiogalactopyranoside (IPTG) at 30℃ for 3 hours. Cultures were harvested by centrifugation, resuspended in 50 mM Tris buffer, pH 8.0 and lysed by sonication. Cell free extract was gently mixed with 1 g DE-52 resin to form a slurry at 4℃ for 15 minutes. DE-52 was removed by centrifugation and this step was repeated. The supernatant was adjusted to pH 6.5 with a saturated 4-morpholineethanesulfonic acid monohydrate (MES) solution. This crude protein mixture was loaded onto an 8 mL SP-sepharose column (8 cm X 1 cm) equilibrated with 50 mM Tris buffer, pH 6.5. AcpS protein was eluted with a linear gradient of NaCl and the fractions were analyzed by UV (monitoring the absorbance at 280 nm) and SDS-PAGE. Pure fractions were concentrated using a YM-10 centricon concentrator. Protein was stored at -20℃ or -80℃ with 50% glycerol.

ecACP Expression and Purification

The *E. coli* acyl-carrier protein (ecACP) was overexpressed and purified as previously described (*58*). Briefly, the pET-ecACP plasmid containing the coding region for ecACP was transformed into *E. coli* BL21-DE3 competent cells. After selection on solid LB media containing kanamycin (30 µg/mL), individual colonies were used to inoculate 1 L of LB media. The culture was incubated at 37℃ until the OD_{600} reached 0.6-0.8, after

which protein expression was induced with 0.1 mM IPTG, 2 g/L casamino acids, and 0.05 g/L pantothenic acid. After incubating for a further 3 hr at 30℃ cells were harvested by centrifugation, resuspended in 50 mL of 100 mM Tris buffer, pH 8.0, containing 0.15 mg/mL of lysozyme, DNase, and RNase and sonicated for 6 min using 30-s pulses at 4℃. Cell debris was removed by centrifugation at 33,000 rpm, and the cell free extract was then diluted with one volume of 25 mM MES buffer, pH 6.1 (buffer A). The mixture was then loaded onto a Q-sepharose (Amersham Biosciences) column (50 x 150 mm) equilibrated in buffer A, and the column was washed with 400 mL of buffer A. The protein was eluted from the column in 10 mL fractions with an 800 mL linear gradient from 0.1 to 0.85 M NaCl in buffer A. The fractions containing ecACP were further purified by subsequently loading them onto a Hi-load 16/60 Superdex-75 column pre-equilibrated in buffer A, containing 100 mM NaCl. The fractions containing apo-ecACP were identified by SDS-PAGE and indicated that the ACP was predominantly in the apo form. ESI mass spectrometry (ESI-MS) revealed that the apo-ACP sample was comprised of two forms in which the N-terminal Met was present (8637 Da) or had been cleaved (8506 Da) (*30*).

ecACP and AcpM Substrate Synthesis

Substrates based on ecACP and AcpM: Apo-AcpM or apo-ecACP (100 µM) was incubated in 1.5 mL of AcpS reaction buffer (50 mM Tris, 5 mM $MgCl_2$, 1 mM DTT, pH 8.5) with 200 µM of either malonyl-CoA (Mal-CoA), palmitoyl-CoA or lauroyl-CoA and 6 µM AcpS for 1 hr at 37℃. Acyl ACPs were isolated from the reaction mixture by ion exchange chromatography using a Mono Q 5/50 GL column (GE healthcare) pre-

equilibrated with 20 mM Tris buffer, pH 8.0 (buffer A). Elution of the different ACP substrates was achieved using a shallow linear gradient with buffer A containing 1 M NaCl. Malonyl-AcpM/ecACP, palmitoyl-AcpM and lauroyl-ecACP eluted at ~330 mM NaCl. ESI-MS determined the molecular weights of all products as expected based off the primary amino acid sequence. ESI-MS: malonyl-AcpM 1304 Da, malonyl-ecACP 8932 Da (9036 Da with N-terminal Met), palmitoyl-AcpM 13200 Da lauroyl-ecACP 9027.

Peptide Synthesis and Purification

Peptides containing 8 (DSLDMLEI), 14 (DSLSMLEIAVQTED) and 16 (DPDSLSMLEIAVQTED) residues were synthesized on a 0.25 mmol scale using an Applied Biosystems 433A Peptide Synthesizer, with 9-fluornylmethoxycarbonyl (Fmoc) chemistry. Use of a 5-(4'-Fmocaminomethyl-3', 5-dimethoxyphenol) valeric acid (PAL-PEG) resin afforded an amidated C-terminus. Standard Fmoc reaction cycles were used. Peptides were cleaved from the resin using 90% Trifluoroacetic acid (TFA), 3.33% anisole, 3.33% thioanisole and 3.33% ethanedithiol.

To increase solubility, the crude peptides were partially dissolved in 20% acetic acid (v/v), frozen in liquid nitrogen and lyophilized. This procedure was repeated several times prior to purification. The crude peptides were redissolved in 0.5% NH_4OH and purified using reversed-phase HPLC. Chromatography was performed at a flow rate of 4 mL/min with a Vydac protein/peptide semipreparative column (10 x 250 mm) and by running a linear gradient of 100% buffer A (95% H_2O, 5% acetonitrile, 0.1% TFA) to 100% buffer B (95% acetonitrile, 5% H_2O, 0.1% TFA) over 30 min. The 8mer, 14mer and 16mer peptides eluted at around 19 min and were subsequently analyzed by ESI-

MS: 8mer ($[M+H]^+$) calcd. $C_{39}H_{67}N_9O_{15}S$, 934.07 *m/z* found 934.0. Yield 25%, 14mer ($[M+H]^+$) calcd. $C_{64}H_{108}N_{16}O_{26}S$ 775.35 *m/z* found 775.0. Yield 10%, 16mer ($[M+H]^+$) calcd. $C_{73}H_{120}N_{18}O_{30}S$ 880.40 *m/z* found 880.0. Yield 50%.

Acyl-phosphopantetheine peptide preparation:

Peptides (200 µM) were incubated in 1 mL of AcpS reaction buffer (50 mM Tris, 10 mM $MgCl_2$, 1 mM DTT, pH 6.5) with 400 µM malonyl-CoA and 6 µM AcpS for 30 min at 37℃ and purified using reversed-phase HPLC. Chromatography was performed at a flow rate of 1 mL/min with a Vydac protein/peptide analytical column (10 x 250 mm) and by running a linear gradient of 100% buffer A (95% H_2O, 5% acetonitrile, 0.1% TFA) to 100% buffer B (95% acetonitrile, 5% H_2O, 0.1% TFA) over 45 min. The Malonyl-phosphopantetheine-8mer (MalPPant-8mer), Malonyl-phosphopantetheine-14mer (MalPPant-14mer) and Malonyl-phosphopantetheine-16mer (MalPPant-16mer) eluted around 21 min and were subsequently analyzed by ESI-MS: MalPPant8mer $[M+2H]^+$ calcd. $C_{53}H_{90}N_{11}O_{24}PS_2$ 680.25 *m/z* found 680.0. Yield 33%, MalPPant-14mer $[M+2H]^+$ calcd. $C_{78}H_{131}N_{18}O_{35}PS_2$ 988.42 *m/z* found 988.0. Yield 20%, MalPPant-16mer $[M+2H]^+$ calcd. $C_{87}H_{143}N_{20}O_{39}PS_2$ 1094.45 *m/z* found 1094.0. Yield 50%.

Peptide Substrate Synthesis

Purified peptide was incubated in AcpS reaction buffer (50 mM Tris, pH 6.5, 10 mM $MgCl_2$, 1 mM DTT) with a 2 molar excess of either malonyl-CoA (Mal-CoA, Sigma) and 6 µM AcpS for 30 minutes at 37℃. Purification via reversed phase HPLC, using a Vydac protein/peptide analytical column (10 mm X 250 mm). The buffer gradient used

was as follows: 0-45 minutes, 100% buffer A (95% H_2O, 5% acetonitrile, 0.1% TFA) to 100% buffer B (95% acetonitrile, 5% H_2O, 0.1% TFA) at a flow rate of 1 mL/min. The 8mer, 14mer and 16mer eluted around 21 minutes and were subsequently analyzed by ESI-MS: $[M+2H]^+$ calcd. $C_{53}H_{90}N_{11}O_{24}PS_2$, $C_{78}H_{131}N_{18}O_{35}PS_2$, $C_{87}H_{143}N_{20}O_{39}PS_2$ 680.25, 988.42 and 1094.45, *m/z* found 680.0, 988.0 and 1094.0, respectively.

*Synthesis of Malonyl-phosphopantetheine **(4)**:*

Pantetheine **(1)**: Pantethine (271 μmoles) and *tris*(2-carboxyethyl)phosphine (1.2 mmoles) were dissolved in 1 mL of deionized water and stirred at RT overnight with subsequent purification using reversed-phase HPLC. Chromatography was performed at a flow rate of 4 mL/min with a Vydac C18 semipreparative column (10 mm X 250 mm) and by running a linear gradient of 95% buffer A (20 mM ammonium acetate, pH 6.7) to 95% buffer B (acetonitrile) over 20 min. Product **1** eluted at 8.5 min and was subsequently concentrated and lyophilized to afford a viscous clear oil. Yield 50%. ESI-MS: $[M-H]^-$ calcd. $C_{11}H_{22}N_2O_2S$ 277.1, *m/z* found 277.1.

Phosphopantetheine **(2)**: PanK (1 mg) was added slowly to a solution of ATP (180 μmoles, pH 7) and **1** (72 μmoles) dissolved in 2.6 mL of 20 mM Tris, 0.1 M NaCl, 50 mM $MgCl_2$ buffer, pH 8 and stirred at RT for 3 hr with subsequent purification using reversed-phase HPLC. Chromatography was performed at a flow rate of 4 mL/min with a Vydac C18 semipreparative column (10 mm X 250 mm) and by running a linear gradient of 95% buffer A (20 mM ammonium acetate , pH 6.7) to 95% buffer B (acetonitrile) over 20 min. Product **2** eluted at 11 min and was subsequently

concentrated and lyophilized to afford a white solid. Yield 20%. ESI-MS: $[M-H]^-$ calcd. $C_{11}H_{22}N_2O_7PS^-$ 356.09, *m/z* found 356.0.

Malonylthiophenol **(3)**

The chemical synthesis of malonylthiophenol is based on the procedure of Bressler and Wakil (*60*). Typically, 10 mmoles of malonic acid was dissolved in 5 mL of anhydrous tetrahydrofuran (THF) at -20℃ followed by the drop wise addition of 5 mmoles of ethyl chloroformate in 1 mL of THF. Precipitation of triethylamine hydrochloride was observed after several min. The mixture was incubated for 30 min at -20℃ to ensure completion of the reaction.

The mixed anhydride was treated with 5 mmoles of thiophenol and incubated at RT for 24 hr. The solvent was then removed under vacuum and the residue was suspended in 2 mL of water. The oily product was extracted in diethyl ether and dried over sodium sulfate. Evaporation removed the ether layer to afford **3** as a viscous oily residue. Yield 85%. ESI-MS: $[M-H]^-$ calcd. $C_9H_8O_3S$ 196.02, *m/z* found 196.0.

Malonyl-phosphopantetheine **(4)**: **3** (25 μmoles) dissolved in 1 mL of THF was added to 5 μmoles of **2** dissolved in 1 mL of 100 mM $NaHCO_3$ buffer, pH 8.2. The mixture was stirred vigorously for 3 hr and acidified with Dowex 50 to pH. The Dowex was removed by centrifugation and washed once with 1.5 mL of water. The supernatant and the wash were combined and the thiophenol was extracted with diethyl ether. The aqueous solution containing the malonyl-phosphopantetheine was then lyophilized and purified using reversed-phase HPLC. Chromatography was performed at a flow rate of 1 mL/min

with a Varian analytical column (4.6 mm X 150 mm) and by running a linear gradient of 95% buffer A (20 mM ammonium acetate, pH 6.7) to 75% buffer B (acetonitrile) over 16 min. The final product **4** eluted at 12 min and was subsequently concentrated and lyophilized to afford a white solid. Yield 25%. ESI-MS: $[M-H]^-$ calcd. $C_{14}H_{25}N_2O_{10}PS$ 443.10, *m/z* found 443.0.

KAS Enzyme Assays

KasA activity was monitored in 50 mM Tris, 1 mM DTT buffer, pH 8.5 at 25℃ using a coupled assay with MabA, the NADPH-dependent FAS-II β-ketoacyl-ACP reductase (**Figure 2.4** (*22*)), allowing the reaction to be monitored at 340 nm. MabA was expressed in *E. coli* BL21-DE3 cells and purified by metal ion affinity chromatography as described previously (*61*). The kinetic studies were performed by varying the concentration of one substrate while at a saturating concentration of the other substrate. Initial velocities were measured after the initiation of the reaction with the appropriate KAS enzyme. The reaction mixtures contained 250 μM NADPH, 10 μM MabA, varying concentrations of acyl and malonyl substrates and 100 nM KasA. K_m was calculated by fitting data to the Michaelis-Menton Equation (**Equation 1**) using GraFit 4.0. k_{cat} values were calculated by using the relationship between k_{cat} and V_{max} (**Equation 2**) and kinetic K_d values were calculated by fitting the data to a substrate inhibition equation (**Equation 3**), also using GraFit 4.0.

$$v = V_{max} [S] / (K_m + [S]) \qquad \textbf{Equation 1}$$

$k_{cat} = V_{max} / [E]$ **Equation 2**

$v = V_{max}*[S] / (K_m + [S] + [S]^2 / K_d)$ **Equation 3**

v is the initial velocity, V_{max} is the maximal velocity, S is the substrate concentration, K_m is the Michaelis constant and K_d is the dissociation constant.

The activity of ecFabF and ecFabB were assayed in a similar fashion except the kinetic parameters were determined in a buffer containing 50 mM potassium phosphate, 50 mM NaCl, 1 mM DTT, pH 6.5. The oxidation of NADPH by MabA was again coupled to the production of the β-ketoacyl product. The kinetic studies were performed by varying the concentration of one substrate while at a saturating concentration of the other substrate. The reaction mixtures contained 250 μM NADPH, 10 μM MabA, varying concentrations of acyl and malonyl substrates and either 770 nM ecFabB or 3 μM ecFabF, unless otherwise noted. K_m was calculated by fitting data to the Michaelis-Menton Equation (**Equation 1)** using GraFit 4.0. k_{cat} values were calculated by using the relationship between k_{cat} and V_{max} (**Equation 2)**.

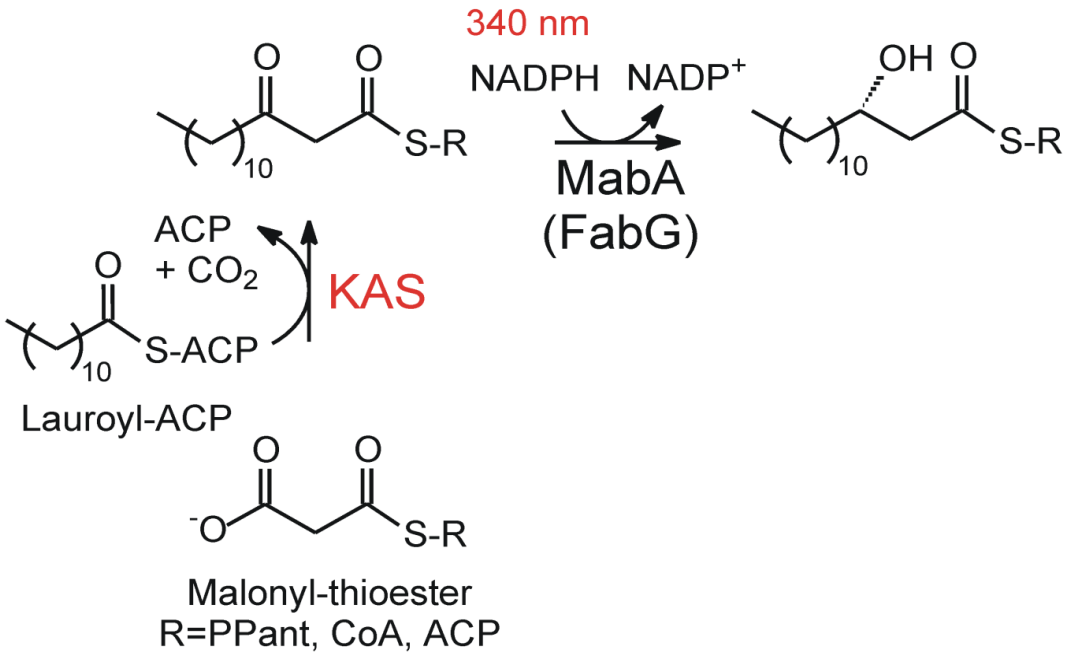

Figure 2.4: Coupled Assay for KAS Activity. Oxidation of NADPH cofactor by coupling enzyme MabA is monitored at 340 nm

Direct Binding Fluorescence Titrations

Direct Binding Fluorescence Titrations: Palmitoyl-CoA binding was quantified by monitoring the intrinsic tryptophan fluorescence of KasA using a Quanta Master fluorimeter (Photon Technology International). Excitation and emission wavelengths were 280 and 337 nm with an excitation slit width of 4.0 nm and an emission slit width of 8.0 nm. Titrations were performed at 25 ℃ by making microliter additions of palmitoyl-CoA (0.1-320 µM) to a solution (970 µL) containing 500 nM enzyme in buffer (50 mM Tris, pH 8.5, 1 mM dithiothreitol). All solutions were filtered and equilibrated to 25℃.

Titration curves were corrected for inner filter effects, and K_d values were calculated using the Scatchard equation (**Equation 4,** Grafit 4.0).

$$[\text{Bound}] = (\text{Capacity} * [\text{Free}]) / (K_d + [\text{Free}]) \qquad \textbf{Equation 4}$$

Results

Kinetic Characterization of KAS Enzymes with ACP and CoA Substrates

ecFabF and ecFabB were obtained as soluble proteins after overexpression in *E. coli*. Expression of KasA was carried out in *M. smegmatis* due to insolubility after expression in *E. coli* (22). Previously, KasA and ecFabB were thought to be inactive with CoA-based substrates, so the natural malonyl, palmitoyl, and lauroyl ecACP based substrates were synthesized using apo-AcpM and apo-ecACP respectively, by AcpS (**Figure 2.5**). Kinetic parameters were determined by monitoring the NADPH-dependent reduction of the β-ketoacyl-ACP product in a coupled assay with MabA, the subsequent enzyme in the FAS-II pathway in MTb (*22*).

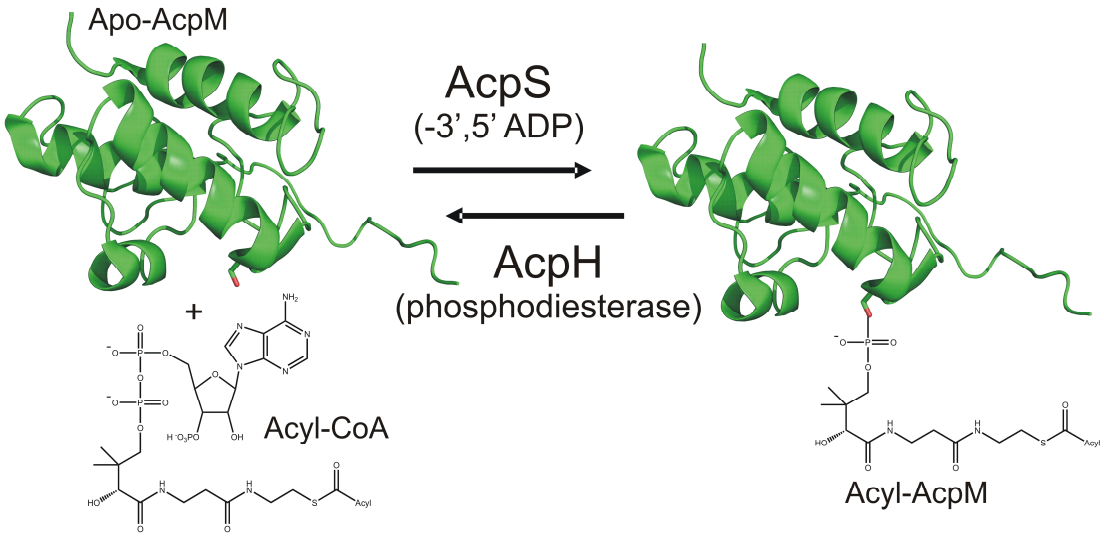

Figure 2.5: Synthesis of ACP Substrates. Reaction catalyzed by AcpS used to synthesize ACP based substrates from apo-ACP and CoA for KAS activity assays

ecFabF Activity with CoA

Kinetic parameters have been previously reported (*62*) for ecFabF with CoA-based substrates, with k_{cat} and K_m values of 2.48 ± 0.06 min^{-1} and 502 ± 54 µM, respectively, when malonyl-CoA was varied at a fixed concentration of lauroyl-CoA (100 µM). These parameters were tested again for accuracy of our assay and the results closely matched what was previously reported with k_{cat} and K_m values of 2.20 ± 0.03 min^{-1} and 510 ± 84 µM, respectively when malonyl-CoA was varied at a fixed concentration of lauroyl-CoA (75 µM, **Figure 2.6**). In addition, we determined the k_{cat} and K_m for ecFabF when lauroyl-CoA was varied at a fixed concentration of malonyl-CoA (600 µM) with values of 2.8 ± 0.03 min^{-1} and 53.7 ± 15 µM (**Figure 2.7**). Kinetic parameters have not been reported for the natural ecACP substrates for ecFabF, and so these were determined with k_{cat} and K_m values of 1.74 ± 0.02 min^{-1} and 8.2 ± 2.1 µM, respectively when malonyl-ecACP was varied at a fixed concentration of lauroyl-ecACP (10 µM, **Table 2.2, Figure 2.7**).

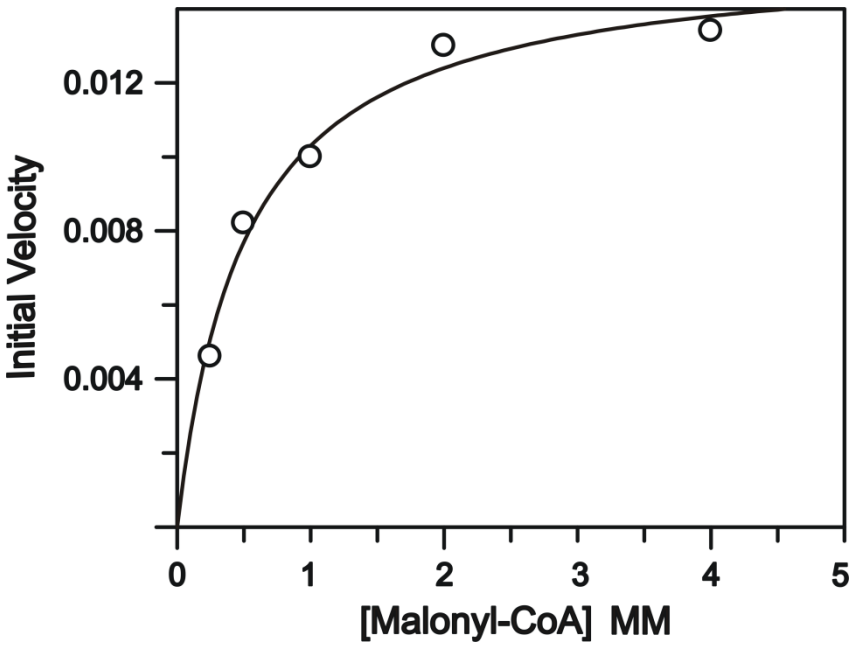

Figure 2.6: Kinetic Analysis of ecFabF for Malonyl-CoA. The initial velocities of product formation were measured with 1 µM ecFabF in the presence of increasing concentrations of malonyl-CoA with respect to 75 µM lauroyl-CoA. k_{cat} and K_m values were determined by fitting the data to the **Equation 1** and **Equation 2** as 2.20 ± 0.03 min^{-1} and 510 ± 84 µM, respectively. The solid line represents the best fit of the data.

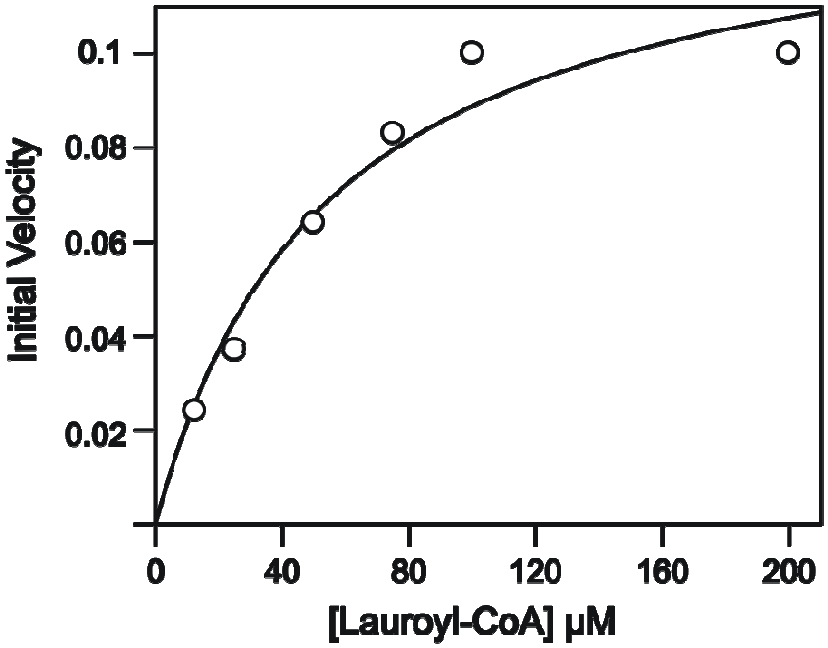

Figure 2.7: Kinetic Analysis of ecFabF for Lauroyl-CoA. The initial velocities of product formation were measured with 7.5 µM ecFabF in the presence of increasing concentrations of lauroyl-CoA with respect to 500 µM malonyl-CoA. k_{cat} and K_m values were determined by fitting the data to the **Equation 1** and **Equation 2** as 2.8 ± 0.03 min^{-1} and 53.7 ± 15 µM, respectively. The solid line represents the best fit of the data.

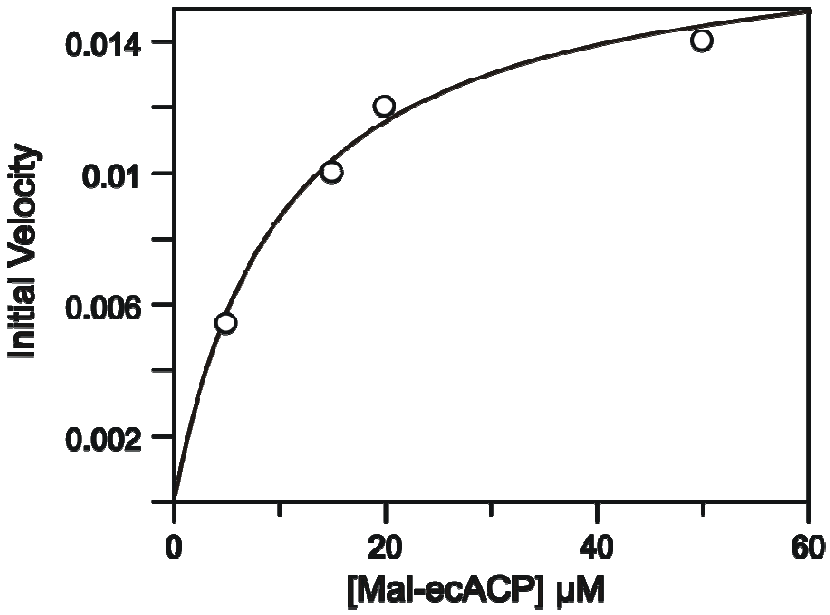

Figure 2.8: Kinetic Analysis of ecFabF for Malonyl-ecACP. The initial velocities of product formation were measured with 3 µM ecFabF in the presence of increasing concentrations of malonyl-ecACP with respect to 10 µM lauoryl-ecACP. k_{cat} and K_m values were determined by fitting the data to the **Equation 1** and **Equation 2** as 1.74 ± 0.02 min^{-1} and 8.2 ± 2.1 µM, respectively. The solid line represents the best fit of the data.

,

Table 2.2: Kinetic Parameters for ecFabF

Donor	Acceptor	K_m (μM)	k_{cat} (min^{-1})	k_{cat}/K_m(μM/min^1)	% Activity
lauroyl-CoA	malonyl-CoA[a]	510 ± 84	2.20 ± 0.02	0.0043 ± 0.0007	2
lauroyl-CoA[b]	malonyl-CoA	53.7 ± 15	2.8 ± 0.03	0.052 ± 0.011	25
lauroyl-CoA	MalPPant[a]	590 ± 133	1.33 ± 0.03	0.0022 ± 0.0005	1
lauroyl-CoA	MalPPant8mer[a]	23.7 ± 5.22	1.11 ± 0.02	0.047 ± 0.011	22
lauroyl-CoA	MalPPant14mer[a]	6.1 ± 1.50	1.36 ± 0.03	0.22 ± 0.057	100
lauroyl-CoA	MalPPant16mer[a]	6.2 ± 1.4	1.34 ± 0.01	0.23 ± 0.060	100
lauroyl-ecACP	malonyl-ecACP[a]	8.2 ± 2.1	1.74 ± 0.4	0.21 ± 0.057	100

a. Calculated by varying the malonyl substrate with respect to 75 μM lauroyl-CoA
b. Calculated by varying the lauroyl substrate with respect to 500 μM malonyl-CoA
c. Calculated by varying the malonyl substrate with respect to 10 μM lauroyl-ecACP

ecFabB Activity with CoA

ecFabB has previously shown to accept an acylated CoA molecule but shows no activity when assaying with both malonyl and lauroyl CoA (unpublished data). Kinetic parameters have so far not been reported for ecFabB, so these were determined using the natural malonyl-ecACP and lauroyl-ecACP substrates, with k_{cat} values of 6.6 ± 0.01 min^{-1} and 3.4 ± 0.02 min^{-1} and K_m values of 11.5 ± 2.2 µM and 3.2 ± 0.5 µM, respectively, when either lauroyl-ecACP was varied at a fixed concentration of malonyl-ecACP (12 µM) or malonyl-ecACP was varied at a fixed concentration of lauroyl-ecACP (10 µM, **Table 2.3, Figure 2.9, 2.10**). Interestingly, ecFabB also had activity when one carrier molecule was a CoA while the other was an ecACP. For instance, when the concentration of malonyl-CoA was varied at a fixed concentration of lauroyl-ecACP (10 µM), the k_{cat} and K_m values were 5.4 ± 0.03 min^{-1} and 88 ± 3.5 µM, respectively. In addition, when the concentration of lauroyl-CoA was varied at a fixed concentration of malonyl-ecACP (12 µM), the k_{cat} and K_m values were 4.40 ± 0.04 min^{-1} and 58.6 ± 5.4 µM, respectively **(Table 2.3, Figure 2.11, 2.12)**.

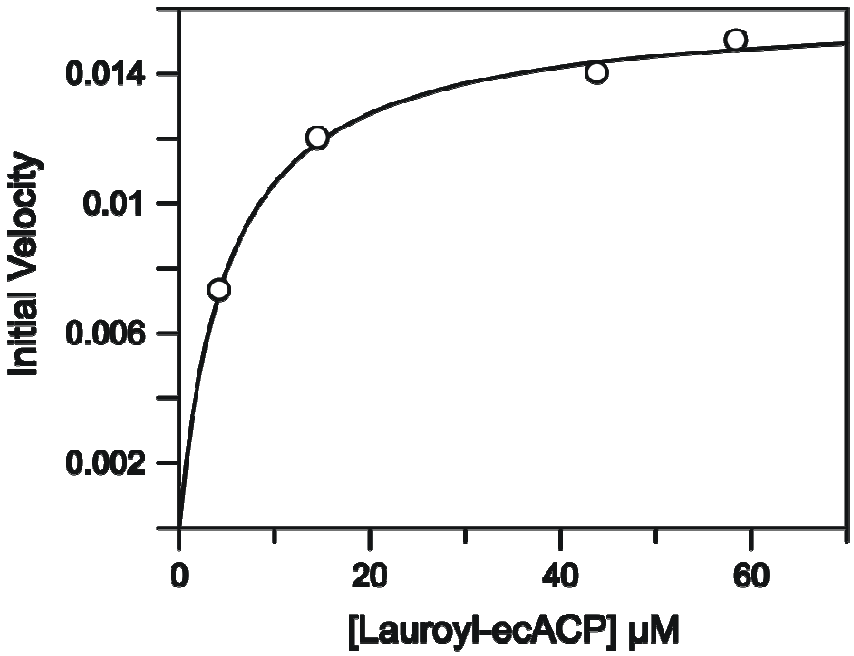

Figure 2.9: Kinetic Analysis of ecFabB for Lauroyl-ecACP. The initial velocities of product formation were measured with 620 nM ecFabB in the presence of increasing concentrations of lauroyl-ecACP with respect to 12 µM malonyl-ecACP. k_{cat} and K_m values were determined by fitting the data to the **Equation 1** and **Equation 2** as 3.4 ± 0.02 min^{-1} and 3.2 ± 0.5 µM, respectively. The solid line represents the best fit of the data.

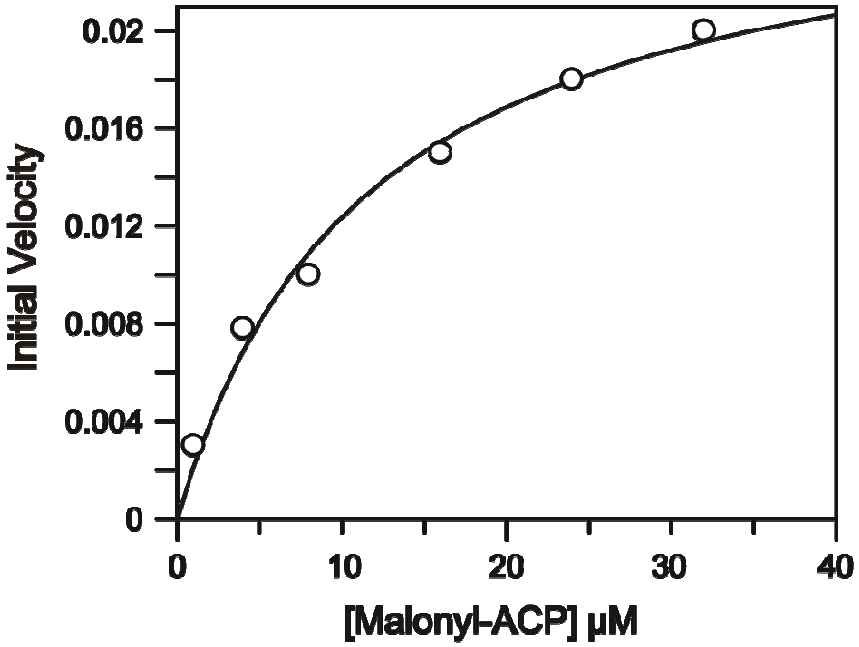

Figure 2.10: Kinetic Analysis of ecFabB for Malonyl-ecACP. The initial velocities of product formation were measured with 620 nM ecFabB in the presence of increasing concentrations of malonyl-ecACP with respect to 10 µM lauoryl-ecACP. k_{cat} and K_m values were determined by fitting the data to the **Equation 1** and **Equation 2** as 6.6 ± 0.01 min^{-1} and 11.5 ± 2.2 µM, respectively. The solid line represents the best fit of the data.

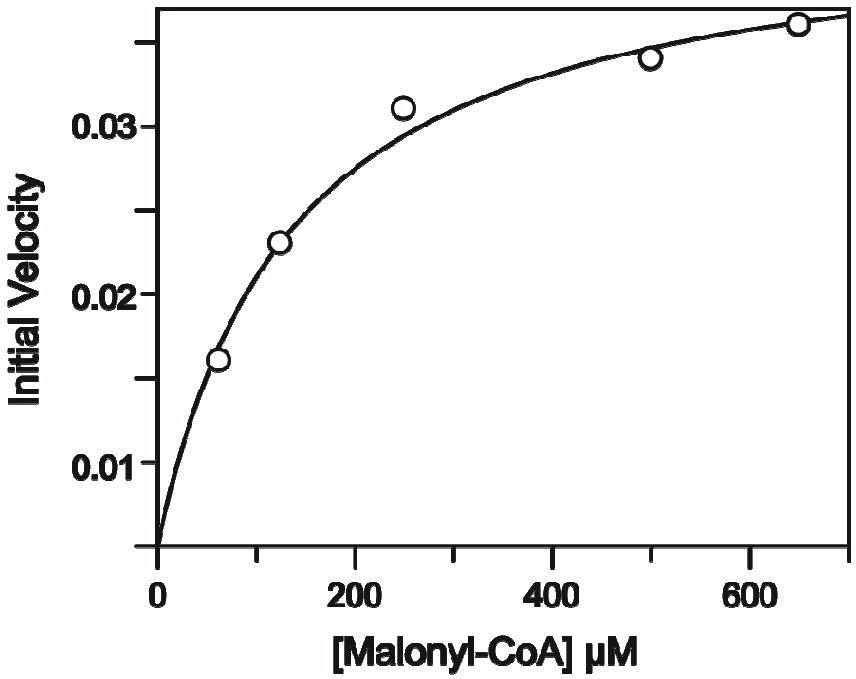

Figure 2.11: Kinetic Analysis of ecFabB for Malonyl-CoA. The initial velocities of product formation were measured with 770 nM ecFabB in the presence of increasing concentrations of malonyl-CoA with respect to 10 µM lauroyl-ecACP. k_{cat} and K_m values were determined by fitting the data to the **Equation 1** and **Equation 2** as 7.1 ± 0.03 min^{-1} and 153 ± 19 µM, respectively. The solid line represents the best fit of the data.

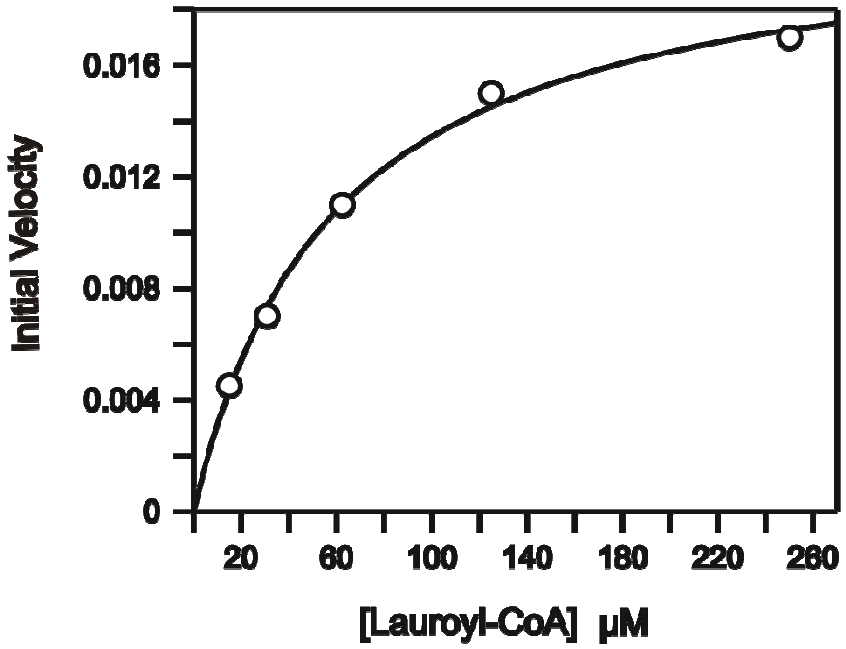

Figure 2.12: Kinetic Analysis of ecFabB for Lauroyl-CoA. The initial velocities of product formation were measured with 770 nM ecFabB in the presence of increasing concentrations of lauroyl-CoA with respect to 12 µM malonyl-ecACP. k_{cat} and K_m values were determined by fitting the data to the **Equation 1** and **Equation 2** as 4.4 ± 0.04 min^{-1} and 58.6 ± 5.4 µM, respectively. The solid line represents the best fit of the data.

Table 2.3: Kinetic Parameters for ecFabB

Donor	Acceptor	K_m (μM)	k_{cat} (min^{-1})	k_{cat}/K_m (μM/min^{-1})	% Activity
lauroyl-ecACP	malonyl-CoA[a]	153 ± 19	7.1 ± 0.03	0.061 ± 0.0024	10
lauroyl-CoA[b]	malonyl-ecACP	58.6 ± 5.4	4.4 ± 0.04	0.075 ± 0.0075	7
lauroyl-ecACP	MalPPant8mer[a]	14.2 ± 2.5	1.13 ± 0.02	0.081 ± 0.015	14
lauroyl-ecACP	MalPPant14mer[a]	15.8 ± 6	2.4 ± 0.01	0.16 ± 0.060	27
lauroyl-ecACP	MalPPant16mer[a]	29 ± 5.5	6.5 ± 0.02	0.22 ± 0.044	37
lauroyl-ecACP[b]	malonyl-ecACP	3.2 ± 0.5	3.4 ± 0.02	1.05 ± 0.18	100
lauroyl-ecACP	malonyl-ecACP[a]	11.5 ± 2.2	6.6 ± 0.01	0.59 ± 0.11	100

a. Calculated by varying the malonyl substrate with respect to 10 μM lauroyl-ecACP
b. Calculated by varying the lauroyl substrate with respect to 10 μM malonyl-ecACP

KasA Activity with CoA

Similar to ecFabB, KasA has previously shown to accept an acylated CoA molecule but shows no activity when both acceptor and donor molecules are CoA ((*63*), unpublished data). The K_m value for malonyl-AcpM of 9 ± 0.8 µM determined at a fixed concentration of palmitoyl-AcpM (10 µM) is similar to the K_m value determined previously (13.5 µM) while the k_{cat} value of 28 ± 0.02 min^{-1} is 6-fold larger than that determined by Schaeffer *et al*., which we speculate could be due to the use of mycobacterial acyl carrier protein in our study compared to the ACP from *E. coli* **(Table 2.4, Figure 2.13)** (*22*). Interestingly, KasA also showed activity when the carrier molecule was CoA and the donor was AcpM. For instance, when the concentration of malonyl-CoA was varied at a fixed concentration of palmitoyl-AcpM (12 µM), the k_{cat} and K_m values were 21 ± 0.01 min^{-1} and 5.8 ± 1.5 µM, respectively **(Table 2.4, Figure 2.14)**. In contrast, when palmitoyl-CoA was used as the donor molecule at a fixed concentration of malonyl-AcpM (10 µM), substrate inhibition was detected with a K_d of 36 µM and k_{cat} and K_m values were 5 ± 0.02 min^{-1} and 0.4 ± 0.09 µM, respectively **(Figure 2.15).**

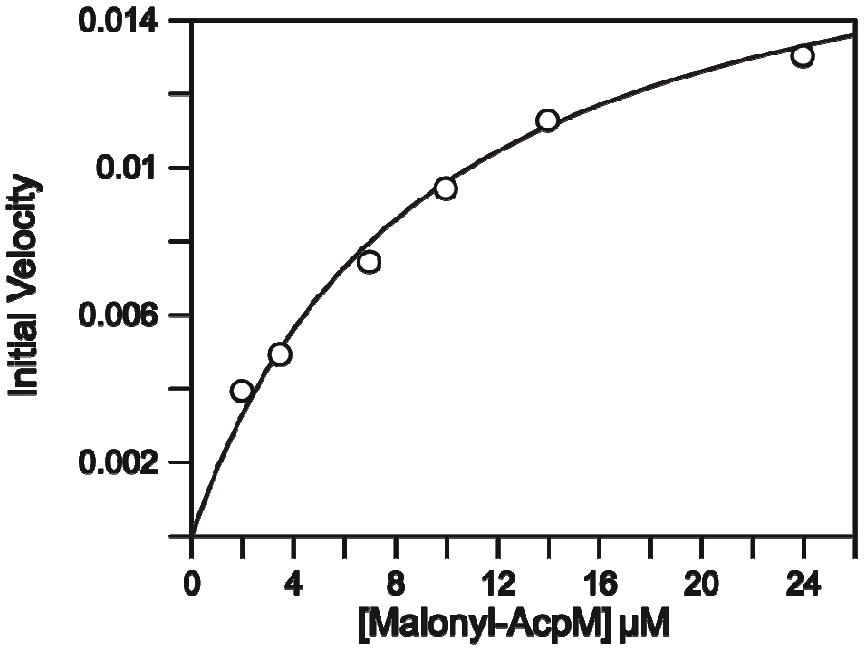

Figure 2.13: Kinetic Analysis of KasA for Malonyl-AcpM. The initial velocities of product formation were measured with 100 nM KasA in the presence of increasing concentrations of malonyl-AcpM with respect to 12 µM palmitoyl-AcpM. k_{cat} and K_m values were determined by fitting the data to the **Equation 1** and **Equation 2** as 28 ± 0.02 min^{-1} and 9 ± 0.8 µM, respectively. The solid line represents the best fit of the data.

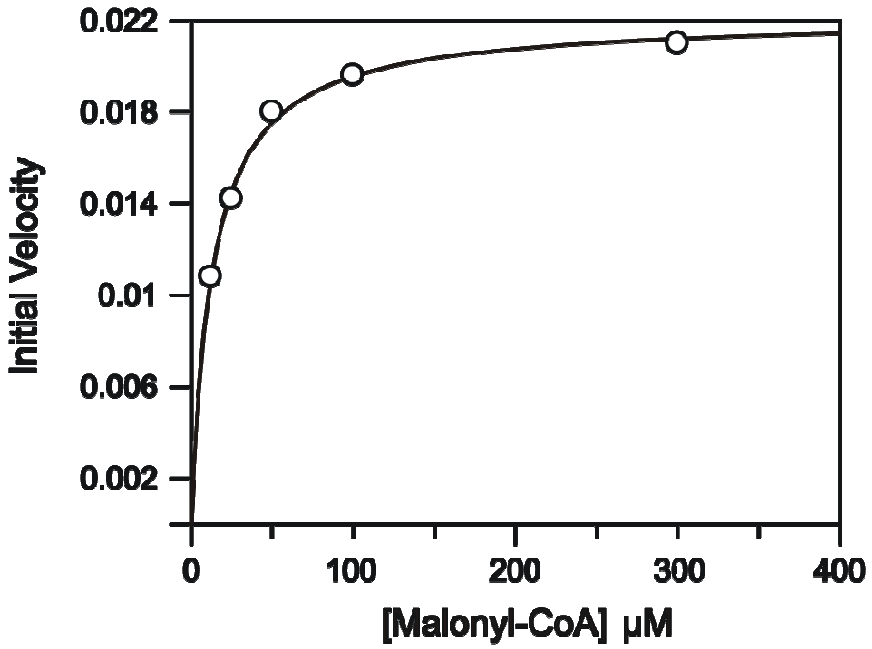

Figure 2.14: Kinetic Analysis of KasA for Malonyl-CoA. The initial velocities of product formation were measured with 100 nM KasA in the presence of increasing concentrations of malonyl-CoA with respect to 12 µM palmitoyl-AcpM. k_{cat} and K_m values were determined by fitting the data to the **Equation 1** and **Equation 2** as 21 ± 0.01 min^{-1} and 5.8 ± 1.5 µM, respectively. The solid line represents the best fit of the data.

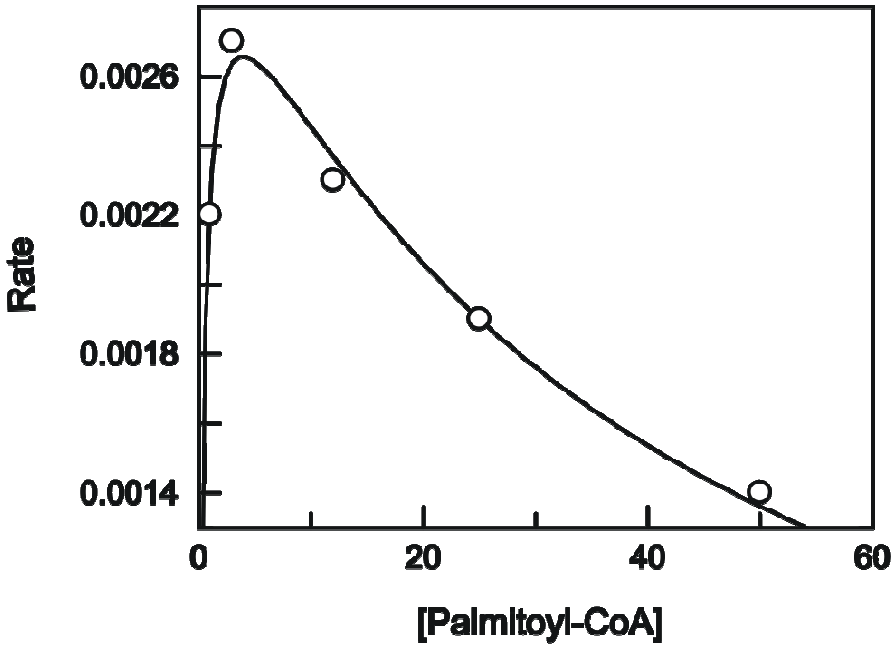

Figure 2.15: Interaction of KasA with Palmitoyl-CoA. Kinetic analysis of KasA for palmitoyl-CoA. The initial velocities of product formation were measured with 100 nM KasA in the presence of increasing concentrations of palmitoyl-CoA with respect to 10 µM malonyl-AcpM. The K_d value was determined by fitting the data to **Equation 3** as 36 ± 5.1 µM. The solid line represents the best fit of the data.

Table 2.4: Kinetics Parameters for KasA

Donor	Acceptor	K_m (μM)	k_{cat} (min^{-1})	k_{cat}/K_m (μM/min^{-1})	% Activity
palmitoyl-AcpM	malonyl-CoA[a]	5.8 ± 1.5	21 ± 0.01	2.3 ± 0.23	48
palmitoyl-AcpM	MalPPant8mer[a]	4.7 ± 0.6	21 ± 0.01	4.4 ± 0.62	99
palmitoyl-AcpM	MalPPant14mer[a]	8.6 ± 1.9	23 ± 0.02	2.7 ± 0.62	66
palmitoyl-AcpM	MalPPant16mer[a]	5.1 ± 0.6	18 ± 0.01	3.5 ± 0.45	73
palmitoyl-AcpM	malonyl-AcpM[a]	9 ± 0.8	28 ± 0.02	4.8 ± 1.25	100
palmitoyl-CoA[b]	malonyl-AcpM	0.4 ± 0.09 36 ± 5.1 (K_d) [d]	5 ± 0.02	12.5 ± 1.43	----
PalmPPant16mer[c]	malonyl-CoA	NA[e]	NA[e]	NA	0

a. Calculated by varying the malonyl substrate with respect to 12 μM palmitoyl-AcpM
b. Calculated by varying the palmitoyl substrate with respect to 10 μM malonyl-AcpM
c. Calculated by varying the palmitoyl substrate with respect to 50 μM malonyl-CoA
d. Substrate inhibition, K_d value was calculated by fitting the data to **Equation 3**
e. Not active

Direct Binding Experiment

The interaction between palmitoyl-CoA and KasA was further examined using a direct binding experiment in which the intrinsic tryptophan fluorescence of KasA was used to measure the affinity of palmitoyl-CoA for KasA. The interaction of palmitoyl-CoA with free enzyme resulted in a decrease of fluorescence and after correction of the data for the inner filter effect, the fluorescent titrations yielded a K_d of 7 ± 0.3 µM. To determine if palmitoyl-CoA was also binding to the acyl enzyme, we synthesized the acyl-KasA intermediate by incubation with palmitoyl-CoA with KasA for ten minutes, where the excess palmitoyl-CoA was removed through excessive washing (*29*). When the titration was repeated with the acylated form of the enzyme, it yielded a K_d of 8 ± 0.6 µM for the interaction between acyl-KasA and palmitoyl-CoA. The fluorescence titration was repeated with C171Q KasA, a mutant shown to mimic the structural change accompanying acyl-KasA formation (*29*). After data analysis, the K_d yielded a similar value, 13 ± 0.9 µM, as the acyl and apo-KasA enzymes **(Table 2.5, Figure 2.16, 2.17, 2.18)**.

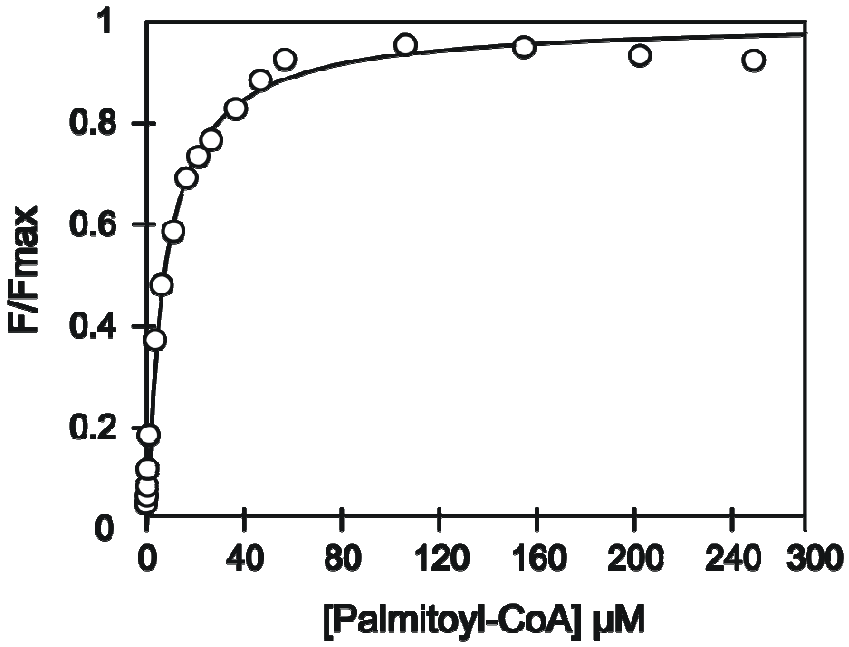

Figure 2.16: Interaction Between Apo-KasA and Palmitoyl-CoA. The change of fluorescence when 500 nM of apo-KasA is titrated with palmitoyl-CoA is shown. The K_d value of 7 ± 0.3 µM was determined by fitting the data to **Equation 4**, where the solid line represents the best fit of the data.

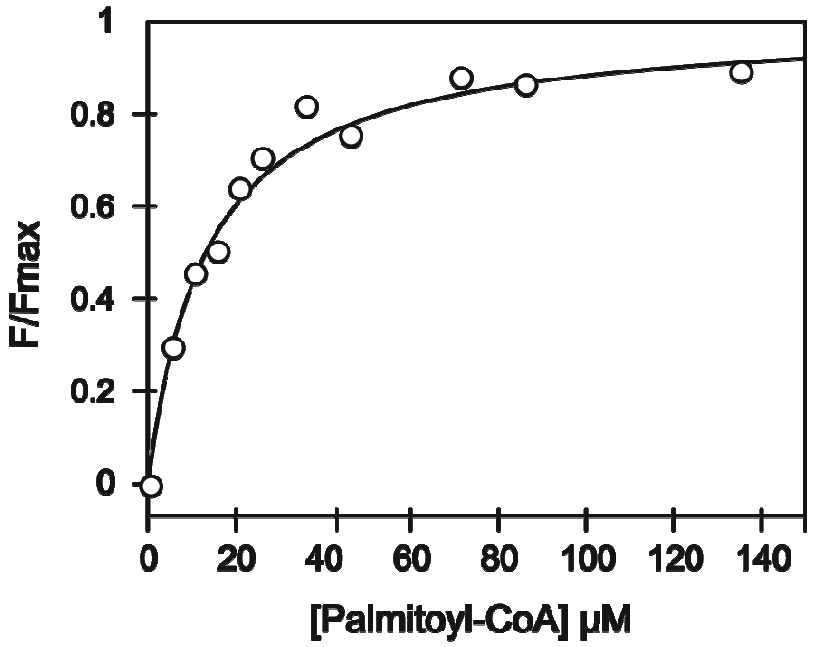

Figure 2.17: Interaction Between Acyl-KasA and Palmitoyl-CoA. The change of fluorescence when 500 nM of acyl-KasA is titrated with palmitoyl-CoA is shown. The K_d value of 13 ± 0.9 µM was determined by fitting the data to **Equation 4**, where the solid line represents the best fit of the data.

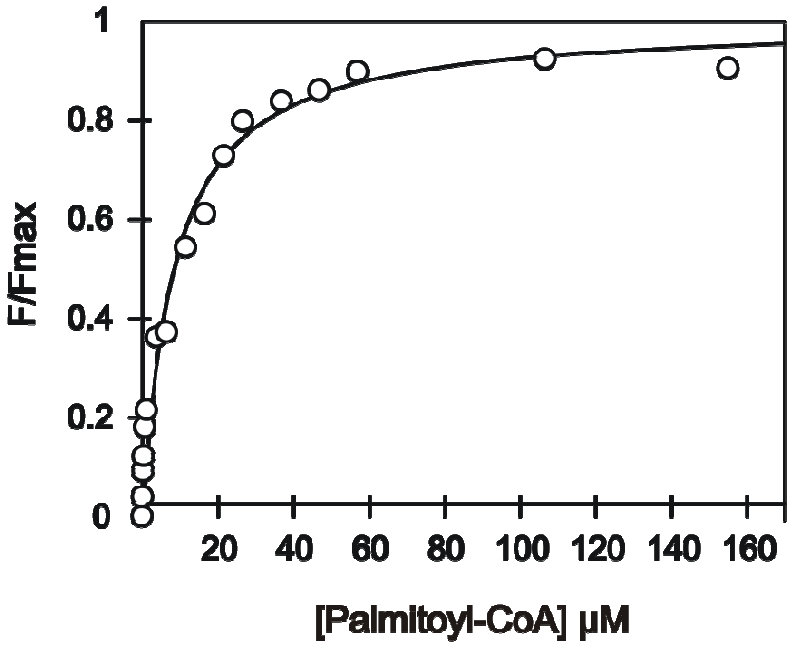

Figure 2.18: Interaction Between C171Q KasA and Palmitoyl-CoA. The change of fluorescence when 500 nM of C171Q KasA is titrated with palmitoyl-CoA is shown. The K_d value of 8 ± 0.6 µM was determined by fitting the data to **Equation 4**, where the solid line represents the best fit of the data.

Table 2.5: Interaction of KasA and C171Q KasA with palmitoyl-CoA

Protein	Ligand	K_d (µM)
Apo-KasA	Palm-CoA	7 ± 0.3
C171Q KasA	Palm-CoA	8 ± 0.6
Acyl-KasA	Palm-CoA	13 ± 0.9

Protein concentration: 500 nM, K_d values were calculated by fitting the data to **Equation 4**

KAS Discrimination of ACP vs. CoA

In order to elucidate the structural changes that have occurred in KASI and KASII resulting in the preference of ACP over CoA, we compared the important residues required for binding of CoA and ACP to the well characterized KASIII enzyme (ecFabH) with those in ecFabF and KasA. Upon alignment of the ecFabH and ecFabF structures, the position of an arginine stood out as playing an important role in selectivity. In ecFabH, R151 is in the correct position to form contacts with the adenine portion of CoA. However, in ecFabF, the arginine is clearly hindering the binding of CoA. To test the possibly that R206 was preventing efficient binding of CoA, we made an ecFabF R206G. A ten fold increase in k_{cat}/K_m of ecFabF R206G was detected with k_{cat} and K_m values of 2.1 ± 0.01 min^{-1} and 47.9 ± 17 μM when varying the concentration of malonyl-CoA at a fixed concentration of lauroyl-CoA (100 μM) (**Figure 2.19)**. The increase in k_{cat}/K_m of ecFabF results mainly from an effect on K_m, suggesting that R206 was preventing favorable binding of CoA.

In addition, a second arginine in ecFabH, R229 has been determined as important for binding to α-helix 2 of ACP. Upon alignment of the ecFabH and KasA structures, R214 in KasA and R229 in ecFabH are at a similar distance to the active site. To test the hypothesis that R214 is important for α-helix 2 binding, we made an R214G mutant. A ten fold decrease in k_{cat}/K_m was detected with R214G KasA with k_{cat} and K_m values of 8 ± 0.02 min^{-1} and 16.6 ± 2 μM when varying the concentration of malonyl-CoA at a fixed concentration of palmitoyl-AcpM (15 μM) (**Figure 2.20)**, suggesting the involvement of R214 in binding to α-helix 2.

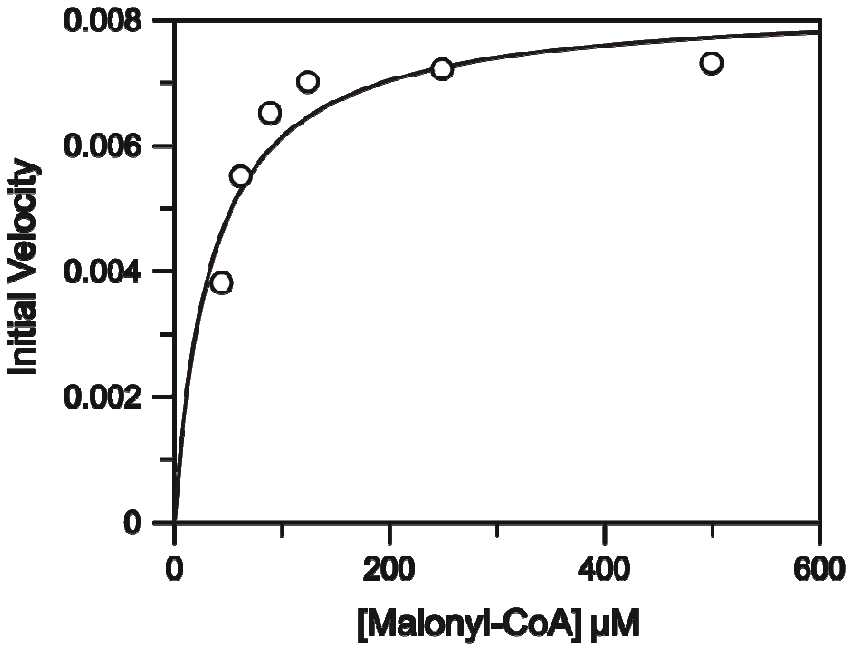

Figure 2.19: Kinetic Analysis of R206G ecFabF for Malonyl-CoA. The initial velocities of product formation were measured with 1 µM ecFabF in the presence of increasing concentrations of malonyl-CoA with respect to 100 µM lauroyl-CoA. k_{cat} and K_m values were determined by fitting the data to the **Equation 1** and **Equation 2** as of 2.1 ± 0.01 min^{-1} and 47.9 ± 17 µM, respectively. The solid line represents the best fit of the data.

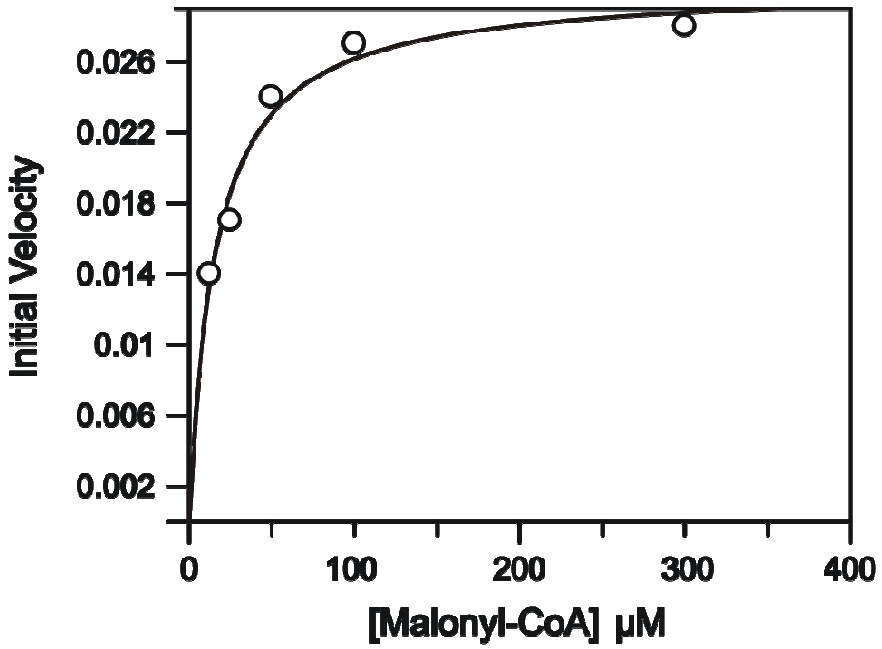

Figure 2.20: Kinetic Analysis of R214G KasA for Malonyl-CoA. The initial velocities of product formation were measured with 500 nM KasA in the presence of increasing concentrations of malonyl-CoA with respect to 15 µM palmitoyl-AcpM. k_{cat} and K_m values were determined by fitting the data to the **Equation 1** and **Equation 2** as of 8 ± 0.02 min^{-1} and 16.6 ± 2 µM, respectively. The solid line represents the best fit of the data.

Kinetic Characterization of KAS Enzymes with Malonyl-phosphopantetheine

To explore minimum requirements for catalysis, malonyl-phosphopantetheine (MalPPant) was synthesized **(Scheme 1)** and tested for activity against ecFabF, ecFabB and KasA using a coupled assay with MabA. It did not show activity with ecFabB when using a fixed concentration of lauroyl-CoA nor with KasA when using a fixed

concentration of palmitoyl-AcpM. However, it did show activity with ecFabF with k_{cat} and K_m values of 1.33 ± 0.03 min^{-1} and 590 ± 133 µM, respectively when MalPPant was varied at a fixed concentration of lauroyl-CoA (100 µM, **Table 2.3, Figure 2.21**). The kinetic parameters were similar to those of malonyl-CoA indicating no improvement on specificity.

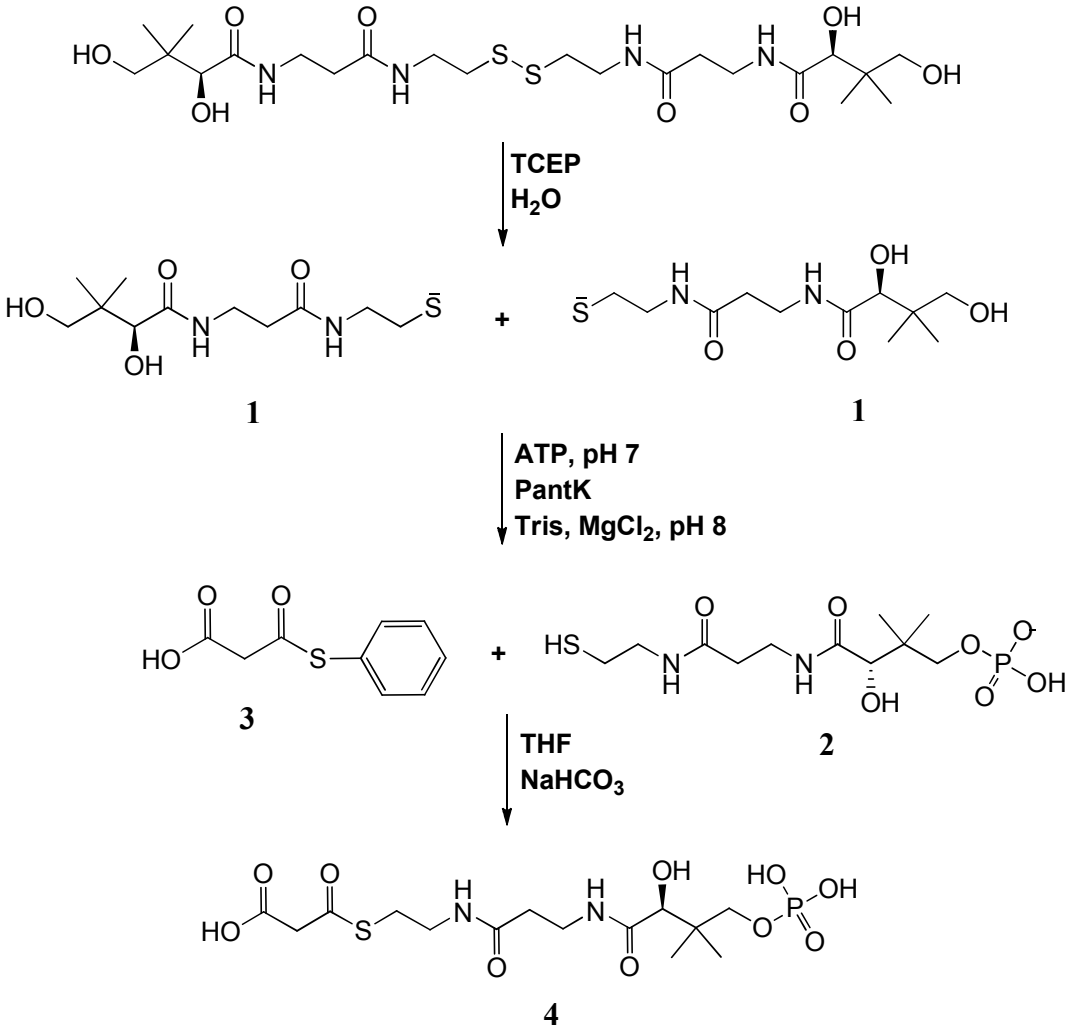

Scheme 1: Synthesis of Malonyl-phosphopantetheine

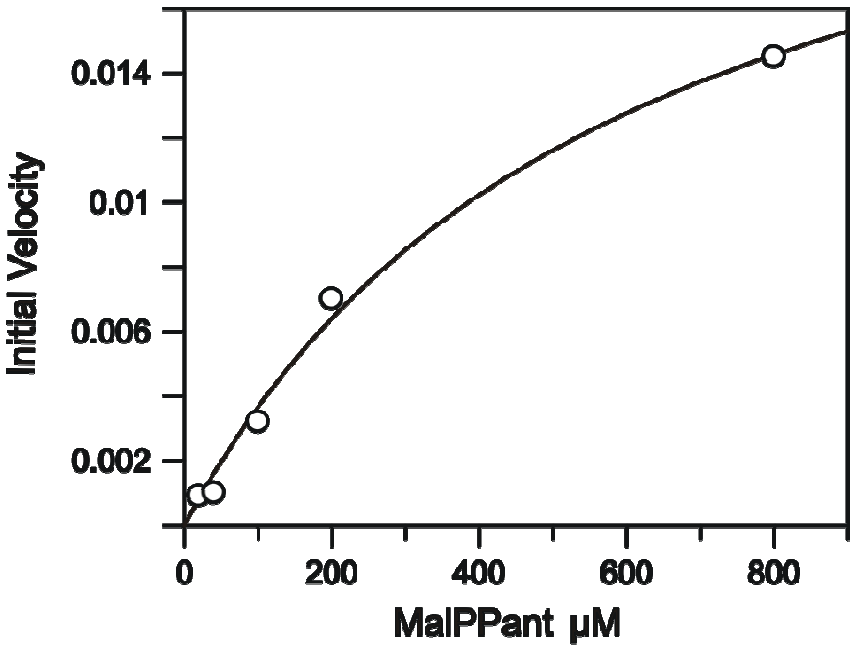

Figure 2.21: Kinetic Analysis of ecFabF for MalPPant. The initial velocities of product formation were measured with 3 µM ecFabF in the presence of increasing concentrations of MalPPant with respect to 100 µM lauroyl-CoA. k_{cat} and K_m values were determined by fitting the data to the **Equation 1** and **Equation 2** as of 1.33 ± 0.03 min^{-1} and 590 ± 133 µM, respectively. The solid line represents the best fit of the data.

Kinetic Characterization of KAS Enzymes with Short Peptide Mimics of ACP

Since removing the adenine and ribose of a CoA substrate did not improve specificity towards the KAS enzymes, a different approach was used to explore the minimal substrate requirements for catalysis. This involved synthesizing short peptide substrates of 8 (DSLDMLEI), 14 (DSLSMLEIAVQTED) and 16 (DPDSLSMLEIAVQTED) residues. The peptides were designed to mimic α-helix 2 of AcpM

(DSLSMVEIAVQTED), which resulted in a 75-90% sequence homology between AcpM and the peptide mimics **(Table 2.6)**. The underlined residue in the previous sequences is the conserved serine that the PPant chain is attached to.

Table 2.6: Sequence Homology of α-helix 2 between ACPs

Protein	Sequence of α-helix 2	Percent homology to peptide mimic
ecACP	DSLDTVELVMALEE	36
AcpM	DSLSMVEIAVQTED	90
Peptide mimic	DSLSMLEIAVQTED	100

All peptides were recognized and post-translationally converted to the respective MalPPant or palmitoyl-phosphopantetheine (PalmPPant) peptide substrate by AcpS **(Figure 2.22)** (*54*). The circular dichroism spectrum of the MalPPant-14mer indicated it did not have any secondary structure and was mostly a random coil which was expected since ACP is extremely flexible in solution. Even so, we designed a peptide with a beginning sequence starting with an aspartic acid followed by a proline which is known to enhance stabilization of α-helical structure (*64*) , as was seen in the CD spectra of MalPPant-16mer. The spectra indicated slight alpha helical content showing characteristic minima at 222 and 208 (**Figure 2.23, 2.24**). The activity of the KAS enzymes with the peptide substrates was assayed in a similar fashion as with ACP and

CoA substrates, where the kinetic parameters were determined by monitoring the NADPH-dependent reduction of the β-ketoacyl product in a coupled assay with MabA.

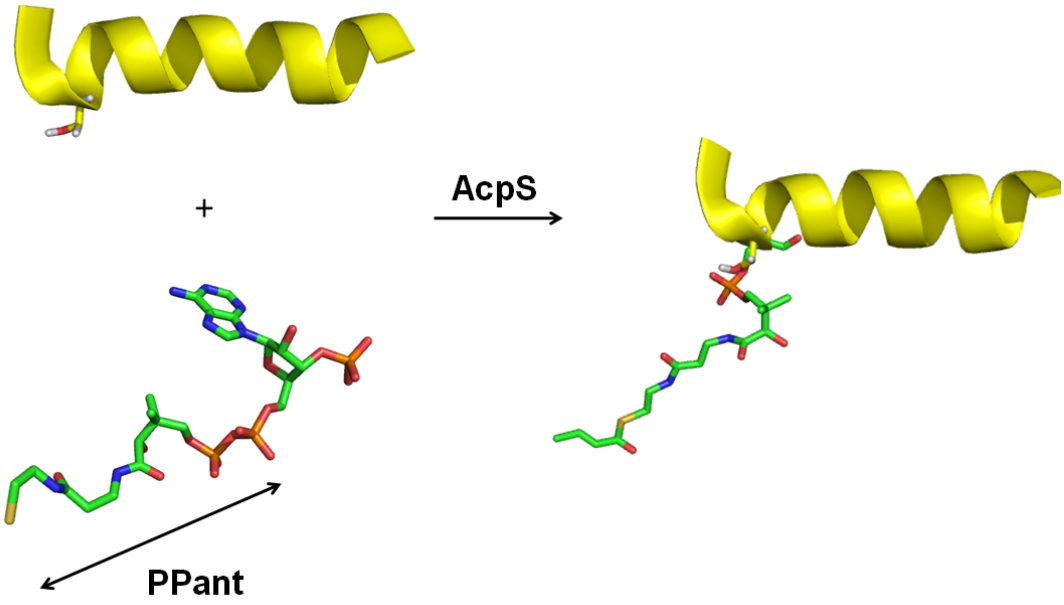

Figure 2.22: Phosphopantethenylation Reaction Catalyzed by AcpS.

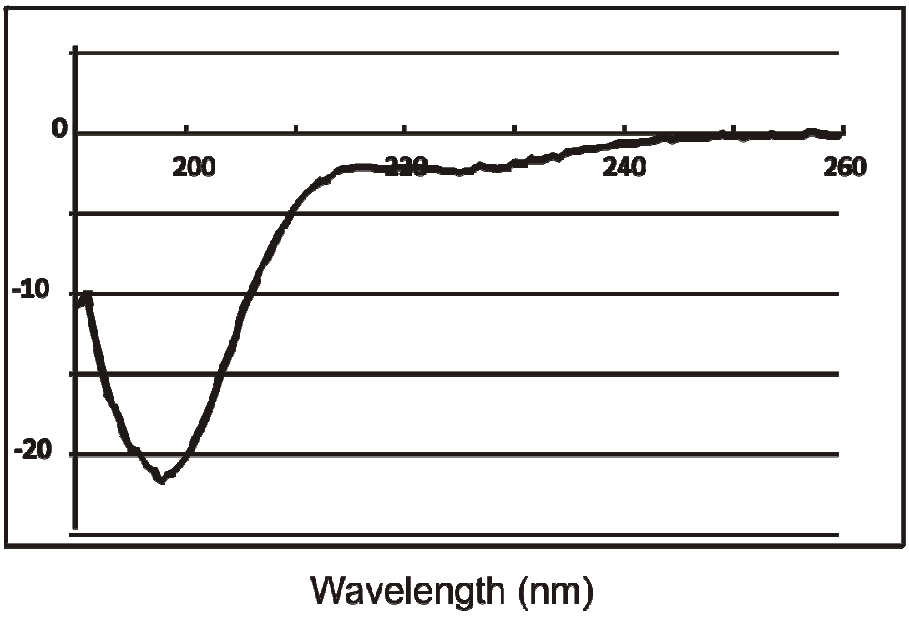

Figure 2.23: CD Spectra of MalPPant-14mer. The spectrum was collected at 25ºC with 75 µM MalPPant-14mer in 50 mM Tris buffer, 0.1% NH_4OH, pH 6.5.

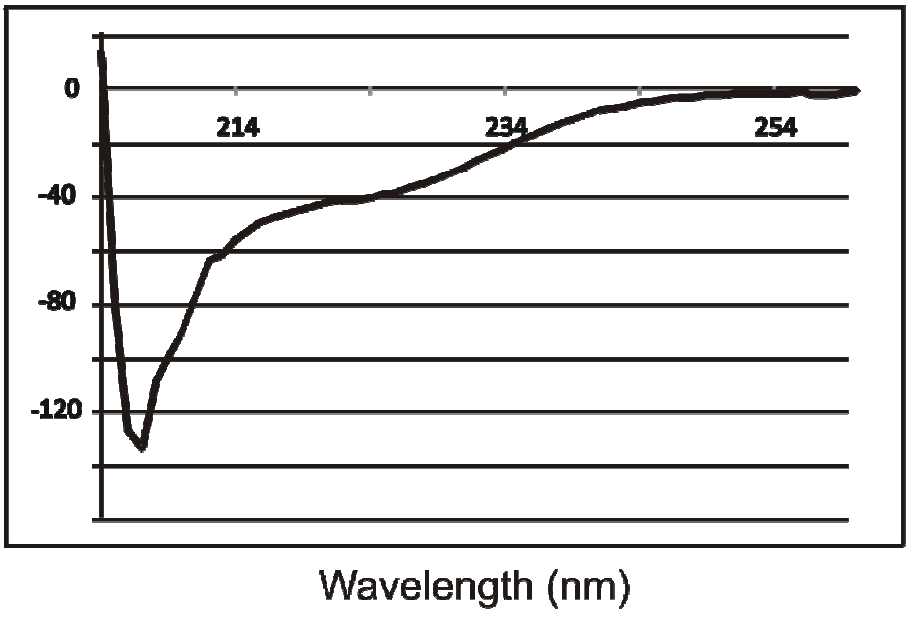

Figure 2.24: CD Spectra of MalPPant-16mer. The spectrum was collected at 25ºC with 75 µM MalPPant-16mer in 50 mM Tris buffer, 0.1% NH_4OH, pH 6.5.

ecFabF Activity with Peptide Mimics

All peptide substrates were first assayed with ecFabF. MalPPant-8mer, MalPPant-14mer and MalPPant-16mer exhibited activity with k_{cat} values of 1.11 ± 0.02 min^{-1}, 1.36 ± 0.03 min^{-1}, 1.34 ± 0.01 min^{-1} and K_m values of 23.7 ± 4.8 µM, 6.10 ± 1.50 µM and 6.2 ± 1.4 µM respectively, when the peptide based substrates were varied at a fixed concentration of lauroyl-CoA (100 µM). The k_{cat}/K_m with the peptides increased 50 fold relative to malonyl-CoA, resulting primarily from an effect on K_m **(Table 2.2, Figure 2.25, 2.26, 2.27)**. In addition, the k_{cat}/K_m of MalPPant-14mer is nearly identical to malonyl-ecACP, indicating the peptide can efficiently replace ACP.

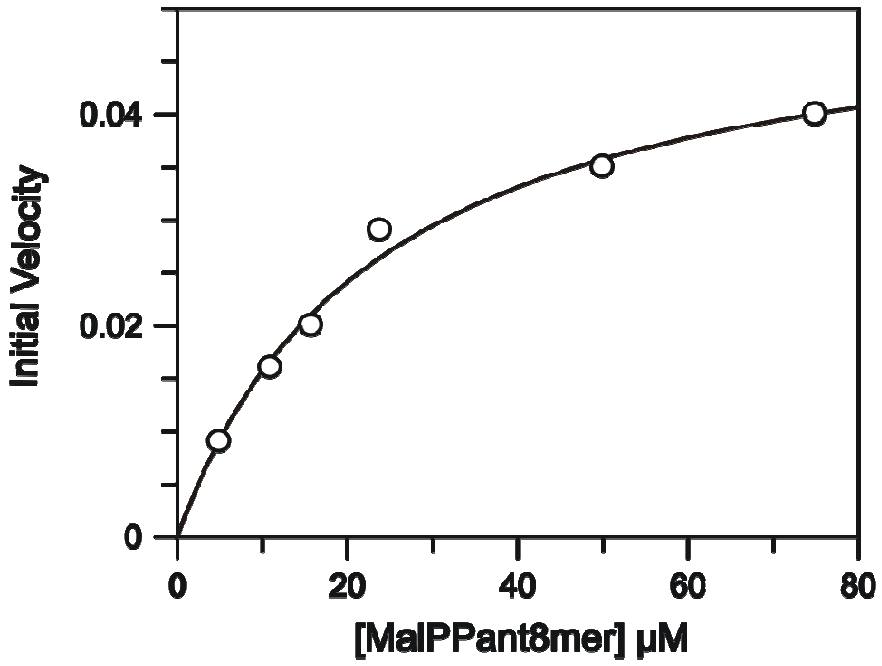

Figure 2.25: Kinetic Analysis of ecFabF for MalPPant-8mer. The initial velocities of product formation were measured with 7.5 µM ecFabF in the presence of increasing concentrations of MalPPant-8mer with respect to 100 µM lauroyl-CoA. k_{cat} and K_m values were determined by fitting the data to the **Equation 1** and **Equation 2** as of 1.11 ± 0.02 min^{-1} and 23.7 ± 5.22 µM, respectively. The solid line represents the best fit of the data.

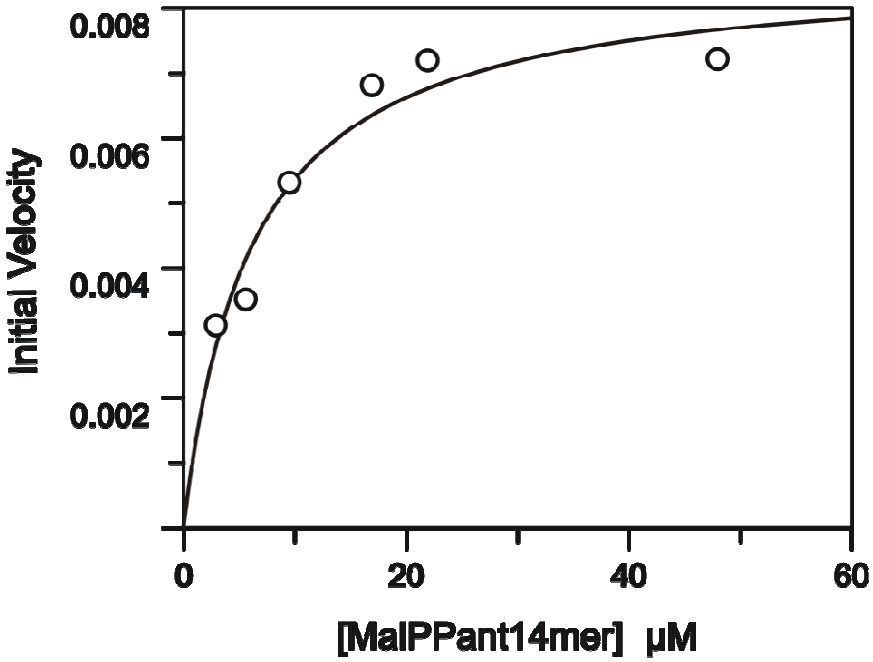

Figure 2.26: Kinetic Analysis of ecFabF for MalPPant-14mer. The initial velocities of product formation were measured with 1 µM ecFabF in the presence of increasing concentrations of MalPPant-14mer with respect to 100 µM lauroyl-CoA. k_{cat} and K_m values were determined by fitting the data to the **Equation 1** and **Equation 2** as of 1.36 ± 0.03 min^{-1} and 6.1 ± 1.5 µM, respectively. The solid line represents the best fit of the data.

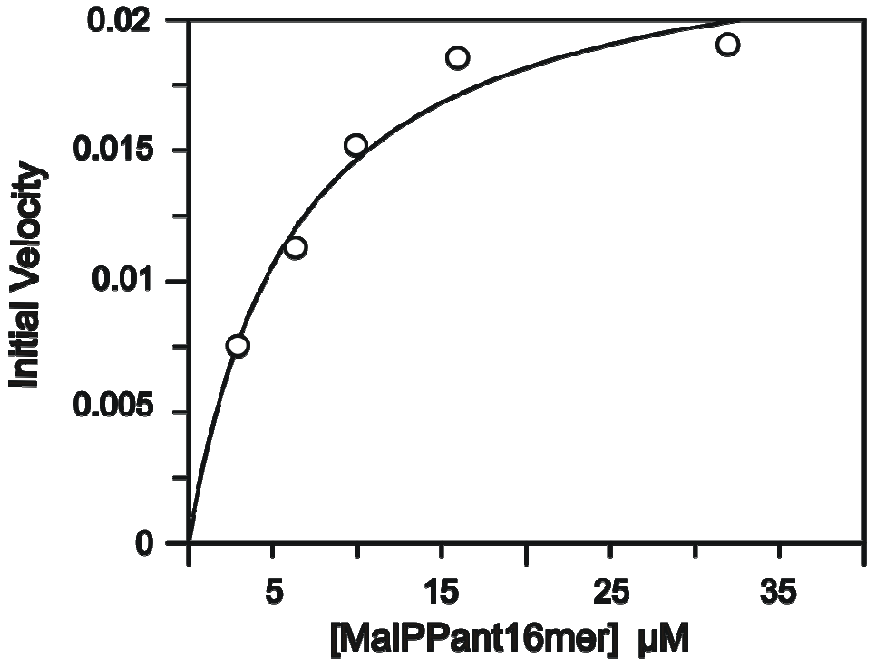

Figure 2.27: Kinetic Analysis of ecFabF for MalPPant-16mer. The initial velocities of product formation were measured with 3 µM ecFabF in the presence of increasing concentrations of MalPPant-16mer with respect to 100 µM lauroyl-CoA. k_{cat} and K_m values were determined by fitting the data to the **Equation 1** and **Equation 2** as of 1.34 ± 0.01 min^{-1} and 6.2 ± 1.4 µM, respectively. The solid line represents the best fit of the data.

ecFabB Activity with Peptide Mimics

In addition, MalPPant-8mer, MalPPant-14mer and MalPPant-16mer also exhibited activity with ecFabB with k_{cat} values of 1.13 ± 0.02 min^{-1}, 2.4 ± 0.01 min^{-1}, 6.5 ± 0.02 min^{-1} and K_m values of 14.2 ± 2.5 µM, 15.8 ± 6.0 µM and 29 ± 5.5 µM respectively when the peptide based substrates were varied at a fixed concentration of lauroyl-ecACP (10 µM, **Table 2.3, Figure 2.28, 2.29, 2.30**). In comparison to malonyl-ecACP, the k_{cat}/K_m with MalPPant-16mer and malonyl-CoA are 3 and 10 fold lower, respectively, when lauroyl-ecACP is used as the donor. This indicates that as long as ACP is used as the donor substrate, ecFabB has a lack of discrimination for the acceptor substrate.

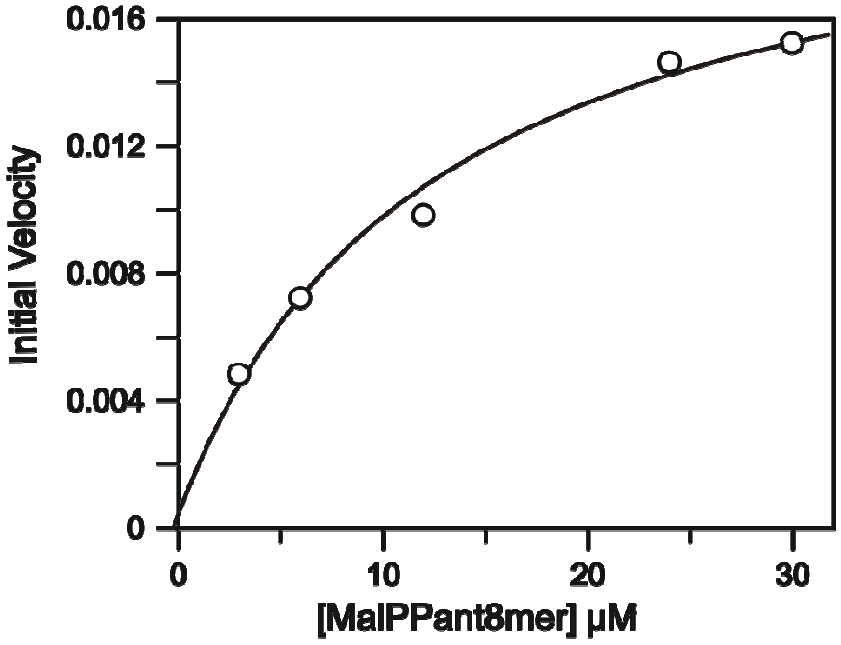

Figure 2.28: Kinetic Analysis of ecFabB for MalPPant-8mer. The initial velocities of product formation were measured with 3 µM ecFabB in the presence of increasing concentrations of MalPPant-8mer with respect to 10 µM lauroyl-ecACP. k_{cat} and K_m values were determined by fitting the data to the **Equation 1** and **Equation 2** as of 1.13 ± 0.02 min^{-1} and 14.2 ± 2.5 µM, respectively. The solid line represents the best fit of the data.

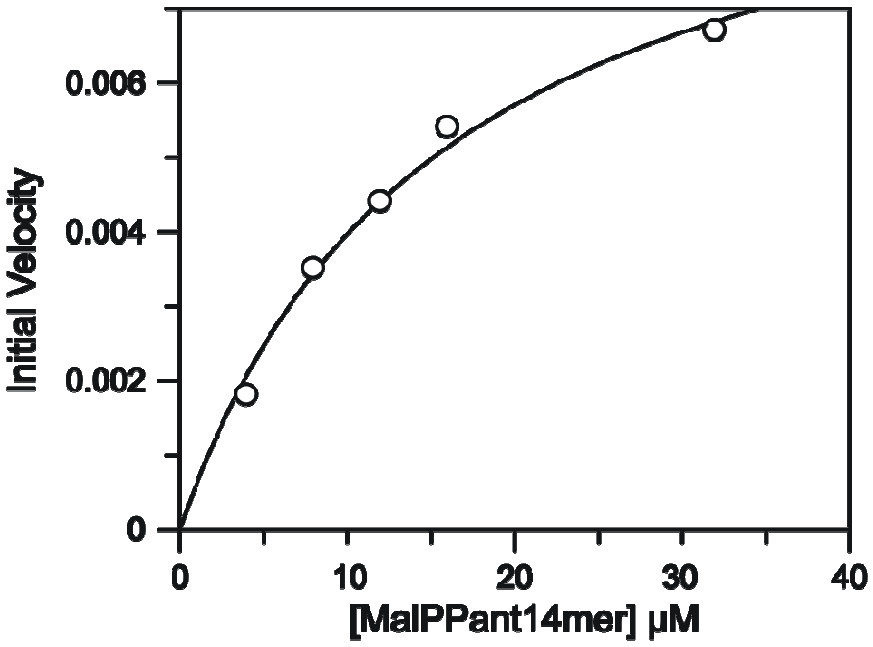

Figure 2.29: Kinetic Analysis of ecFabB for MalPPant-14mer. The initial velocities of product formation were measured with 670 nM ecFabB in the presence of increasing concentrations of MalPPant-14mer with respect to 10 µM lauroyl-ecACP. k_{cat} and K_m values were determined by fitting the data to the **Equation 1** and **Equation 2** as of 2.4 ± 0.01 min^{-1} and 15.8 ± 6 µM, respectively. The solid line represents the best fit of the data.

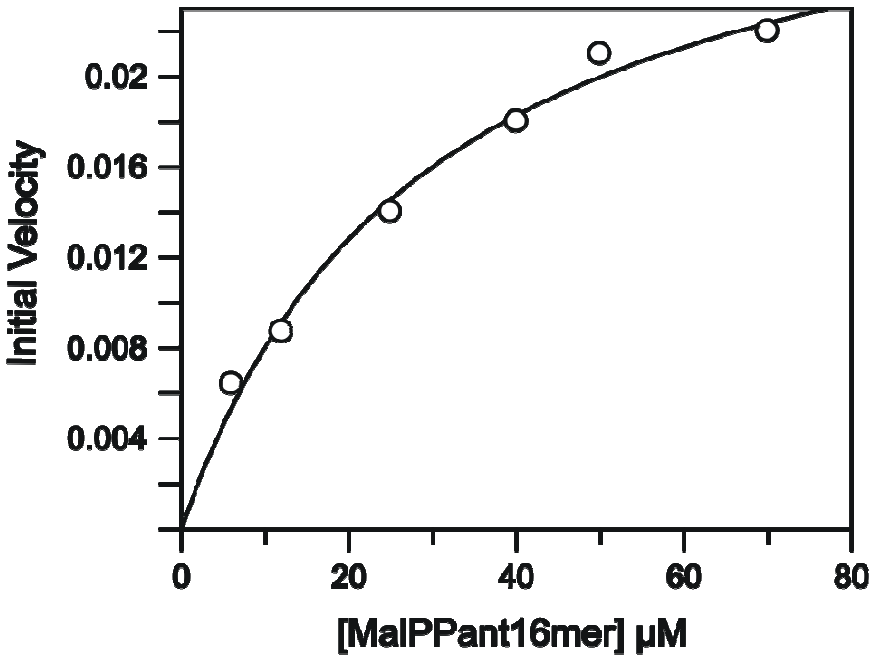

Figure 2.30: Kinetic Analysis of ecFabB for MalPPant-16mer. The initial velocities of product formation were measured with 770 nM ecFabB in the presence of increasing concentrations of MalPPant-16mer with respect to 10 µM lauroyl-ecACP. k_{cat} and K_m values were determined by fitting the data to the **Equation 1** and **Equation 2** as of 6.5 ± 0.02 min^{-1} and 29 ± 5.5 µM, respectively. The solid line represents the best fit of the data.

KasA Activity with Peptide Mimics

Lastly, MalPPant-8mer, MalPPant-14mer, MalPPant-16mer were shown to be substrates of KasA with k_{cat} values of 21 ± 1.5 min^{-1}, 23 ± 1 min^{-1}, 18 ± 0.7 min^{-1} and K_m values of 4.7 ± 1.5 µM, 8.6 ± 1.9 µM and 5.1 ± 0.6 µM respectively, when the peptide based substrates were varied at a fixed concentration of palmitoyl-AcpM (12 µM, **Table 2.4, Figure 2.31, 2.32, 2.33**). Similar to ecFabB, the small variation of k_{cat}/K_m values between the acceptor substrates indicate a lack of preference for the acceptor molecule as long as AcpM is present. We were also interested in knowing if the peptide mimics could be an efficient substitute for AcpM. To address this, KasA was assayed with one peptide substrate and one CoA substrate. KasA activity was not detected with an acyl-peptide and malonyl-CoA or with malonyl-peptide and acyl-CoA. To be certain this was not an effect of using an acyl peptide as the donor molecule, the enzyme was assayed using the acyl peptide and malonyl-AcpM, which showed activity. Together these results indicate the absolute requirement for at least one AcpM based substrate.

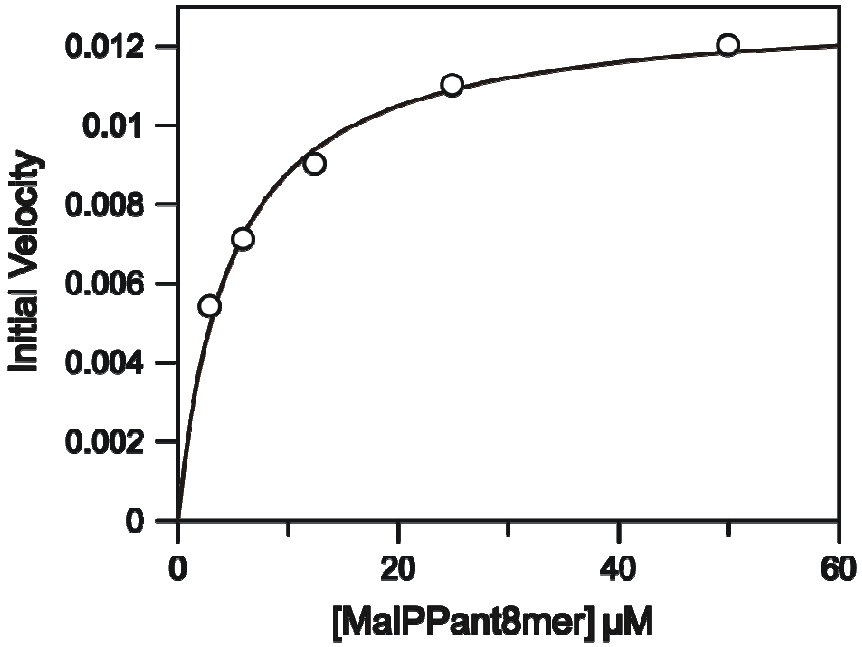

Figure 2.31: Kinetic Analysis of KasA for MalPPant-8mer. The initial velocities of product formation were measured with 100 nM KasA in the presence of increasing concentrations of MalPPant-8mer with respect to 12 µM palmitoyl-AcpM. k_{cat} and K_m values were determined by fitting the data to the **Equation 1** and **Equation 2** as of 21 ± 0.01 min^{-1} and 4.7 ± 0.6 µM, respectively. The solid line represents the best fit of the data.

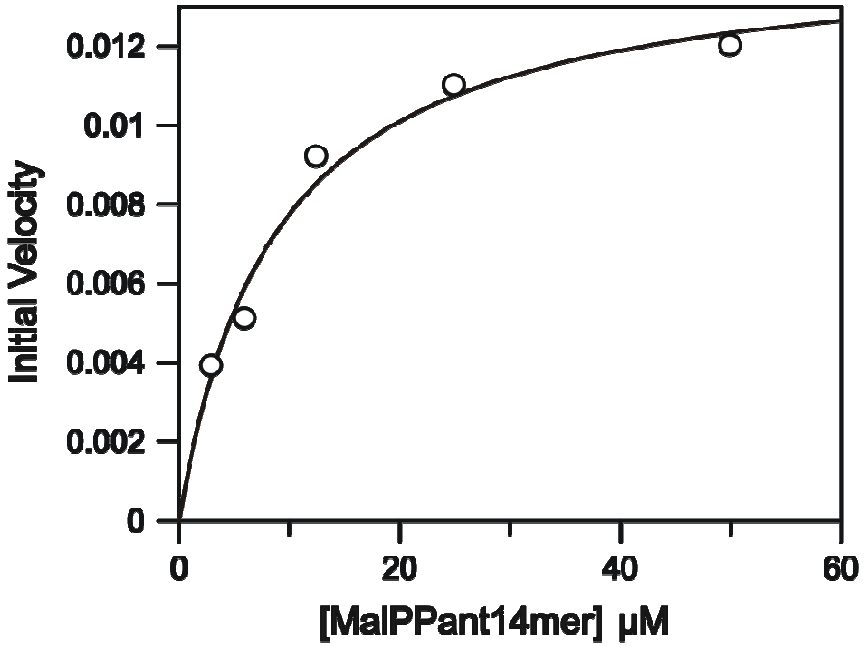

Figure 2.32: Kinetic Analysis of KasA for MalPPant-14mer. The initial velocities of product formation were measured with 100 nM KasA in the presence of increasing concentrations of MalPPant-14mer with respect to 12 µM palmitoyl-AcpM. k_{cat} and K_m values were determined by fitting the data to the **Equation 1** and **Equation 2** as of 23 ± 0.02 min^{-1} and 8.6 ± 1.9 µM, respectively. The solid line represents the best fit of the data.

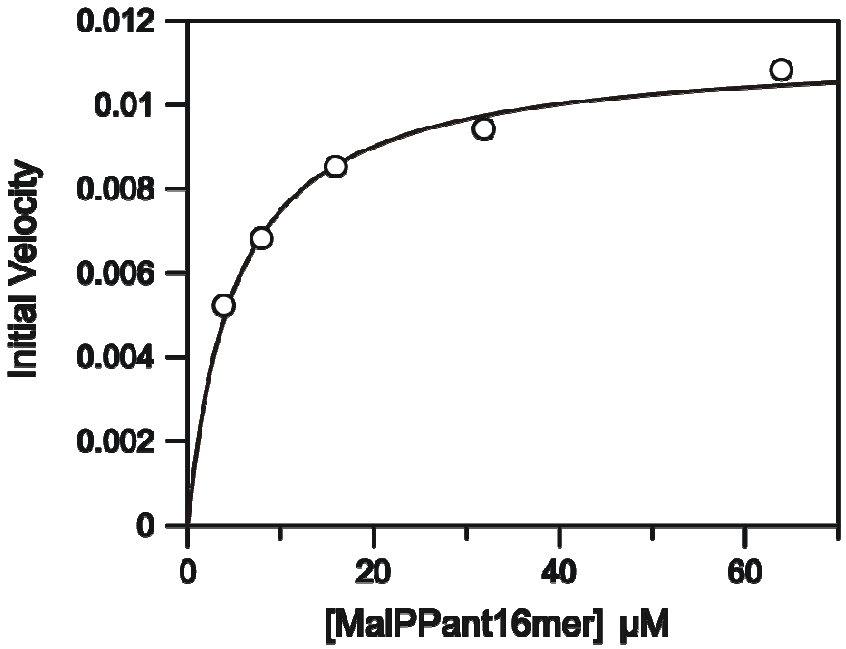

Figure 2.33: Kinetic Analysis of KasA for MalPPant-16mer. The initial velocities of product formation were measured with 100 nM KasA in the presence of increasing concentrations of MalPPant-16mer with respect to 12 µM palmitoyl-AcpM. k_{cat} and K_m values were determined by fitting the data to the **Equation 1** and **Equation 2** as of 18 ± 0.01 min^{-1} and 5.1 ± 0.6 µM, respectively. The solid line represents the best fit of the data.

Discussion

Fatty acid synthase enzymes in bacteria differ significantly from their eukaryotic counterparts. Hence, they have been studied extensively as potential drug targets for the discovery of novel chemotherapeutics. A key feature of the FASII system is the substrates are shuttled between the FASII enzymes by ACP. While the KAS enzyme(s) involved in fatty acid elongation (KASI and KASII) utilize ACP-based substrates, the priming KAS enzyme (KASIII) is initially acylated by an acyl-CoA substrate. In order to compare and contrast the specificity of KASI/II and KASIII for the substrate carrier, we have synthesized substrates based on PPant, CoA, ACP and ACP peptide mimics (**Figure 2.34)**, and explored their interactions with the KASI enzyme from *M. tuberculosis* (KasA) as well as with the KASI and KASII enzymes from *E. coli* (ecFabB and ecFabF).

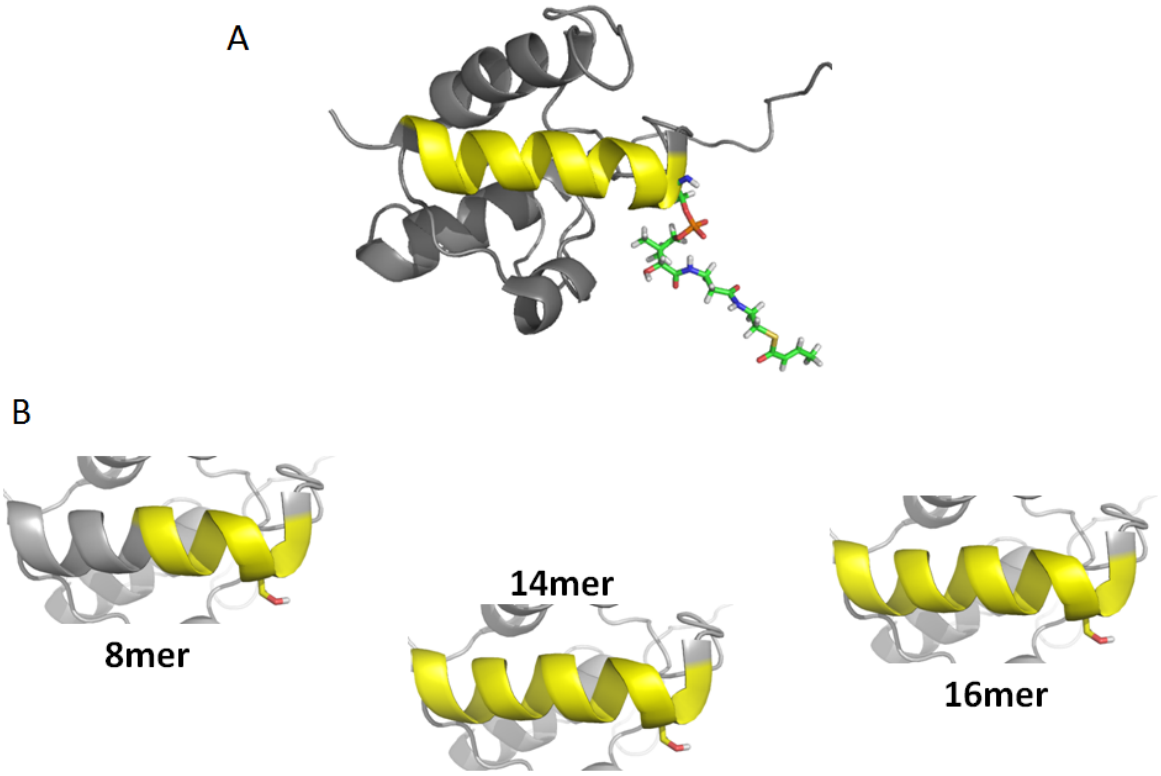

Figure 2.34: Synthesized AcpM Peptide Mimic.

Typically in CoA binding proteins, the phosphate groups are stabilized by surrounding basic residues. CoA is further stabilized by amino acids within hydrogen bonding distance to the adenine and PPant group. In ACP binding proteins, acidic residues from ACP α-helix 2 have been shown to interact with basic residues on the surface of the protein (*53, 68*). The specific structural changes that have occurred resulting in the preference of ACP over CoA are still unclear throughout KASI and KASII enzymes. However, substrate specificity has been well characterized in ecFabH

(KASIII), a protein evolved to bind ACP and CoA with similar affinity. Structural analysis of CoA bound to ecFabH resulted in the identification of R249, which functions to stabilize CoA through an interaction with the pyrophosphate group. ecFabF discriminates against CoA through a 50 fold weaker binding over ACP. Although there is no published crystal structure for the interaction of ecFabF and either ACP or CoA, Reynolds *et al* solved the structure of CoA bound to ecFabH (*7*). By aligning the structures of ecFabH with that of ecFabF, we were able to postulate the binding site of CoA. Upon examination of the proposed binding structure, R249 of ecFabH is replaced by a P308 in ecFabF **(Figure 2.35b)**. This substitution prevents ecFabF from providing the required stabilization to the pyrophosphate group of CoA thus affording the first clues toward elucidating the discriminatory nature of the protein. This is supported by Smith *et al* who identified evolutionary evidence that the replacement of an arginine normally required to stabilize the pyrophosphate of CoA with a tyrosine resulted in the discrimination of the ACP-specific decarboxylase, CurF, to select against CoA based substrates (*69*).

In addition, when overlaying the structures of ecFabH and ecFabF, the position of a second arginine stood out as playing an important role in selectivity against CoA. In ecFabH, R151 is in the correct position to form contacts with the adenine portion of CoA. However, in ecFabF, R206 is clearly forming an unfavorable interaction with the ribose portion of CoA and therefore unable to form the same contacts as ecFabH with the adenine **(Figure 2.35a).** In order to determine if R206 was preventing efficient binding of CoA we developed an R206G mutant. Upon removal of the steric hindrance posed by R206, the catalytic efficiency of ecFabF for malonyl-CoA at a constant

concentration of lauroyl-CoA increased 10 fold, supporting our hypothesis that R206 was preventing favorable binding of CoA, thus elucidating the mechanism for discrimination even further.

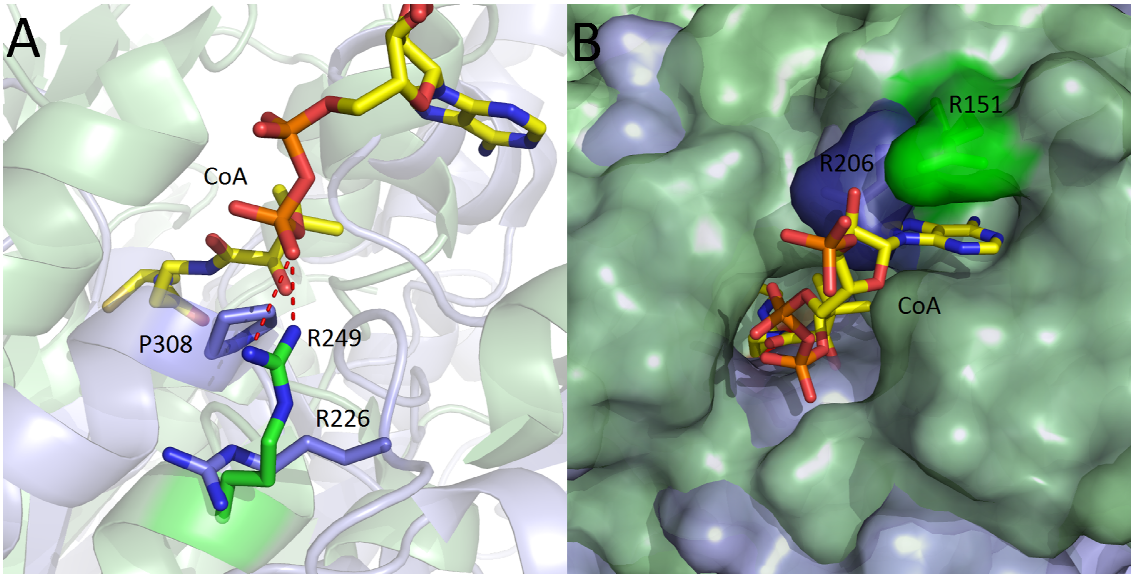

Figure 2.35: Structure of ecFabH-CoA complex superimposed with ecFabF. (a) Comparison between CoA binding with R206 of ecFabF (blue) and R151 of ecFabH (green), where R206 appears to be hindering binding and R151 is clearly stabilizing CoA binding. (b) While R249 in ecFabH (green) forms an interaction to the pyrophosphate of the PPant chain, R226 in ecFabF (blue) is flipped 90 degrees and replaced by P308, preventing bond formation to the pyrophophate of CoA. This figure was made using PyMol and the PDB entries 2eft (ecFabH), 2gfw (ecFabF)

It is also noteworthy to mention that although there are different binding sites in ecFabH for CoA and ACP, R249 (responsible for binding CoA) is also involved in binding an acidic residue on α-helix 2 of ACP. R249 is in close proximity to the active site and to a patch of basic residues also important for ACP binding**.** In ecFabF, R206 is in the same proximity to the active site as R249 in ecFabH and is therefore also likely involved in helix binding **(Figure 2.36b)**.

Similarly to ecFabF, structural analysis of the proposed binding of CoA to KasA and ecFabB also revealed that the side chain of R226 and R234, respectively, is facing away from the pyrophosphate preventing it from performing the same function as R249 in ecFabH. Also as in ecFabF, a proline is sharing the same space as the side chain of R249 in both KasA and ecFabB. The mutant data indicated that R206 in ecFabF is clearly not involved in CoA binding. Consequently, we proposed its involvement in binding to ACP α-helix 2 since it exhibits a similar proximity to the active site as R249, which is responsible for binding α-helix 2 in ecFabH. In KasA and ecFabB, R214 and R45 respectively, are in a similar position and at a similar distance to the active site as R206 and R249 of ecFabF and ecFabH respectively, **(Figure 2.36b**) and we therefore propose they are also important for binding ACP α-helix 2**.** This is supported by the ACP dependent CurF which also contains basic residues flanking the active site that are likely involved in ACP binding (*69*). The importance of these residues was supported by our binding model obtained by docking ecACP to ecFabB where they are located within bonding distance to the pyrophosphate group of ecACP. Since KasA and ecFabF have structural homology to ecFabB, the binding model can be extended to ACP binding interactions with these enzymes as well.

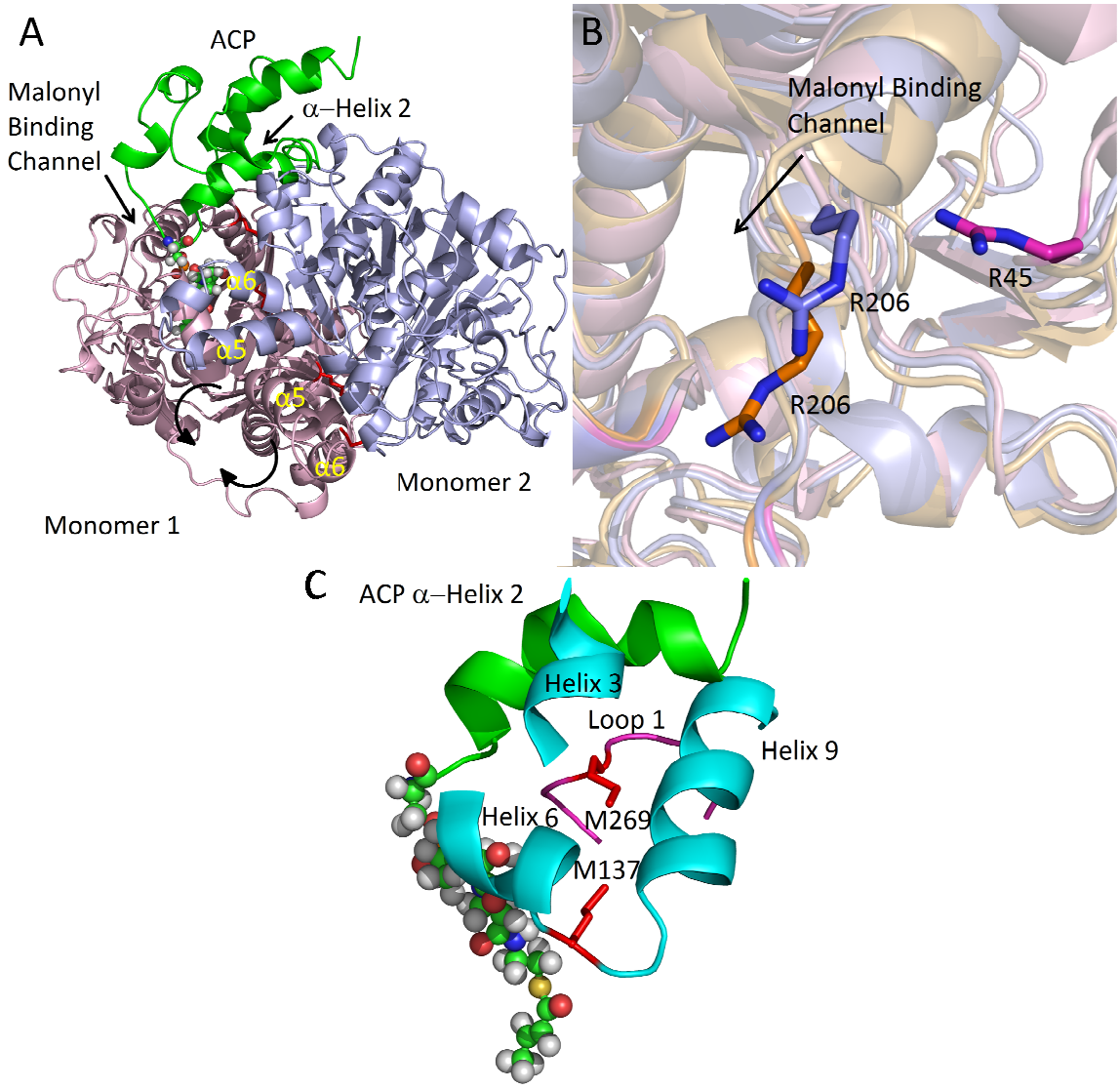

Figure 2.36: Proposed binding interactions between ACP and ecFabB, ecFabF and KasA. (a) Shown is the homodimeric structure of ecFabB. Monomer 1 is colored in blue, monomer 2 is colored in purple and ecACP is colored in green. ACP is shown binding to the interface between the two monomers. Key residues M137 and M269 that link the active site to helices α5 and α6 are shown in red. Arrows indicate the movement of helices α5 and α6 on adjacent subunits upon ACP binding (b) Overlay of ecFabF,

ecFabB and KasA indicating the location of R206, R45 and R214 respectively. All three are in close proximity to the active site and are therefore likely involved in binding to ACP. (c) A detailed view of the locations of the conserved methionines (colored in red), which alter their position upon ACP binding (green) and aid in the transition from free enzyme to the acyl-enzyme. M269 is located in the middle of loop 1 of monomer 1 and M137 is part of helix 6 of monomer 2. ACP is shown interacting with helix 3 and 9 of monomer 1 and loop 1 of monomer 2 of ecFabB. This figure was made using DOCK and PyMoL and the PDB entries 2gfw (ecFabF, blue), 2WGF (KasA, orange) 1FJ4 (ecFabB with TLM) and (ecACP).

ACP and CoA differ by the replacement of AMP with the carrier protein. To determine if the AMP portion of CoA was affecting binding to the KAS enzymes, we synthesized malonyl-PPant. However, the k_{cat}/K_m was similar to that of malonyl-CoA indicating that the AMP portion is not affecting the binding of CoA to ecFabF.

In order to determine the minimum ACP sequence required for recognition and catalysis by the KAS enzymes we synthesized short ACP peptide substrates mimics. For ecFabF, the k_{cat}/K_m of MalPPant-14mer is nearly identical to malonyl-ecACP, indicating that the peptide can effectively replace its activity. This, coupled with the 50 fold increase in k_{cat}/K_m relative to malonyl-CoA indicates binding interactions between ecFabF and ACP α-helix 2 that are important for transition state stabilization.

Unlike ecFabF which shows discrimination against CoA, but does not require the presence of the natural substrate for efficient catalysis, ecFabB and KasA have an

absolute requirement for an ACP substrate as the donor substrate, and provided this requirement was met, variation in the acceptor carrier had only had a small effect on k_{cat}/K_m. We hypothesize that ACP is allosterically interacting with the surface of the protein resulting in a conformational change that facilitates the binding of the second substrate, regardless of the carrier molecule. This is supported by Reynolds *et al* who determined that ecFabH adopts multiple conformations, the distribution of which is influenced by the carrier molecule (*33*). Studies indicate that ecFabH exists in a distribution of conformations where the binding of CoA substrate to one subunit induces a closed conformation and concomitant reduced affinity for CoA substrate binding to the second subunit. This negative cooperatively is only observed in the absence of ACP. This indicates the binding of ACP leads to a disordering of the ecFabH structure and shift in distribution toward a more accessible open form therefore facilitating the binding of the second substrate. In addition, the existence of multiple conformations is further supported by Machutta *et al,* who identified a hinge region in KasA that allows for the adoption of open and closed forms (*58*). The change in position of M137 and M269 between acylated and apo KasA cause helices α5 and α6 to move in a scissor like fashion allowing direct access to the acyl channel where this opening is thought to be further guided by the binding of ACP **(Figure 2.36a, c)**. Our hypothesis parallels these findings where we propose the binding of the donor ACP to the first subunit causes the second subunit to adopt an open conformation resulting in a lower specificity for the acceptor substrate. The binding mechanism would proceed as follows, the first subunit becomes acylated by ACP and while that subunit closes, the second subunit can adopt an open conformation. The acylation of the second subunit by ACP and subsequent

closing allows the first subunit to re-adopt an open conformation allowing the acceptor substrate to bind easily and also facilitate the release of the long hydrophobic product. Interestingly, our binding model generated from docking indicates that ACP is interacting with loop 1, where M269 is located **(Figure 2.36c)**. It is plausible to imagine that the binding of ACP causes M137 to move closer to M269 which subsequently causes the helices to flex. This binding model is in support of our kinetic data where KasA and ecFabB have an absolute requirement for ACP since the residues that are responsible for the hinge movement and thus the presence of multiple conformations are conserved in ecFabB and KasA but not in ecFabF. This suggests that ecFabF can freely adopt open and closed conformations irrespective of ACP binding.

In addition, although the KASIII enzyme in *Escherichia coli* (ecFabH) is essential, the corresponding enzyme in *Mycobacterium tuberculosis* (mtFabH) is not, suggesting that the KASI or II enzyme in *M. tuberculosis* (KasA or KasB, respectively) must be able to accept a CoA donor substrateIn addition, if mtFabH However, our data indicated that KasA undergoes substrate inhibition with palmitoyl-CoA implying that mtFabH is essential.

Our studies demonstrated a clear distinction between the substrate specificity of KASI (ecFabB and KasA) and KASII (ecFabF) enzymes and potentially confirmed mtFabH as essential for the first step in the FASII pathway. In addition, the evolutionary change that resulted in the absolute requirement for ACP for KASI enzymes could also explain why they are essential in *E. coli,* while KASII are not.

Summary

β-Ketoacyl-ACP synthase (KAS) enzymes catalyze Claisen condensation reactions in the fatty acid biosynthesis pathway. These reactions follow a ping-pong mechanism in which a donor substrate acylates the active site KAS cysteine residue after which the acyl group is condensed with the malonyl-ACP acceptor substrate to form a β-ketoacyl-ACP. In the priming KASIII enzymes the donor substrate is an acyl-CoA while in the elongating KASI and KASII enzymes the donor is an acyl-ACP. Although the KASIII enzyme in *Escherichia coli* (ecFabH) is essential, the corresponding enzyme in *Mycobacterium tuberculosis* (mtFabH) is not, suggesting that the KASI or II enzyme in *M. tuberculosis* (KasA or KasB, respectively) must be able to accept a CoA donor substrate. Since KasA is known to be essential we have focused our attention on exploring the substrate specificity of this KASI enzyme using substrates based on phosphopantetheine, CoA, ACP and ACP peptide mimics. This analysis has been extended to the KASI and KASII enzymes from *E. coli* (ecFabB and ecFabF) where we show that a 14 residue malonyl-phosphopantetheine peptide can efficiently replace malonyl-ACP as the acceptor substrate in the ecFabF reaction. While ecFabF is able to catalyze the condensation reaction when CoA is the carrier for both substrates, the KASI enzymes ecFabB and KasA have an absolute requirement for an ACP substrate as the acyl donor. Provided that this requirement is met, variation in the acceptor carrier substrate has little impact on the k_{cat}/K_m for the KASI reaction. For the KASI enzymes we propose that the binding of ACP results in a conformational change that leads to an open form of the enzyme to which the malonyl acceptor substrate binds. In

addition, for KasA substrate inhibition is observed when palmitoyl-CoA is the donor. The implications of these results regarding the essentiality of mtFabH are discussed.

References

1. Haapalainen, A. M., Merilainen, G., and Wierenga, R. K. (2006) The thiolase superfamily: condensing enzymes with diverse reaction specificities, *Trends Biochem Sci 31*, 64-71.
2. Heath, R. J., and Rock, C. O. (2002) The Claisen condensation in biology, *Nat Prod Rep 19*, 581-596.
3. Mathieu, M., Modis, Y., Zeelen, J. P., Engel, C. K., Abagyan, R. A., Ahlberg, A., Rasmussen, B., Lamzin, V. S., Kunau, W. H., and Wierenga, R. K. (1997) The 1.8 A crystal structure of the dimeric peroxisomal 3-ketoacyl-CoA thiolase of Saccharomyces cerevisiae: implications for substrate binding and reaction mechanism, *J Mol Biol 273*, 714-728.
4. Mathieu, M., Zeelen, J. P., Pauptit, R. A., Erdmann, R., Kunau, W. H., and Wierenga, R. K. (1994) The 2.8 A crystal structure of peroxisomal 3-ketoacyl-CoA thiolase of Saccharomyces cerevisiae: a five-layered alpha beta alpha beta alpha structure constructed from two core domains of identical topology, *Structure 2*, 797-808.
5. Davies, C., Heath, R. J., White, S. W., and Rock, C. O. (2000) The 1.8 A crystal structure and active-site architecture of beta-ketoacyl-acyl carrier protein synthase III (FabH) from escherichia coli, *Structure 8*, 185-195.
6. Luckner, S. R., Machutta, C. A., Tonge, P. J., and Kisker, C. (2009) Crystal structures of Mycobacterium tuberculosis KasA show mode of action within cell wall biosynthesis and its inhibition by thiolactomycin, *Structure 17*, 1004-1013.

7. Musayev, F., Sachdeva, S., Scarsdale, J. N., Reynolds, K. A., and Wright, H. T. (2005) Crystal structure of a substrate complex of Mycobacterium tuberculosis beta-ketoacyl-acyl carrier protein synthase III (FabH) with lauroyl-coenzyme A, *J Mol Biol 346*, 1313-1321.

8. Sachdeva, S., and Reynolds, K. A. (2008) Mycobacterium tuberculosis beta-ketoacyl acyl carrier protein synthase III (mtFabH) assay: principles and method, *Methods Mol Med 142*, 205-213.

9. Choi, K. H., Heath, R. J., and Rock, C. O. (2000) beta-ketoacyl-acyl carrier protein synthase III (FabH) is a determining factor in branched-chain fatty acid biosynthesis, *J Bacteriol 182*, 365-370.

10. Choi, K. H., Kremer, L., Besra, G. S., and Rock, C. O. (2000) Identification and substrate specificity of beta -ketoacyl (acyl carrier protein) synthase III (mtFabH) from Mycobacterium tuberculosis, *J Biol Chem 275*, 28201-28207.

11. Heath, R. J., and Rock, C. O. (1996) Inhibition of beta-ketoacyl-acyl carrier protein synthase III (FabH) by acyl-acyl carrier protein in Escherichia coli, *J Biol Chem 271*, 10996-11000.

12. Heath, R. J., and Rock, C. O. (1996) Regulation of fatty acid elongation and initiation by acyl-acyl carrier protein in Escherichia coli, *J Biol Chem 271*, 1833-1836.

13. Jackowski, S., and Rock, C. O. (1987) Acetoacetyl-acyl carrier protein synthase, a potential regulator of fatty acid biosynthesis in bacteria, *J Biol Chem 262*, 7927-7931.

14. Tsay, J. T., Oh, W., Larson, T. J., Jackowski, S., and Rock, C. O. (1992) Isolation and characterization of the beta-ketoacyl-acyl carrier protein synthase III gene (fabH) from Escherichia coli K-12, *J Biol Chem 267*, 6807-6814.

15. Olsen, J. G., Kadziola, A., von Wettstein-Knowles, P., Siggaard-Andersen, M., Lindquist, Y., and Larsen, S. (1999) The X-ray crystal structure of beta-ketoacyl [acyl carrier protein] synthase I, *FEBS Lett 460*, 46-52.

16. Price, A. C., Choi, K. H., Heath, R. J., Li, Z., White, S. W., and Rock, C. O. (2001) Inhibition of beta-ketoacyl-acyl carrier protein synthases by thiolactomycin and cerulenin. Structure and mechanism, *J Biol Chem 276*, 6551-6559.

17. White, S. W., Zheng, J., Zhang, Y. M., and Rock. (2005) The structural biology of type II fatty acid biosynthesis, *Annu Rev Biochem 74*, 791-831.

18. Jez, J. M., and Noel, J. P. (2000) Mechanism of chalcone synthase. pKa of the catalytic cysteine and the role of the conserved histidine in a plant polyketide synthase, *J Biol Chem 275*, 39640-39646.

19. Olsen, J. G., Kadziola, A., von Wettstein-Knowles, P., Siggaard-Andersen, M., and Larsen, S. (2001) Structures of beta-ketoacyl-acyl carrier protein synthase I complexed with fatty acids elucidate its catalytic machinery, *Structure 9*, 233-243.

20. Price, A. C., Rock, C. O., and White, S. W. (2003) The 1.3-Angstrom-resolution crystal structure of beta-ketoacyl-acyl carrier protein synthase II from Streptococcus pneumoniae, *J Bacteriol 185*, 4136-4143.

21. Edwards, P., Nelsen, J. S., Metz, J. G., and Dehesh, K. (1997) Cloning of the fabF gene in an expression vector and in vitro characterization of recombinant fabF and fabB encoded enzymes from Escherichia coli, *FEBS Lett 402*, 62-66.

22. Schaeffer, M. L., Agnihotri, G., Volker, C., Kallender, H., Brennan, P. J., and Lonsdale, J. T. (2001) Purification and biochemical characterization of the Mycobacterium tuberculosis beta-ketoacyl-acyl carrier protein synthases KasA and KasB, *J Biol Chem 276*, 47029-47037.

23. Rosenfeld, I. S., D'Agnolo, G., and Vagelos, P. R. (1973) Synthesis of unsaturated fatty acids and the lesion in fab B mutants, *J Biol Chem 248*, 2452-2460.

24. D'Agnolo, G., Rosenfeld, I. S., and Vagelos, P. R. (1975) Multiple forms of beta-ketoacyl-acyl carrier protein synthetase in Escherichia coli, *J Biol Chem 250*, 5289-5294.

25. Garwin, J. L., Klages, A. L., and Cronan, J. E., Jr. (1980) Beta-ketoacyl-acyl carrier protein synthase II of Escherichia coli. Evidence for function in the thermal regulation of fatty acid synthesis, *J Biol Chem 255*, 3263-3265.

26. de Mendoza, D., Klages Ulrich, A., and Cronan, J. E., Jr. (1983) Thermal regulation of membrane fluidity in Escherichia coli. Effects of overproduction of beta-ketoacyl-acyl carrier protein synthase I, *J Biol Chem 258*, 2098-2101.

27. Bhatt, A., Kremer, L., Dai, A. Z., Sacchettini, J. C., and Jacobs, W. R., Jr. (2005) Conditional depletion of KasA, a key enzyme of mycolic acid biosynthesis, leads to mycobacterial cell lysis, *J Bacteriol 187*, 7596-7606.

28. Slayden, R. A., Lee, R. E., Armour, J. W., Cooper, A. M., Orme, I. M., Brennan, P. J., and Besra, G. S. (1996) Antimycobacterial action of thiolactomycin: an inhibitor of fatty acid and mycolic acid synthesis, *Antimicrob Agents Chemother 40*, 2813-2819.

29. Wang, J., Soisson, S. M., Young, K., Shoop, W., Kodali, S., Galgoci, A., Painter, R., Parthasarathy, G., Tang, Y. S., Cummings, R., Ha, S., Dorso, K., Motyl, M., Jayasuriya, H., Ondeyka, J., Herath, K., Zhang, C., Hernandez, L., Allocco, J., Basilio, A., Tormo, J. R., Genilloud, O., Vicente, F., Pelaez, F., Colwell, L., Lee, S. H., Michael, B., Felcetto, T., Gill, C., Silver, L. L., Hermes, J. D., Bartizal, K., Barrett, J., Schmatz, D., Becker, J. W., Cully, D., and Singh, S. B. (2006) Platensimycin is a selective FabF inhibitor with potent antibiotic properties, *Nature 441*, 358-361.

30. Young, K., Jayasuriya, H., Ondeyka, J. G., Herath, K., Zhang, C., Kodali, S., Galgoci, A., Painter, R., Brown-Driver, V., Yamamoto, R., Silver, L. L., Zheng, Y., Ventura, J. I., Sigmund, J., Ha, S., Basilio, A., Vicente, F., Tormo, J. R., Pelaez, F., Youngman, P., Cully, D., Barrett, J. F., Schmatz, D., Singh, S. B., and Wang, J. (2006) Discovery of FabH/FabF inhibitors from natural products, *Antimicrob Agents Chemother 50*, 519-526.

31. Lai, C. Y., and Cronan, J. E. (2003) Beta-ketoacyl-acyl carrier protein synthase III (FabH) is essential for bacterial fatty acid synthesis, *J Biol Chem 278*, 51494-51503.

32. Sassetti, C. M., Boyd, D. H., and Rubin, E. J. (2003) Genes required for mycobacterial growth defined by high density mutagenesis, *Mol Microbiol 48*, 77-84.

33. Alhamadsheh, M. M., Musayev, F., Komissarov, A. A., Sachdeva, S., Wright, H. T., Scarsdale, N., Florova, G., and Reynolds, K. A. (2007) Alkyl-CoA disulfides as inhibitors and mechanistic probes for FabH enzymes, *Chem Biol 14*, 513-524.

34. Magnuson, K., Jackowski, S., Rock, C. O., and Cronan, J. E., Jr. (1993) Regulation of fatty acid biosynthesis in Escherichia coli, *Microbiol Rev 57*, 522-542.

35. Rumley, M. K., Therisod, H., Weissborn, A. C., and Kennedy, E. P. (1992) Mechanisms of regulation of the biosynthesis of membrane-derived oligosaccharides in Escherichia coli, *J Biol Chem 267*, 11806-11810.

36. Shen, B., Summers, R. G., Gramajo, H., Bibb, M. J., and Hutchinson, C. R. (1992) Purification and characterization of the acyl carrier protein of the Streptomyces glaucescens tetracenomycin C polyketide synthase, *J Bacteriol 174*, 3818-3821.

37. Summers, R. G., Ali, A., Shen, B., Wessel, W. A., and Hutchinson, C. R. (1995) Malonyl-coenzyme A:acyl carrier protein acyltransferase of Streptomyces glaucescens: a possible link between fatty acid and polyketide biosynthesis, *Biochemistry 34*, 9389-9402.

38. Therisod, H., Weissborn, A. C., and Kennedy, E. P. (1986) An essential function for acyl carrier protein in the biosynthesis of membrane-derived oligosaccharides of Escherichia coli, *Proc Natl Acad Sci U S A 83*, 7236-7240.

39. Keating, D. H., Carey, M. R., and Cronan, J. E., Jr. (1995) The unmodified (apo) form of Escherichia coli acyl carrier protein is a potent inhibitor of cell growth, *J Biol Chem 270*, 22229-22235.

40. Lambalot, R. H., and Walsh, C. T. (1995) Cloning, overproduction, and characterization of the Escherichia coli holo-acyl carrier protein synthase, *J Biol Chem 270*, 24658-24661.

41. Cryle, M. J., and Schlichting, I. (2008) Structural insights from a P450 Carrier Protein complex reveal how specificity is achieved in the P450(BioI) ACP complex, *Proc Natl Acad Sci U S A 105*, 15696-15701.

42. Holak, T. A., Kearsley, S. K., Kim, Y., and Prestegard, J. H. (1988) Three-dimensional structure of acyl carrier protein determined by NMR pseudoenergy and distance geometry calculations, *Biochemistry 27*, 6135-6142.

43. Kim, Y., and Prestegard, J. H. (1990) Refinement of the NMR structures for acyl carrier protein with scalar coupling data, *Proteins 8*, 377-385.

44. Parris, K. D., Lin, L., Tam, A., Mathew, R., Hixon, J., Stahl, M., Fritz, C. C., Seehra, J., and Somers, W. S. (2000) Crystal structures of substrate binding to Bacillus subtilis holo-(acyl carrier protein) synthase reveal a novel trimeric arrangement of molecules resulting in three active sites, *Structure 8*, 883-895.

45. Ploskon, E., Arthur, C. J., Kanari, A. L., Wattana-amorn, P., Williams, C., Crosby, J., Simpson, T. J., Willis, C. L., and Crump, M. P. (2010) Recognition of intermediate functionality by acyl carrier protein over a complete cycle of fatty acid biosynthesis, *Chem Biol 17*, 776-785.

46. Qiu, X., and Janson, C. A. (2004) Structure of apo acyl carrier protein and a proposal to engineer protein crystallization through metal ions, *Acta Crystallogr D Biol Crystallogr 60*, 1545-1554.

47. Roujeinikova, A., Baldock, C., Simon, W. J., Gilroy, J., Baker, P. J., Stuitje, A. R., Rice, D. W., Slabas, A. R., and Rafferty, J. B. (2002) X-ray crystallographic studies on butyryl-ACP reveal flexibility of the structure around a putative acyl chain binding site, *Structure 10*, 825-835.

48. Roujeinikova, A., Simon, W. J., Gilroy, J., Rice, D. W., Rafferty, J. B., and Slabas, A. R. (2007) Structural studies of fatty acyl-(acyl carrier protein) thioesters reveal a hydrophobic binding cavity that can expand to fit longer substrates, *J Mol Biol 365*, 135-145.

49. Wu, B. N., Zhang, Y. M., Rock, C. O., and Zheng, J. J. (2009) Structural modification of acyl carrier protein by butyryl group, *Protein Sci 18*, 240-246.

50. Xu, G. Y., Tam, A., Lin, L., Hixon, J., Fritz, C. C., and Powers, R. (2001) Solution structure of B. subtilis acyl carrier protein, *Structure 9*, 277-287.

51. Jones, P. J., Cioffi, E. A., and Prestegard, J. H. (1987) [19F]-1H heteronuclear nuclear Overhauser effect studies of the acyl chain-binding site of acyl carrier protein, *J Biol Chem 262*, 8963-8965.

52. Zornetzer, G. A., Fox, B. G., and Markley, J. L. (2006) Solution structures of spinach acyl carrier protein with decanoate and stearate, *Biochemistry 45*, 5217-5227.

53. Zhang, Y. M., Rao, M. S., Heath, R. J., Price, A. C., Olson, A. J., Rock, C. O., and White, S. W. (2001) Identification and analysis of the acyl carrier protein (ACP) docking site on beta-ketoacyl-ACP synthase III, *J Biol Chem 276*, 8231-8238.

54. Zhang, Y. M., Wu, B., Zheng, J., and Rock, C. O. (2003) Key residues responsible for acyl carrier protein and beta-ketoacyl-acyl carrier protein reductase (FabG) interaction, *J Biol Chem 278*, 52935-52943.

55. Yin, J., Straight, P. D., McLoughlin, S. M., Zhou, Z., Lin, A. J., Golan, D. E., Kelleher, N. L., Kolter, R., and Walsh, C. T. (2005) Genetically encoded short

peptide tag for versatile protein labeling by Sfp phosphopantetheinyl transferase, *Proc Natl Acad Sci U S A 102*, 15815-15820.

56. Zhou, Z., Cironi, P., Lin, A. J., Xu, Y., Hrvatin, S., Golan, D. E., Silver, P. A., Walsh, C. T., and Yin, J. (2007) Genetically encoded short peptide tags for orthogonal protein labeling by Sfp and AcpS phosphopantetheinyl transferases, *ACS Chem Biol 2*, 337-346.

57. Zhou, Z., Koglin, A., Wang, Y., McMahon, A. P., and Walsh, C. T. (2008) An eight residue fragment of an acyl carrier protein suffices for post-translational introduction of fluorescent pantetheinyl arms in protein modification in vitro and in vivo, *J Am Chem Soc 130*, 9925-9930.

58. Machutta, C. A., Bommineni, G. R., Luckner, S. R., Kapilashrami, K., Ruzsicska, B., Simmerling, C., Kisker, C., and Tonge, P. J. (2010) Slow onset inhibition of bacterial beta-ketoacyl-acyl carrier protein synthases by thiolactomycin, *J Biol Chem 285*, 6161-6169.

59. Das, S., Kumar, P., Bhor, V., Surolia, A., and Vijayan, M. (2005) Expression, purification, crystallization and preliminary X-ray crystallographic analysis of pantothenate kinase from Mycobacterium tuberculosis, *Acta Crystallogr Sect F Struct Biol Cryst Commun 61*, 65-67.

60. Rawat, R., Whitty, A., and Tonge, P. J. (2003) The isoniazid-NAD adduct is a slow, tight-binding inhibitor of InhA, the Mycobacterium tuberculosis enoyl reductase: adduct affinity and drug resistance, *Proc Natl Acad Sci U S A 100*, 13881-13886.

61. Haas, J. A., Frederick, M. A., and Fox, B. G. (2000) Chemical and posttranslational modification of Escherichia coli acyl carrier protein for preparation of dansyl-acyl carrier proteins, *Protein Expr Purif 20*, 274-284.

62. Nazi, I., Koteva, K. P., and Wright, G. D. (2004) One-pot chemoenzymatic preparation of coenzyme A analogues, *Anal Biochem 324*, 100-105.

63. Wieland. T., a. K., H. . (1953) *Ann. Chem. Liebigs 581*.

64. Cohen-Gonsaud, M., Ducasse, S., Hoh, F., Zerbib, D., Labesse, G., and Quemard, A. (2002) Crystal structure of MabA from Mycobacterium tuberculosis, a reductase involved in long-chain fatty acid biosynthesis, *J Mol Biol 320*, 249-261.

65. Silva, R. G., Rosado, L. A., Santos, D. S., and Basso, L. A. (2008) Mycobacterium tuberculosis beta-ketoacyl-ACP reductase: alpha-secondary kinetic isotope effects and kinetic and equilibrium mechanisms of substrate binding, *Arch Biochem Biophys 471*, 1-10.

66. Schaeffer, M. L., Carson, J. D., Kallender, H., and Lonsdale, J. T. (2004) Development of a scintillation proximity assay for the Mycobacterium tuberculosis KasA and KasB enzymes involved in mycolic acid biosynthesis, *Tuberculosis (Edinb) 84*, 353-360.

67. Hollenbeck, J. J., McClain, D. L., and Oakley, M. G. (2002) The role of helix stabilizing residues in GCN4 basic region folding and DNA binding, *Protein Sci 11*, 2740-2747.

68. Rafi, S., Novichenok, P., Kolappan, S., Zhang, X., Stratton, C. F., Rawat, R., Kisker, C., Simmerling, C., and Tonge, P. J. (2006) Structure of acyl carrier

protein bound to FabI, the FASII enoyl reductase from Escherichia coli, *J Biol Chem 281*, 39285-39293.

69. Geders, T. W., Gu, L., Mowers, J. C., Liu, H., Gerwick, W. H., Hakansson, K., Sherman, D. H., and Smith, J. L. (2007) Crystal structure of the ECH2 catalytic domain of CurF from Lyngbya majuscula. Insights into a decarboxylase involved in polyketide chain beta-branching, *J Biol Chem 282*, 35954-35963.

Chapter III: The Use of Short Lived Isotopes for Exploring Drug Binding Partners in *Mycobacterium Tuberculosis*

Challenges of Identifying Protein Targets

In general, drug design programs are focused on lead optimization and *in vitro* studies focusing on how structural changes introduced into the lead compound affect its interaction with the target and the biological activity of the molecule. A good relationship between target affinity and cellular potency suggests that the compounds bind to the target in the cell. However, the complex cellular environment of cell penetration, efflux and metabolism can complicate the correlation. In addition, biological activity could result from interactions with other targets in the cell. Therefore, identifying drug-target interactions and verifying that the small molecules do in fact bind to the projected target is an important step in order to advance inhibitors through the drug discovery pipeline.

We have developed a novel drug-target identification method that relies on the incorporation of short-lived isotopes such as carbon-11 into clinically approved anti-TB drugs such as rifampicin and isoniazid (INH) along with the alkyl diaryl ether, PT70. Radiolabeling is accomplished without altering the structure of the drug and size exclusion chromatography (SEC) is used to fractionate proteins following exposure to the radiotracer. Proof of concept experiments have revealed a non covalent interaction between *M. smegmatis* protein lysate and ^{11}C-rifampicin, and demonstrated interactions between the enoyl-ACP reductase, FabI, and ^{11}C-INH as well as with the ^{11}C-PT70 FabI inhibitor.

Rifampicin

Rifampicin is a semisynthetic derivative of the macrolide rifamycin, a class of antibiotics that are fermentation products of *Nocardia mediterranei* (*1, 2*). Rifampicin is a broad spectrum antibiotic and is active against mycobacteria and gram-positive organisms at low concentrations (*3*). The drug is now in wide clinical use and has shown particular efficacy against *Mycobacterium tuberculosis* (MTb) (MIC = 0.1-0.2 µg/mL) (*4*). The mechanism of rifampicin has been heavily studied and shown to inhibit DNA-dependent RNA synthesis by binding to the β-subunit of RNA polymerase, thus preventing transcription to RNA and subsequent translation to proteins (*5*). The stability of the rifampicin-RNA polymerase complex is proposed to result from van der Waals interactions between the napthoquinone and nearby aromatic amino acids (*6*). Multi-drug-resistant MTb correlate to mutations in the *rpoB* gene where aromatic amino acids are replaced with non-aromatic amino acids and thereby disrupt the interactions between rifampicin and RNA polymerase (*7*).

Enoyl-ACP Reductase Structure Activity Relationship and Target Validation

Since INH resistance mainly results from a dysfunction in INH activation, compounds that do not depend on activation by the catalase-peroxidase enzyme, KatG but still inhibit the cellular targets are anticipated to be effective against INH resistant MTb. The FASII enoyl-ACP reductase (ER) has been one of the main targets for inhibitor design in a variety of bacteria such as MTb (InhA), *E. coli, S. aureus, P. falciparum* and more recently, *F. tularensis and Burkholderia pseudomallei* (*8-14*). The early classes of ER inhibitors explored were based on substituted piperazines and pyrazoles. The most

potent piperazine possessed an IC_{50} value for InhA of 0.16 µM while the most potent pyrazole showed better efficacy *in vivo*, inhibiting a drug resistant MTb strains with MIC values of 1-30 µM (*12*). Moreover, Tonge *et al* have developed a class of InhA inhibitors based on the biocide triclosan (*9*). Using the SAR data from the ligands binding to the *E. coli* enoyl-ACP reductase, FabI and InhA (previously described in chapter 1), a series of alkyl diaryl ether inhibitors were developed, where the most potent is a slow onset inhibitor of InhA with a K_i^* of 22 pM **(Figure 3.1)**. This inhibitor also exhibited activity against MTb with an MIC of 3 µg/mL (*9*). The alkyl diaryl ethers also possess potency towards 5 additional clinical strains, some of which have mutations in KatG, supporting the theory that compounds can inhibit InhA by a mechanism irrespective of KatG activation. In order to provide evidence that InhA is a potential target for the analogues, an InhA overexpression strain of MTb was exposed to inhibitors which resulted in a 9-12 fold increase in MIC values. In addition, gene dosing experiments showed an increase in *inhA* gene expression supporting the evidence that InhA is targeted in the cell (*9*).

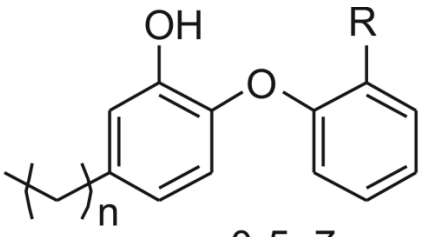

n = 0-5, 7

Inhibitor	Organism	K_i (nM)	MIC (μg/mL)
8PP n = 7, R = H	MTB	1	1-2
PT70 n = 7, R=Me	MTB	0.022	3

Figure 3.1: InhA Inhibitors. Structures of most potent rapid reversible inhibitor 5-octyl-2-phenoxyphenol (8PP) and the slow onset inhibitor 2-(o-tolyloxy)-5-hexylphenol (PT70)

Reactive Species of INH

Isoniazid has been a cornerstone in TB chemotherapy ever since its discovery in 1952 (*15, 16*). The re-emergence of TB in the mid-1980s along with the rising number of INH-resistant strains (*17, 18*) encouraged numerous studies to elucidate its mechanism. Although the exact mechanism is still unclear, it has been established that INH is activated by KatG in MTb, and that mutations in *katG* confer resistance *(19, 20)*. KatG activates INH by peroxidation, utilizing a variety of oxidants, including hydrogen peroxide, superoxide and simple alkyl hydroperoxides (*21-23*). Activation of INH can also be achieved by the addition of exogenous Mn^{2+} or Mn^{3+}, termed autoxidation (*24-26*). Enzyme and metal catalyzed INH oxidation have shown to result in the formation of multiple activated species, mainly isonicotinic acid, but also detectable levels of the aldehyde and amide **(Figure 3.2)** (*27*).

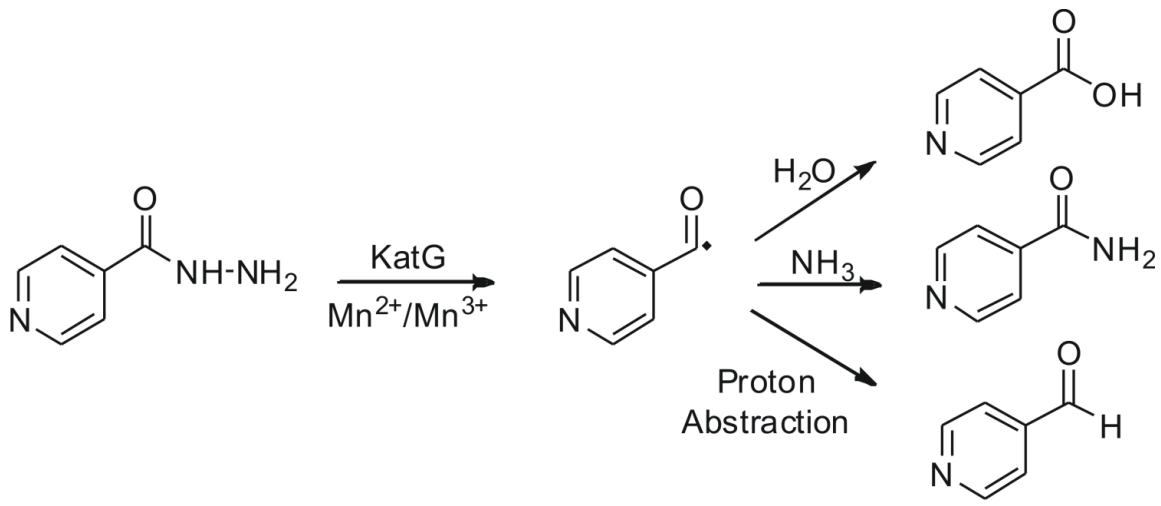

Figure 3.2: INH Oxidation Products. The activation of INH by the endogenous KatG or exogenous Mn^{2+}, Mn^{3+}, results in the formation of a radical on the carbonyl carbon. Shown are the additional oxidation products that are formed (other than the INH-NAD adduct) which include, nicotinic acid, amide and aldehyde.

Mechanism of Action of INH

When NAD(H) is present, the activation of INH leads to the formation of a covalent adduct with the nicotinamide head group of NAD(H) forming the INH-NAD adduct **(Figure 3.3)**. While the definitive target of this adduct has been the subject of much debate, it has been well established that it prevents the synthesis of mycolic acids by inhibiting InhA, the enoyl-ACP reductase of the FASII pathway, leading to an accumulation of hexacosanoic acid (*28-30*). However, there is significant evidence that the mode of action of INH is complex. For instance, through *in vitro* inhibition studies using the purified INH-NAD adduct, Tonge *et al* found no indication that the InhA

mutations correlating with INH resistance *in vivo* affect the affinity of InhA for the adduct (*31*). In addition, the mutations in *inhA* and *katG* that correlate to INH resistance, do not appear to be sufficient to account for all the observed resistance, suggesting that INH interacts with other proteins in the cell (*32*). Barry *et al* discovered an 80 kD complex consisting of KasA, AcpM and INH by analyzing two-dimensional gel electrophoresis protein profiles of MTb that were exposed to low levels of INH treatment (*33*). Subsequently, Blanchard *et al* discovered that an INH-NADP adduct can inhibit other mycobacterial enzymes such as dihydrofolate reductase (*34*). They also employed an affinity purification technique using the INH-NAD adduct, where they identified over 20 proteins that although discovered *in vitro*, have the potential to interact *in vivo (35)*. In addition, transcriptional profiling has revealed that INH treatment resulted in an increase in the expression levels of the *kas* operon that encodes KasA, KasB and AcpM, while there was no affect on the expression of the *mab* operon that encodes InhA and MabA (*36-38*). While extensive evidence proves INH interferes with cell wall biosynthesis by targeting InhA, these data indicate the presence of additional components regulating the action of these drugs. Therefore, it is important to develop new target identification methods in order to elucidate additional drug binding partners in the cell.

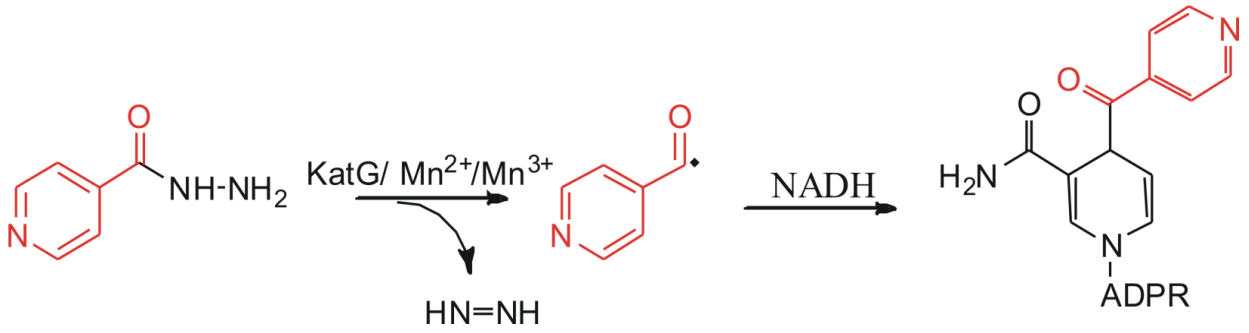

Figure 3.3: Scheme for the Formation of the INH-NAD Adduct. INH can be activated by either KatG or Mn^{2+}, Mn^{3+}, producing a radical intermediate which in turn forms a covalent adduct with the nicotinamide head group of NAD(P)H.

Current Methods to Study Drug Binding Partners

To date, all target identification techniques fall into two main categories: affinity based chromatography where explicit binding events can be identified and phenotype based methods where physiological responses elucidate drug targets/pathways.

Proteomic and Genomic Approaches

Proteomics is widely used to examine the physiological response of cells (*39*). For example, Marcotte *et al* investigated the proteomic response of *M. smegmatis* when exposed to anti-TB drugs, where they were able to identify specific proteins and metabolic pathways that were affected by the drugs (*40*). This method involves the use of quantitative spectrometry which allows the drug induced protein profiles to serve as a depiction of a drug's mode of action. While progress has been made in proteomic research, the technical challenges are still remarkable. For instance, the high number of

modified and unmodified proteins in the cell complicates the analysis of the protein profiles and it is believed that future progress will require innovative discoveries in chemistry, biology, and bioinformatics (*41*).

Oltvai *et al* took a different approach toward improving the target discovery process (*42*). To accomplish this, they combined the methods of genome analysis, network biology and virtual screening. By analyzing bacterial metabolic networks, they identified essential metabolic enzymes in *E. coli*, which they virtually screened against a library of small molecule compounds. The drug targets that were identified were then verified *in vitro*, thus demonstrating the effectiveness of their approach (*42*). Although this method can provide early drug discovery leads, *in vitro* and *in silico* experiments do not reflect a biologically relevant environment.

Affinity Chromatography Using Small Molecules

Another technique used for the determination of drug binding partners in cell utilizes the old but effective method of affinity chromatography. Blanchard *et al* chemically immobilized the INH-NAD(P) adduct to a resin, which resulted in the selective purification of 20 identified proteins that bound to the adduct (*35*). Although affinity chromatography has identified a number of important molecular targets, it is not a commonly used technique for several reasons. Firstly, it is laborious to prepare the affinity reagents and the attachment often entails a chemical modification that may affect the chemical structure and binding properties of the small molecule (*43*). Also, extensive washing of the resin is required to eliminate non specific binding which can decrease the probability of capturing the more weakly bound proteins (*44*).

Drug Affinity Response Target Stability (DARTS)

Non-affinity based target identification is limited due to the reliance on the drugs capability to influence specific cellular and biochemical responses (*45, 46*). Huang *et al* developed a method to overcome this limitation which allows for the direct identification of drug binding targets by exploiting increased stability of the drug bound target to proteolysis (*47*). An advantage of this method is it allows for the identification of the drug target without derivitization or immobilization of the small molecule. However, there are limitations to the DARTS method. For instance, the technique depends on *in vitro* proteolysis using exogenous proteases which is not indicative of the natural more complicated *in vivo* environment (*48*). In addition, an extrinsic limitation of DARTS is the sensitivity limitations of mass spectrometry where the visualization of lower abundance proteins may not be possible.

Positron Emission Tomography and Radioisotopes

Positron emission tomography (PET) is a molecular visualization technique in nuclear medicine that produces an image based on the distribution of a biologically active molecule containing a positron-emitting radionuclide *(49, 50).* During radioactive decay, emitted positrons are annihilated by colliding with electrons, which generates detectable radiation **(Figure 3.4)**. The most commonly used radioisotopes that possess the chemical and physical properties required for PET are those with short half lives, such as carbon-11 (^{11}C), nitrogen-13 (^{13}N), oxygen-15 (^{15}O) and fluorine-18 (^{18}F) **(Table 3.1)** (*51*). Uniquely, the high energy of the annihilation (511 keV) associated with these isotopes result in greater tissue penetration and consequently, better detectability than

the more commonly used technetium-99m (^{99m}Tc) whose annihilation energy is only 140 keV (*52*). Furthermore, by utilizing the attractive characteristics of radioisotopes, the biological pathway of any radiolabeled compound can be traced with high detectability, making the processes and applications that can be explored, virtually limitless.

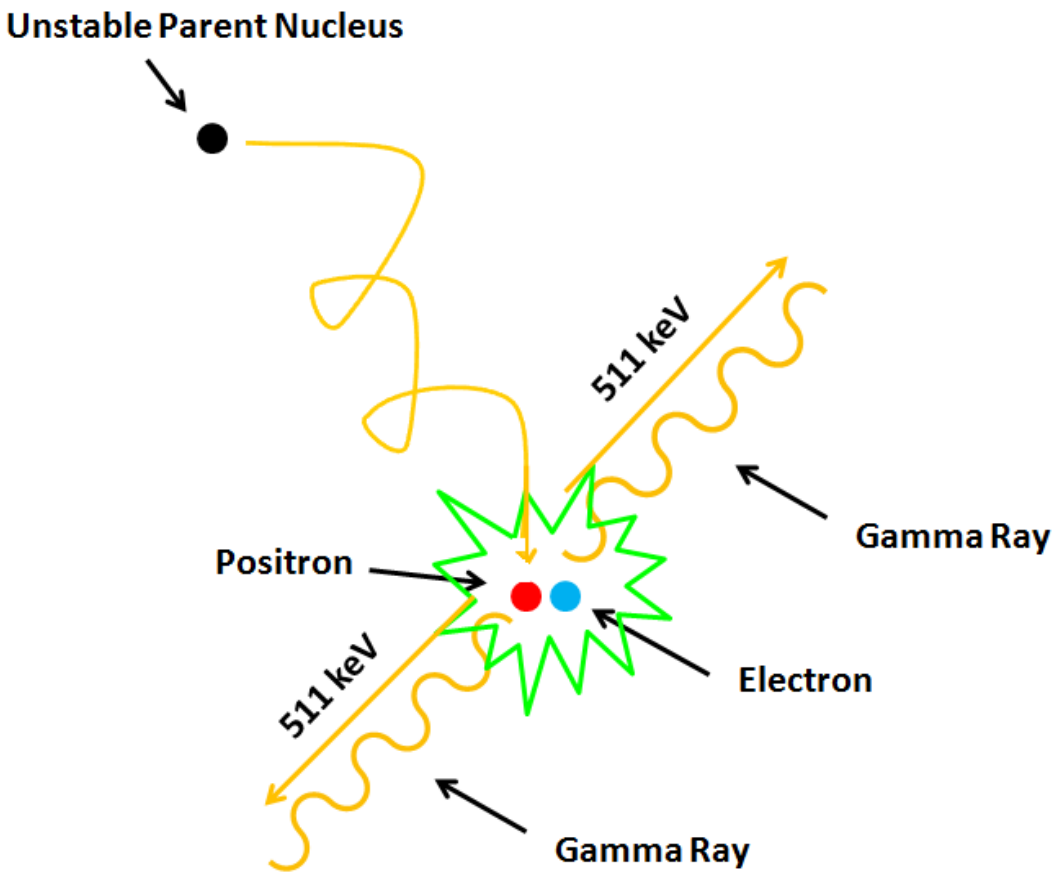

Figure 3.4: Radioactive Decay by Positron Emission. Positively charged electrons (positrons), are emitted from the nucleus of an unstable radionuclide. The positrons quickly lose their kinetic energy and interact with an electron. The positron and electron annihilate one another, resulting in two photons traveling in approximately opposite directions with an energy of 511 keV

Table 3.1: **Short Lived Radioactive Isotopes and Their Half Lives**

	Radio-isotope	Half Life (min)
γ-emitter	^{99m}Tc	6 hrs
β-emitter	^{11}C	20
	^{13}N	10
	^{15}O	2
	^{18}F	110

Incorporation of Short Lived Radioisotopes

In order to bridge the gap in the drug discovery process, we propose a new target identification method which utilizes the attractive characteristics of short lived radioisotopes. This involves incorporating short lived radioisotopes such as ^{11}C and ^{18}F, into small molecules without altering the structure of the molecule. An advantage of this method is that radio-isotopes possess a high specific activity which allows binding events with low abundant proteins to be identified. Also, the constant emission of gamma rays enables real time tracking during protein fractionation methods. Lastly, the incorporation of radioisotopes with short lived half lives facilitates post separation analysis without the concern of radioactivity.

We have incorporated ^{11}C into clinically approved anti-TB drugs, such as rifampicin and INH along with PT70, developed in our lab, resulting in the development of a traceable drug whose structure has been unaltered. Efforts towards identifying new

protein targets along with verifying already known interactions were explored using methods which preserve non-covalent interactions. Early experiments employing SEC combined with native PAGE, revealed a non covalent interaction between *M. smegmatis* protein lysate and ^{11}C-rifampicin. In addition, we were able to detect the ^{11}C-INH-NAD adduct bound to isolated InhA and to *E. coli* protein lysate overexpressing InhA, through SEC with an in line radiation detector. Similarly, we confirmed the genetic and *in vitro* data that the alkyl diaryl ethers inhibit InhA by detecting the binding of ^{11}C-PT70 to isolated InhA.

Materials and Methods

Expression and Purification of InhA

The pET15b vector containing the *InhA* gene with an N-terminal hexahistidine tag, was transformed into E. *coli* pLysS competent cells. Colonies selected on LB solid media containing 200 µg/mL ampicillin were cultivated in LB media and grown to an optical density (OD_{600}) of 1.2, after which protein expression was induced with 0.3 mM isopropyl β-D-thiogalactoside (IPTG). The InhA protein was subsequently purified using standard nickel affinity chromatography followed by chromatography on G-25 resin using a buffer containing 30 mM Pipes, 150 mM NaCl and 1 mM EDTA, pH 6.8. The fractions were analyzed by sodium dodecyl sulfate polyacrylamide gel electrophoresis (SDS-PAGE) and Ultraviolet (UV) visible spectroscopy (monitoring the absorbance at 280 nm) using a Nano Drop ND-1000 spectrophotometer. Protein was stored at -20℃.

The Synthesis of ^{11}C-rifampicin, ^{11}C-INH and ^{11}C-PT70

The ^{11}C labeled compounds shown in **Scheme 3.1, 3.2 and 3.3** were synthesized by Li Lui, a graduate student in the Tonge lab (*53*).

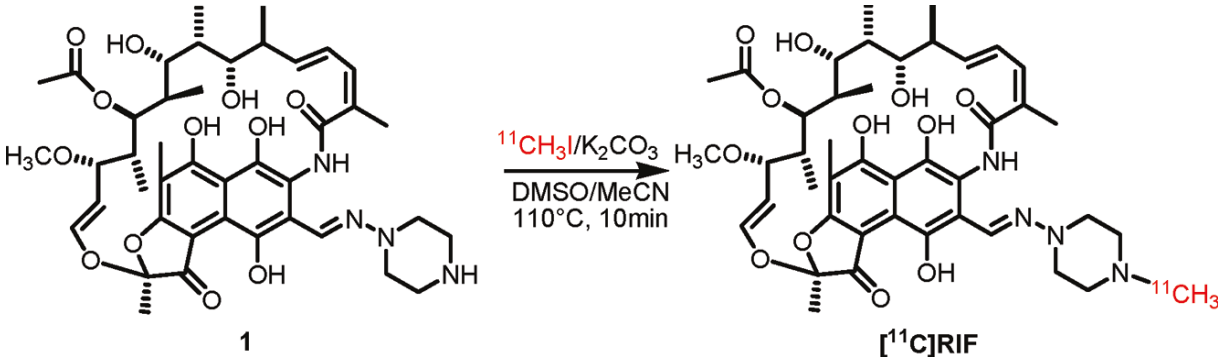

Scheme 3.1: **Radiosynthesis of ^{11}C-rifampicin**

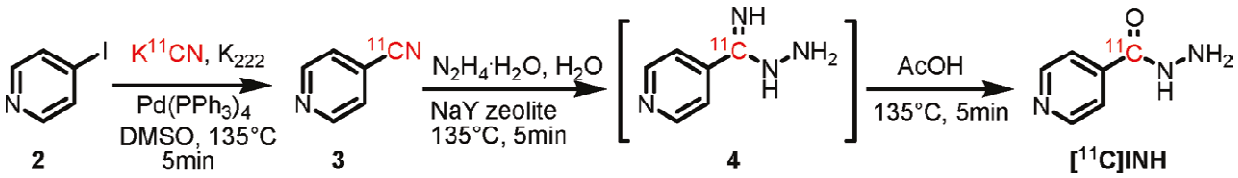

Scheme 3.2: **Radiosynthesis of ^{11}C-INH**

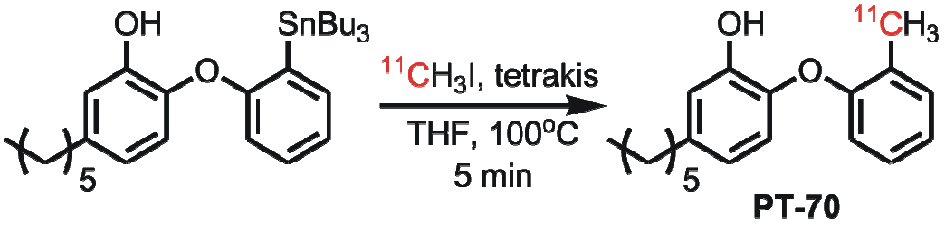

Scheme 3.3: **Radiosynthesis of ^{11}C-PT70**

Identification of Protein Targets Using ^{11}C-rifampicin

M. smegmatis mc^{2}155 cells were grown on 7H9 solid media containing 200 µg/mL ampicillin and 15 µg/mL cyclohexamide. Selected colonies were subsequently cultivated in 7H9 liquid media supplemented with glycerol, and grown to mid log phase (OD_{600} 0.5-0.8). The cells were then harvested, resuspended in 1 mL of 100 mM sodium phosphate buffer, pH 7 and lysed by sonication. ^{11}C-rifampicin was then added to the supernatant and incubated at room temperature for 30 minutes. The mixture was then loaded onto a PD-10 gel filtration column, pre-equilibrated with phosphate buffer. Fractions were collected every 500 µL and quantified on a Packard MINAXI y 5000 automated gamma counter.

Conditions for INH-NAD Adduct Formation

The reaction mixtures generally contained 250 µM INH, 250 µM NAD+, and 200 µM Mn(III) pyrophosphate. Time points from the reaction mixture were taken at 1, 2, 5, 10, 20, 30 and 60 minutes and adduct formation was analyzed on a UV spectrophotometer at 326 nm.

InhA Inactivation

Cold inactivation reactions contained 3 µM InhA, 250 µM INH, 2 mM Mn(III) pyrophosphate, and 250 µM NADH in 100 mM sodium phosphate buffer, pH 7.5. The reaction mixture was incubated at room temperature for up to 30 minutes. Kinetic assays were performed on a Cary 100 Bio spectrophotometer and also on a Nano Drop ND-1000 spectrophotometer in phosphate buffer at 25°C by following the oxidation of

NADH to NAD+ at 340 nm. The activity of InhA was monitored by the addition of DD-CoA (25 µM) and NADH (250 µM) to the inactivation reaction mixtures. Initial velocities were compared for reactions with and without inhibitor to determine the percent inhibition.

^{11}C-INH Binds to InhA

In order to establish a control experiment, ^{11}C-INH was added to a mixture of InhA (3 µM), NADH (500 µM) and Mn(III) pyrophosphate (2 mM) in 100 mM sodium phosphate buffer, pH 7, and incubated at room temperature for 20 minutes. The reaction mixture was subsequently loaded onto a size exclusion column (G3000SW, 7.5 mm x 60 cm), pre-equilibrated with phosphate buffer. INH interactions were identified by an HPLC based SEC system equipped with a radioactive detector. HPLC quantization was performed using an isocratic gradient of 100 mM sodium phosphate buffer at a flow rate of 1 mL/min. InhA eluted off the column with radioactivity at 16 minutes.

The procedure is similar for experiments involving the verification of InhA as the target for PT70 except, due to the hydrophobic nature of PT70, it does not solubilize well in phosphate buffer. This led to a decreased amount of initial radioactivity and to account for this, we decreased the incubation time to 10 minutes instead of 20 minutes. In addition, PT70 does not require activation and therefore Mn(III) pyrophosphate was not added to the incubation mixture.

Identification of Cellular Protein Targets Using ^{11}C-INH

M. smegmatis cells or an *E. coli* strain overexpressing InhA were grown to mid log phase and harvested by centrifugation. The cells were then resuspended in 1 mL of 100 mM sodium phosphate buffer, pH 7 and lysed by sonication. The lysate (1.5 mg/mL) was then loaded onto a G25 gel filtration spin column, pre-equilibrated with phosphate buffer in order to remove lower molecular weight proteins. ^{11}C-INH was then added to the supernatant and incubated at room temperature for 20 minutes. The reaction mixture was subsequently loaded onto a size exclusion column (G3000SW, 7.5 mm x 60 cm), pre-equilibrated with phosphate buffer. Drug binding was identified by an HPLC based SEC system equipped with a radioactive detector or by applying the mixture onto a gravity PD-10 size exclusion column. HPLC quantization was performed using an isocratic gradient of 100 mM sodium phosphate buffer, pH 7 at a flow rate of 1 mL/min. Fractions were collected when protein eluted with radioactivity and were immediately analyzed by SDS-PAGE and native PAGE. The native and denaturing gels were run at 90 V for 5 minutes followed by 250 volts for approximately an hour. Phosphor plates were used for imaging the positron emissions, and quantified using Science Laboratory 99 Image Gauge software (Fuji Photo Film Co). All fractions were additionally quantified on a Packard MINAXI γ 5000 automated gamma counter (*Packard* Instrument, Meriden, CT)

Results

Expression and Purification of InhA, AcpM and KasA

The proteins were purified by using hexahistidine-tag affinity purification chromatography, yielding pure recombinant protein with the predicted molecular weights of ~30 kDa, 15 kDa and 42 kDa, respectively as determined by SDS-PAGE.

^{11}C-rifampicin Binds to High Molecular Weight Proteins

Since it has been well characterized that rifampicin exhibits its activity by targeting the β-subunit of RNA polymerase, we used this system for a proof of principle experiment. In our experiments, *M. smegmatis* was used because it is fast growing and non-pathogenic compared to MTb. After ^{11}C-rifampicin was incubated with *M. smegmatis* cell lysate, fractionation was accomplished by applying the mixture onto a PD-10 size exclusion column. The resulting fractions were then run under native PAGE, and subsequently phosphorimaged. We found that ~100 µCi at the beginning of protein incubation was sufficient to determine the position of radioactivity on electrophoresis bands up to 4 hours later even after a ten-fold dilution of activity. We demonstrated that 34% of the radioactivity elutes with biomaterial that has a molecular weight > 5,000 Da. In a control, the ^{11}C-rifampicin only starts to elute off the column after fraction 10 (**Figure 3.5**).

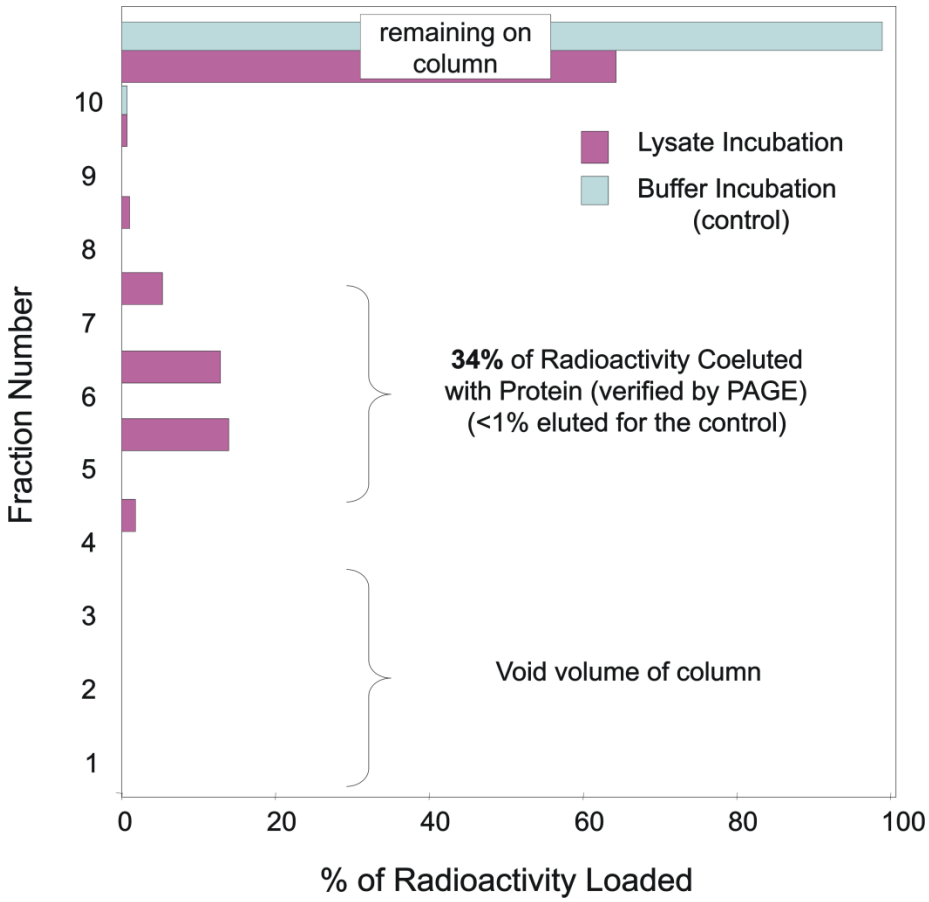

Figure 3.5: **^{11}C-rifampicin Binding to *M. smegmatis* Protein Lysate**.

Size exclusion chromatography indicated a non covalent interaction between protein lysate and ^{11}C-rifampicin.

^{11}C-PT70 Binds to InhA

InhA has been the well established target for PT70 through *in vitro* and gene expression experiments (*9*). Unlike INH, PT70 does not require activation and is therefore a better model to start with before determining the more complicated mode of action of INH. After the incubation of ^{11}C-PT70 with InhA and NADH, HPLC based SEC

indicated that InhA eluted off the column with radioactivity around 18 minutes, confirming that ^{11}C-PT70 binds to InhA **(Figure 3.6)**. In addition, by analyzing the radioactive HPLC trace, there was no radioactive peak corresponding to unbound ^{11}C-PT70. This suggests that all of the ^{11}C-PT70 that was incubated with InhA, bound to InhA.

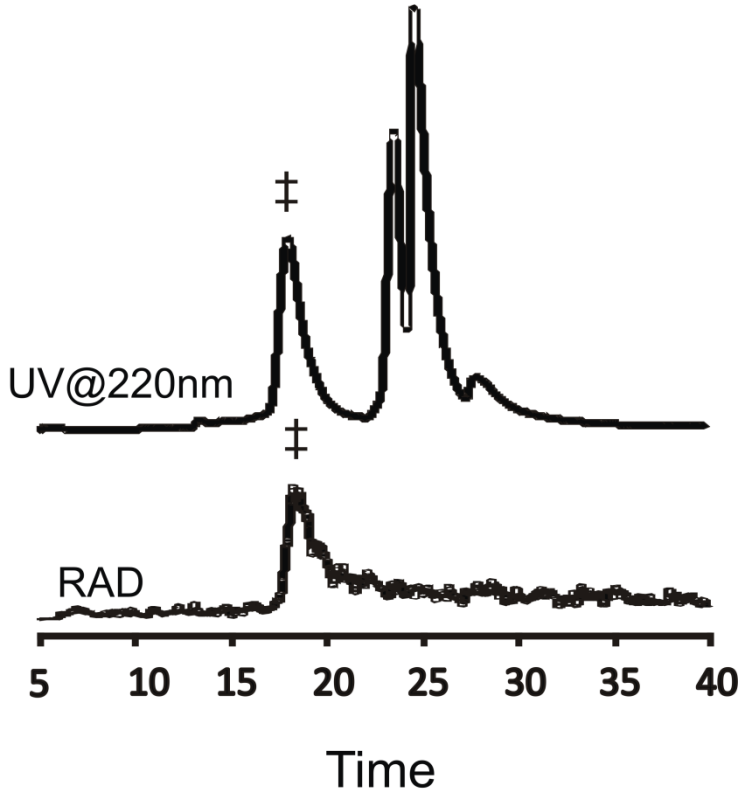

Figure 3.6: **HPLC Based SEC of ^{11}C-PT70 Incubated with InhA**. The upper UV trace is monitored at 220 nm where the peak at 18 and 23 minutes is InhA, and NADH, respectively. The lower radioactive trace also shows a peak at 16 minutes, indicating a binding event between InhA and ^{11}C-PT70.

Proof of INH-NAD Adduct Formation

INH-NAD adduct formation is dependent on KatG to activate INH (*20*). It has previously been shown that $MnCl_2$ and Mn(III) pyrophosphate are capable of activating INH in the absence of KatG (*25, 54*). In addition, while we are aware that KatG will be present in *M. smegmatis* and *E. coli* cell lysates during the experiments involving the identification of drug binding partners in complex mixtures, the MIC of INH for *M. smegmatis* and *E. coli* is 8 µg/mL and 500 µg/mL respectively, compared to 0.02 µg/mL for MTb, suggesting that they cannot activate INH as efficiently as MTb (*32, 55*). Therefore, in our initial experiments it was necessary to supplement the lysate with a manganese source. Since our radiolabeling experiments are time sensitive, it is important to establish the minimal amount of time required for INH-NAD adduct formation. INH and NAD were incubated in the presence of 200 µM Mn(III) pyrophosphate, where the formation of the adduct was monitored at 326 nm. By comparing the absorbance at 326 nm for 1 minute (0.1) versus 10 minutes (0.2), there is a 50% increase in adduct formation **(Figure 3.7)**. As expected, the amount of adduct formed continues to increase with time.

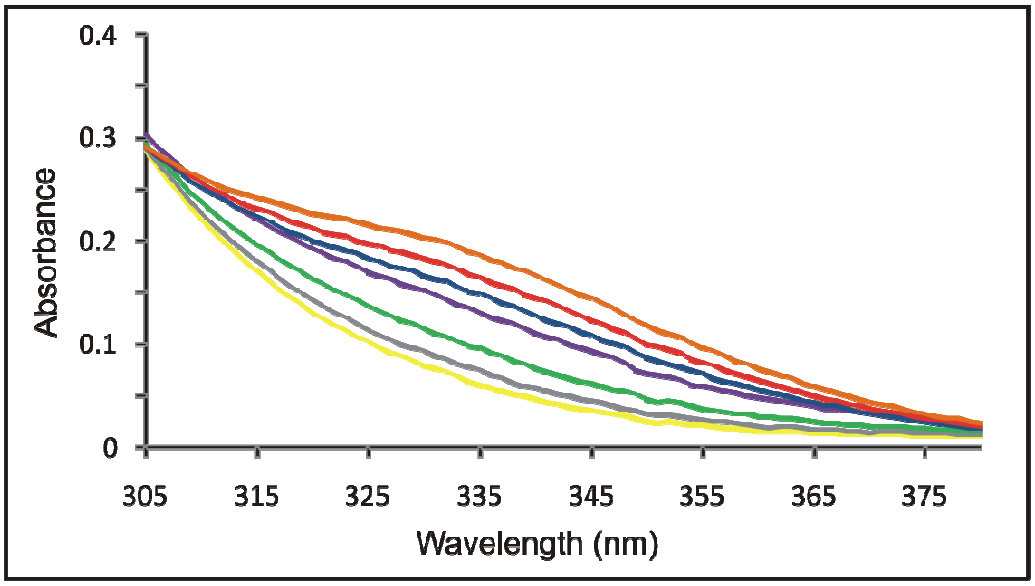

Figure 3.7: UV Analysis of INH-NAD Adduct Formation. Time points from a reaction mixture of 250 µM NAD+, 200 µM Mn(III) pyrophosphate and 250 µM INH were taken at 1, 2, 5, 10, 20, 30 and 60 minutes and analyzed on a UV spectrophotometer. The traces indicate an increase of a peak at 326 nm, which is indicative of INH-NAD formation.

InhA Inactivation Conditions

Our labeling technique is challenging due to the short half life of ^{11}C. Therefore, it is necessary to establish the quickest and most efficient conditions for InhA inactivation. **Figure 3.8** shows the results of different inactivation reaction conditions. As expected, in the absence of INH, InhA retains 100% activity. Upon incubation of the adduct with 3 uM InhA for 1 min, InhA is still 67% active. In contrast, after incubating the adduct with 3 µM InhA for 3 minutes, nearly complete inhibition with only 1% of remaining activity is detected.

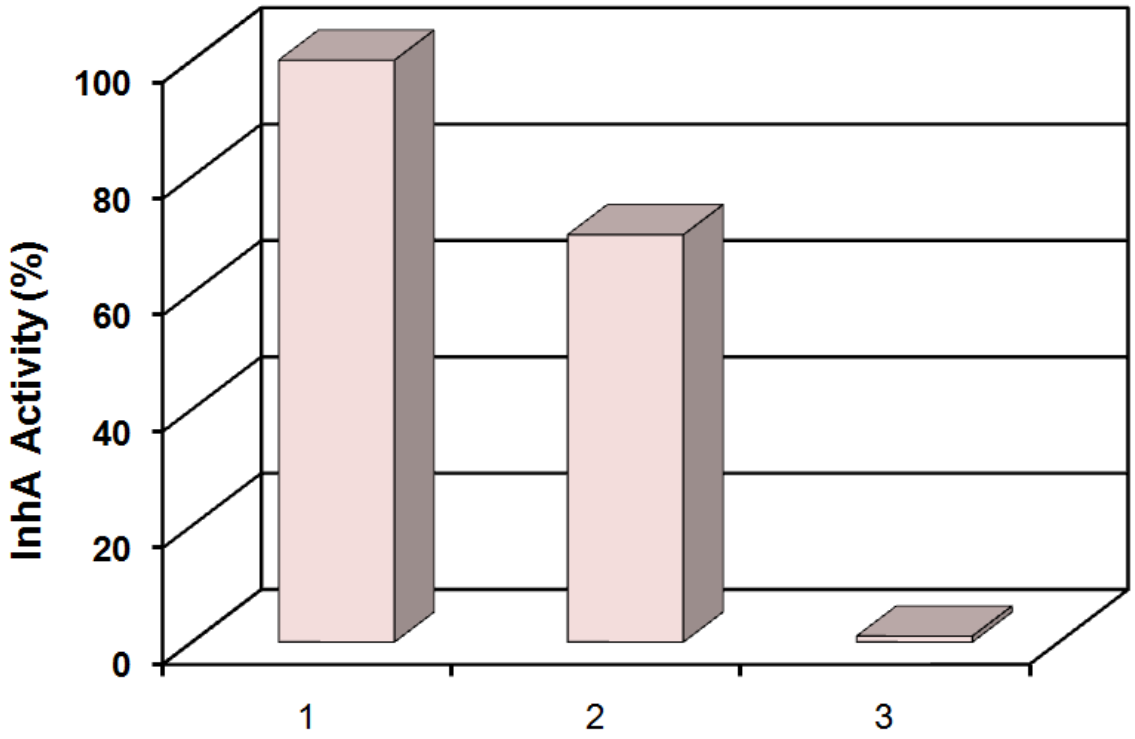

Figure 3.8: Remaining InhA activity. Column 1) 3 µM InhA, 250 µM NAD+, 200 µM Mn(III) pyrophosphate, in the absence of INH; Column 2) 3 µM InhA, 250 µM NADH, 250 µM INH, 200 µM Mn(III) pyrophosphate, after 1 minute; Column 3) 3 µM InhA, 250 µM NADH, 250 µM INH, 200 µM Mn(III) pyrophosphate, after 3 minutes.

As mentioned above, Mn(III) pyrophosphate is able to activate INH in the absence of KatG. After the purification of ^{11}C-INH, there is excess hydrazine present which will compete with INH for activation by Mn(III) pyrophosphate. In order to account for this, we needed to determine the maximal amount of Mn(III) pyrophosphate we can use without affecting the activity of InhA. **Figure 3.9** shows the effect on InhA activity in the presence of each component of the inactivation reaction mixture. Each column

represents the activity of InhA in the absence of one of the reaction components, where it is shown that InhA is not inhibited unless all reaction components are present (NAD+, INH, Mn(III) pyrophosphate and InhA). Also, column two shows 100% activity when 2 mM Mn(III) pyrophosphate is used indicating that InhA in unaffected by such a high concentration.

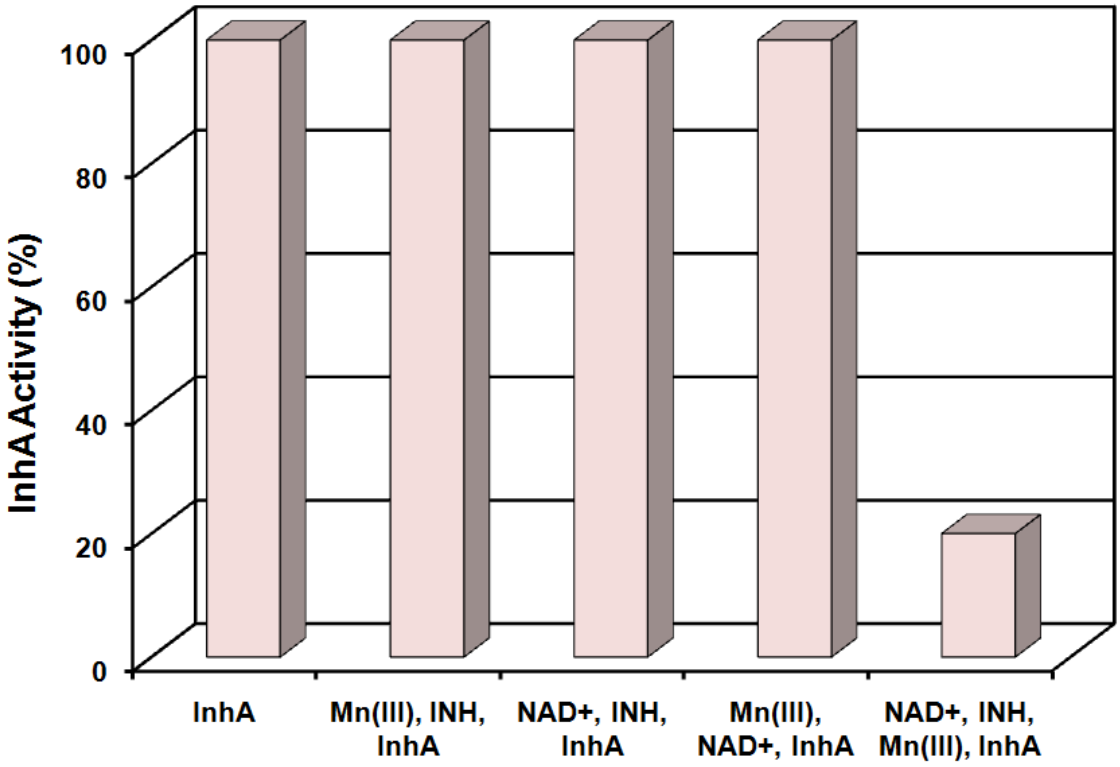

Figure 3.9: Remaining InhA activity. Column 1) 3 µM InhA; Colum 2) 3 µM InhA, 250 µM INH, 2 mM Mn(III) pyrophosphate, in the absence of NAD+; Column 3) 3 µM InhA, 250 µM NAD+, 250 µM INH in the absence of 2 mM Mn(III) pyrophosphate; Column 4) 3 µM InhA, 250 µM NAD+, 2 mM Mn(III) pyrophosphate, in the absence of INH; Colum 5) 3 µM InhA, 250 µM NAD+, 250 µM INH, 2 mM Mn(III) pyrophosphate.

^{11}C-INH Binds to and Inhibits InhA

Since InhA has been a well established target for INH, detecting the binding of ^{11}C-INH to InhA is a good starting point to determine the applicability of our radiolabeling target identification technique. After the incubation of ^{11}C-INH with InhA, NADH and Mn(III) pyrophosphate, HPLC based SEC indicated that InhA eluted off the column with radioactivity around 17 minutes **(Figure 3.10)**, confirming that ^{11}C-INH binds to InhA and also verifies the use of this technique to study additional protein-drug interactions.

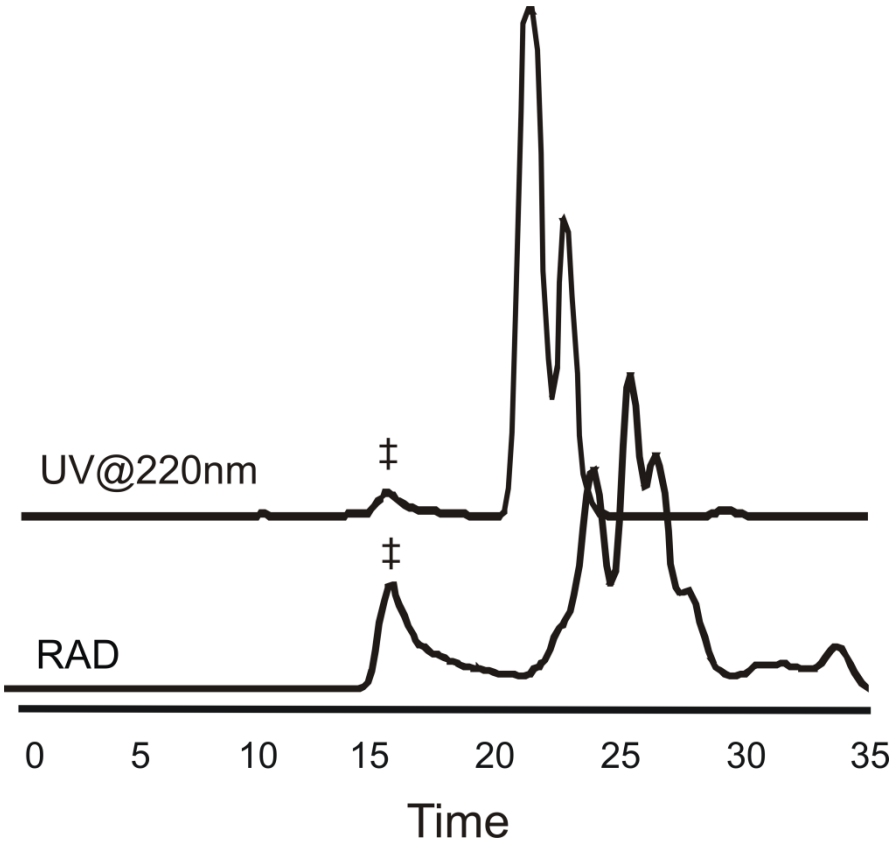

Figure 3.10: **HPLC Based SEC of ^{11}C-INH Incubated with InhA.**

The upper UV trace is monitored at 220 nm where the peak at 17, 22 and 24 minutes is InhA, Mn(III) pyrophosphate/NADH respectively and INH. The lower radioactive trace shows the ^{11}C-INH-NAD adduct at 17 minutes and possibly the side products of the activation reaction eluting from 22-30 minutes. The same elution time of ^{11}C-INH-NAD and InhA indicates a binding event between the two.

HPLC based SEC suffers from both UV and radioactive detection limits. Therefore it was important to use a secondary method to verify the binding of ^{11}C-INH to InhA. Due to our inability to remove the radioactivity, we brought in a portable UV spectrometer (Nano Drop) to monitor the inhibition of InhA by ^{11}C-INH through a discontinuous assay

following the oxidation of NADH at 340 nm. The blue trace in **Figure 3.11** indicates the activity of InhA without inhibitor present, while the green and red traces represent the activity of InhA with ^{11}C-INH and ^{11}C-INH with supplemented cold INH, respectively. Compared to the activity of InhA without inhibitor present, the blue and yellow traces show 33% and 11% remaining InhA activity, respectively, confirming binding ^{11}C-INH to InhA.

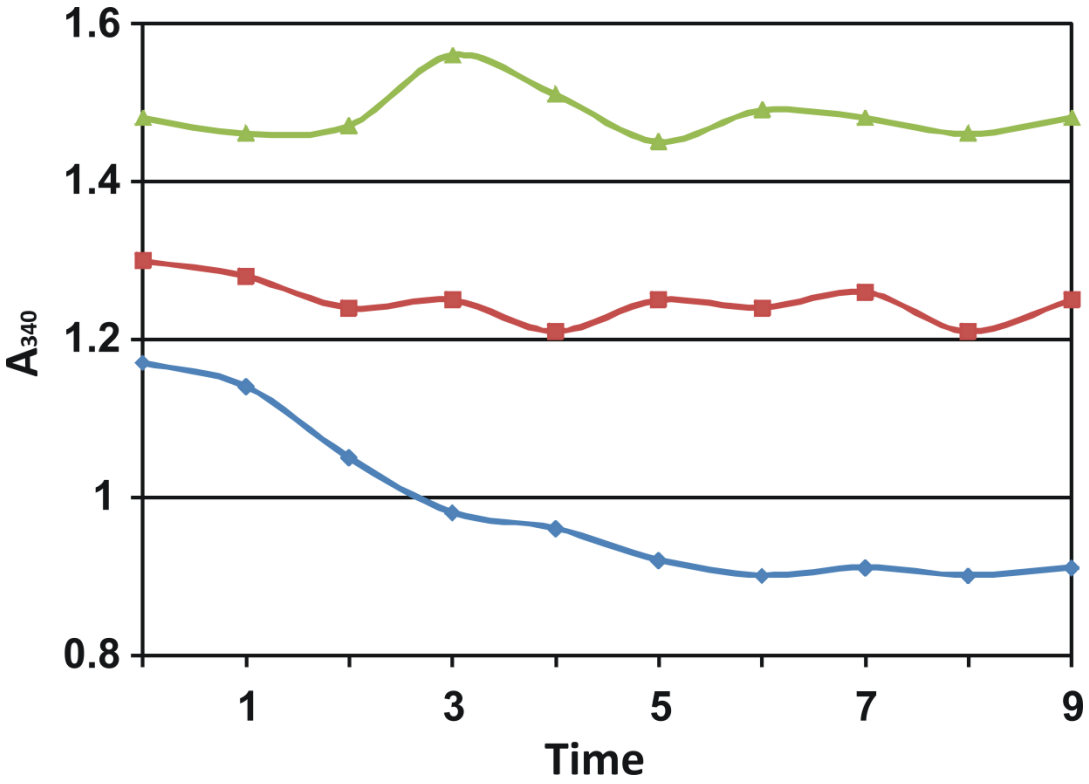

Figure 3.11 NADH Oxidation. Blue trace reaction conditions: 3 μM InhA, 2 mM Mn(III) pyrophosphate, 500 μM NAD+; Green trace reaction conditions: 3 μM InhA, 2 mM Mn(III) pyrophosphate, 500 μM NAD+ and ^{11}C-INH; Red trace reaction conditions: 3 μM InhA, 2 mM Mn(III) pyrophosphate, 500 μM NAD+, ^{11}C-INH and 100 μM INH.

^{11}C- INH Binding in a Complex Mixture

Considerable evidence suggests that INH has a complex mode of action inside the cell. In order to elucidate the complexity, we performed drug binding experiments in cell lysate and applied two different separation techniques. First, we incubated ^{11}C-INH,

NADH and Mn(III) pyrophosphate with *M. smegmatis* cell lysate and fractionated the lysate through a gravity gel filtration column. The fractions were subsequently subject to SDS and native gel electrophoresis, which were then phosphorimaged. The resulting phosphor images showed no detectable radioactive protein gel bands, after 4 hours from the start of the radiosynthesis. However radioactive counts were detected by inserting the whole gel into a gamma counter, which has a lower limit of detection than a phosphorimager but cannot identify individual radioactive gel bands.

The second experiment involved the incubation of ^{11}C-INH, NADH and Mn(III) pyrophosphate with an *E. coli* strain overexpressing InhA and subsequent analysis by HPLC based SEC. Radioactivity eluted off the column at the same retention time as InhA (18 minutes) and possibly at earlier retention times as well. However, the radioactive signal for this experiment was very low (indicated by the noisiness of the signal) so this experiment needs to be repeated in order to confidently draw any conclusions **(Figure 3.12)**.

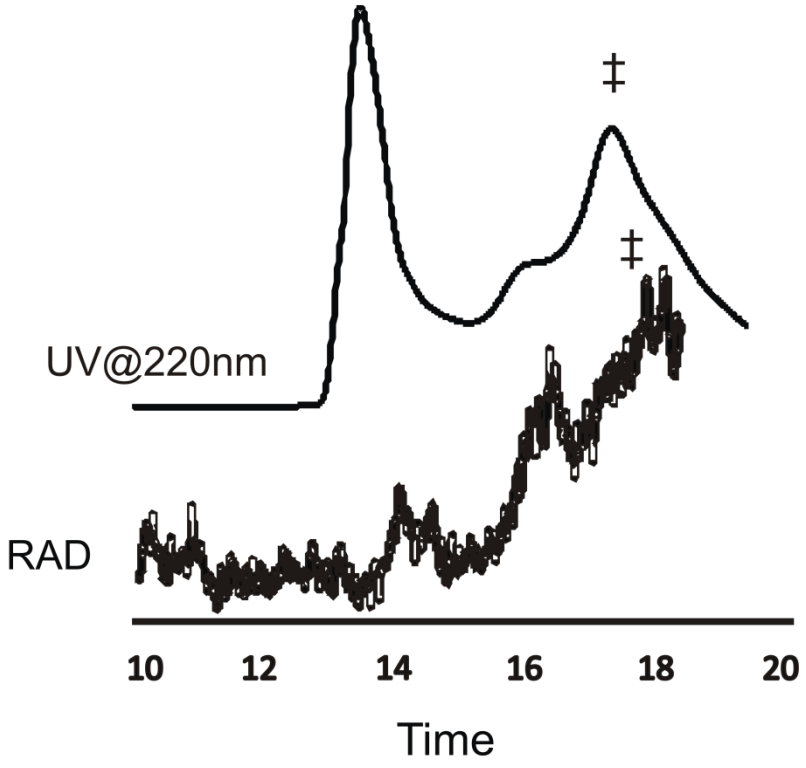

Figure 3.12: **HPLC Based SEC of ^{11}C-INH Incubated with an *E. coli* Strain Overexpression InhA**. The upper UV trace is monitored at 220 nm where smaller molecular weight species elute at earlier time points while the larger proteins elute at later time points. Overexpressed InhA is shown by the large peak at 18 minutes. The lower radioactive trace shows peaks corresponding to all UV peaks, possibly as a result of non specific binding.

Discussion

Rational drug design involves the use of structural and mechanistic information of a target to direct the design and synthesis of small molecules that bind to it with a high affinity. Current methods for drug target identification involve affinity based methods which involve the chemical immobilization of drugs or phenotype based methods which infer the drug target/pathway from physiological responses. Affinity based purification suffers from the possibility that a covalent modification of the drug may alter the chemical structure and binding properties of the molecule. An inherent effect of phenotype based methods is that they are only applicable to drugs that affect cell growth and viability and the analysis of the proteomic response can be difficult to detect and analyze with currently available technology. In addition, both of these methods may identify targets that bind to the drug *in vitro*, but do not do so in living cells. In order to address this fault in the drug discovery pipeline, we have incorporated short lived radioisotopes into frontline MTb drugs rifampicin and INH as well as the alkyl diaryl ether inhibitors, developed in our lab.

Rifampicin is a front line MTb drug known to inhibit the bacterial RNA polymerase, where mutations in the β-subunit (*rpoB*) correlate to drug resistance to rifampicin (*56*). The incorporation of ^{11}C into rifampicin and subsequent experiments with *M. smegmatis* cell lysate served as a control for the method we are developing. We have demonstrated that ^{11}C-rifampicin co-elutes with high molecular weight proteins from a gel filtration column. In this preliminary experiment we also determined the maximal amount of time we have to perform our experiments without losing traceable radioactivity. We found that ~100 μCi of activity with protein was sufficient to detect the

position of radioactivity on electrophoresis bands up to 4 hours later even after a ten-fold dilution of activity. From our experiments and the detection limits of the instrument, we estimate that < 1 nCi/mm^2 is sufficient for detection. This tells us the half lives of the radionuclides are long enough to permit cell treatment, protein fractionation and detection, but short enough so that proteins can be analyzed after the radionuclides have decayed. The crucial information learned from this control experiment allowed us to apply our technique to identify additional drugs-target interactions.

The diaryl ethers have broad spectrum antibacterial activity, where PT70 is active against *M. smegmatis, S. aureus and E. coli*. Although we know that PT70 is a potent inhibitor of InhA (*57*), we are very interested to know if the compound binds to other proteins in the cell. Unlike INH, PT70 does not require activation and is therefore a better model to start with before determining the more complicated mode of action of INH. Detecting the binding of PT70 to InhA is the first logical step before attempting to identify additional binding partners. HPLC based SEC with an in-line radiation detector, indicated that InhA eluted off the column with radioactivity confirming that ^{11}C-PT70 binds to InhA. In addition, by analyzing the radioactive HPLC trace, there was no later time point peak corresponding to unbound ^{11}C-PT70, suggesting potent and specific inhibition of InhA by ^{11}C-PT70. This supports the *in vitro* and gene expression data that InhA is the target for PT70.

Isoniazid is the most effective frontline drug to treat MTb. Despite considerable effort, there is still uncertainty concerning the precise mode of action of isoniazid. For instance, Tonge *et al* found no indication that the InhA mutations correlating with INH resistance *in vivo* affect the affinity of InhA for the purified INH-NAD adduct (*31*). In

addition, Blanchard *et al* later discovered that an INH-NADP adduct inhibits the dihydrofolate reductase (*34*) and also used affinity purification with an INH-NAD adduct, where they identified 20 new proteins *(35)*. Given the importance of INH as a frontline MTb drug, there is great interest in determining its specific mode of action. It is clear that once activated, INH forms a covalent adduct with NADH which then inhibits InhA. We used this knowledge as a starting point for our INH experiments. Due to the short half lives of the radionuclides, we established proper experimental conditions for a fast and efficient INH adduct formation and InhA inhibition.

Nguyen *et a*l showed that Mn(III) pyrophosphate can be used to effectively activate INH. While we are aware that KatG will be present in the lysate for the experiments which identify drug binding partners in complex mixtures, the MIC of INH for *M. smegmatis* and *E. coli* are 400-25,000 fold higher than for MTb, indicating that they cannot activate INH as efficiently as MTb (*32, 55*). Therefore, in our initial experiments it was necessary to supplement the lysate with a manganese source. In the presence of Mn(III) pyrophosphate, a 50% increase in adduct formation was detected after 10 minutes, supporting the data of Nguyen *et al*, where he showed a 93% conversion of INH within a few minutes after incubation (*54*).

Initially, we were experiencing great difficulty activating ^{11}C-INH and subsequently inhibiting InhA. Through a long trial and error process, we determined that excess hydrazine could be affecting INH activation. Hydrazine is a reaction component in the synthesis of INH, and it proved difficult to remove all of the excess hydrazine during the purification process. Similar to INH, hydrazine will also undergo radical formation in the presence of Mn(III) pyrophosphate, and therefore will reduce the amount of Mn(III)

pyrophosphate available to activate INH (*58*). In order to overcome this, we determined that concentrations as high as 2 mM Mn(III) pyrophosphate has no affect on the activity of InhA. Due to our time limitations it was crucial to determine the shortest time necessary to inhibit InhA. In addition, it has been shown that the INH-NAD adduct is a slow tight binding inhibitor of InhA (*31*) and therefore we must ensure that incubation times are sufficient to allow the complex to form and bind to protein targets. By incubating the adduct with InhA for 3 minutes, the degree of inhibition increased 66-fold in comparison to the incubation of 1 minute, suggesting that the incubation time is crucial for efficient inhibition. These together determined that 3 µM InhA is efficiently inhibited in the presence of 2 mM Mn(III) pyrophosphate, INH and NADH with a <10 minute incubation time.

With the proper experimental controls in place, we were able to perform the ^{11}C-INH radiolabeling experiment. HPLC based SEC with an in-line radiation detector, indicated that InhA eluted off the column with radioactivity, confirming that ^{11}C-INH binds to InhA. The remaining activity of InhA after incubation with ^{11}C-INH was determined as 11-33%, consistent with our cold inhibition studies.

As previously stated, there is considerable evidence to suggest that INH has a complex mode of action. In order to elucidate the complexity, we performed drug binding experiments in cell lysate and applied two different separation techniques. The first involved the fractionation of *M. smegmatis* cell lysate through a gravity gel filtration column and subsequently running denaturing and native PAGE which were then phosphorimaged. The resulting phosphor images showed no traces of radioactivity indicating that we needed a faster non covalent separation method. This led to the

second experiment involving HPLC based SEC with an in-line radiation detector. By analyzing the HPLC traces, of a reaction mixture containing the cell lysate of an *E. coli* strain overexpressing InhA and ^{11}C-INH, radioactivity eluted off the column at the same retention time as InhA and possibly at earlier retention times as well. However, the radioactive signal for this experiment was very low (indicated by the noisiness of the signal) so the experiment needs to be repeated in order to confidently draw any conclusions.

The success of these preliminary experiments suggests that our labeling technique can be applied to many systems to help elucidate the mode of action of drugs without altering its chemical structure. Also, as long as a drug can be taken up by the bacteria, this technique can be used to explore *in vivo* cellular complexes in whole cells. Our results give us confidence that this technique will bridge the gap in the drug discovery process and open up doors for the development of future novel chemotherapeutics by identifying new protein targets.

Summary

The bacterial fatty acid biosynthesis (FASII) pathway is a promising target for antibacterial drug discovery. This chapter was focused on studying the interaction of current enzyme inhibitors with components of the pathway in whole cells.

A novel drug-target identification method has been developed that relies on the incorporation of short-lived isotopes such as carbon-11 into the drug of interest. Radiolabeling is accomplished without altering the structure of the drug and size exclusion chromatography (SEC) is used to fractionate proteins following exposure to the radiotracer. Proof of concept experiments have so demonstrated interactions between the FabI enoyl-ACP reductase and the front-line tuberculosis drug ^{11}C-isoniazid as well as with a carbon-11 labeled alkyl diaryl ether FabI inhibitor.

References

1. Sensi, P., Margalith, P., and Timbal, M. T. (1959) Rifomycin, a new antibiotic; preliminary report, *Farmaco Sci 14*, 146-147.
2. Maggi, N., Pasqualucci, C. R., Ballotta, R., and Sensi, P. (1966) Rifampicin: a new orally active rifamycin, *Chemotherapy 11*, 285-292.
3. Piddock, L. J., Williams, K. J., and Ricci, V. (2000) Accumulation of rifampicin by Mycobacterium aurum, Mycobacterium smegmatis and Mycobacterium tuberculosis, *J Antimicrob Chemother 45*, 159-165.
4. Blanchard, J. S. (1996) Molecular mechanisms of drug resistance in Mycobacterium tuberculosis, *Annu Rev Biochem 65*, 215-239.
5. Wehrli, W. (1983) Rifampin: mechanisms of action and resistance, *Rev Infect Dis 5 Suppl 3*, S407-411.
6. Aristoff, P. A., Garcia, G. A., Kirchhoff, P. D., and Hollis Showalter, H. D. (2010) Rifamycins--obstacles and opportunities, *Tuberculosis (Edinb) 90*, 94-118.
7. Anthony, R. M., Schuitema, A. R., Bergval, I. L., Brown, T. J., Oskam, L., and Klatser, P. R. (2005) Acquisition of rifabutin resistance by a rifampicin resistant mutant of Mycobacterium tuberculosis involves an unusual spectrum of mutations and elevated frequency, *Ann Clin Microbiol Antimicrob 4*, 9.
8. Lu, H., England, K., am Ende, C., Truglio, J. J., Luckner, S., Reddy, B. G., Marlenee, N. L., Knudson, S. E., Knudson, D. L., Bowen, R. A., Kisker, C., Slayden, R. A., and Tonge, P. J. (2009) Slow-onset inhibition of the FabI enoyl reductase from francisella tularensis: residence time and in vivo activity, *ACS Chem Biol 4*, 221-231.

9. Sullivan, T. J., Truglio, J. J., Boyne, M. E., Novichenok, P., Zhang, X., Stratton, C. F., Li, H. J., Kaur, T., Amin, A., Johnson, F., Slayden, R. A., Kisker, C., and Tonge, P. J. (2006) High affinity InhA inhibitors with activity against drug-resistant strains of Mycobacterium tuberculosis, *ACS Chem Biol 1*, 43-53.

10. Xu, H., Sullivan, T. J., Sekiguchi, J., Kirikae, T., Ojima, I., Stratton, C. F., Mao, W., Rock, F. L., Alley, M. R., Johnson, F., Walker, S. G., and Tonge, P. J. (2008) Mechanism and inhibition of saFabI, the enoyl reductase from Staphylococcus aureus, *Biochemistry 47*, 4228-4236.

11. Heath, R. J., White, S. W., and Rock, C. O. (2001) Lipid biosynthesis as a target for antibacterial agents, *Prog Lipid Res 40*, 467-497.

12. Kuo, M. R., Morbidoni, H. R., Alland, D., Sneddon, S. F., Gourlie, B. B., Staveski, M. M., Leonard, M., Gregory, J. S., Janjigian, A. D., Yee, C., Musser, J. M., Kreiswirth, B., Iwamoto, H., Perozzo, R., Jacobs, W. R., Jr., Sacchettini, J. C., and Fidock, D. A. (2003) Targeting tuberculosis and malaria through inhibition of Enoyl reductase: compound activity and structural data, *J Biol Chem 278*, 20851-20859.

13. Payne, D. J., Miller, W. H., Berry, V., Brosky, J., Burgess, W. J., Chen, E., DeWolf Jr, W. E., Jr., Fosberry, A. P., Greenwood, R., Head, M. S., Heerding, D. A., Janson, C. A., Jaworski, D. D., Keller, P. M., Manley, P. J., Moore, T. D., Newlander, K. A., Pearson, S., Polizzi, B. J., Qiu, X., Rittenhouse, S. F., Slater-Radosti, C., Salyers, K. L., Seefeld, M. A., Smyth, M. G., Takata, D. T., Uzinskas, I. N., Vaidya, K., Wallis, N. G., Winram, S. B., Yuan, C. C., and Huffman, W. F.

(2002) Discovery of a novel and potent class of FabI-directed antibacterial agents, *Antimicrob Agents Chemother 46*, 3118-3124.

14. Surolia, N., and Surolia, A. (2001) Triclosan offers protection against blood stages of malaria by inhibiting enoyl-ACP reductase of Plasmodium falciparum, *Nat Med 7*, 167-173.
15. Middlebrook, G. (1954) Isoniazid-resistance and catalase activity of tubercle bacilli; a preliminary report, *Am Rev Tuberc 69*, 471-472.
16. Youatt, J. (1969) A review of the action of isoniazid, *Am Rev Respir Dis 99*, 729-749.
17. Heym, B., Alzari, P. M., Honore, N., and Cole, S. T. (1995) Missense mutations in the catalase-peroxidase gene, katG, are associated with isoniazid resistance in Mycobacterium tuberculosis, *Mol Microbiol 15*, 235-245.
18. Stoeckle, M. Y., Guan, L., Riegler, N., Weitzman, I., Kreiswirth, B., Kornblum, J., Laraque, F., and Riley, L. W. (1993) Catalase-peroxidase gene sequences in isoniazid-sensitive and -resistant strains of Mycobacterium tuberculosis from New York City, *J Infect Dis 168*, 1063-1065.
19. Shoeb, H. A., Bowman, B. U., Jr., Ottolenghi, A. C., and Merola, A. J. (1985) Peroxidase-mediated oxidation of isoniazid, *Antimicrob Agents Chemother 27*, 399-403.
20. Zhang, Y., Heym, B., Allen, B., Young, D., and Cole, S. (1992) The catalase-peroxidase gene and isoniazid resistance of Mycobacterium tuberculosis, *Nature 358*, 591-593.

21. Ghiladi, R. A., Medzihradszky, K. F., Rusnak, F. M., and Ortiz de Montellano, P. R. (2005) Correlation between isoniazid resistance and superoxide reactivity in mycobacterium tuberculosis KatG, *J Am Chem Soc 127*, 13428-13442.

22. Wengenack, N. L., and Rusnak, F. (2001) Evidence for isoniazid-dependent free radical generation catalyzed by Mycobacterium tuberculosis KatG and the isoniazid-resistant mutant KatG(S315T), *Biochemistry 40*, 8990-8996.

23. Zhao, X., Yu, H., Yu, S., Wang, F., Sacchettini, J. C., and Magliozzo, R. S. (2006) Hydrogen peroxide-mediated isoniazid activation catalyzed by Mycobacterium tuberculosis catalase-peroxidase (KatG) and its S315T mutant, *Biochemistry 45*, 4131-4140.

24. Johnsson, K., Froland, W. A., and Schultz, P. G. (1997) Overexpression, purification, and characterization of the catalase-peroxidase KatG from Mycobacterium tuberculosis, *J Biol Chem 272*, 2834-2840.

25. Nagy, J. M., Cass, A. E., and Brown, K. A. (1997) Purification and characterization of recombinant catalase-peroxidase, which confers isoniazid sensitivity in Mycobacterium tuberculosis, *J Biol Chem 272*, 31265-31271.

26. Marcinkeviciene, R. S. M. a. J. A. (1996) Evidence for Isoniazid Oxidation by Oxyferrous Mycobacterial Catalase−Peroxidase, *J. Am. Chem. Soc. 118*, 11303-11304.

27. Jacques Bodiguel, J. M. N., Katherine A. Brown,and Brigitte Jamart-Grégoire. (2000) Oxidation of Isoniazid by Manganese and Mycobacterium tuberculosis Catalase−Peroxidase Yields a New Mechanism of Activation, *J. Am. Chem. Soc. 123*, 3832-3833.

28. Quemard, A., Sacchettini, J. C., Dessen, A., Vilcheze, C., Bittman, R., Jacobs, W. R., Jr., and Blanchard, J. S. (1995) Enzymatic characterization of the target for isoniazid in Mycobacterium tuberculosis, *Biochemistry 34*, 8235-8241.

29. Takayama, K., Schnoes, H. K., Armstrong, E. L., and Boyle, R. W. (1975) Site of inhibitory action of isoniazid in the synthesis of mycolic acids in Mycobacterium tuberculosis, *J Lipid Res 16*, 308-317.

30. Vilcheze, C., Morbidoni, H. R., Weisbrod, T. R., Iwamoto, H., Kuo, M., Sacchettini, J. C., and Jacobs, W. R., Jr. (2000) Inactivation of the inhA-encoded fatty acid synthase II (FASII) enoyl-acyl carrier protein reductase induces accumulation of the FASI end products and cell lysis of Mycobacterium smegmatis, *J Bacteriol 182*, 4059-4067.

31. Rawat, R., Whitty, A., and Tonge, P. J. (2003) The isoniazid-NAD adduct is a slow, tight-binding inhibitor of InhA, the Mycobacterium tuberculosis enoyl reductase: adduct affinity and drug resistance, *Proc Natl Acad Sci U S A 100*, 13881-13886.

32. Mdluli, K., Sherman, D. R., Hickey, M. J., Kreiswirth, B. N., Morris, S., Stover, C. K., and Barry, C. E., 3rd. (1996) Biochemical and genetic data suggest that InhA is not the primary target for activated isoniazid in Mycobacterium tuberculosis, *J Infect Dis 174*, 1085-1090.

33. Mdluli, K., Slayden, R. A., Zhu, Y., Ramaswamy, S., Pan, X., Mead, D., Crane, D. D., Musser, J. M., and Barry, C. E., 3rd. (1998) Inhibition of a Mycobacterium tuberculosis beta-ketoacyl ACP synthase by isoniazid, *Science 280*, 1607-1610.

34. Argyrou, A., Vetting, M. W., Aladegbami, B., and Blanchard, J. S. (2006) Mycobacterium tuberculosis dihydrofolate reductase is a target for isoniazid, *Nat Struct Mol Biol 13*, 408-413.

35. Argyrou, A., Jin, L., Siconilfi-Baez, L., Angeletti, R. H., and Blanchard, J. S. (2006) Proteome-wide profiling of isoniazid targets in Mycobacterium tuberculosis, *Biochemistry 45*, 13947-13953.

36. Betts, J. C., McLaren, A., Lennon, M. G., Kelly, F. M., Lukey, P. T., Blakemore, S. J., and Duncan, K. (2003) Signature gene expression profiles discriminate between isoniazid-, thiolactomycin-, and triclosan-treated Mycobacterium tuberculosis, *Antimicrob Agents Chemother 47*, 2903-2913.

37. Slayden, R. A., Lee, R. E., and Barry, C. E., 3rd. (2000) Isoniazid affects multiple components of the type II fatty acid synthase system of Mycobacterium tuberculosis, *Mol Microbiol 38*, 514-525.

38. Wilson, M., DeRisi, J., Kristensen, H. H., Imboden, P., Rane, S., Brown, P. O., and Schoolnik, G. K. (1999) Exploring drug-induced alterations in gene expression in Mycobacterium tuberculosis by microarray hybridization, *Proc Natl Acad Sci U S A 96*, 12833-12838.

39. Washburn, M. P., and Yates, J. R., 3rd. (2000) Analysis of the microbial proteome, *Curr Opin Microbiol 3*, 292-297.

40. Marcotte, R. W. a. E. M. (2008) The Proteomic Response of Mycobacterium smegmatis to Anti-Tuberculosis Drugs Suggests Targeted Pathways, *The Journal of Proteome Research 7*, 855-865.

41. MacKeigan, J. P., Clements, C. M., Lich, J. D., Pope, R. M., Hod, Y., and Ting, J. P. (2003) Proteomic profiling drug-induced apoptosis in non-small cell lung carcinoma: identification of RS/DJ-1 and RhoGDIalpha, *Cancer Res 63*, 6928-6934.

42. Shen, Y., Liu, J., Estiu, G., Isin, B., Ahn, Y. Y., Lee, D. S., Barabasi, A. L., Kapatral, V., Wiest, O., and Oltvai, Z. N. (2010) Blueprint for antimicrobial hit discovery targeting metabolic networks, *Proc Natl Acad Sci U S A 107*, 1082-1087.

43. Lin, M. Z., and Wang, L. (2008) Selective labeling of proteins with chemical probes in living cells, *Physiology (Bethesda) 23*, 131-141.

44. Ong, S. E., Schenone, M., Margolin, A. A., Li, X., Do, K., Doud, M. K., Mani, D. R., Kuai, L., Wang, X., Wood, J. L., Tolliday, N. J., Koehler, A. N., Marcaurelle, L. A., Golub, T. R., Gould, R. J., Schreiber, S. L., and Carr, S. A. (2009) Identifying the proteins to which small-molecule probes and drugs bind in cells, *Proc Natl Acad Sci U S A 106*, 4617-4622.

45. Giaever, G., Shoemaker, D. D., Jones, T. W., Liang, H., Winzeler, E. A., Astromoff, A., and Davis, R. W. (1999) Genomic profiling of drug sensitivities via induced haploinsufficiency, *Nat Genet 21*, 278-283.

46. Hughes, T. R., Marton, M. J., Jones, A. R., Roberts, C. J., Stoughton, R., Armour, C. D., Bennett, H. A., Coffey, E., Dai, H., He, Y. D., Kidd, M. J., King, A. M., Meyer, M. R., Slade, D., Lum, P. Y., Stepaniants, S. B., Shoemaker, D. D., Gachotte, D., Chakraburtty, K., Simon, J., Bard, M., and Friend, S. H. (2000) Functional discovery via a compendium of expression profiles, *Cell 102*, 109-126.

47. Lomenick, B., Hao, R., Jonai, N., Chin, R. M., Aghajan, M., Warburton, S., Wang, J., Wu, R. P., Gomez, F., Loo, J. A., Wohlschlegel, J. A., Vondriska, T. M., Pelletier, J., Herschman, H. R., Clardy, J., Clarke, C. F., and Huang, J. (2009) Target identification using drug affinity responsive target stability (DARTS), *Proc Natl Acad Sci U S A 106*, 21984-21989.

48. Foit, L., Morgan, G. J., Kern, M. J., Steimer, L. R., von Hacht, A. A., Titchmarsh, J., Warriner, S. L., Radford, S. E., and Bardwell, J. C. (2009) Optimizing protein stability in vivo, *Mol Cell 36*, 861-871.

49. Fowler, J. S., Volkow, N. D., Wang, G. J., Ding, Y. S., and Dewey, S. L. (1999) PET and drug research and development, *J Nucl Med 40*, 1154-1163.

50. Gambhir, S. S. (2002) Molecular imaging of cancer with positron emission tomography, *Nat Rev Cancer 2*, 683-693.

51. Phelps, M. E. (2002) Nuclear medicine, molecular imaging, and molecular medicine, *J Nucl Med 43*, 13N-14N.

52. Raichle, M. E. (1983) Positron emission tomography, *Annu Rev Neurosci 6*, 249-267.

53. Liu, L., Xu, Y., Shea, C., Fowler, J. S., Hooker, J. M., and Tonge, P. J. (2010) Radiosynthesis and bioimaging of the tuberculosis chemotherapeutics isoniazid, rifampicin and pyrazinamide in baboons, *J Med Chem 53*, 2882-2891.

54. Nguyen, M., Quemard, A., Broussy, S., Bernadou, J., and Meunier, B. (2002) Mn(III) pyrophosphate as an efficient tool for studying the mode of action of isoniazid on the InhA protein of Mycobacterium tuberculosis, *Antimicrob Agents Chemother 46*, 2137-2144.

55. Rastogi, N., Goh, K. S., Horgen, L., and Barrow, W. W. (1998) Synergistic activities of antituberculous drugs with cerulenin and trans-cinnamic acid against Mycobacterium tuberculosis, *FEMS Immunol Med Microbiol 21*, 149-157.

56. White, R. J., Lancini, G. C., and Silvestri, L. G. (1971) Mechanism of action of rifampin on Mycobacterium smegmatis, *J Bacteriol 108*, 737-741.

57. Luckner, S. R., Liu, N., am Ende, C. W., Tonge, P. J., and Kisker, C. (2010) A slow, tight binding inhibitor of InhA, the enoyl-acyl carrier protein reductase from Mycobacterium tuberculosis, *J Biol Chem 285*, 14330-14337.

58. Kalyanaraman, B., and Sinha, B. K. (1985) Free radical-mediated activation of hydrazine derivatives, *Environ Health Perspect 64*, 179-184.

Chapter IV: Studying Protein-Protein Interactions in the FASII Pathway

Protein-Protein Interactions

Protein-protein interactions are central to a vast amount of biological processes. These include, DNA replication, transcription, translation, splicing, secretion, cell cycle control, signal transduction, and intermediary metabolism (*1*). In consequence, what used to be a field exclusively for biochemists is now gaining valuable insight from geneticists, cell biologists, developmental biologists, molecular biologists, and biophysicists.

It is clear that protein-protein interactions are much more complex than once assumed, where their involvement in regulating cellular events is large (*2-6*). Identification of the components of multiprotein complexes and determining their sites of interaction will provide crucial information towards understanding these processes and can also be used to develop therapies and specific drugs to overcome diseases. Consequently, a growing interest has emerged in the development of methods suitable to study these protein–protein interactions.

Evidence of a Fatty Acid Biosynthesis Pathway Complex

The fatty acid biosynthetic pathway is essential, specific for mycobacteria and represents a valuable system for the search of new anti-tuberculosis agents. A key feature of the fatty acid biosynthesis (FASII) pathway is that the hydrophobic fatty acyl intermediates are shuttled from enzyme to enzyme attached to a phosphopantetheine (PPant) prosthetic group on a small, highly acidic ACP (*7*). There is increasing evidence that the components of the FASII pathway associate with each other in vivo. Bloch *et al*

isolated a high molecular weight protein fraction displaying FASII activity from *M. smegmatis*, where both InhA and MabA have been specifically identified in this complex (*8*). More recently, Zerbib *et al* demonstrated the existence of both heterotropic and homotropic protein-protein interactions within the member of the FASII pathway. In addition, the enzyme responsible for dehydration of hydroxyacyl-ACP during the elongation cycles of the FASII pathway remains unknown. This step is catalyzed by FabZ- and FabA-type enzymes in bacteria, but no homologous proteins are present in mycobacteria (*9*).

In order to gain more structural insight towards identifying protein-protein interactions between the members of the FASII pathway and discovering the dehydratase, we have utilized a variety of techniques to identify protein-protein interactions. These include the use of a photoreactive crosslinker, a bioorthogonal probe and fluorescent labels.

General Protein-Protein Identification Methods

Techniques developed to identify protein-protein interactions which offer high throughput and low resolution include phage display and yeast or bacteria two hybrid screens. In contrast, methods developed which offer low throughput and high resolution include affinity chromatography, crosslinking and utilizing bioorthogonal probes. Lastly, fluorescence spectroscopy can be used to quantitate the identified interaction.

Yeast or Bacterial Hybrid (Y2H, B2H)

In Y2H/B2H, a transcription factor is split into two fragments, the DNA-binding domain (BD) fragment and the activation domain (AD) fragment. Each fragment is then fused to separate proteins or peptide fragments. If these two proteins interact, then the AD and BD are brought in close proximity, which leads to the transcription of reporter gene (*10*). Through B2H, Tonge *et al* discovered a novel interaction between KasA and PpsB as well as PpsD, two polyketide modules involved in the biosynthesis of the virulence lipid phthiocerol dimycocerosate (PDIM) (*11*). One major drawback to consider with this method is that false positives are often detected and therefore the analysis of the results must be carefully controlled.

Phage Display

Phage display is one of the oldest and most robust combinatorial biology methods. The technology is based on the fact that polypeptides fused to bacteriophage coat proteins can be displayed on the surface of the viral particle (*12-14*). By entering into a bacterial host, the phage particles will be transformed, where the incorporation of many different DNA fragments will result in a phage-displayed library (*15*). Protein-protein interactions are identified by passing a phage-displayed library over the surface of an immobilized target protein. Following binding selection, proteins can be analyzed by using simple enzyme-linked immunosorban assays (ELISAs) to quantify binding in a high-throughput fashion (*16*).

Protein Affinity Chromatography

Another common method to study protein-protein interactions is by affinity chromatography. Proteins of interest can either be coupled directly to preactivated resins or they can be noncovalently tethered through high-affinity binding interactions. Both methods were demonstrated by Beeckmans and Kanarek who identified an interaction between fumarase and malate dehydrogenase by immobilizing fumarase to an antibody bound to protein A-Sepharose, as well as by directly coupling fumarase to Sepharose (*17*).

There are both advantages and disadvantages to this technique. One advantage is, protein affinity chromatography is extremely sensitive, detecting interactions with a binding constant as weak as 10^{-5} M (*18*). One disadvantage of this technique is the possibility of affecting the biological activity of the protein during coupling, which can lead to a failure to detect binding partners of the immobilized protein. A second potential problem derives from the very sensitivity of the method, where secondary techniques are required to determine if the interaction is physiologically relevant (*1*). The detection of a false-positives can occur for a variety of reasons, including, binding due to charged interactions; secondary protein interactions; or the proteins may interact with high specificity *in vitro* but not in the cell. A well known example of the latter is the high affinity of actin for DNase I (*19*).

Crosslinkers

Cross-linking techniques do not have the advantage of phage display or yeast two-hybrid systems, where libraries of potential protein partners can be rapidly screened,

nor does it offer information about the strength of an interaction. It does however allow for the production of higher resolution structural data, where protein-protein interactions can be mapped to specific domains or amino acids (*20, 21*). Significantly, crosslinking allows non covalent interactions which are often transient or may depend on specific physiological conditions, to be captured into long lived covalent complexes for subsequent purification and analysis (*22*).

Chemical Crosslinkers

There are many readily available chemical crosslinkers which are commonly used to probe protein-protein interactions. Even so, Brown *et al* developed a new class of crosslinkers utilizing metal catalyzed oxidation to cross-link proteins (*23*). Specifically, chelated Ni(II) can be used to introduce zero-length crosslinks between proteins. This reaction entails the oxidation of Ni(II) to a highly reactive Ni(III)-oxo species in the presence of a peracid that can in turn take electrons from aromatic amino acid side chains. Bond formation results from the quenching of the radical cation by a nearby electron rich or nucleophilic residue. Brown *et al* demonstrated this chemistry by tethering a nickel-based crosslinker to the protein ecotin and subsequently crosslinking ecotin to itself, and to its protease target, trypsin (*24*). Other metal complexes such as palladium, ruthenium and manganese in concert with peracids have also been used to crosslink proteins in a site specific manor (*25-27*). Although many important protein-protein interactions have been discovered by this technique, it is limited to only metal binding proteins.

Photo Crosslinkers

Photochemical cross linkers were also developed to examine protein-protein interactions and usually consist of fluorescent or radiolabeled aryl azides, carbenes, or benzophenones attached to an electrophile. The attachment is through either a cleavable linker, which includes a disulfide, azo or ester linker or a non-cleavable linker, such as carbon (*28, 29*). The reagents are first tethered to a known protein by the electrophilic end of the crosslinker, with subsequent activation by UV light, resulting in a crosslink to a nearby protein (*26*). If the crosslinker contains a cleavable linker, it is severed in a last step, resulting in a label transfer, and thus the identification of the binding partner. Ebright and coworkers demonstrated the effectiveness of this method by attaching a photoactivatable azide crosslinker to an engineered cysteine in the *E. coli* catabolite activating protein (CAP) which crosslinked to RNA polymerase, forming the CAP-RNA-polymerase complex (*30*). After photolysis, the crosslinker disulfide bond was reduced thus transferring the tag to the RNA-polymerase α subunit. The use of photoaffinity crosslinkers with an attached electrophile is becoming more popular because it allows for the selective attachment of the reagent to the protein and provides a simple and effective way to identify multiprotein complexes.

Bio-orthogonal Probes

A relatively new methods to study biomolecules is through the use of bioorthogonal chemical reactions, or reactions that do not interfere with biology (*31*). Bioorthogonal chemical reactions have successfully been used to study proteins, glycans, lipids, and nucleic acids in living systems (*32*).

The first step of this approach involves the incorporation of a functional group into a biomolecule through metabolic uptake of an unnatural substrate. The size of the functional group is crucial, in that it must be small enough that the organism's biosynthetic machinery accepts the modified metabolite (*33-35*). The second step involves the detection of the biomolecule through a bioorthogonal ligation with the complementary reactive group attached to a probe (fluorophore or affinity tag). Initially, chemical reporters that were used included ketones, aldehydes or azides. However, the reactions with ketones and aldehydes were found inefficient at physiological pH and the presence of intracellular ketones and aldehydes limit their use to cell surface labeling (*36*). Azides are an attractive alternative because they are small, kinetically stable and are not present in endogenous metabolites. In consequence, the azide has taken the place of the ketone/aldehyde as a chemical reporter group (*37*). The detection of azides can be accomplished by three click chemistry methods, the Staudinger ligation with triarylphosphine reagents (*35*), the copper-catalyzed cycloaddition between terminal alkynes and azides (*38, 39*), or [3 + 2] cycloaddition with strained cyclooctynes (*40, 41*). There are many examples that indicate the use of bioorthogonal probes with azide moieties resulting in high sensitivity protein labeling with superior kinetics (*31*).

Fluorescence

Once the protein-protein interactions have been identified, researchers can turn to a wide range of tools and techniques to gather real-time functional data about binding events. This is especially necessary for techniques that may identify false positives such as Y2H/B2H. Fluorescence is a highly sensitive method for detecting and quantifying

protein-protein interactions. There are two ways in which fluorescence can be applied to measure the interactions of proteins, either by monitoring changes in the intrinsic tryptophan fluorescence or by changes in a fluorescent tag (42-44). Sensitivity is dependent on the intensity of the fluorescent change and since fluorescent tags are developed to have a high fluorescent signal, the latter technique allows for greater sensitivity (45). An example of this approach is the interaction between calmodulin and smooth myosin light chain kinase. Johnson *et al* were able to quantitatively determine the binding event by fluorescently labeling calmodulin through a native cysteine (*44*).

Elucidating a FASII Complex

This biosynthetic pathway is essential and specific for mycobacteria and still represents a valuable system for the search of new anti-tuberculosis agents. As previously stated, several data in the literature suggest the existence of protein–protein interactions within the FASII pathway. An isolated protein fraction exhibiting FASII activity containing InhA and MabA was identified (*8*). In addition, through Y2H and co-immunoprecipitation techniques, Zerbib *et al* demonstrated the condensing enzymes KasA, KasB and mtFabH interact with each other, along with the reductases MabA (*46*). In addition, through B2H a novel interaction between InhA and KasA was discovered. The interactions between the components of the FASII pathway might be critical for modulating their activity and inhibition and therefore elucidating these interactions is a vital step toward drug discovery.

In order to identify the interactions between the components of the FASII pathway and discover the unknown dehydratase, we have utilized a variety of protein-protein

identification techniques. With the knowledge that AcpM interacts with many proteins in the cell, we developed an AcpM photoprobe by attaching a benzophenone group to the prosthetic PPant arm and incubated it *M. smegmatis* cell lysate in an attempt to identify the unknown dehydratase. A separate method employed to identify the dehydratase was through the use of an ω-azido fatty acid probe, which was developed to target the fatty acylated proteins in the cell. Lastly, due to the evidence of an interaction between InhA and KasA, we have incorporated fluorescent labels into InhA in order to quantitate the interaction to KasA.

Materials and Methods

Chemical Synthesis of ω-Azido-dodecanoic Acid

The chemical synthesis of the ω-azido-fatty acids was performed as previously described by Hang *et al* (**Scheme 4.1**, (*47*)). Briefly, commercially available ω-azido-dodecanoic acid was converted to corresponding methyl esters with acetyl chloride (AcCl) and methanol (MeOH). The ω-hydroxy fatty acid methyl ester was then reacted with mesyl chloride (MsCl) and triethylamine (TEA) to afford the corresponding ω-mesyl fatty acid methyl ester, which were displaced with sodium azide in N,N-dimethyl formamide (DMF). The resulting ω-azido-fatty acid methyl ester were saponified with 1 M sodium hydroxide (NaOH) in tetrahydrofuran (THF):water (1:1) to yield the ω-azido-dodecanoic acid.

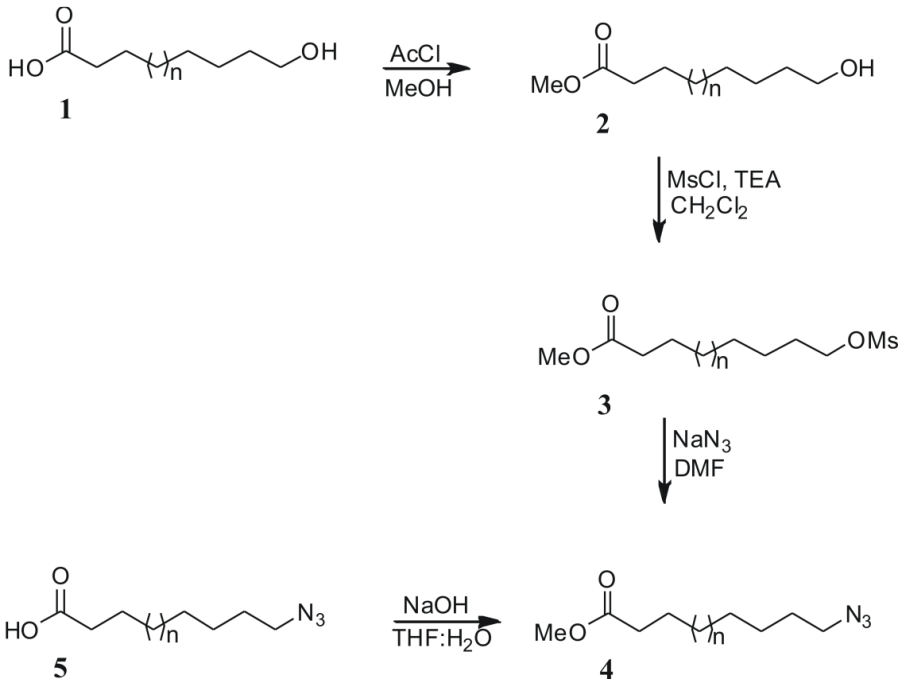

Scheme 4.1: Synthesis of ω-azido-hexadecanoic acid

ω-Hydroxy-dodecanoic Acid Methyl Ester ***(2)***

16-hydroxyhexadodecanoic acid (2 mmol), MeOH (5 mL) and AcCl (10 mmol) were added to a 25 mL round-bottom flask. The solution was stirred for 3 hours at room temperature and the solvent was removed under vacuum. The resulting white solid was resuspended in CH_2Cl_2 (50 mL), washed with $NaHCO_3$ (2 x 50 mL) and brine (50 mL). The organic phase was separated, dried over Na_2SO4 and concentrated. The crude material was purified by silica gel flash chromatography eluting with 10:1 hexanes:ethyl acetate (EtOAc) to afford the corresponding ω-hydroxy fatty acid methyl ester as a white solid in excellent yield (90%). ESI-MS: $[M\text{-}N_2+H]^+$ calcd. $C_{12}H_{24}NO_2$ 214.18, found 214.18.

ω-Mesyl-dodecanoic Acid Methyl Ester ***(3)***

The ω-hydroxy fatty acid methyl ester (**2,** 2 mmol) was dissolved in anhydrous CH_2Cl_2 (10 mL) and added to a 50 mL round-bottom flask. After the addition of TEA (2.2 mmol), the flask was placed in an ice-bath for 30 minutes followed by a dropwise addition of MsCl (2.2 mmol). The reaction mixture was stirred for an additional 30 minutes in the ice-bath followed by 1 hour at room temperature. The reaction mixture was then diluted with CH_2Cl_2 (50 mL), washed with deionized water (50 mL), $NaHCO_3$ (2 x 50 mL) and brine (50 mL). The organic phase was separated, dried over Na_2SO4 and concentrated to afford the corresponding ω-mesyl fatty acid methyl ester as a white solid in good yield (70%). ESI-MS: $[M\text{-}N_2+H]^+$ calcd. $C_{14}H_{28}NO_2$ 242.21, found 242.20.

*ω-Azido-dodecanoic Acid Methyl Ester **(4)***

ω-Mesyl fatty acid methyl ester (**3,** 2 mmol), anhydrous dimethyl formamide (DMF,10 mL) and sodium azide (10 mmol) were added to a 50 mL round-bottom flask. The solution was stirred for 16 hours at 45ºC, cooled to room temperature and concentrated. The crude material was resuspended in CH_2Cl_2 (50 mL), washed with deionized water (3 x 50 mL) and brine (50 mL). The organic phase was separated, dried over Na_2SO4 and concentrated. The crude material was purified by silica gel flash chromatography eluting with 10:1 hexanes:ethyl acetate (EtOAc) to afford ω-azido fatty acid methyl ester as a white solid in good yield (75%). ESI-MS: $[M-N_2+H]^+$ calcd. $C_{15}H_{30}NO_2$ 256.22, found 256.24.

*ω-Azido-hexadecanoic Acid **(5)***

ω-Azido fatty acid methyl ester (**4,** 2 mmol), THF (10 mL) and deionized water (10 mL) were added to a 50 mL round-bottom flask. NaOH (1 M, 10 mmol) was then added dropwise and the reaction mixture was stirred for 16 hours at room temperature. After diluting with EtOAc (50 mL), and washing with 10% HCl (25 mL), deionized water (2 x 50 mL) and brine (50 mL), the organic phase was separated, dried over Na_2SO4 and concentrated to afford the corresponding ω-azido fatty acid as a white solid in good yield (80%). ESI-MS: $[M-N_2+H]^+$ calcd. $C_{16}H_{32}NO_2$ 270.24, found 270.23.

*Benzophenone-4-maleimide Coenzyme A (B4M-CoA) Synthesis **(Scheme 4.2)***

Benzophenone-4-maleimide (Sigma, 18 μM), THF (2 mL), CoA (18 μM) and deionized water (2 mL) were added to a 10 mL round-bottom flask and the solution was

stirred at room temperature. The progression of the reaction was monitored by measuring the amount of free thiol in solution by using a 5'5'-dithiolbis(2-nitrobenzoic acid) (DTNB) assay (*48, 49*). The reaction was completed after 90 minutes, reading an A_{412} of 0.02. The THF was removed using a rotory evaporator and the resulting solution was flash frozen and dried under vacuum. All steps of the reaction were performed under light restrictive conditions. ESI-MS: $[M+H]^+$ calcd. $C_{38}H_{47}N_8O_{19}P_3S$ 1044.17, found 1044.2.

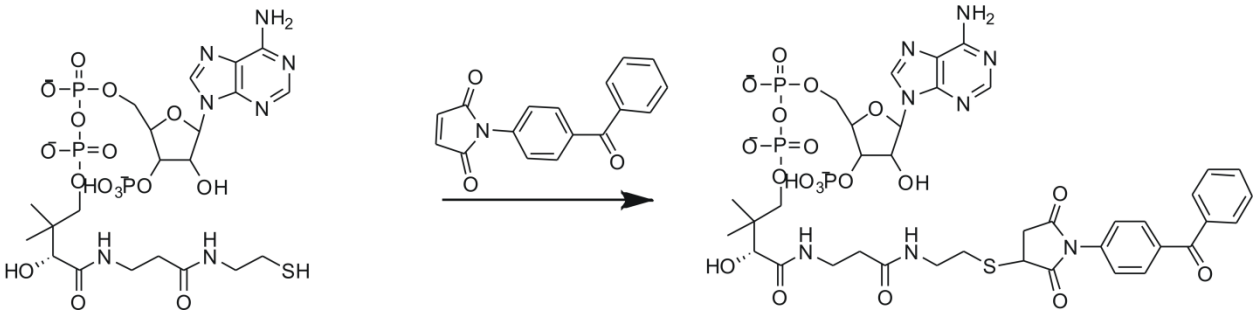

Scheme 4.2: Synthesis of B4M-CoA. Synthetic scheme for the reaction involving the production of the modified CoA. A michael attack from the thiol on the CoA will promote the formation of a carbon bond to the maleimide group, resulting in B4M-CoA.

Expression and Purification of AcpM

The pET24b vector containing the *AcpM* gene with an in-frame C-terminal hexahistidine-tag was transformed into E. *coli* pLysS competent cells. Colonies selected on LB solid media containing 30 µg/mL kanamycin were cultivated in LB media and

grown to an OD_{600} of 0.6-0.8, after which AcpM expression was induced with 0.3 mM IPTG at 37℃ for 3 hours. The cells were harvested by centrifugation and lysed by sonication. The AcpM protein was subsequently purified using standard nickel affinity chromatography which yielded three AcpM forms, apo, holo and acyl-AcpM. The fractions were analyzed by SDS-PAGE and UV spectroscopy (monitoring the absorbance at 280 nm) using a Nano Drop ND-1000 spectrophotometer. Fractions containing pure protein were subsequently dialyzed into a 75 mM Tris-HCl and 10 mM $MgCl_2$ buffer, pH 7.8. An ÄKTA fast protein liquid chromatography (FPLC) protein purification system was used to obtain pure apo protein by injecting the concentrated protein onto a Mono Q 5/50 GL column (GE healthcare) which had been equilibrated with 20 mM Tris buffer, pH 8.0 (buffer A). Elution of the different ACP substrates was achieved using a shallow linear gradient with buffer A containing 1 M NaCl. Fractions containing apo-AcpM were concentrated as previously described and stored at -20℃.

Expression and Purification of KasA

KasA was expressed as an N-terminally hexahistidine tagged construct in *M. smegmatis* mc^2155 competent cells and purified using standard nickel affinity chromatography as previously described in chapter 2.

Expression and Purification of InhA

InhA was expressed as an N-terminal hexahistidine tagged construct in *E. coli* pLysS cells and purified using standard nickel affinity chromatography as previously described in chapter 3.

Expression and Purification of S200C and S73C InhA

S200C and S73C InhA (available from previous studies) were expressed as a N-terminal hexahistidine tagged construct in *E. coli* pLysS cells and purified in the same manner as wild type InhA, by using standard nickel affinity chromatography as previously described in chapter 3.

B4M-AcpM Synthesis

AcpM (apo, holo, acyl) was incubated in reaction buffer (75 mM Tris, pH 8.5, 10 mM $MgCl_2$) with a 4 molar excess of B4M-CoA and 200 nM Sfp for 1.5 hour at 37℃. The reaction was stopped by flash freezing and stored at -20^{o}C. The product was verified by ESI-MS. All reactions were performed in under light restrictive conditions.

M. Smegmatis Growth

M. smegmatis mc^{2}155 cells were grown on 7H9 solid media containing 200 µg/mL ampicillin and 15 µg/mL cyclohexamide. Selected colonies were subsequently cultivated in 7H9 liquid media supplemented with glycerol, and grown to mid log phase (OD_{600} 0.5-0.8). The cells were then harvested, resuspended in 75 mM Tris-HCl, 10 mM $MgCl_2$, pH 7 and lysed by sonication.

Identifying Protein-Protein Interactions with B4M-AcpM

B4M-AcpM (10 µM) was incubated with *smegmatis* cell lysate (1 mg/mL), under light sensitive conditions for 1.5 hours at 35.5℃. The reaction mixture was then irradiated with 365 nm light (Spectroline, 60 Hz) for 10 min and subsequently purified by standard

nickel chromatography. Fractions containing protein were then separated by SDS-PAGE and transferred to a nitrocellulose membrane, which was blocked with PBST (PBS, 0.1% Tween-20) containing 5% non-fat dried milk for 1 hour at room temperature or overnight at 4ºC. The membrane was washed with PBST (3x) and incubated with anti polyhistidine alkaline phosphotase (1:2000 in PBST) for 1 hour at room temperature. The membrane was washed with PBST (3x) and subsequently developed with phosphotase substrate BGP/NBT (KPL). Any bands that were identified by western blot were then extracted out of an SDS protein gel and subject to tryptic digestion for proteomic analysis.

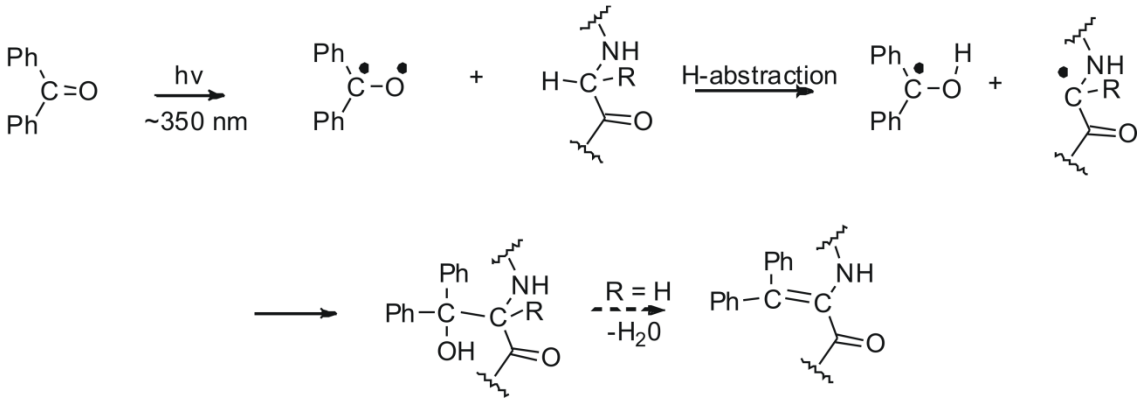

Scheme 4.3: Benzophenone Photochemistry. After irradiation with 350 nm light, a radical forms on the carbonyl carbon and oxygen. The carbonyl oxygen will then readily abstract a hydrogen from a nearby peptide bond, producing a radical on the carbon peptide backbone. Carbon-carbon bond formation and subsequent dehydration produces the covalent product (*50*).

Metabolic Labeling with ω-azido-hexadecanoic Acid

The ω-azido-hexadecanoic acid was dissolved in DMSO to generate 50 mM stock solutions. Fatty acids were added to 7H9 media and when necessary, the fatty acid-media solutions were sonicated to dissolve lipids. Fatty acid-media solutions were then added to *M. smegmatis* cells (1 mg/mL) and incubated for 6 hours at 35.5°. Cells were harvested washed with PBS and lysed with breaking buffer (100 mM phosphate buffer, pH 6.8) at 4ºC. Cell lysates were centrifuged at 20,000 g for 10 min at 4 ºC and concentrated.

Reaction of Azide Labeled Cells with a Biotin Alkyne or Alkyne-FLAG Tag

To the concentrated lysates, either a biotin alkyne tag (Invitrogen, Click-It Kit) with $CuSO_4$ as the catalyst were added, or the lysates were mixed with bathophenanthroline disulphonic acid disodium salt (3 mM), alkyne-FLAG (500 µM, gift from Prof Isaac Carrico) and CuBr (1 mM) for 1 hour. The samples were then analyzed by western blotting technique to determine incorporation of biotin alkyne or alkyne-FLAG Tag.

Western Blotting

The reaction mixture was separated by SDS-PAGE and transferred to a nitrocellulose membrane, which was blocked with PBST (PBS, 0.1% Tween-20) containing 5% non-fat dried milk for 1 hour at room temperature or overnight at 4ºC. The membrane was washed with PBST (3x) and incubated with an anti biotinylated alkaline phosphotase (1:2000 in PBST) or anti-FLAG M2 horseradish peroxidase (HRP) conjugate (1:12000 in PBST) for 1 hour at room temperature. The membrane was

washed with PBST (3x) and subsequently developed colorimetrically with phosphotase substrate BGP/NBT (KPL) or by chemiluminescence with an HRP substrate (Millipore Immobilon Western kit)

Fluorescently Labeling InhA

A 10-fold molar excess of TCEP was added to InhA (75 μM) in 100 mM phosphate buffer, pH 7.2. Then, a 10 mM solution of Alexa Fluor 350 C_5-maleimide dye or bimane C_3-maleimide (Invitrogen, **Figure 4.1, 4.2**) was prepared by adding 1 mg of dye into 175 μl of DMSO, which was added slowly to the InhA mixture and stirred for 2 hours at room temperature, wrapped in foil. Upon completion of the reaction, an excess of mecaptoethanol was added to quench any unreacted Alexa Fluor. To remove unreacted Alexa Fluor, the reaction was then subject to a sephadex G25 column, pre-equilibrated in 30 mM Pipes, 150 mM NaCl and 1mM EDTA at pH 6.8. The fractions were collected and the degree of labeling was determined by using the absorbance and the molar extinction coefficient of the dye. This identical method was used for labeling S73C and S200C InhA.

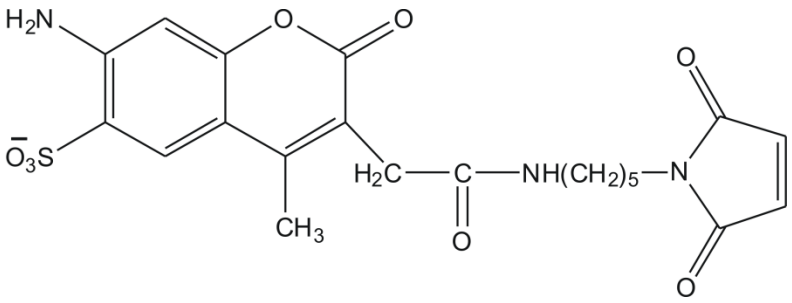

Figure 4.1: Structure of Alexa Fluor 350. Alexa Fluor 350 that was used for fluorescent experiments where it was attached to the cysteine on InhA. Excitation and emission wavelengths are 345 and 444 nm.

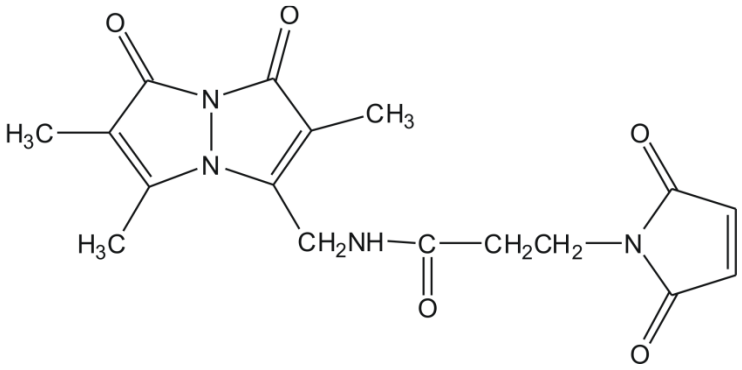

Figure 4.2: **Structure of Bimane Fluorophore.** Bimane that was used for fluorescent experiments where it was attached to the cysteine on InhA. Excitation and emission wavelengths are 388 and 474 nm.

Direct Binding Fluorescence Titrations

A direct binding experiment was employed in which the fluorescence of Alexa Fluor 350 or Bimane bound to InhA was used to measure the affinity of KasA for InhA, using a Flurolog.Quanta Master fluorimeter (Photon Technology International). Excitation

wavelengths for the Alexa Fluor and Bimane were 345 and 388, where the emission wavelengths were 444 and 474, respectively, with excitation slit width of 4.0 nm and an emission slit width of 8.0 nm. KasA was titrated at 0-1000 nm concentrations, and the concentration of enzyme in the direct binding measurements was 30 nM. All solutions were filtered and equilibrated to 25℃.

Results

Expression and Purification of InhA (wild type, S200C, S73C), AcpM and KasA

The proteins were purified by using hexahistidine-tag affinity purification chromatography, yielding pure recombinant protein with the predicted molecular weights of ~30 kDa, 15 kDa and 42 kDa, respectively as determined by SDS-PAGE.

Identifying Protein Interactions with B4M-AcpM

ACPs are highly conserved, small acidic proteins that are involved in many biosynthetic pathways, including, fatty acid synthesis (FAS), lipopolysaccharide synthesis and polyketide synthesis (*51-55*). ACP is responsible for shuttling the growing fatty acid chain between a collection of enzymes during fatty acid elongation and modification.

As discussed, small molecule probes are commonly used to detect novel protein-protein interactions, where the elucidation of these interactions is an important step in the drug discovery process. We developed a photoreactive probe by attaching a benzophenone to the prosthetic PPant arm of AcpM (B4M-AcpM). To determine if our photoreactive probe can be used to identify protein-protein interactions, controls were done with proteins known to interact with AcpM. These proteins include but are not limited to, KasA, InhA, and MabA **(Figure 4.3)**. After incubation of B4M-AcpM with the said proteins and subsequent western blot, KasA (**Figure 4.3**; ln 2b) and InhA (**Figure 4.3**; ln 6b) both show an appearance of a higher molecular weight band (**Figure 4.3**; lanes 1b, MW ~ 58190 Da and 6b, MW ~ 45190 Da respectively), indicating that B4M-

AcpM can be used to identify protein-protein interactions. This positive control allowed us to try our system in *M. smegmatis* cell lysate with the purpose of identifying the dehydratase. The resulting western blot indicated the presence of many protein bands, four of which were extracted out of an SDS-PAGE gel, subject to trypsin digestion and sequenced. All four sequencing results identified AcpM, however, the other most abundant proteins in the samples were identified as chaperones and bovine serum albumin (BSA, **Figure 4.4**).

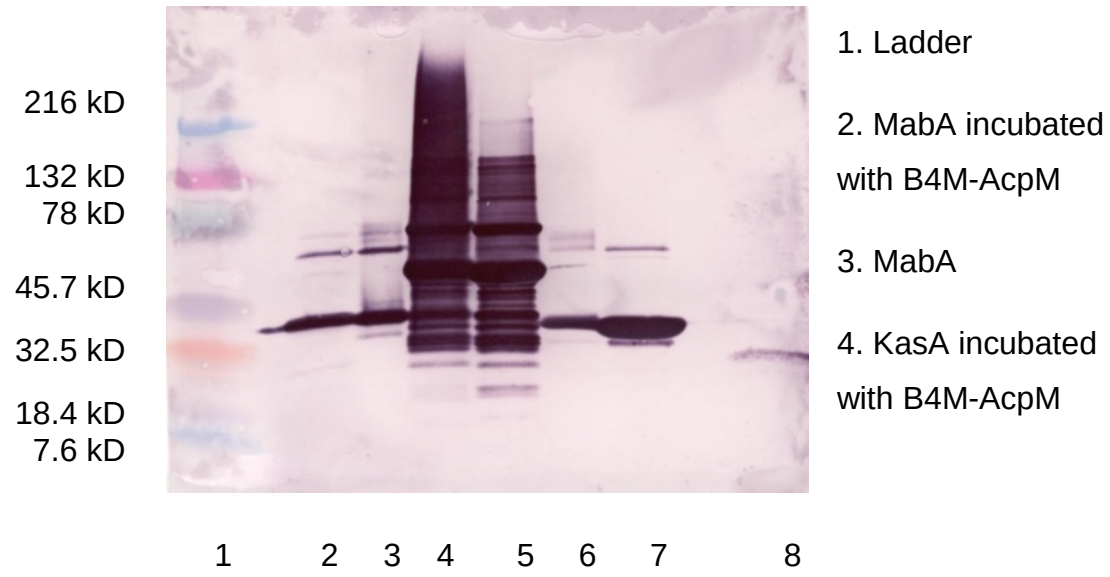

Figure 4.3: Reaction with Purified MabA, KasA and InhA and B4M-AcpM. By comparing 4 and 5 on the western blot, a light shift in the monomeric weight of KasA is seen, possibly indicating a covalent interaction between KasA and B4M-AcpM. The same upward shift is seen with InhA when comparing lanes 6 and 7.

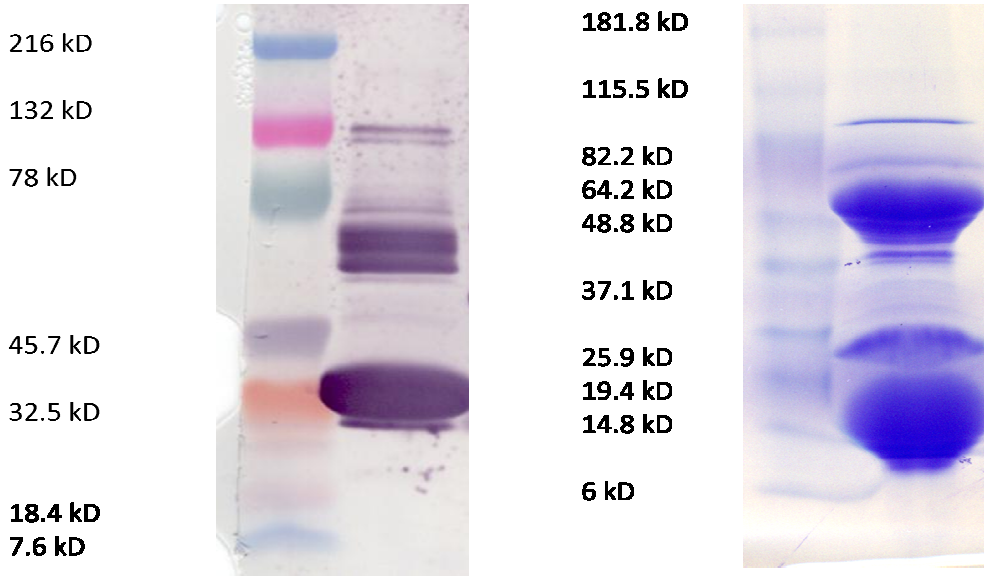

Figure 4.4: Reaction with *M. smegmatis* Cell Lysate and B4M-AcpM. By comparing the western blot and SDS gel, 4 large bands were identified as possible proteins covalently bound to B4M-AcpM. These proteins were then analyzed by ESI-MS.

Incorporation of ω-Azido-fatty Acids

Acylation is a key step for all the enzymes of the fatty acid biosynthesis pathway. To explore whether ω-azido-fatty acids could serve as chemical probes for fatty acylated proteins and potentially identify the dehydratase, we synthesized ω-azido-hexadecanoic acid and incubated it with *M. smegmatis* and *E. coli* cells.

Upon analysis of the western blot which compares the lysates of *M. smegmatis* and *E. coli* with and without addition of ω-azido-hexadecanoic acid and subsequent reaction with an alkyne biotinylated tag, it appeared that only natively biotinylated proteins were being detected **(Figure 4.5)**. These results indicate that either the click chemistry is not occurring or the fatty acids are not entering into the cells. The results from western blot

development by chemiluminescence yielded a similar conclusion. However, product formation between ω-azido- hexadecanoic acid and 1-octyne in the presence of $CuSO_4$, led towards favoring the latter conclusion.

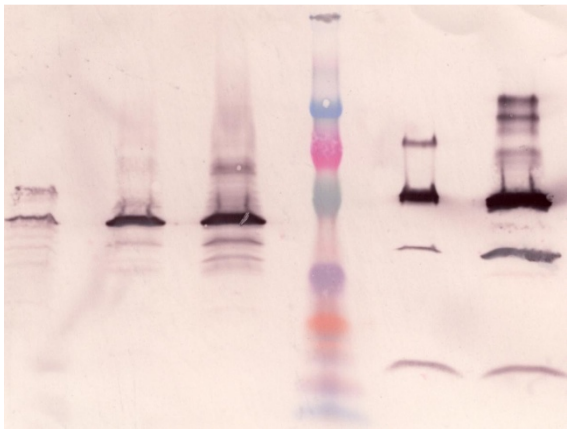

1. *M. smegmatis* lysate with fatty acid (lysed before incubation)

2. *M. smegmatis* lysate with fatty acid (lysed after incubation)

3. *M. smegmatis* lysate without fatty acid

Ladder

4. *E. coli* lysate with fatty acid

5. *E.Coli* lysate without fatty acid

Figure 4.5: Reaction of ω-Azido-hexadecanoic Acid with Protein Lysate. Western blot of *M. smegmatis* and *E. coli* with and without addition of ω-azido- hexadecanoic acid and subsequent reaction with an alkyne biotinylated tag. By comparing lanes 1/2 with 3 and 4 with 5, it appears that only native biotinylated proteins are present.

InhA-KasA Fluorescence

Bacterial two hybrid (B2H) studies previously performed in our lab identified a novel interaction between KasA and InhA. In order to investigate the InhA-KasA interaction further, we incorporated fluorophores into wild type and clinical mutants of InhA to be used for direct binding experiments. Both fluorophores are thiol reactive probe which react with cysteines. InhA has one native cysteine at position 243. The degree of

labeling for each protein was determined using the absorbance and extinction coefficient of the probe. Wild type InhA had a degree of labeling of 0.5, which supports the idea that the native cysteine is less accessible due to its buried position in the protein **(Figure 4.6)**. This led us to our first mutant, S73C. It was engineered so the mutation would produce a cysteine on the surface of the protein **(Figure 4.7)** in order to gain to a higher degree of labeling, which was determined as 1.02. In an attempt to gain a higher success of detecting an interaction between KasA and InhA, a second mutant was made, S200C which was also engineered to produce a surface cysteine **(Figure 4.7)** but this time on the opposite face of the first mutation. The distance between the two mutations is 32 Å apart. The degree of labeling of S200C was determined as 1.50. Fluorescent titration experiments were performed, where a decrease in fluorescence was detected for wild type, S200C and S73C InhA upon addition of KasA. However, the buffer controls showed a similar decrease in fluorescence, indicating this method cannot be used to detect the binding interaction between InhA and KasA.

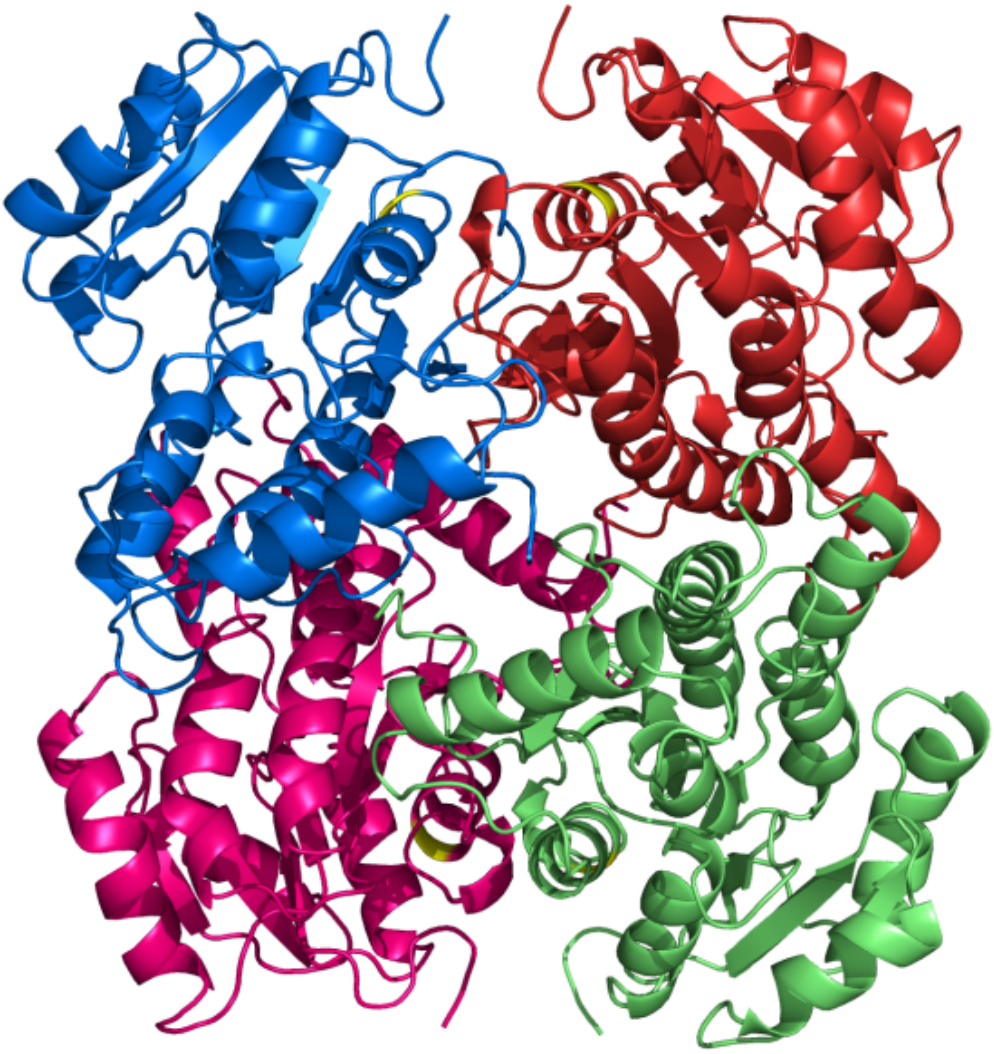

Figure 4.6: Structure of the InhA Tetramer. The native cysteine is colored in yellow.

This figure was made by PyMoL (1BVR.pdb)

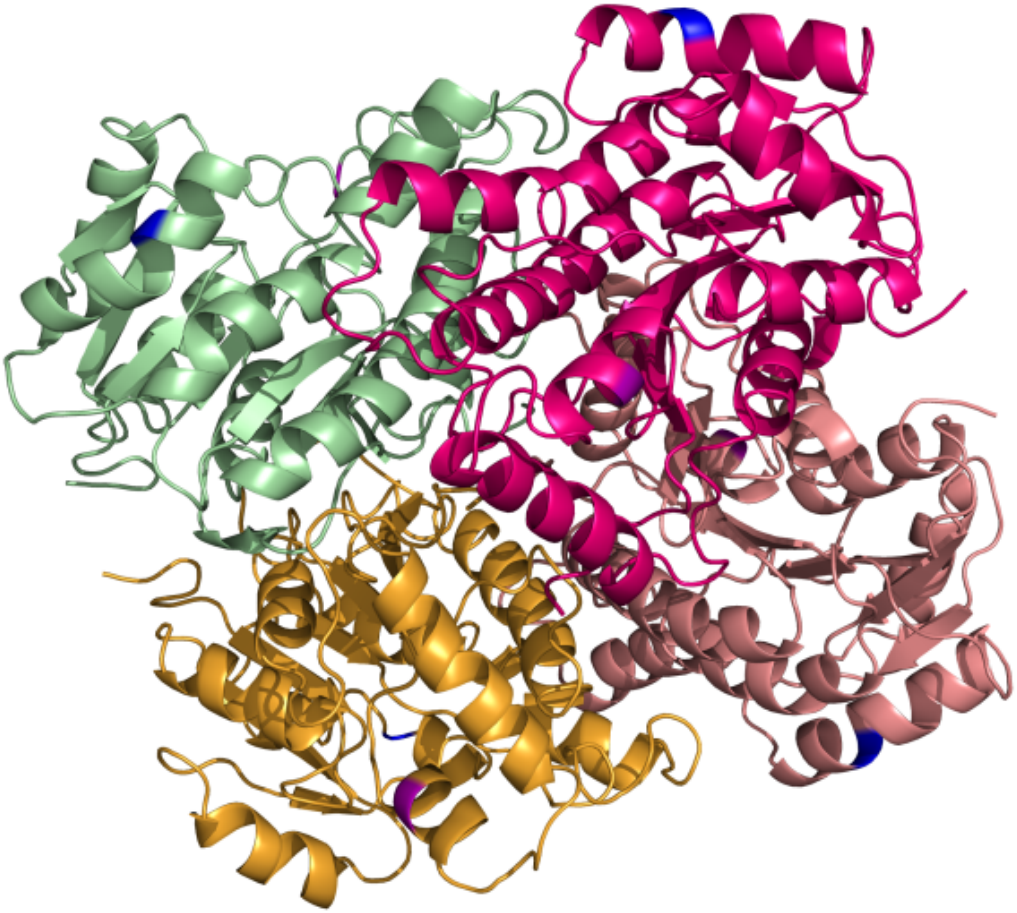

Figure 4.7: Structure of InhA Tetramer. The S200C mutation is colored in blue and the S73C mutation is colored in purple. This figure was made using PyMoL (1BVR.pdb)

Discussion

This biosynthetic pathway is essential and specific for mycobacteria and thus represents a valuable system for the search of new anti-tuberculosis agents. An important feature of the FASII system is that the hydrophobic fatty acyl intermediates are shuttled from enzyme to enzyme attached to a phosphopantetheine prosthetic group on a small, highly acidic ACP (*7*). Several data in the literature suggest the existence of a non covalent complex between the components of the FASII pathway (*8, 46*), where these interactions may modulate their activity and inhibition. In addition, Barry *et al* isolated an 80 kD complex consisting of KasA, AcpM and INH, confirming the role of AcpM within this multi-subunit complex.

ACP interacts with all components of the FASII system, including the unknown dehydratase. In an attempt to identify the dehydratase, we developed a photoprobe by tethering a benzophenone moiety to the prosthetic PPant arm of AcpM. A benzophenone photoprobe was chosen due to specific biochemical and chemical advantages (*56*). First, benzophenones are more stable than other photoactivatable probes such as diazo esters, aryl azides and diazarines. They can also be manipulated in ambient light and activated at wavelengths that are not harmful to proteins. Lastly, benzophenones will favor bond formation to nearby carbons that are unreactive even in the presence of solvent and nucleophiles **(Scheme 4.3)**. These properties combined make benzophenones a top choice for covalent modifications. Although our lysate incubation experiments were unable to identify novel interactions, the photoprobe successfully crosslinked to KasA and InhA, along with chaperones and BSA in the lysate. Therefore, these initial results substantiate the use of B4M-AcpM as a

photoprobe. This is supported by Tonge *et al* who confirmed an interactions between PpsB and KasA by transferring B4M-CoA to the ACP domain of PpsB, resulting in a B4M-PpsB which was then shown to form a crosslink with KasA (*11*). Future experiments that eliminate the presence of BSA (M. smegmatis cells grown in the absence of ADS supplement which contains BSA) and those that reduce the amount of chaperones, could be promising experiments to detect AcpM-protein interactions in the cell. Chaperone proteins are present to reduce aggregation of intracellular protein (*57*), therefore growing the cells to a lower OD could result in less chaperone expression.

Acylation is a key step for all the enzymes of the fatty acid biosynthesis pathway. Therefore, in a separate attempt to identify the dehydratase, we synthesized a ω-azido hexadecanoic acid bioorthogonal probe. Azides are small, kinetically stable and are not present in endogenous metabolites, making them the most versatile bioorthogonal chemical probe available. Our results suggest that the ω-azido hexadecanoic acid was unable to identify fatty acylated proteins. Two possibilities could arise from this, either the click chemistry is not occurring or the fatty acids are not entering into the cells. A control experiment which detected product formation between ω-azido hexadecanoic acid and 1-octyne in the presence of $CuSO_4$, led towards favoring the latter conclusion.

Future experiments towards the success of metabolic labeling of cells with azido fatty acids will include optimizing the feeding conditions for entrance into the cells. Fatty acid solubilization experiments were performed by Smith and Lough who determined that at physiological pH, saturated fatty acids have the highest solubility in aqueous solution containing bile salts and phospholipids such as phosphatidylethanolamine and

lecithin (*58*). In addition, there are also commercially available reagents we can use such as solutol® which facilitate the entrance of hydrophobic molecules into the cell.

B2H studies previously performed in our lab identified a novel interaction between KasA and InhA. Although B2H studies are an effective method in detecting *in vivo* interactions between proteins, they cannot provide information on the site of the interaction. This technique also suffers from the detection of false positives. In order to investigate the InhA-KasA interaction further, we incorporated fluorophores into wild type and clinical mutants of InhA for their use in direct binding experiments. However, the fluorescent titration experiments were unable to detect binding between InhA and KasA. InhA is a 120 kD tetramer and KasA is an 80 kD dimer, therefore, the surface area over the two proteins is quite large. The inability to detect an interaction could suggest that KasA is simply not interacting with the surface of InhA near residues S200 or S73 or that fluorescence is not an appropriate method to further characterize the binding interaction. Future experiments that entail engineering additional mutations to InhA are thus required to elucidate the binding site.

The preliminary results we discussed from our protein-protein interaction techniques exemplify their potential in identifying protein binding partners in a complex cellular environment. However, they also emphasize the requirement for optimization in order to succeed further. We have hope that by employing these techniques in future optimized experiments, the discovery of novel protein-protein interactions will ensue.

Summary

Protein-protein interactions are central to biological processes. There has been increasing evidence that the components of the FASII pathway interact with one other, where this interaction might be critical for modulating their activity and inhibition and therefore elucidating these interactions is a vital step toward drug discovery. In addition, the enzyme responsible for dehydration of hydroxyacyl-ACP during the elongation cycles of the FASII pathway remains unknown.

In order to identify the interactions between the components of the FASII pathway and discovering the unknown dehydratase, we have utilized a variety of protein-protein identification techniques. First, we developed an AcpM photoprobe in an attempt to identify the unknown dehydratase. Although our lysate incubation experiments were unable to identify novel interactions, the photoprobe successfully crosslinked to KasA and InhA, along with chaperones and BSA in the lysate. With future experimental optimization, the photoprobe could prove to be a useful tool. A separate method employed to identify the dehydratase was through the use of an ω-azido fatty acid probe, which was developed to target the fatty acylated proteins in the cell. Similar to the previous experiment, our incubation experiments were unable to identify acylated proteins, suggesting the requirement for future optimization of this technique. Lastly, due to the evidence of an interaction between InhA and KasA, we have incorporated fluorescent labels into InhA in order to quantitate the interaction to KasA. Our results indicate that either fluorescence cannot be used to further characterize this interaction or the fluorophore is not in an optimal position to detect an interaction.

Addressing and overcoming the problems we encountered when employing our techniques could give way to the discovery of novel protein-protein interactions.

References

1. Phizicky, E. M., and Fields, S. (1995) Protein-protein interactions: methods for detection and analysis, *Microbiol Rev 59*, 94-123.
2. Evans, P. R., Farrants, G. W., and Hudson, P. J. (1981) Phosphofructokinase: structure and control, *Philos Trans R Soc Lond B Biol Sci 293*, 53-62.
3. Kellogg, D. R., Field, C. M., and Alberts, B. M. (1989) Identification of microtubule-associated proteins in the centrosome, spindle, and kinetochore of the early Drosophila embryo, *J Cell Biol 109*, 2977-2991.
4. Kerppola, T. K., and Curran, T. (1991) Fos-Jun heterodimers and Jun homodimers bend DNA in opposite orientations: implications for transcription factor cooperativity, *Cell 66*, 317-326.
5. Monod, J., Wyman, J., and Changeux, J. P. (1965) On the Nature of Allosteric Transitions: A Plausible Model, *J Mol Biol 12*, 88-118.
6. Yanofsky, C., and Rachmeler, M. (1958) The exclusion of free indole as an intermediate in the biosynthesis of tryptophan in Neurospora crassa, *Biochim Biophys Acta 28*, 640-641.
7. Schaeffer, M. L., Agnihotri, G., Kallender, H., Brennan, P. J., and Lonsdale, J. T. (2001) Expression, purification, and characterization of the Mycobacterium tuberculosis acyl carrier protein, AcpM, *Biochim Biophys Acta 1532*, 67-78.
8. Odriozola, J. M., Ramos, J. A., and Bloch, K. (1977) Fatty acid synthetase activity in Mycobacterium smegmatis. Characterization of the acyl carrier protein-dependent elongating system, *Biochim Biophys Acta 488*, 207-217.

9. Heath, R. J., and Rock, C. O. (1996) Roles of the FabA and FabZ beta-hydroxyacyl-acyl carrier protein dehydratases in Escherichia coli fatty acid biosynthesis, *J Biol Chem 271*, 27795-27801.

10. Young, K. H. (1998) Yeast two-hybrid: so many interactions, (in) so little time, *Biol Reprod 58*, 302-311.

11. Kruh, N. A., Borgaro, J. G., Ruzsicska, B. P., Xu, H., and Tonge, P. J. (2008) A novel interaction linking the FAS-II and phthiocerol dimycocerosate (PDIM) biosynthetic pathways, *J Biol Chem 283*, 31719-31725.

12. Bass, S., Greene, R., and Wells, J. A. (1990) Hormone phage: an enrichment method for variant proteins with altered binding properties, *Proteins 8*, 309-314.

13. Scott, J. K., and Smith, G. P. (1990) Searching for peptide ligands with an epitope library, *Science 249*, 386-390.

14. Smith, G. P. (1985) Filamentous fusion phage: novel expression vectors that display cloned antigens on the virion surface, *Science 228*, 1315-1317.

15. Smith, G. P., and Petrenko, V. A. (1997) Phage Display, *Chem Rev 97*, 391-410.

16. Sidhu, S. S., Lowman, H. B., Cunningham, B. C., and Wells, J. A. (2000) Phage display for selection of novel binding peptides, *Methods Enzymol 328*, 333-363.

17. Beeckmans, S., and Kanarek, L. (1981) Demonstration of physical interactions between consecutive enzymes of the citric acid cycle and of the aspartate-malate shuttle. A study involving fumarase, malate dehydrogenase, citrate synthesis and aspartate aminotransferase, *Eur J Biochem 117*, 527-535.

18. Formosa, T., Barry, J., Alberts, B. M., and Greenblatt, J. (1991) Using protein affinity chromatography to probe structure of protein machines, *Methods Enzymol 208*, 24-45.

19. Lazarides, E., and Lindberg, U. (1974) Actin is the naturally occurring inhibitor of deoxyribonuclease I, *Proc Natl Acad Sci U S A 71*, 4742-4746.

20. Fancy, D. A. (2000) Elucidation of protein-protein interactions using chemical cross-linking or label transfer techniques, *Curr Opin Chem Biol 4*, 28-33.

21. Trakselis, M. A., Alley, S. C., and Ishmael, F. T. (2005) Identification and mapping of protein-protein interactions by a combination of cross-linking, cleavage, and proteomics, *Bioconjug Chem 16*, 741-750.

22. Beeckmans, S. (1999) Chromatographic methods to study protein-protein interactions, *Methods 19*, 278-305.

23. Brown, K. C., Yang, S. H., and Kodadek, T. (1995) Highly specific oxidative cross-linking of proteins mediated by a nickel-peptide complex, *Biochemistry 34*, 4733-4739.

24. Brown, K. C., Yu, Z., Burlingame, A. L., and Craik, C. S. (1998) Determining protein-protein interactions by oxidative cross-linking of a glycine-glycine-histidine fusion protein, *Biochemistry 37*, 4397-4406.

25. Campbell, L. A., Kodadek, T., and Brown, K. C. (1998) Protein cross-linking mediated by metalloporphyrins, *Bioorg Med Chem 6*, 1301-1307.

26. Fancy, D. A., and Kodadek, T. (1999) Chemistry for the analysis of protein-protein interactions: rapid and efficient cross-linking triggered by long wavelength light, *Proc Natl Acad Sci U S A 96*, 6020-6024.

27. Kim, K., Fancy, D. A., Carney, D., and Kodadek, T. (1999) Photoinduced Protein Cross-linking Mediated by Palladium Porphyrins, *J. Am. Chem. Soc 121*, 11896-11897.

28. Marriott, G., and Ottl, J. (1998) Synthesis and applications of heterobifunctional photocleavable cross-linking reagents, *Methods Enzymol 291*, 155-175.

29. Cornish, V. W., Hahn, K. M., Schultz, P. G. (1996) Site-specific protein modification using a ketone handle, *J. Am. Chem. Soc 118*, 8150-8151.

30. Chen, Y., Ebright, Y. W., and Ebright, R. H. (1994) Identification of the target of a transcription activator protein by protein-protein photocrosslinking, *Science 265*, 90-92.

31. Prescher, J. A., and Bertozzi, C. R. (2005) Chemistry in living systems, *Nat Chem Biol 1*, 13-21.

32. Sletten, E. M., and Bertozzi, C. R. (2009) Bioorthogonal chemistry: fishing for selectivity in a sea of functionality, *Angew Chem Int Ed Engl 48*, 6974-6998.

33. Kho, Y., Kim, S. C., Jiang, C., Barma, D., Kwon, S. W., Cheng, J., Jaunbergs, J., Weinbaum, C., Tamanoi, F., Falck, J., and Zhao, Y. (2004) A tagging-via-substrate technology for detection and proteomics of farnesylated proteins, *Proc Natl Acad Sci U S A 101*, 12479-12484.

34. Kiick, K. L., Saxon, E., Tirrell, D. A., and Bertozzi, C. R. (2002) Incorporation of azides into recombinant proteins for chemoselective modification by the Staudinger ligation, *Proc Natl Acad Sci U S A 99*, 19-24.

35. Saxon, E., and Bertozzi, C. R. (2000) Cell surface engineering by a modified Staudinger reaction, *Science 287*, 2007-2010.

36. Mahal, L. K., Yarema, K. J., and Bertozzi, C. R. (1997) Engineering chemical reactivity on cell surfaces through oligosaccharide biosynthesis, *Science 276*, 1125-1128.

37. Baskin, J. M., Bertozzi, C.R. (2007) Bioorthogonal Click Chemistry: Covalent Labeling in Living Systems, *QSAR Comb. Sci. 26*.

38. Rostovtsev, V. V., Green, L. G., Fokin, V. V., and Sharpless, K. B. (2002) A stepwise huisgen cycloaddition process: copper(I)-catalyzed regioselective "ligation" of azides and terminal alkynes, *Angew Chem Int Ed Engl 41*, 2596-2599.

39. Tornoe, C. W., Christensen, C., and Meldal, M. (2002) Peptidotriazoles on solid phase: [1,2,3]-triazoles by regiospecific copper(i)-catalyzed 1,3-dipolar cycloadditions of terminal alkynes to azides, *J Org Chem 67*, 3057-3064.

40. Agard, N. J., Prescher, J. A., and Bertozzi, C. R. (2004) A strain-promoted [3 + 2] azide-alkyne cycloaddition for covalent modification of biomolecules in living systems, *J Am Chem Soc 126*, 15046-15047.

41. Baskin, J. M., Prescher, J. A., Laughlin, S. T., Agard, N. J., Chang, P. V., Miller, I. A., Lo, A., Codelli, J. A., and Bertozzi, C. R. (2007) Copper-free click chemistry for dynamic in vivo imaging, *Proc Natl Acad Sci U S A 104*, 16793-16797.

42. Kwon, O. S., and Churchich, J. E. (1994) Interaction of 70-kDA heat shock cognate protein with peptides and myo-inositol monophosphatase, *J Biol Chem 269*, 266-271.

43. Lee, F. S., Auld, D. S., and Vallee, B. L. (1989) Tryptophan fluorescence as a probe of placental ribonuclease inhibitor binding to angiogenin, *Biochemistry 28*, 219-224.

44. Mills, J. S., Walsh, M. P., Nemcek, K., and Johnson, J. D. (1988) Biologically active fluorescent derivatives of spinach calmodulin that report calmodulin target protein binding, *Biochemistry 27*, 991-996.

45. Wine, R. N., Dial, J. M., Tomer, K. B., and Borchers, C. H. (2002) Identification of components of protein complexes using a fluorescent photo-cross-linker and mass spectrometry, *Anal Chem 74*, 1939-1945.

46. Veyron-Churlet, R., Guerrini, O., Mourey, L., Daffe, M., and Zerbib, D. (2004) Protein-protein interactions within the Fatty Acid Synthase-II system of Mycobacterium tuberculosis are essential for mycobacterial viability, *Mol Microbiol 54*, 1161-1172.

47. Hang, H. C., Geutjes, E. J., Grotenbreg, G., Pollington, A. M., Bijlmakers, M. J., and Ploegh, H. L. (2007) Chemical probes for the rapid detection of Fatty-acylated proteins in Mammalian cells, *J Am Chem Soc 129*, 2744-2745.

48. Bulaj, G., Kortemme, T., and Goldenberg, D. P. (1998) Ionization-reactivity relationships for cysteine thiols in polypeptides, *Biochemistry 37*, 8965-8972.

49. Ellman, G. L. (1959) Tissue sulfhydryl groups, *Arch Biochem Biophys 82*, 70-77.

50. Sarikonda, G., Wang, H., Puan, K. J., Liu, X. H., Lee, H. K., Song, Y., Distefano, M. D., Oldfield, E., Prestwich, G. D., and Morita, C. T. (2008) Photoaffinity antigens for human gammadelta T cells, *J Immunol 181*, 7738-7750.

51. Magnuson, K., Jackowski, S., Rock, C. O., and Cronan, J. E., Jr. (1993) Regulation of fatty acid biosynthesis in Escherichia coli, *Microbiol Rev 57*, 522-542.

52. Rumley, M. K., Therisod, H., Weissborn, A. C., and Kennedy, E. P. (1992) Mechanisms of regulation of the biosynthesis of membrane-derived oligosaccharides in Escherichia coli, *J Biol Chem 267*, 11806-11810.

53. Shen, B., Summers, R. G., Gramajo, H., Bibb, M. J., and Hutchinson, C. R. (1992) Purification and characterization of the acyl carrier protein of the Streptomyces glaucescens tetracenomycin C polyketide synthase, *J Bacteriol 174*, 3818-3821.

54. Summers, R. G., Ali, A., Shen, B., Wessel, W. A., and Hutchinson, C. R. (1995) Malonyl-coenzyme A:acyl carrier protein acyltransferase of Streptomyces glaucescens: a possible link between fatty acid and polyketide biosynthesis, *Biochemistry 34*, 9389-9402.

55. Therisod, H., Weissborn, A. C., and Kennedy, E. P. (1986) An essential function for acyl carrier protein in the biosynthesis of membrane-derived oligosaccharides of Escherichia coli, *Proc Natl Acad Sci U S A 83*, 7236-7240.

56. Dorman, G., and Prestwich, G. D. (1994) Benzophenone photophores in biochemistry, *Biochemistry 33*, 5661-5673.

57. Yoo, B. C., Fountoulakis, M., Dierssen, M., and Lubec, G. (2001) Expression patterns of chaperone proteins in cerebral cortex of the fetus with Down syndrome: dysregulation of T-complex protein 1, *J Neural Transm Suppl*, 321-334.

58. Smith, A., and Lough, A. K. (1976) Micellar solubilization of fatty acids in aqueous media containing bile salts and phospholipids, *Br J Nutr 35*, 77-87.

Bibliography

Chapter I

1. Snider, D. E., Jr., and La Montagne, J. R. (1994) The neglected global tuberculosis problem: a report of the 1992 World Congress on Tuberculosis, *J Infect Dis 169*, 1189-1196.
2. Dye, C., Scheele, S., Dolin, P., Pathania, V., and Raviglione, M. C. (1999) Consensus statement. Global burden of tuberculosis: estimated incidence, prevalence, and mortality by country. WHO Global Surveillance and Monitoring Project, *JAMA 282*, 677-686.
3. Raviglione, M. C., Snider, D. E., Jr., and Kochi, A. (1995) Global epidemiology of tuberculosis. Morbidity and mortality of a worldwide epidemic, *JAMA 273*, 220-226.
4. Antonucci, G., Girardi, E., Raviglione, M. C., and Ippolito, G. (1995) Risk factors for tuberculosis in HIV-infected persons. A prospective cohort study. The Gruppo Italiano di Studio Tubercolosi e AIDS (GISTA), *JAMA 274*, 143-148.
5. Zink, A. R., Sola, C., Reischl, U., Grabner, W., Rastogi, N., Wolf, H., and Nerlich, A. G. (2003) Characterization of Mycobacterium tuberculosis complex DNAs from Egyptian mummies by spoligotyping, *J Clin Microbiol 41*, 359-367.
6. Schnappinger, D., Schoolnik, G. K., and Ehrt, S. (2006) Expression profiling of host pathogen interactions: how Mycobacterium tuberculosis and the macrophage adapt to one another, *Microbes Infect 8*, 1132-1140.
7. (2000) Diagnostic Standards and Classification of Tuberculosis in Adults and Children. This official statement of the American Thoracic Society and the

Centers for Disease Control and Prevention was adopted by the ATS Board of Directors, July 1999. This statement was endorsed by the Council of the Infectious Disease Society of America, September 1999, *Am J Respir Crit Care Med 161*, 1376-1395.

8. Sacchettini, J. C., Rubin, E. J., and Freundlich, J. S. (2008) Drugs versus bugs: in pursuit of the persistent predator Mycobacterium tuberculosis, *Nat Rev Microbiol 6*, 41-52.

9. Middlebrook, G. (1952) Sterilization of tubercle bacilli by isonicotinic acid hydrazide and the incidence of variants resistant to the drug in vitro, *Am Rev Tuberc 65*, 765-767.

10. Rawat, R., Whitty, A., and Tonge, P. J. (2003) The isoniazid-NAD adduct is a slow, tight-binding inhibitor of InhA, the Mycobacterium tuberculosis enoyl reductase: adduct affinity and drug resistance, *Proc Natl Acad Sci U S A 100*, 13881-13886.

11. Zhang, Y., and Mitchison, D. (2003) The curious characteristics of pyrazinamide: a review, *Int J Tuberc Lung Dis 7*, 6-21.

12. Zimhony, O., Cox, J. S., Welch, J. T., Vilcheze, C., and Jacobs, W. R., Jr. (2000) Pyrazinamide inhibits the eukaryotic-like fatty acid synthetase I (FASI) of Mycobacterium tuberculosis, *Nat Med 6*, 1043-1047.

13. Boshoff, H. I., Mizrahi, V., and Barry, C. E., 3rd. (2002) Effects of pyrazinamide on fatty acid synthesis by whole mycobacterial cells and purified fatty acid synthase I, *J Bacteriol 184*, 2167-2172.

14. Zhang, Y., Wade, M. M., Scorpio, A., Zhang, H., and Sun, Z. (2003) Mode of action of pyrazinamide: disruption of Mycobacterium tuberculosis membrane transport and energetics by pyrazinoic acid, *J Antimicrob Chemother 52*, 790-795.

15. Takayama, K., and Kilburn, J. O. (1989) Inhibition of synthesis of arabinogalactan by ethambutol in Mycobacterium smegmatis, *Antimicrob Agents Chemother 33*, 1493-1499.

16. Yarbrough, L. R., Wu, F. Y., and Wu, C. W. (1976) Molecular mechanism of the rifampicin -RNA polymerase interaction, *Biochemistry 15*, 2669-2676.

17. CDC. (2003) Treatment of Tuberculosis, *MMWR 52(RR11)*, 1-77.

18. Lim, S. A. (2006) Ethambutol-associated optic neuropathy, *Ann Acad Med Singapore 35*, 274-278.

19. Lopez-Cortes, L. F., Ruiz-Valderas, R., Viciana, P., Alarcon-Gonzalez, A., Gomez-Mateos, J., Leon-Jimenez, E., Sarasanacenta, M., Lopez-Pua, Y., and Pachon, J. (2002) Pharmacokinetic interactions between efavirenz and rifampicin in HIV-infected patients with tuberculosis, *Clin Pharmacokinet 41*, 681-690.

20. Addington, W. W. (1979) The side effects and interactions of antituberculosis drugs, *Chest 76*, 782-784.

21. Gustafson, J. E., Candelaria, P. V., Fisher, S. A., Goodridge, J. P., Lichocik, T. M., McWilliams, T. M., Price, C. T., O'Brien, F. G., and Grubb, W. B. (1999) Growth in the presence of salicylate increases fluoroquinolone resistance in Staphylococcus aureus, *Antimicrob Agents Chemother 43*, 990-992.

22. Lemaitre, N., Sougakoff, W., Truffot-Pernot, C., and Jarlier, V. (1999) Characterization of new mutations in pyrazinamide-resistant strains of Mycobacterium tuberculosis and identification of conserved regions important for the catalytic activity of the pyrazinamidase PncA, *Antimicrob Agents Chemother 43*, 1761-1763.

23. Addington, W. W. (1979) Patient compliance: the most serious remaining problem in the control of tuberculosis in the United States, *Chest 76*, 741-743.

24. Frieden, T. R., Sterling, T., Pablos-Mendez, A., Kilburn, J. O., Cauthen, G. M., and Dooley, S. W. (1993) The emergence of drug-resistant tuberculosis in New York City, *N Engl J Med 328*, 521-526.

25. Hayward, A. C., and Coker, R. J. (2000) Could a tuberculosis epidemic occur in London as it did in New York?, *Emerg Infect Dis 6*, 12-16.

26. Kwon, H. H., Tomioka, H., and Saito, H. (1995) Distribution and characterization of beta-lactamases of mycobacteria and related organisms, *Tuber Lung Dis 76*, 141-148.

27. Liu, J., Takiff, H. E., and Nikaido, H. (1996) Active efflux of fluoroquinolones in Mycobacterium smegmatis mediated by LfrA, a multidrug efflux pump, *J Bacteriol 178*, 3791-3795.

28. Cox, H. S., Morrow, M., and Deutschmann, P. W. (2008) Long term efficacy of DOTS regimens for tuberculosis: systematic review, *BMJ 336*, 484-487.

29. Heath, R. J., and Rock, C. O. (2004) Fatty acid biosynthesis as a target for novel antibacterials, *Curr Opin Investig Drugs 5*, 146-153.

30. Liu, J., Shworak, N. W., Fritze, L. M., Edelberg, J. M., and Rosenberg, R. D. (1996) Purification of heparan sulfate D-glucosaminyl 3-O-sulfotransferase, *J Biol Chem 271*, 27072-27082.

31. Barry, C. E., 3rd, Lee, R. E., Mdluli, K., Sampson, A. E., Schroeder, B. G., Slayden, R. A., and Yuan, Y. (1998) Mycolic acids: structure, biosynthesis and physiological functions, *Prog Lipid Res 37*, 143-179.

32. Smith, I. (2003) Mycobacterium tuberculosis pathogenesis and molecular determinants of virulence, *Clin Microbiol Rev 16*, 463-496.

33. Brennan, P. J., and Nikaido, H. (1995) The envelope of mycobacteria, *Annu Rev Biochem 64*, 29-63.

34. Kremer, L., Douglas, J. D., Baulard, A. R., Morehouse, C., Guy, M. R., Alland, D., Dover, L. G., Lakey, J. H., Jacobs, W. R., Jr., Brennan, P. J., Minnikin, D. E., and Besra, G. S. (2000) Thiolactomycin and related analogues as novel anti-mycobacterial agents targeting KasA and KasB condensing enzymes in Mycobacterium tuberculosis, *J Biol Chem 275*, 16857-16864.

35. Smith, S., Witkowski, A., and Joshi, A. K. (2003) Structural and functional organization of the animal fatty acid synthase, *Prog Lipid Res 42*, 289-317.

36. Kremer, L., Dover, L. G., Carrere, S., Nampoothiri, K. M., Lesjean, S., Brown, A. K., Brennan, P. J., Minnikin, D. E., Locht, C., and Besra, G. S. (2002) Mycolic acid biosynthesis and enzymic characterization of the beta-ketoacyl-ACP synthase A-condensing enzyme from Mycobacterium tuberculosis, *Biochem J 364*, 423-430.

37. Lu, Y. J., Zhang, Y. M., and Rock, C. O. (2004) Product diversity and regulation of type II fatty acid synthases, *Biochem Cell Biol 82*, 145-155.

38. Campbell, J. W., and Cronan, J. E., Jr. (2001) Bacterial fatty acid biosynthesis: targets for antibacterial drug discovery, *Annu Rev Microbiol 55*, 305-332.

39. Banerjee, A., Dubnau, E., Quemard, A., Balasubramanian, V., Um, K. S., Wilson, T., Collins, D., de Lisle, G., and Jacobs, W. R., Jr. (1994) inhA, a gene encoding a target for isoniazid and ethionamide in Mycobacterium tuberculosis, *Science 263*, 227-230.

40. Dessen, A., Quemard, A., Blanchard, J. S., Jacobs, W. R., Jr., and Sacchettini, J. C. (1995) Crystal structure and function of the isoniazid target of Mycobacterium tuberculosis, *Science 267*, 1638-1641.

41. Quemard, A., Sacchettini, J. C., Dessen, A., Vilcheze, C., Bittman, R., Jacobs, W. R., Jr., and Blanchard, J. S. (1995) Enzymatic characterization of the target for isoniazid in Mycobacterium tuberculosis, *Biochemistry 34*, 8235-8241.

42. Rozwarski, D. A., Grant, G. A., Barton, D. H., Jacobs, W. R., Jr., and Sacchettini, J. C. (1998) Modification of the NADH of the isoniazid target (InhA) from Mycobacterium tuberculosis, *Science 279*, 98-102.

43. Mdluli, K., Slayden, R. A., Zhu, Y., Ramaswamy, S., Pan, X., Mead, D., Crane, D. D., Musser, J. M., and Barry, C. E., 3rd. (1998) Inhibition of a Mycobacterium tuberculosis beta-ketoacyl ACP synthase by isoniazid, *Science 280*, 1607-1610.

44. Magnuson, K., Jackowski, S., Rock, C. O., and Cronan, J. E., Jr. (1993) Regulation of fatty acid biosynthesis in Escherichia coli, *Microbiol Rev 57*, 522-542.

45. Marrakchi, H., Zhang, Y. M., and Rock, C. O. (2002) Mechanistic diversity and regulation of Type II fatty acid synthesis, *Biochem Soc Trans 30*, 1050-1055.

46. White, S. W., Zheng, J., Zhang, Y. M., and Rock. (2005) The structural biology of type II fatty acid biosynthesis, *Annu Rev Biochem 74*, 791-831.

47. Price, A. C., Zhang, Y. M., Rock, C. O., and White, S. W. (2001) Structure of beta-ketoacyl-[acyl carrier protein] reductase from Escherichia coli: negative cooperativity and its structural basis, *Biochemistry 40*, 12772-12781.

48. Silva, R. G., de Carvalho, L. P., Blanchard, J. S., Santos, D. S., and Basso, L. A. (2006) Mycobacterium tuberculosis beta-ketoacyl-acyl carrier protein (ACP) reductase: kinetic and chemical mechanisms, *Biochemistry 45*, 13064-13073.

49. Kimber, M. S., Martin, F., Lu, Y., Houston, S., Vedadi, M., Dharamsi, A., Fiebig, K. M., Schmid, M., and Rock, C. O. (2004) The structure of (3R)-hydroxyacyl-acyl carrier protein dehydratase (FabZ) from Pseudomonas aeruginosa, *J Biol Chem 279*, 52593-52602.

50. Leesong, M., Henderson, B. S., Gillig, J. R., Schwab, J. M., and Smith, J. L. (1996) Structure of a dehydratase-isomerase from the bacterial pathway for biosynthesis of unsaturated fatty acids: two catalytic activities in one active site, *Structure 4*, 253-264.

51. Roujeinikova, A., Sedelnikova, S., de Boer, G. J., Stuitje, A. R., Slabas, A. R., Rafferty, J. B., and Rice, D. W. (1999) Inhibitor binding studies on enoyl reductase reveal conformational changes related to substrate recognition, *J Biol Chem 274*, 30811-30817.

52. Edwards, P., Nelsen, J. S., Metz, J. G., and Dehesh, K. (1997) Cloning of the fabF gene in an expression vector and in vitro characterization of recombinant fabF and fabB encoded enzymes from Escherichia coli, *FEBS Lett 402*, 62-66.

53. Schaeffer, M. L., Agnihotri, G., Volker, C., Kallender, H., Brennan, P. J., and Lonsdale, J. T. (2001) Purification and biochemical characterization of the Mycobacterium tuberculosis beta-ketoacyl-acyl carrier protein synthases KasA and KasB, *J Biol Chem 276*, 47029-47037.

54. Olsen, J. G., Kadziola, A., von Wettstein-Knowles, P., Siggaard-Andersen, M., and Larsen, S. (2001) Structures of beta-ketoacyl-acyl carrier protein synthase I complexed with fatty acids elucidate its catalytic machinery, *Structure 9*, 233-243.

55. Bergler, H., Fuchsbichler, S., Hogenauer, G., and Turnowsky, F. (1996) The enoyl-[acyl-carrier-protein] reductase (FabI) of Escherichia coli, which catalyzes a key regulatory step in fatty acid biosynthesis, accepts NADH and NADPH as cofactors and is inhibited by palmitoyl-CoA, *Eur J Biochem 242*, 689-694.

56. Sullivan, T. J., Truglio, J. J., Boyne, M. E., Novichenok, P., Zhang, X., Stratton, C. F., Li, H. J., Kaur, T., Amin, A., Johnson, F., Slayden, R. A., Kisker, C., and Tonge, P. J. (2006) High affinity InhA inhibitors with activity against drug-resistant strains of Mycobacterium tuberculosis, *ACS Chem Biol 1*, 43-53.

57. Lai, C. Y., and Cronan, J. E. (2003) Beta-ketoacyl-acyl carrier protein synthase III (FabH) is essential for bacterial fatty acid synthesis, *J Biol Chem 278*, 51494-51503.

58. Sassetti, C. M., and Rubin, E. J. (2003) Genetic requirements for mycobacterial survival during infection, *Proc Natl Acad Sci U S A 100*, 12989-12994.

59. Bhatt, A., Kremer, L., Dai, A. Z., Sacchettini, J. C., and Jacobs, W. R., Jr. (2005) Conditional depletion of KasA, a key enzyme of mycolic acid biosynthesis, leads to mycobacterial cell lysis, *J Bacteriol 187*, 7596-7606.

60. Parish, T., Roberts, G., Laval, F., Schaeffer, M., Daffe, M., and Duncan, K. (2007) Functional complementation of the essential gene fabG1 of Mycobacterium tuberculosis by Mycobacterium smegmatis fabG but not Escherichia coli fabG, *J Bacteriol 189*, 3721-3728.

61. Silva, R. G., Rosado, L. A., Santos, D. S., and Basso, L. A. (2008) Mycobacterium tuberculosis beta-ketoacyl-ACP reductase: alpha-secondary kinetic isotope effects and kinetic and equilibrium mechanisms of substrate binding, *Arch Biochem Biophys 471*, 1-10.

62. Khandekar, S. S., Daines, R. A., and Lonsdale, J. T. (2003) Bacterial beta-ketoacyl-acyl carrier protein synthases as targets for antibacterial agents, *Curr Protein Pept Sci 4*, 21-29.

63. Zhang, Y. M., White, S. W., and Rock, C. O. (2006) Inhibiting bacterial fatty acid synthesis, *J Biol Chem 281*, 17541-17544.

64. Baldock, C., Rafferty, J. B., Sedelnikova, S. E., Baker, P. J., Stuitje, A. R., Slabas, A. R., Hawkes, T. R., and Rice, D. W. (1996) A mechanism of drug action revealed by structural studies of enoyl reductase, *Science 274*, 2107-2110.

65. Argyrou, A., Jin, L., Siconilfi-Baez, L., Angeletti, R. H., and Blanchard, J. S. (2006) Proteome-wide profiling of isoniazid targets in Mycobacterium tuberculosis, *Biochemistry 45*, 13947-13953.

66. Ramaswamy, S. V., Reich, R., Dou, S. J., Jasperse, L., Pan, X., Wanger, A., Quitugua, T., and Graviss, E. A. (2003) Single nucleotide polymorphisms in genes associated with isoniazid resistance in Mycobacterium tuberculosis, *Antimicrob Agents Chemother 47*, 1241-1250.

67. McMurry, L. M., Oethinger, M., and Levy, S. B. (1998) Triclosan targets lipid synthesis, *Nature 394*, 531-532.

68. Heath, R. J., and Rock, C. O. (1996) Inhibition of beta-ketoacyl-acyl carrier protein synthase III (FabH) by acyl-acyl carrier protein in Escherichia coli, *J Biol Chem 271*, 10996-11000.

69. Levy, C. W., Roujeinikova, A., Sedelnikova, S., Baker, P. J., Stuitje, A. R., Slabas, A. R., Rice, D. W., and Rafferty, J. B. (1999) Molecular basis of triclosan activity, *Nature 398*, 383-384.

70. Xu, H., Sullivan, T. J., Sekiguchi, J., Kirikae, T., Ojima, I., Stratton, C. F., Mao, W., Rock, F. L., Alley, M. R., Johnson, F., Walker, S. G., and Tonge, P. J. (2008) Mechanism and inhibition of saFabI, the enoyl reductase from Staphylococcus aureus, *Biochemistry 47*, 4228-4236.

71. Chhibber, M., Kumar, G., Parasuraman, P., Ramya, T. N., Surolia, N., and Surolia, A. (2006) Novel diphenyl ethers: design, docking studies, synthesis and inhibition of enoyl ACP reductase of Plasmodium falciparum and Escherichia coli, *Bioorg Med Chem 14*, 8086-8098.

72. Freundlich, J. S., Yu, M., Lucumi, E., Kuo, M., Tsai, H. C., Valderramos, J. C., Karagyozov, L., Jacobs, W. R., Jr., Schiehser, G. A., Fidock, D. A., Jacobus, D. P., and Sacchettini, J. C. (2006) Synthesis and biological activity of diaryl ether

inhibitors of malarial enoyl acyl carrier protein reductase. Part 2: 2'-substituted triclosan derivatives, *Bioorg Med Chem Lett 16*, 2163-2169.

73. Perozzo, R., Kuo, M., Sidhu, A. S., Valiyaveettil, J. T., Bittman, R., Jacobs, W. R., Jr., Fidock, D. A., and Sacchettini, J. C. (2002) Structural elucidation of the specificity of the antibacterial agent triclosan for malarial enoyl acyl carrier protein reductase, *J Biol Chem 277*, 13106-13114.

74. Parikh, S. L., Xiao, G., and Tonge, P. J. (2000) Inhibition of InhA, the enoyl reductase from Mycobacterium tuberculosis, by triclosan and isoniazid, *Biochemistry 39*, 7645-7650.

75. Lu, H., England, K., am Ende, C., Truglio, J. J., Luckner, S., Reddy, B. G., Marlenee, N. L., Knudson, S. E., Knudson, D. L., Bowen, R. A., Kisker, C., Slayden, R. A., and Tonge, P. J. (2009) Slow-onset inhibition of the FabI enoyl reductase from francisella tularensis: residence time and in vivo activity, *ACS Chem Biol 4*, 221-231.

76. Price, A. C., Choi, K. H., Heath, R. J., Li, Z., White, S. W., and Rock, C. O. (2001) Inhibition of beta-ketoacyl-acyl carrier protein synthases by thiolactomycin and cerulenin. Structure and mechanism, *J Biol Chem 276*, 6551-6559.

77. Rastogi, N., Goh, K. S., Horgen, L., and Barrow, W. W. (1998) Synergistic activities of antituberculous drugs with cerulenin and trans-cinnamic acid against Mycobacterium tuberculosis, *FEMS Immunol Med Microbiol 21*, 149-157.

78. Omura, S. (1981) Cerulenin, *Methods Enzymol 72*, 520-532.

79. Machutta, C. A., Bommineni, G. R., Luckner, S. R., Kapilashrami, K., Ruzsicska, B., Simmerling, C., Kisker, C., and Tonge, P. J. (2010) Slow onset inhibition of

bacterial beta-ketoacyl-acyl carrier protein synthases by thiolactomycin, *J Biol Chem 285*, 6161-6169.

80. Douglas, J. D., Senior, S. J., Morehouse, C., Phetsukiri, B., Campbell, I. B., Besra, G. S., and Minnikin, D. E. (2002) Analogues of thiolactomycin: potential drugs with enhanced anti-mycobacterial activity, *Microbiology 148*, 3101-3109.

81. He, X., Reeve, A. M., Desai, U. R., Kellogg, G. E., and Reynolds, K. A. (2004) 1,2-dithiole-3-ones as potent inhibitors of the bacterial 3-ketoacyl acyl carrier protein synthase III (FabH), *Antimicrob Agents Chemother 48*, 3093-3102.

82. Jones, S. M., Urch, J. E., Brun, R., Harwood, J. L., Berry, C., and Gilbert, I. H. (2004) Analogues of thiolactomycin as potential anti-malarial and anti-trypanosomal agents, *Bioorg Med Chem 12*, 683-692.

83. Kamal, A., Shaik, A. A., Sinha, R., Yadav, J. S., and Arora, S. K. (2005) Antitubercular agents. Part 2: new thiolactomycin analogues active against Mycobacterium tuberculosis, *Bioorg Med Chem Lett 15*, 1927-1929.

84. McFadden, J. M., Medghalchi, S. M., Thupari, J. N., Pinn, M. L., Vadlamudi, A., Miller, K. I., Kuhajda, F. P., and Townsend, C. A. (2005) Application of a flexible synthesis of (5R)-thiolactomycin to develop new inhibitors of type I fatty acid synthase, *J Med Chem 48*, 946-961.

85. Sakya, S. M., Suarez-Contreras, M., Dirlam, J. P., O'Connell, T. N., Hayashi, S. F., Santoro, S. L., Kamicker, B. J., George, D. M., and Ziegler, C. B. (2001) Synthesis and structure-activity relationships of thiotetronic acid analogues of thiolactomycin, *Bioorg Med Chem Lett 11*, 2751-2754.

86. Senior, S. J., Illarionov, P. A., Gurcha, S. S., Campbell, I. B., Schaeffer, M. L., Minnikin, D. E., and Besra, G. S. (2004) Acetylene-based analogues of thiolactomycin, active against Mycobacterium tuberculosis mtFabH fatty acid condensing enzyme, *Bioorg Med Chem Lett 14*, 373-376.

87. Senior, S. J., Illarionov, P. A., Gurcha, S. S., Campbell, I. B., Schaeffer, M. L., Minnikin, D. E., and Besra, G. S. (2003) Biphenyl-based analogues of thiolactomycin, active against Mycobacterium tuberculosis mtFabH fatty acid condensing enzyme, *Bioorg Med Chem Lett 13*, 3685-3688.

88. Daines, R. A., Pendrak, I., Sham, K., Van Aller, G. S., Konstantinidis, A. K., Lonsdale, J. T., Janson, C. A., Qiu, X., Brandt, M., Khandekar, S. S., Silverman, C., and Head, M. S. (2003) First X-ray cocrystal structure of a bacterial FabH condensing enzyme and a small molecule inhibitor achieved using rational design and homology modeling, *J Med Chem 46*, 5-8.

89. Herath, K. B., Jayasuriya, H., Guan, Z., Schulman, M., Ruby, C., Sharma, N., MacNaul, K., Menke, J. G., Kodali, S., Galgoci, A., Wang, J., and Singh, S. B. (2005) Anthrabenzoxocinones from Streptomyces sp. as liver X receptor ligands and antibacterial agents, *J Nat Prod 68*, 1437-1440.

90. Khandekar, S. S., Gentry, D. R., Van Aller, G. S., Warren, P., Xiang, H., Silverman, C., Doyle, M. L., Chambers, P. A., Konstantinidis, A. K., Brandt, M., Daines, R. A., and Lonsdale, J. T. (2001) Identification, substrate specificity, and inhibition of the Streptococcus pneumoniae beta-ketoacyl-acyl carrier protein synthase III (FabH), *J Biol Chem 276*, 30024-30030.

91. Kodali, S., Galgoci, A., Young, K., Painter, R., Silver, L. L., Herath, K. B., Singh, S. B., Cully, D., Barrett, J. F., Schmatz, D., and Wang, J. (2005) Determination of selectivity and efficacy of fatty acid synthesis inhibitors, *J Biol Chem 280*, 1669-1677.

92. Young, K., Jayasuriya, H., Ondeyka, J. G., Herath, K., Zhang, C., Kodali, S., Galgoci, A., Painter, R., Brown-Driver, V., Yamamoto, R., Silver, L. L., Zheng, Y., Ventura, J. I., Sigmund, J., Ha, S., Basilio, A., Vicente, F., Tormo, J. R., Pelaez, F., Youngman, P., Cully, D., Barrett, J. F., Schmatz, D., Singh, S. B., and Wang, J. (2006) Discovery of FabH/FabF inhibitors from natural products, *Antimicrob Agents Chemother 50*, 519-526.

Chatper II

1. Haapalainen, A. M., Merilainen, G., and Wierenga, R. K. (2006) The thiolase superfamily: condensing enzymes with diverse reaction specificities, *Trends Biochem Sci 31*, 64-71.

2. Heath, R. J., and Rock, C. O. (2002) The Claisen condensation in biology, *Nat Prod Rep 19*, 581-596.

3. Mathieu, M., Modis, Y., Zeelen, J. P., Engel, C. K., Abagyan, R. A., Ahlberg, A., Rasmussen, B., Lamzin, V. S., Kunau, W. H., and Wierenga, R. K. (1997) The 1.8 A crystal structure of the dimeric peroxisomal 3-ketoacyl-CoA thiolase of Saccharomyces cerevisiae: implications for substrate binding and reaction mechanism, *J Mol Biol 273*, 714-728.

4. Mathieu, M., Zeelen, J. P., Pauptit, R. A., Erdmann, R., Kunau, W. H., and Wierenga, R. K. (1994) The 2.8 A crystal structure of peroxisomal 3-ketoacyl-CoA thiolase of Saccharomyces cerevisiae: a five-layered alpha beta alpha beta alpha structure constructed from two core domains of identical topology, *Structure 2*, 797-808.
5. Davies, C., Heath, R. J., White, S. W., and Rock, C. O. (2000) The 1.8 A crystal structure and active-site architecture of beta-ketoacyl-acyl carrier protein synthase III (FabH) from escherichia coli, *Structure 8*, 185-195.
6. Luckner, S. R., Machutta, C. A., Tonge, P. J., and Kisker, C. (2009) Crystal structures of Mycobacterium tuberculosis KasA show mode of action within cell wall biosynthesis and its inhibition by thiolactomycin, *Structure 17*, 1004-1013.
7. Musayev, F., Sachdeva, S., Scarsdale, J. N., Reynolds, K. A., and Wright, H. T. (2005) Crystal structure of a substrate complex of Mycobacterium tuberculosis beta-ketoacyl-acyl carrier protein synthase III (FabH) with lauroyl-coenzyme A, *J Mol Biol 346*, 1313-1321.
8. Sachdeva, S., and Reynolds, K. A. (2008) Mycobacterium tuberculosis beta-ketoacyl acyl carrier protein synthase III (mtFabH) assay: principles and method, *Methods Mol Med 142*, 205-213.
9. Choi, K. H., Heath, R. J., and Rock, C. O. (2000) beta-ketoacyl-acyl carrier protein synthase III (FabH) is a determining factor in branched-chain fatty acid biosynthesis, *J Bacteriol 182*, 365-370.

10. Choi, K. H., Kremer, L., Besra, G. S., and Rock, C. O. (2000) Identification and substrate specificity of beta -ketoacyl (acyl carrier protein) synthase III (mtFabH) from Mycobacterium tuberculosis, *J Biol Chem 275*, 28201-28207.

11. Heath, R. J., and Rock, C. O. (1996) Inhibition of beta-ketoacyl-acyl carrier protein synthase III (FabH) by acyl-acyl carrier protein in Escherichia coli, *J Biol Chem 271*, 10996-11000.

12. Heath, R. J., and Rock, C. O. (1996) Regulation of fatty acid elongation and initiation by acyl-acyl carrier protein in Escherichia coli, *J Biol Chem 271*, 1833-1836.

13. Jackowski, S., and Rock, C. O. (1987) Acetoacetyl-acyl carrier protein synthase, a potential regulator of fatty acid biosynthesis in bacteria, *J Biol Chem 262*, 7927-7931.

14. Tsay, J. T., Oh, W., Larson, T. J., Jackowski, S., and Rock, C. O. (1992) Isolation and characterization of the beta-ketoacyl-acyl carrier protein synthase III gene (fabH) from Escherichia coli K-12, *J Biol Chem 267*, 6807-6814.

15. Olsen, J. G., Kadziola, A., von Wettstein-Knowles, P., Siggaard-Andersen, M., Lindquist, Y., and Larsen, S. (1999) The X-ray crystal structure of beta-ketoacyl [acyl carrier protein] synthase I, *FEBS Lett 460*, 46-52.

16. Price, A. C., Choi, K. H., Heath, R. J., Li, Z., White, S. W., and Rock, C. O. (2001) Inhibition of beta-ketoacyl-acyl carrier protein synthases by thiolactomycin and cerulenin. Structure and mechanism, *J Biol Chem 276*, 6551-6559.

17. White, S. W., Zheng, J., Zhang, Y. M., and Rock. (2005) The structural biology of type II fatty acid biosynthesis, *Annu Rev Biochem 74*, 791-831.

18. Jez, J. M., and Noel, J. P. (2000) Mechanism of chalcone synthase. pKa of the catalytic cysteine and the role of the conserved histidine in a plant polyketide synthase, *J Biol Chem 275*, 39640-39646.

19. Olsen, J. G., Kadziola, A., von Wettstein-Knowles, P., Siggaard-Andersen, M., and Larsen, S. (2001) Structures of beta-ketoacyl-acyl carrier protein synthase I complexed with fatty acids elucidate its catalytic machinery, *Structure 9*, 233-243.

20. Price, A. C., Rock, C. O., and White, S. W. (2003) The 1.3-Angstrom-resolution crystal structure of beta-ketoacyl-acyl carrier protein synthase II from Streptococcus pneumoniae, *J Bacteriol 185*, 4136-4143.

21. Edwards, P., Nelsen, J. S., Metz, J. G., and Dehesh, K. (1997) Cloning of the fabF gene in an expression vector and in vitro characterization of recombinant fabF and fabB encoded enzymes from Escherichia coli, *FEBS Lett 402*, 62-66.

22. Schaeffer, M. L., Agnihotri, G., Volker, C., Kallender, H., Brennan, P. J., and Lonsdale, J. T. (2001) Purification and biochemical characterization of the Mycobacterium tuberculosis beta-ketoacyl-acyl carrier protein synthases KasA and KasB, *J Biol Chem 276*, 47029-47037.

23. Rosenfeld, I. S., D'Agnolo, G., and Vagelos, P. R. (1973) Synthesis of unsaturated fatty acids and the lesion in fab B mutants, *J Biol Chem 248*, 2452-2460.

24. D'Agnolo, G., Rosenfeld, I. S., and Vagelos, P. R. (1975) Multiple forms of beta-ketoacyl-acyl carrier protein synthetase in Escherichia coli, *J Biol Chem 250*, 5289-5294.

25. Garwin, J. L., Klages, A. L., and Cronan, J. E., Jr. (1980) Beta-ketoacyl-acyl carrier protein synthase II of Escherichia coli. Evidence for function in the thermal regulation of fatty acid synthesis, *J Biol Chem 255*, 3263-3265.

26. de Mendoza, D., Klages Ulrich, A., and Cronan, J. E., Jr. (1983) Thermal regulation of membrane fluidity in Escherichia coli. Effects of overproduction of beta-ketoacyl-acyl carrier protein synthase I, *J Biol Chem 258*, 2098-2101.

27. Bhatt, A., Kremer, L., Dai, A. Z., Sacchettini, J. C., and Jacobs, W. R., Jr. (2005) Conditional depletion of KasA, a key enzyme of mycolic acid biosynthesis, leads to mycobacterial cell lysis, *J Bacteriol 187*, 7596-7606.

28. Slayden, R. A., Lee, R. E., Armour, J. W., Cooper, A. M., Orme, I. M., Brennan, P. J., and Besra, G. S. (1996) Antimycobacterial action of thiolactomycin: an inhibitor of fatty acid and mycolic acid synthesis, *Antimicrob Agents Chemother 40*, 2813-2819.

29. Wang, J., Soisson, S. M., Young, K., Shoop, W., Kodali, S., Galgoci, A., Painter, R., Parthasarathy, G., Tang, Y. S., Cummings, R., Ha, S., Dorso, K., Motyl, M., Jayasuriya, H., Ondeyka, J., Herath, K., Zhang, C., Hernandez, L., Allocco, J., Basilio, A., Tormo, J. R., Genilloud, O., Vicente, F., Pelaez, F., Colwell, L., Lee, S. H., Michael, B., Felcetto, T., Gill, C., Silver, L. L., Hermes, J. D., Bartizal, K., Barrett, J., Schmatz, D., Becker, J. W., Cully, D., and Singh, S. B. (2006) Platensimycin is a selective FabF inhibitor with potent antibiotic properties, *Nature 441*, 358-361.

30. Young, K., Jayasuriya, H., Ondeyka, J. G., Herath, K., Zhang, C., Kodali, S., Galgoci, A., Painter, R., Brown-Driver, V., Yamamoto, R., Silver, L. L., Zheng, Y.,

Ventura, J. I., Sigmund, J., Ha, S., Basilio, A., Vicente, F., Tormo, J. R., Pelaez, F., Youngman, P., Cully, D., Barrett, J. F., Schmatz, D., Singh, S. B., and Wang, J. (2006) Discovery of FabH/FabF inhibitors from natural products, *Antimicrob Agents Chemother 50*, 519-526.

31. Magnuson, K., Jackowski, S., Rock, C. O., and Cronan, J. E., Jr. (1993) Regulation of fatty acid biosynthesis in Escherichia coli, *Microbiol Rev 57*, 522-542.

32. Rumley, M. K., Therisod, H., Weissborn, A. C., and Kennedy, E. P. (1992) Mechanisms of regulation of the biosynthesis of membrane-derived oligosaccharides in Escherichia coli, *J Biol Chem 267*, 11806-11810.

33. Shen, B., Summers, R. G., Gramajo, H., Bibb, M. J., and Hutchinson, C. R. (1992) Purification and characterization of the acyl carrier protein of the Streptomyces glaucescens tetracenomycin C polyketide synthase, *J Bacteriol 174*, 3818-3821.

34. Summers, R. G., Ali, A., Shen, B., Wessel, W. A., and Hutchinson, C. R. (1995) Malonyl-coenzyme A:acyl carrier protein acyltransferase of Streptomyces glaucescens: a possible link between fatty acid and polyketide biosynthesis, *Biochemistry 34*, 9389-9402.

35. Therisod, H., Weissborn, A. C., and Kennedy, E. P. (1986) An essential function for acyl carrier protein in the biosynthesis of membrane-derived oligosaccharides of Escherichia coli, *Proc Natl Acad Sci U S A 83*, 7236-7240.

36. Keating, D. H., Carey, M. R., and Cronan, J. E., Jr. (1995) The unmodified (apo) form of Escherichia coli acyl carrier protein is a potent inhibitor of cell growth, *J Biol Chem 270*, 22229-22235.

37. Lambalot, R. H., and Walsh, C. T. (1995) Cloning, overproduction, and characterization of the Escherichia coli holo-acyl carrier protein synthase, *J Biol Chem 270*, 24658-24661.

38. Cryle, M. J., and Schlichting, I. (2008) Structural insights from a P450 Carrier Protein complex reveal how specificity is achieved in the P450(BioI) ACP complex, *Proc Natl Acad Sci U S A 105*, 15696-15701.

39. Holak, T. A., Kearsley, S. K., Kim, Y., and Prestegard, J. H. (1988) Three-dimensional structure of acyl carrier protein determined by NMR pseudoenergy and distance geometry calculations, *Biochemistry 27*, 6135-6142.

40. Kim, Y., and Prestegard, J. H. (1990) Refinement of the NMR structures for acyl carrier protein with scalar coupling data, *Proteins 8*, 377-385.

41. Parris, K. D., Lin, L., Tam, A., Mathew, R., Hixon, J., Stahl, M., Fritz, C. C., Seehra, J., and Somers, W. S. (2000) Crystal structures of substrate binding to Bacillus subtilis holo-(acyl carrier protein) synthase reveal a novel trimeric arrangement of molecules resulting in three active sites, *Structure 8*, 883-895.

42. Ploskon, E., Arthur, C. J., Kanari, A. L., Wattana-amorn, P., Williams, C., Crosby, J., Simpson, T. J., Willis, C. L., and Crump, M. P. (2010) Recognition of intermediate functionality by acyl carrier protein over a complete cycle of fatty acid biosynthesis, *Chem Biol 17*, 776-785.

43. Qiu, X., and Janson, C. A. (2004) Structure of apo acyl carrier protein and a proposal to engineer protein crystallization through metal ions, *Acta Crystallogr D Biol Crystallogr 60*, 1545-1554.

44. Roujeinikova, A., Baldock, C., Simon, W. J., Gilroy, J., Baker, P. J., Stuitje, A. R., Rice, D. W., Slabas, A. R., and Rafferty, J. B. (2002) X-ray crystallographic studies on butyryl-ACP reveal flexibility of the structure around a putative acyl chain binding site, *Structure 10*, 825-835.

45. Roujeinikova, A., Simon, W. J., Gilroy, J., Rice, D. W., Rafferty, J. B., and Slabas, A. R. (2007) Structural studies of fatty acyl-(acyl carrier protein) thioesters reveal a hydrophobic binding cavity that can expand to fit longer substrates, *J Mol Biol 365*, 135-145.

46. Wu, B. N., Zhang, Y. M., Rock, C. O., and Zheng, J. J. (2009) Structural modification of acyl carrier protein by butyryl group, *Protein Sci 18*, 240-246.

47. Xu, G. Y., Tam, A., Lin, L., Hixon, J., Fritz, C. C., and Powers, R. (2001) Solution structure of B. subtilis acyl carrier protein, *Structure 9*, 277-287.

48. Jones, P. J., Cioffi, E. A., and Prestegard, J. H. (1987) [19F]-1H heteronuclear nuclear Overhauser effect studies of the acyl chain-binding site of acyl carrier protein, *J Biol Chem 262*, 8963-8965.

49. Zornetzer, G. A., Fox, B. G., and Markley, J. L. (2006) Solution structures of spinach acyl carrier protein with decanoate and stearate, *Biochemistry 45*, 5217-5227.

50. Zhang, Y. M., Rao, M. S., Heath, R. J., Price, A. C., Olson, A. J., Rock, C. O., and White, S. W. (2001) Identification and analysis of the acyl carrier protein

(ACP) docking site on beta-ketoacyl-ACP synthase III, *J Biol Chem 276*, 8231-8238.

51. Zhang, Y. M., Wu, B., Zheng, J., and Rock, C. O. (2003) Key residues responsible for acyl carrier protein and beta-ketoacyl-acyl carrier protein reductase (FabG) interaction, *J Biol Chem 278*, 52935-52943.

52. Yin, J., Straight, P. D., McLoughlin, S. M., Zhou, Z., Lin, A. J., Golan, D. E., Kelleher, N. L., Kolter, R., and Walsh, C. T. (2005) Genetically encoded short peptide tag for versatile protein labeling by Sfp phosphopantetheinyl transferase, *Proc Natl Acad Sci U S A 102*, 15815-15820.

53. Zhou, Z., Cironi, P., Lin, A. J., Xu, Y., Hrvatin, S., Golan, D. E., Silver, P. A., Walsh, C. T., and Yin, J. (2007) Genetically encoded short peptide tags for orthogonal protein labeling by Sfp and AcpS phosphopantetheinyl transferases, *ACS Chem Biol 2*, 337-346.

54. Zhou, Z., Koglin, A., Wang, Y., McMahon, A. P., and Walsh, C. T. (2008) An eight residue fragment of an acyl carrier protein suffices for post-translational introduction of fluorescent pantetheinyl arms in protein modification in vitro and in vivo, *J Am Chem Soc 130*, 9925-9930.

55. Machutta, C. A., Bommineni, G. R., Luckner, S. R., Kapilashrami, K., Ruzsicska, B., Simmerling, C., Kisker, C., and Tonge, P. J. (2010) Slow onset inhibition of bacterial beta-ketoacyl-acyl carrier protein synthases by thiolactomycin, *J Biol Chem 285*, 6161-6169.

56. Das, S., Kumar, P., Bhor, V., Surolia, A., and Vijayan, M. (2005) Expression, purification, crystallization and preliminary X-ray crystallographic analysis of

pantothenate kinase from Mycobacterium tuberculosis, *Acta Crystallogr Sect F Struct Biol Cryst Commun 61*, 65-67.

57. Rawat, R., Whitty, A., and Tonge, P. J. (2003) The isoniazid-NAD adduct is a slow, tight-binding inhibitor of InhA, the Mycobacterium tuberculosis enoyl reductase: adduct affinity and drug resistance, *Proc Natl Acad Sci U S A 100*, 13881-13886.

58. Haas, J. A., Frederick, M. A., and Fox, B. G. (2000) Chemical and posttranslational modification of Escherichia coli acyl carrier protein for preparation of dansyl-acyl carrier proteins, *Protein Expr Purif 20*, 274-284.

59. Nazi, I., Koteva, K. P., and Wright, G. D. (2004) One-pot chemoenzymatic preparation of coenzyme A analogues, *Anal Biochem 324*, 100-105.

60. Wieland, T., and Koppe, H. (1953) *Ann. Chem. 581*.

61. Cohen-Gonsaud, M., Ducasse, S., Hoh, F., Zerbib, D., Labesse, G., and Quemard, A. (2002) Crystal structure of MabA from Mycobacterium tuberculosis, a reductase involved in long-chain fatty acid biosynthesis, *J Mol Biol 320*, 249-261.

62. Silva, R. G., Rosado, L. A., Santos, D. S., and Basso, L. A. (2008) Mycobacterium tuberculosis beta-ketoacyl-ACP reductase: alpha-secondary kinetic isotope effects and kinetic and equilibrium mechanisms of substrate binding, *Arch Biochem Biophys 471*, 1-10.

63. Schaeffer, M. L., Carson, J. D., Kallender, H., and Lonsdale, J. T. (2004) Development of a scintillation proximity assay for the Mycobacterium tuberculosis

KasA and KasB enzymes involved in mycolic acid biosynthesis, *Tuberculosis (Edinb) 84*, 353-360.

64. Hollenbeck, J. J., McClain, D. L., and Oakley, M. G. (2002) The role of helix stabilizing residues in GCN4 basic region folding and DNA binding, *Protein Sci 11*, 2740-2747.

65. Zhang, Y. M., Marrakchi, H., White, S. W., and Rock, C. O. (2003) The application of computational methods to explore the diversity and structure of bacterial fatty acid synthase, *J Lipid Res 44*, 1-10.

66. Alhamadsheh, M. M., Musayev, F., Komissarov, A. A., Sachdeva, S., Wright, H. T., Scarsdale, N., Florova, G., and Reynolds, K. A. (2007) Alkyl-CoA disulfides as inhibitors and mechanistic probes for FabH enzymes, *Chem Biol 14*, 513-524.

67. Gavilanes, J. G., Lizarbe, M. A., Municio, A. M., and Onaderra, M. (1982) Effects of palmitoyl-CoA on the structure-function of the fatty acid synthetase complex from Ceratitis capitata, *Int J Biochem 14*, 1061-1066.

Chapter III

1. Sensi, P., Margalith, P., and Timbal, M. T. (1959) Rifomycin, a new antibiotic; preliminary report, *Farmaco Sci 14*, 146-147.

2. Maggi, N., Pasqualucci, C. R., Ballotta, R., and Sensi, P. (1966) Rifampicin: a new orally active rifamycin, *Chemotherapy 11*, 285-292.

3. Piddock, L. J., Williams, K. J., and Ricci, V. (2000) Accumulation of rifampicin by Mycobacterium aurum, Mycobacterium smegmatis and Mycobacterium tuberculosis, *J Antimicrob Chemother 45*, 159-165.

4. Blanchard, J. S. (1996) Molecular mechanisms of drug resistance in Mycobacterium tuberculosis, *Annu Rev Biochem 65*, 215-239.

5. Wehrli, W. (1983) Rifampin: mechanisms of action and resistance, *Rev Infect Dis 5 Suppl 3*, S407-411.

6. Aristoff, P. A., Garcia, G. A., Kirchhoff, P. D., and Hollis Showalter, H. D. (2010) Rifamycins--obstacles and opportunities, *Tuberculosis (Edinb) 90*, 94-118.

7. Anthony, R. M., Schuitema, A. R., Bergval, I. L., Brown, T. J., Oskam, L., and Klatser, P. R. (2005) Acquisition of rifabutin resistance by a rifampicin resistant mutant of Mycobacterium tuberculosis involves an unusual spectrum of mutations and elevated frequency, *Ann Clin Microbiol Antimicrob 4*, 9.

8. Lu, H., England, K., am Ende, C., Truglio, J. J., Luckner, S., Reddy, B. G., Marlenee, N. L., Knudson, S. E., Knudson, D. L., Bowen, R. A., Kisker, C., Slayden, R. A., and Tonge, P. J. (2009) Slow-onset inhibition of the FabI enoyl reductase from francisella tularensis: residence time and in vivo activity, *ACS Chem Biol 4*, 221-231.

9. Sullivan, T. J., Truglio, J. J., Boyne, M. E., Novichenok, P., Zhang, X., Stratton, C. F., Li, H. J., Kaur, T., Amin, A., Johnson, F., Slayden, R. A., Kisker, C., and Tonge, P. J. (2006) High affinity InhA inhibitors with activity against drug-resistant strains of Mycobacterium tuberculosis, *ACS Chem Biol 1*, 43-53.

10. Xu, H., Sullivan, T. J., Sekiguchi, J., Kirikae, T., Ojima, I., Stratton, C. F., Mao, W., Rock, F. L., Alley, M. R., Johnson, F., Walker, S. G., and Tonge, P. J. (2008) Mechanism and inhibition of saFabI, the enoyl reductase from Staphylococcus aureus, *Biochemistry 47*, 4228-4236.

11. Heath, R. J., White, S. W., and Rock, C. O. (2001) Lipid biosynthesis as a target for antibacterial agents, *Prog Lipid Res 40*, 467-497.

12. Kuo, M. R., Morbidoni, H. R., Alland, D., Sneddon, S. F., Gourlie, B. B., Staveski, M. M., Leonard, M., Gregory, J. S., Janjigian, A. D., Yee, C., Musser, J. M., Kreiswirth, B., Iwamoto, H., Perozzo, R., Jacobs, W. R., Jr., Sacchettini, J. C., and Fidock, D. A. (2003) Targeting tuberculosis and malaria through inhibition of Enoyl reductase: compound activity and structural data, *J Biol Chem 278*, 20851-20859.

13. Payne, D. J., Miller, W. H., Berry, V., Brosky, J., Burgess, W. J., Chen, E., DeWolf Jr, W. E., Jr., Fosberry, A. P., Greenwood, R., Head, M. S., Heerding, D. A., Janson, C. A., Jaworski, D. D., Keller, P. M., Manley, P. J., Moore, T. D., Newlander, K. A., Pearson, S., Polizzi, B. J., Qiu, X., Rittenhouse, S. F., Slater-Radosti, C., Salyers, K. L., Seefeld, M. A., Smyth, M. G., Takata, D. T., Uzinskas, I. N., Vaidya, K., Wallis, N. G., Winram, S. B., Yuan, C. C., and Huffman, W. F. (2002) Discovery of a novel and potent class of FabI-directed antibacterial agents, *Antimicrob Agents Chemother 46*, 3118-3124.

14. Surolia, N., and Surolia, A. (2001) Triclosan offers protection against blood stages of malaria by inhibiting enoyl-ACP reductase of Plasmodium falciparum, *Nat Med 7*, 167-173.

15. Middlebrook, G. (1954) Isoniazid-resistance and catalase activity of tubercle bacilli; a preliminary report, *Am Rev Tuberc 69*, 471-472.

16. Youatt, J. (1969) A review of the action of isoniazid, *Am Rev Respir Dis 99*, 729-749.

17. Heym, B., Alzari, P. M., Honore, N., and Cole, S. T. (1995) Missense mutations in the catalase-peroxidase gene, katG, are associated with isoniazid resistance in Mycobacterium tuberculosis, *Mol Microbiol 15*, 235-245.

18. Stoeckle, M. Y., Guan, L., Riegler, N., Weitzman, I., Kreiswirth, B., Kornblum, J., Laraque, F., and Riley, L. W. (1993) Catalase-peroxidase gene sequences in isoniazid-sensitive and -resistant strains of Mycobacterium tuberculosis from New York City, *J Infect Dis 168*, 1063-1065.

19. Shoeb, H. A., Bowman, B. U., Jr., Ottolenghi, A. C., and Merola, A. J. (1985) Peroxidase-mediated oxidation of isoniazid, *Antimicrob Agents Chemother 27*, 399-403.

20. Zhang, Y., Heym, B., Allen, B., Young, D., and Cole, S. (1992) The catalase-peroxidase gene and isoniazid resistance of Mycobacterium tuberculosis, *Nature 358*, 591-593.

21. Ghiladi, R. A., Medzihradszky, K. F., Rusnak, F. M., and Ortiz de Montellano, P. R. (2005) Correlation between isoniazid resistance and superoxide reactivity in mycobacterium tuberculosis KatG, *J Am Chem Soc 127*, 13428-13442.

22. Wengenack, N. L., and Rusnak, F. (2001) Evidence for isoniazid-dependent free radical generation catalyzed by Mycobacterium tuberculosis KatG and the isoniazid-resistant mutant KatG(S315T), *Biochemistry 40*, 8990-8996.

23. Zhao, X., Yu, H., Yu, S., Wang, F., Sacchettini, J. C., and Magliozzo, R. S. (2006) Hydrogen peroxide-mediated isoniazid activation catalyzed by Mycobacterium tuberculosis catalase-peroxidase (KatG) and its S315T mutant, *Biochemistry 45*, 4131-4140.

24. Johnsson, K., Froland, W. A., and Schultz, P. G. (1997) Overexpression, purification, and characterization of the catalase-peroxidase KatG from Mycobacterium tuberculosis, *J Biol Chem 272*, 2834-2840.

25. Nagy, J. M., Cass, A. E., and Brown, K. A. (1997) Purification and characterization of recombinant catalase-peroxidase, which confers isoniazid sensitivity in Mycobacterium tuberculosis, *J Biol Chem 272*, 31265-31271.

26. Marcinkeviciene, R. S. M. a. J. A. (1996) Evidence for Isoniazid Oxidation by Oxyferrous Mycobacterial Catalase−Peroxidase, *J. Am. Chem. Soc. 118*, 11303-11304.

27. Jacques Bodiguel, J. M. N., Katherine A. Brown,and Brigitte Jamart-Grégoire. (2000) Oxidation of Isoniazid by Manganese and Mycobacterium tuberculosis Catalase−Peroxidase Yields a New Mechanism of Activation, *J. Am. Chem. Soc. 123*, 3832-3833.

28. Quemard, A., Sacchettini, J. C., Dessen, A., Vilcheze, C., Bittman, R., Jacobs, W. R., Jr., and Blanchard, J. S. (1995) Enzymatic characterization of the target for isoniazid in Mycobacterium tuberculosis, *Biochemistry 34*, 8235-8241.

29. Takayama, K., Schnoes, H. K., Armstrong, E. L., and Boyle, R. W. (1975) Site of inhibitory action of isoniazid in the synthesis of mycolic acids in Mycobacterium tuberculosis, *J Lipid Res 16*, 308-317.

30. Vilcheze, C., Morbidoni, H. R., Weisbrod, T. R., Iwamoto, H., Kuo, M., Sacchettini, J. C., and Jacobs, W. R., Jr. (2000) Inactivation of the inhA-encoded fatty acid synthase II (FASII) enoyl-acyl carrier protein reductase induces

accumulation of the FASI end products and cell lysis of Mycobacterium smegmatis, *J Bacteriol 182*, 4059-4067.

31. Rawat, R., Whitty, A., and Tonge, P. J. (2003) The isoniazid-NAD adduct is a slow, tight-binding inhibitor of InhA, the Mycobacterium tuberculosis enoyl reductase: adduct affinity and drug resistance, *Proc Natl Acad Sci U S A 100*, 13881-13886.

32. Mdluli, K., Sherman, D. R., Hickey, M. J., Kreiswirth, B. N., Morris, S., Stover, C. K., and Barry, C. E., 3rd. (1996) Biochemical and genetic data suggest that InhA is not the primary target for activated isoniazid in Mycobacterium tuberculosis, *J Infect Dis 174*, 1085-1090.

33. Mdluli, K., Slayden, R. A., Zhu, Y., Ramaswamy, S., Pan, X., Mead, D., Crane, D. D., Musser, J. M., and Barry, C. E., 3rd. (1998) Inhibition of a Mycobacterium tuberculosis beta-ketoacyl ACP synthase by isoniazid, *Science 280*, 1607-1610.

34. Argyrou, A., Vetting, M. W., Aladegbami, B., and Blanchard, J. S. (2006) Mycobacterium tuberculosis dihydrofolate reductase is a target for isoniazid, *Nat Struct Mol Biol 13*, 408-413.

35. Argyrou, A., Jin, L., Siconilfi-Baez, L., Angeletti, R. H., and Blanchard, J. S. (2006) Proteome-wide profiling of isoniazid targets in Mycobacterium tuberculosis, *Biochemistry 45*, 13947-13953.

36. Betts, J. C., McLaren, A., Lennon, M. G., Kelly, F. M., Lukey, P. T., Blakemore, S. J., and Duncan, K. (2003) Signature gene expression profiles discriminate between isoniazid-, thiolactomycin-, and triclosan-treated Mycobacterium tuberculosis, *Antimicrob Agents Chemother 47*, 2903-2913.

37. Slayden, R. A., Lee, R. E., and Barry, C. E., 3rd. (2000) Isoniazid affects multiple components of the type II fatty acid synthase system of Mycobacterium tuberculosis, *Mol Microbiol 38*, 514-525.

38. Wilson, M., DeRisi, J., Kristensen, H. H., Imboden, P., Rane, S., Brown, P. O., and Schoolnik, G. K. (1999) Exploring drug-induced alterations in gene expression in Mycobacterium tuberculosis by microarray hybridization, *Proc Natl Acad Sci U S A 96*, 12833-12838.

39. Washburn, M. P., and Yates, J. R., 3rd. (2000) Analysis of the microbial proteome, *Curr Opin Microbiol 3*, 292-297.

40. Marcotte, R. W. a. E. M. (2008) The Proteomic Response of Mycobacterium smegmatis to Anti-Tuberculosis Drugs Suggests Targeted Pathways, *The Journal of Proteome Research 7*, 855-865.

41. MacKeigan, J. P., Clements, C. M., Lich, J. D., Pope, R. M., Hod, Y., and Ting, J. P. (2003) Proteomic profiling drug-induced apoptosis in non-small cell lung carcinoma: identification of RS/DJ-1 and RhoGDIalpha, *Cancer Res 63*, 6928-6934.

42. Shen, Y., Liu, J., Estiu, G., Isin, B., Ahn, Y. Y., Lee, D. S., Barabasi, A. L., Kapatral, V., Wiest, O., and Oltvai, Z. N. (2010) Blueprint for antimicrobial hit discovery targeting metabolic networks, *Proc Natl Acad Sci U S A 107*, 1082-1087.

43. Lin, M. Z., and Wang, L. (2008) Selective labeling of proteins with chemical probes in living cells, *Physiology (Bethesda) 23*, 131-141.

44. Ong, S. E., Schenone, M., Margolin, A. A., Li, X., Do, K., Doud, M. K., Mani, D. R., Kuai, L., Wang, X., Wood, J. L., Tolliday, N. J., Koehler, A. N., Marcaurelle, L. A., Golub, T. R., Gould, R. J., Schreiber, S. L., and Carr, S. A. (2009) Identifying the proteins to which small-molecule probes and drugs bind in cells, *Proc Natl Acad Sci U S A 106*, 4617-4622.

45. Giaever, G., Shoemaker, D. D., Jones, T. W., Liang, H., Winzeler, E. A., Astromoff, A., and Davis, R. W. (1999) Genomic profiling of drug sensitivities via induced haploinsufficiency, *Nat Genet 21*, 278-283.

46. Hughes, T. R., Marton, M. J., Jones, A. R., Roberts, C. J., Stoughton, R., Armour, C. D., Bennett, H. A., Coffey, E., Dai, H., He, Y. D., Kidd, M. J., King, A. M., Meyer, M. R., Slade, D., Lum, P. Y., Stepaniants, S. B., Shoemaker, D. D., Gachotte, D., Chakraburtty, K., Simon, J., Bard, M., and Friend, S. H. (2000) Functional discovery via a compendium of expression profiles, *Cell 102*, 109-126.

47. Lomenick, B., Hao, R., Jonai, N., Chin, R. M., Aghajan, M., Warburton, S., Wang, J., Wu, R. P., Gomez, F., Loo, J. A., Wohlschlegel, J. A., Vondriska, T. M., Pelletier, J., Herschman, H. R., Clardy, J., Clarke, C. F., and Huang, J. (2009) Target identification using drug affinity responsive target stability (DARTS), *Proc Natl Acad Sci U S A 106*, 21984-21989.

48. Foit, L., Morgan, G. J., Kern, M. J., Steimer, L. R., von Hacht, A. A., Titchmarsh, J., Warriner, S. L., Radford, S. E., and Bardwell, J. C. (2009) Optimizing protein stability in vivo, *Mol Cell 36*, 861-871.

49. Fowler, J. S., Volkow, N. D., Wang, G. J., Ding, Y. S., and Dewey, S. L. (1999) PET and drug research and development, *J Nucl Med 40*, 1154-1163.

50. Gambhir, S. S. (2002) Molecular imaging of cancer with positron emission tomography, *Nat Rev Cancer 2*, 683-693.

51. Phelps, M. E. (2002) Nuclear medicine, molecular imaging, and molecular medicine, *J Nucl Med 43*, 13N-14N.

52. Raichle, M. E. (1983) Positron emission tomography, *Annu Rev Neurosci 6*, 249-267.

53. Liu, L., Xu, Y., Shea, C., Fowler, J. S., Hooker, J. M., and Tonge, P. J. (2010) Radiosynthesis and bioimaging of the tuberculosis chemotherapeutics isoniazid, rifampicin and pyrazinamide in baboons, *J Med Chem 53*, 2882-2891.

54. Nguyen, M., Quemard, A., Broussy, S., Bernadou, J., and Meunier, B. (2002) Mn(III) pyrophosphate as an efficient tool for studying the mode of action of isoniazid on the InhA protein of Mycobacterium tuberculosis, *Antimicrob Agents Chemother 46*, 2137-2144.

55. Rastogi, N., Goh, K. S., Horgen, L., and Barrow, W. W. (1998) Synergistic activities of antituberculous drugs with cerulenin and trans-cinnamic acid against Mycobacterium tuberculosis, *FEMS Immunol Med Microbiol 21*, 149-157.

56. White, R. J., Lancini, G. C., and Silvestri, L. G. (1971) Mechanism of action of rifampin on Mycobacterium smegmatis, *J Bacteriol 108*, 737-741.

57. Luckner, S. R., Liu, N., am Ende, C. W., Tonge, P. J., and Kisker, C. (2010) A slow, tight binding inhibitor of InhA, the enoyl-acyl carrier protein reductase from Mycobacterium tuberculosis, *J Biol Chem 285*, 14330-14337.

58. Kalyanaraman, B., and Sinha, B. K. (1985) Free radical-mediated activation of hydrazine derivatives, *Environ Health Perspect 64*, 179-184.

Chapter IV

1. Phizicky, E. M., and Fields, S. (1995) Protein-protein interactions: methods for detection and analysis, *Microbiol Rev 59*, 94-123.
2. Evans, P. R., Farrants, G. W., and Hudson, P. J. (1981) Phosphofructokinase: structure and control, *Philos Trans R Soc Lond B Biol Sci 293*, 53-62.
3. Kellogg, D. R., Field, C. M., and Alberts, B. M. (1989) Identification of microtubule-associated proteins in the centrosome, spindle, and kinetochore of the early Drosophila embryo, *J Cell Biol 109*, 2977-2991.
4. Kerppola, T. K., and Curran, T. (1991) Fos-Jun heterodimers and Jun homodimers bend DNA in opposite orientations: implications for transcription factor cooperativity, *Cell 66*, 317-326.
5. Monod, J., Wyman, J., and Changeux, J. P. (1965) On the Nature of Allosteric Transitions: A Plausible Model, *J Mol Biol 12*, 88-118.
6. Yanofsky, C., and Rachmeler, M. (1958) The exclusion of free indole as an intermediate in the biosynthesis of tryptophan in Neurospora crassa, *Biochim Biophys Acta 28*, 640-641.
7. Schaeffer, M. L., Agnihotri, G., Kallender, H., Brennan, P. J., and Lonsdale, J. T. (2001) Expression, purification, and characterization of the Mycobacterium tuberculosis acyl carrier protein, AcpM, *Biochim Biophys Acta 1532*, 67-78.
8. Odriozola, J. M., Ramos, J. A., and Bloch, K. (1977) Fatty acid synthetase activity in Mycobacterium smegmatis. Characterization of the acyl carrier protein-dependent elongating system, *Biochim Biophys Acta 488*, 207-217.

9. Heath, R. J., and Rock, C. O. (1996) Roles of the FabA and FabZ beta-hydroxyacyl-acyl carrier protein dehydratases in Escherichia coli fatty acid biosynthesis, *J Biol Chem 271*, 27795-27801.

10. Young, K. H. (1998) Yeast two-hybrid: so many interactions, (in) so little time, *Biol Reprod 58*, 302-311.

11. Kruh, N. A., Borgaro, J. G., Ruzsicska, B. P., Xu, H., and Tonge, P. J. (2008) A novel interaction linking the FAS-II and phthiocerol dimycocerosate (PDIM) biosynthetic pathways, *J Biol Chem 283*, 31719-31725.

12. Bass, S., Greene, R., and Wells, J. A. (1990) Hormone phage: an enrichment method for variant proteins with altered binding properties, *Proteins 8*, 309-314.

13. Scott, J. K., and Smith, G. P. (1990) Searching for peptide ligands with an epitope library, *Science 249*, 386-390.

14. Smith, G. P. (1985) Filamentous fusion phage: novel expression vectors that display cloned antigens on the virion surface, *Science 228*, 1315-1317.

15. Smith, G. P., and Petrenko, V. A. (1997) Phage Display, *Chem Rev 97*, 391-410.

16. Sidhu, S. S., Lowman, H. B., Cunningham, B. C., and Wells, J. A. (2000) Phage display for selection of novel binding peptides, *Methods Enzymol 328*, 333-363.

17. Beeckmans, S., and Kanarek, L. (1981) Demonstration of physical interactions between consecutive enzymes of the citric acid cycle and of the aspartate-malate shuttle. A study involving fumarase, malate dehydrogenase, citrate synthesis and aspartate aminotransferase, *Eur J Biochem 117*, 527-535.

18. Formosa, T., Barry, J., Alberts, B. M., and Greenblatt, J. (1991) Using protein affinity chromatography to probe structure of protein machines, *Methods Enzymol 208*, 24-45.

19. Lazarides, E., and Lindberg, U. (1974) Actin is the naturally occurring inhibitor of deoxyribonuclease I, *Proc Natl Acad Sci U S A 71*, 4742-4746.

20. Fancy, D. A. (2000) Elucidation of protein-protein interactions using chemical cross-linking or label transfer techniques, *Curr Opin Chem Biol 4*, 28-33.

21. Trakselis, M. A., Alley, S. C., and Ishmael, F. T. (2005) Identification and mapping of protein-protein interactions by a combination of cross-linking, cleavage, and proteomics, *Bioconjug Chem 16*, 741-750.

22. Beeckmans, S. (1999) Chromatographic methods to study protein-protein interactions, *Methods 19*, 278-305.

23. Brown, K. C., Yang, S. H., and Kodadek, T. (1995) Highly specific oxidative cross-linking of proteins mediated by a nickel-peptide complex, *Biochemistry 34*, 4733-4739.

24. Brown, K. C., Yu, Z., Burlingame, A. L., and Craik, C. S. (1998) Determining protein-protein interactions by oxidative cross-linking of a glycine-glycine-histidine fusion protein, *Biochemistry 37*, 4397-4406.

25. Campbell, L. A., Kodadek, T., and Brown, K. C. (1998) Protein cross-linking mediated by metalloporphyrins, *Bioorg Med Chem 6*, 1301-1307.

26. Fancy, D. A., and Kodadek, T. (1999) Chemistry for the analysis of protein-protein interactions: rapid and efficient cross-linking triggered by long wavelength light, *Proc Natl Acad Sci U S A 96*, 6020-6024.

27. Kim, K., Fancy, D. A., Carney, D., and Kodadek, T. (1999) Photoinduced Protein Cross-linking Mediated by Palladium Porphyrins, *J. Am. Chem. Soc 121*, 11896-11897.

28. Marriott, G., and Ottl, J. (1998) Synthesis and applications of heterobifunctional photocleavable cross-linking reagents, *Methods Enzymol 291*, 155-175.

29. Cornish, V. W., Hahn, K. M., Schultz, P. G. (1996) Site-specific protein modification using a ketone handle, *J. Am. Chem. Soc 118*, 8150-8151.

30. Chen, Y., Ebright, Y. W., and Ebright, R. H. (1994) Identification of the target of a transcription activator protein by protein-protein photocrosslinking, *Science 265*, 90-92.

31. Prescher, J. A., and Bertozzi, C. R. (2005) Chemistry in living systems, *Nat Chem Biol 1*, 13-21.

32. Sletten, E. M., and Bertozzi, C. R. (2009) Bioorthogonal chemistry: fishing for selectivity in a sea of functionality, *Angew Chem Int Ed Engl 48*, 6974-6998.

33. Kho, Y., Kim, S. C., Jiang, C., Barma, D., Kwon, S. W., Cheng, J., Jaunbergs, J., Weinbaum, C., Tamanoi, F., Falck, J., and Zhao, Y. (2004) A tagging-via-substrate technology for detection and proteomics of farnesylated proteins, *Proc Natl Acad Sci U S A 101*, 12479-12484.

34. Kiick, K. L., Saxon, E., Tirrell, D. A., and Bertozzi, C. R. (2002) Incorporation of azides into recombinant proteins for chemoselective modification by the Staudinger ligation, *Proc Natl Acad Sci U S A 99*, 19-24.

35. Saxon, E., and Bertozzi, C. R. (2000) Cell surface engineering by a modified Staudinger reaction, *Science 287*, 2007-2010.

36. Mahal, L. K., Yarema, K. J., and Bertozzi, C. R. (1997) Engineering chemical reactivity on cell surfaces through oligosaccharide biosynthesis, *Science 276*, 1125-1128.

37. Baskin, J. M., Bertozzi, C.R. (2007) Bioorthogonal Click Chemistry: Covalent Labeling in Living Systems, *QSAR Comb. Sci. 26*.

38. Rostovtsev, V. V., Green, L. G., Fokin, V. V., and Sharpless, K. B. (2002) A stepwise huisgen cycloaddition process: copper(I)-catalyzed regioselective "ligation" of azides and terminal alkynes, *Angew Chem Int Ed Engl 41*, 2596-2599.

39. Tornoe, C. W., Christensen, C., and Meldal, M. (2002) Peptidotriazoles on solid phase: [1,2,3]-triazoles by regiospecific copper(i)-catalyzed 1,3-dipolar cycloadditions of terminal alkynes to azides, *J Org Chem 67*, 3057-3064.

40. Agard, N. J., Prescher, J. A., and Bertozzi, C. R. (2004) A strain-promoted [3 + 2] azide-alkyne cycloaddition for covalent modification of biomolecules in living systems, *J Am Chem Soc 126*, 15046-15047.

41. Baskin, J. M., Prescher, J. A., Laughlin, S. T., Agard, N. J., Chang, P. V., Miller, I. A., Lo, A., Codelli, J. A., and Bertozzi, C. R. (2007) Copper-free click chemistry for dynamic in vivo imaging, *Proc Natl Acad Sci U S A 104*, 16793-16797.

42. Kwon, O. S., and Churchich, J. E. (1994) Interaction of 70-kDA heat shock cognate protein with peptides and myo-inositol monophosphatase, *J Biol Chem 269*, 266-271.

43. Lee, F. S., Auld, D. S., and Vallee, B. L. (1989) Tryptophan fluorescence as a probe of placental ribonuclease inhibitor binding to angiogenin, *Biochemistry 28*, 219-224.

44. Mills, J. S., Walsh, M. P., Nemcek, K., and Johnson, J. D. (1988) Biologically active fluorescent derivatives of spinach calmodulin that report calmodulin target protein binding, *Biochemistry 27*, 991-996.

45. Wine, R. N., Dial, J. M., Tomer, K. B., and Borchers, C. H. (2002) Identification of components of protein complexes using a fluorescent photo-cross-linker and mass spectrometry, *Anal Chem 74*, 1939-1945.

46. Veyron-Churlet, R., Guerrini, O., Mourey, L., Daffe, M., and Zerbib, D. (2004) Protein-protein interactions within the Fatty Acid Synthase-II system of Mycobacterium tuberculosis are essential for mycobacterial viability, *Mol Microbiol 54*, 1161-1172.

47. Hang, H. C., Geutjes, E. J., Grotenbreg, G., Pollington, A. M., Bijlmakers, M. J., and Ploegh, H. L. (2007) Chemical probes for the rapid detection of Fatty-acylated proteins in Mammalian cells, *J Am Chem Soc 129*, 2744-2745.

48. Bulaj, G., Kortemme, T., and Goldenberg, D. P. (1998) Ionization-reactivity relationships for cysteine thiols in polypeptides, *Biochemistry 37*, 8965-8972.

49. Ellman, G. L. (1959) Tissue sulfhydryl groups, *Arch Biochem Biophys 82*, 70-77.

50. Sarikonda, G., Wang, H., Puan, K. J., Liu, X. H., Lee, H. K., Song, Y., Distefano, M. D., Oldfield, E., Prestwich, G. D., and Morita, C. T. (2008) Photoaffinity antigens for human gammadelta T cells, *J Immunol 181*, 7738-7750.

51. Magnuson, K., Jackowski, S., Rock, C. O., and Cronan, J. E., Jr. (1993) Regulation of fatty acid biosynthesis in Escherichia coli, *Microbiol Rev 57*, 522-542.

52. Rumley, M. K., Therisod, H., Weissborn, A. C., and Kennedy, E. P. (1992) Mechanisms of regulation of the biosynthesis of membrane-derived oligosaccharides in Escherichia coli, *J Biol Chem 267*, 11806-11810.

53. Shen, B., Summers, R. G., Gramajo, H., Bibb, M. J., and Hutchinson, C. R. (1992) Purification and characterization of the acyl carrier protein of the Streptomyces glaucescens tetracenomycin C polyketide synthase, *J Bacteriol 174*, 3818-3821.

54. Summers, R. G., Ali, A., Shen, B., Wessel, W. A., and Hutchinson, C. R. (1995) Malonyl-coenzyme A:acyl carrier protein acyltransferase of Streptomyces glaucescens: a possible link between fatty acid and polyketide biosynthesis, *Biochemistry 34*, 9389-9402.

55. Therisod, H., Weissborn, A. C., and Kennedy, E. P. (1986) An essential function for acyl carrier protein in the biosynthesis of membrane-derived oligosaccharides of Escherichia coli, *Proc Natl Acad Sci U S A 83*, 7236-7240.

56. Dorman, G., and Prestwich, G. D. (1994) Benzophenone photophores in biochemistry, *Biochemistry 33*, 5661-5673.

57. Yoo, B. C., Fountoulakis, M., Dierssen, M., and Lubec, G. (2001) Expression patterns of chaperone proteins in cerebral cortex of the fetus with Down syndrome: dysregulation of T-complex protein 1, *J Neural Transm Suppl*, 321-334.

58. Smith, A., and Lough, A. K. (1976) Micellar solubilization of fatty acids in aqueous media containing bile salts and phospholipids, *Br J Nutr 35*, 77-87.